THE DYNAMICS AND CONTROL OF GLUCOSE METABOLISM

by

Robert Steven Hillman

B.S., Stanford University

(1976)

Submitted in Partial Fulfillment

of the Requirements for the

Degree of

Master of Science

at the

Massachusetts Institute of Technology

December, 1976

(i.e. February 1978)

Signature of Author _____

Department of Chemical Engineering, Dec., 1977

Certified by _____

Clark K. Colton Thesis Supervisor

Accepted by _____

Glenn C. Williams, Chairman, Department Committee

THE DYNAMICS AND CONTROL OF GLUCOSE METABOLISM

by

Robert Steven Hillman

Submitted to the Department of Chemical Engineering
in partial on fullfillment of the requirements for the degree of
Master of Science.

Abstract

A comprehensive review of models of glucose metabolism is presented. These models fall into three categories 1) compartment models, 2) flow-limited models, and 3) control models. A flow-limited model for insulin and glucose distribution is developed, based on characterizing the body as a system of continuously-stirred tank reactors connected in series according to their anatomical scheme. The concentration in each organ (CSTR) is dependent on the flow rate to the organ, and mass-transfer resistance between tissue and blood regions. The model accurately simulates clinical data obtained from the Joslin Diabetes Research Laboratory. In addition, the model is used to test a variety of schemes for the control of glucose concentration in diabetics. The model is also used to derive an algorithm that can be used in conjunction with an artificial electromechanical pancreas.

Department of Chemical Engineering
Massachusetts Institute of Technology
Cambridge, Massachusetts 02139
December 7, 1977

Professor Irving Kaplan
Secretary of the Faculty
Massachusetts Institute of Technology
Cambridge, Massachusetts 02139

Dear Professor Kaplan:

In accordance with the regulations of the faculty, I herewith submit a thesis, entitled "The Dynamics and Control of Glucose Metabolism", in partial fulfillment of the requirements for the degree of Master of Science in Chemical Engineering at the Massachusetts Institute of Technology.

Respectfully submitted,

Robert S. Hillman

Acknowledgements

This work was supported in part by NIH grant AM-09748, AM-18352, the Doll Medical Research Foundation, N.Y., and the Joslin Diabetes Foundation, Inc., Boston, to whom the author is grateful.

During my stay at M.I.T. I have had the opportunity to work with many people whose help, advice, and friendship have been valuable in many ways. Specifically, I would like to express my appreciation to: Dr. J. Stuart Soeldner, of the Joslin Diabetes Clinic and Research Laboratory, for his generous support of the project. Dr. Soeldner arranged financial support, provided experimental data, and served as my advisor. His appreciation of modeling, insights into the treatment of diabetes, and willingness to constantly make time in his busy schedule to work with me, definitely improved the quality of this thesis.

Professor Clark Colton, my advisor, for reviewing my work and asking questions that have provided direction and guidance.

Dr. John Guyton, whose insights into the physiology and modeling of glucose metabolism led him to develop the model that serves as the basis for this work. I sincerely appreciate his patience in answering all my questions and for getting me started.

Doctors T. Aoki, G. Cahill, Jr, O. Ganda, R. Gleason, and all the staff at the Joslin Research Laboratory for patiently helping me understand the complexities of fuel metabolism.

Michael Nathanson, for his humor and for a friendship I shall always value.

And all the people in my office: Irvin, Irene, Calvin, Selahatin, Rob, Steve and Mitch.

TO

MY

MOTHER

AND

FATHER.

TABLE OF CONTENTS

LIST OF FIGURES

Figure 10 Schematic diagram of apparatus used for monitoring and automatic regulation of blood sugar (from Albisser et al, 1974).

Figure 11 Apparatus used for the automatic regulation of blood glucose (from Mirouze et al, 1977).

Figure 12 The mean glucose concentrations during an oral glucose tolerance test in diabetics given subcutaneous (S.C.) insulin and controlled by the artificial pancreas (from Albisser et al, 1977).

Figure 13 Continuous blood glucose profiles in diabetics sustained by subcutaneous insulin (top curve) and regulated by artificial pancreas (center curve). Infusion patterns (histogram) of insulin (black bars) and dextrose (white) (from Albisser et al, 1974).

Figure 14 Plasma insulin in nine diabetic subjects during continuous treatment with the pulsed insulin-delivery system (closed circle) compared with plasma insulin in eight normal subjects receiving identical meals at 8:00 a.m., 1:00 p.m., and 6:00 p.m. (from Genuth and Martin, 1977).

Figure 15 Mean plasma glucose in nine diabetic subjects prior to treatment (solid line), during pulsed insulin delivery (interrupted line), and during the first day of treatment (hatched line). Double arrows indicate 600 calorie meals and single arrow a 300 calorie snack (from Genuth and Martin, 1977).

Figure 16 Daily substrate flow in a normal fasted man (from Cahill, 1971).

Figure 17 Cycle of glucose homeostasis in a fasting man after liver glycogen has been depleted. FFA = free fatty acid; AA = amino acid (from Cahill, 1974).

Figure 18 Substrate flux following a mixed meal consisting of carbohydrates,

(Figure 18) amino acids and lipids (Courtesy of G. F. Cahill, Jr.).

Figure 19 Spectrum of glucose metabolism, which ranges from (left to right) large glucose meals of 3 g/min, infusion of .2 to .5 g/min, infusion of dextrose and water at 0.1 g/min, and total fasting, to a net carbohydrate deficit as observed in diabetics with hyperglycemia and glycosuria (from Cahill, 1974).

Figure 20 Diagrammatic representation of the morphologic events of the secretory process in an insulin-producing cell. Abbreviations: r = free ribosome; pr = polyribosomes; sv = smooth vesicles; cv = coated vesicles; ig = immature granules; mg = mature granules; mt = microtubules; cw = cell web; bm = basement membrane; mv = microvillus; cm = cell membrane (from Renold, A. et al, 1971).

Figure 21 Effect of glucose on insulin release from mouse and rat islets (from Ashcroft, 1976).

Figure 21A Effect of prolonged glucose infusion and restimulation on insulin secretion from the <u>in vitro</u> perfused pancreas of the rat. Shaded area represents period of glucose stimulation at 300 mg/dl (from Curry et al, 1968).

Figure 22 Insulin secretion during staircase stimulations with 50 mg/100 ml increments of glucose. Values in mg/100 ml refer to glucose concentrations at each five minute step (from Grodsky, 1972).

Figure 23 Effect of gradually increasing glucose concentration on insulin secretion from the <u>in vitro</u> perfused pancreas of rat (from Grodsky, 1972).

Figure 24 Plasma insulin responses of 12 normal weight and 12 obese diabetic subjects to an oral glucose tolerance test (100 gm) and

(Figure 24) infusion maintained glucose profile (from Perley and Kipnis, 1967).

Figure 25 Substrate flow in a diabetic man (Cahill and Soeldner, 1969).

Figure 26 The nonlinear function relating the glucose concentration to the rate of insulin secretion (from Cerasi et al, 1974).

Figure 27 Model of oxidation glucose metabolism. V represents the volume of each compartment, K represents the intercompartmental transfer and elimination rates (from Spencer et al, 1971).

Figure 28 Three compartment model for insulin distribution. U_1 = endogenous insulin secretion rate; U_2 = exogenous insulin infusion rate; M = mass of compartment; and K = rates of intercompartment transfer and removal (from Insel et al, 1975).

Figure 29 Three compartment model for glucose distribution. U_3 = endogenous glucose production rate, U_4 = exogenous glucose infusion rate, K = rate of intercompartmental transfer and removal, and M = mass of compartment (from Insel et al, 1975).

Figure 30 Model for glucose homeostasis. The rectangles represent concentrations. The decanter-shaped figures represent rates (from Foster et al, 1973).

Figure 31 The quantitative relationship between the blood glucose concentration and the nervous system uptake of glucose (NSU). The numbers shown on the y-axis are multiplicative factors (from Foster et al, 1973).

Figure 32 The influence of blood glucose concentration and rate of change of blood glucose concentration on insulin secretion (from Foster et al, 1973).

Figure 33 The influence of plasma free fatty acid concentration on insulin

(Figure 33) secretion. The numbers on the y-axis are multipliers (from Foster, 1973).

Figure 34 Diagram of Guyton's model for glucose distribution in a normal man. Q = blood flow rate; dotted line represents separation between blood and tissue regions.

Figure 35 Diagram of a compartment (heart) in which blood and tissue regions are represented. Q_H is the blood flow rate to the compartment; K_H is the blood-to-tissue (transmembrane) glucose transport rate; K_{TH} of the tissue-to-blood glucose transport rate.

Figure 36 Peripheral glucose uptake as a function of insulin concentrations. NL represents the fasting insulin concentration. The numbers on the axis are multiplicative factors.

Figure 37 Peripheral glucose uptake as a function of glucose concentrations. NL represents the fasting glucose concentration. The numbers on the axis are multiplicative factors.

Figure 38 Peripheral glucose uptake as a function of heart glucose concentrations. The numbers on the y-axis are multipliers.

Figure 39 The influence of insulin concentration on the rate of glycogen breakdown.

Figure 40 The influence of heart glucose concentration on the rate of glycogen breakdown.

Figure 41 The influence of insulin concentration on the rate of glycogen synthesis

Figure 42 The influence of insulin concentration on gluconeogenesis.

Figure 43 The influence of heart glucose concentration on gluconeogenesis.

Figure 44 The influence of liver glucose concentration on glycogen synthesis.

Figure 45 Diagram of Guyton's model for insulin distribution in a normal man. Q = plasma flow rate; dotted line represents separation between plasma and tissue regions.

Figure 46 Model of beta-cell secretion of insulin in response to glucose. lg: granular insulin; lm: releasable insulin at membrane; lp: insulin precursor protein; c, d: intermediates representing trigger mechanism; a,b: unidentified postulated intermediates; G: glucose (from Bergman and Urquhart, 1971).

Figure 47 Total insulin secreted during the early phase (min 1-10) (open circles represent data). Solid line is a graph of the analytic function used to fit the data. Broken line is its mathematical derivative (from Grodsky, 1972).

Figure 48 Maximum secretion rate of insulin release during the second phase as a function of glucose concentration. Open circles represent data. Broken line is a graph of the analytic function used to fit the data.

Figure 49 Model of beta-cell synthesis and storage of insulin. Is: stored insulin; lg: insulin in the Golgi apparatus; Ip: proinsulin, C_H: heart concentration of glucose; G: glucose concantration in the beta-cell; G_M: glucose metabolite; M_{RNA} = messenger RNA.

Figure 50 The effect of heart glucose concentrations on the rate of MRNA synthesis. Numbers on the y-axis are multiplicative factors.

Figure 51 The effect of heart glucose concentrations on the rate of transfer of stored insulin to releasing-holding sites. Numbers on the

(Figure 51) y-axis multiply the fasting rate.

Figure 52 The effect of heart glucose concentrations on the fraction of insulin releasing sites.

Figure 53 The delayed effect on heart glucose concentrations on the secretion of insulin.

Figure 54 Beta-cell model simulation of response to a constant infusion of glucose at a concentration of 300 mg/dl.

Figure 55 Three-minute, 0.5 GM/Kg IVGTT. Comparison of model simulation to experimental data.

Figure 56 Twelve-minute, 0.5 GM/Kg IVGTT. Simulated versus averaged experimental result.

Figure 57 G-30-G double pulse glucose study simulated versus average experimental result.

Figure 58 G-60-G double pulse glucose study simulated versus average experimental result.

Figure 59 Relationship of blood glucose concentration to insulin and dextrose infusion rates (from Botz, 1976).

Figure 60 Algorithms for calculation of the "glucose difference" factor, DF (from Clemens et al, 1977).

Figure 61 Comparison of normal and simulated insulin/blood glucose relationships in response to 60 min glucose load (10 mg/Kg/min) (from Botz, 1976).

Figure 62 Control algorithms relating insulin infusion rate to blood glucose concentrations. (1) control algorithm for blood glucose rises; (2) control algorithm for blood glucose falls; (3) basal insulin secretion rate; (4) maximum insulin secretion rate (from Mirouze et al, 1977).

Figure 63 Control algorithm relating blood glucose concentration to insulin secretion rate. R_I: basal insulin infusion rate; B_I: the glucose set point; Q_I: the steepness of the curve.

Figure 64 100 gram oral glucose tolerance test. Simulated versus experimental results.

Figure 65 100 gram oral glucose tolerance test. Simulated versus experimental results.

Figure 66 100 gram oral glucose tolerance test. Model simulation of liver, heart and kidney glucose concentrations.

Figure 67 100 gram oral glucose tolerance test. Model Simulation of liver, heart, and peripheral glucose concentrations.

Figure 68 The rate of absorption of glucose following a 100 gram oral glucose tolerance test.

Figure 69 The disposition of a glucose load following a 100 gram oral glucose tolerance test. The area under the lower curve indicates total liver utilization; the area between the upper and lower curve indicates the total peripheral tissue utilization.

Figure 70 The disposition of a glucose load following a 35 gram IVGTT.

Figure 71 Simulated rates of peripheral glucose uptake (mgu), glycogen synthesis (glys), gluconeogenosis (gneo), and glycogen breakdown (glyb) following a 100 gram oral glucose tolerance test. Note that fasting glycogen stores were taken to 1/10th of normal.

Figure 72 Simulated rates of peripheral glucose uptake (MGU), glycogen synthesis (GLYS), gluconeogenesis (GNEO), and glycogen breakdown (GLYB) following a 100 gram oral glucose tolerance test.

Figure 73 The rate of insulin secretion in response to a 100 gram oral glucose tolerance test.

Figure 74 The rate of insulin secretion in response to a 100 gram oral glucose tolerance test. Note that in this simulation, the effect of Gl hormones on insulin secretion has been omitted.

Figure 75 Simulation of the peripheral glucose concentration following a 100 gram oral glucose tolerance test, with diminished insulin secretion.

Figure 76 Simulated blood glucose concentration in response to 3 100 gram oral glucose tolerance tests at five hour intervals. (Arrows indicate start of each test.)

Figure 77 Simulated peripheral insulin concentrations in response to three 100 gm oral glucose tolerance tests at five-hour intervals. (Arrows indicate start of each test.)

Figure 78 Simulated rates of peripheral glucose uptake (mgu), glycogen synthesis (glys), glycogen brakdown (glyb) and gluconeogenesis (gnes) in response to three 100 gram oral glucose tolerance tests at five-hour intervals. (Arrows indicate start of each test.)

Figure 79 Phase plot of simulated peripheral insulin versus peripheral glucose concentrations following a 100 gram oral glucose tolerance test.

Figure 80 Phase plot of simulated peripheral insulin versus peripheral glucose concentrations following a 35 gram IVGTT.

Figure 81 Phase plot of simulated insulin secretion rate versus arterial glucose concentrations following a 100 gram oral glucose tolerance test.

Figures 83-84 Experimental data and simulation of a 50 gram oral glucose tolerance test.

Figures 85-90 Intramuscular insulin injection of 40 units of intermediate-acting insulin. Simulation of response to two 100 gram oral tolerance tests at five-hour intervals, under these conditions.

Figures 91-92 Intravenous insulin infusion of 10 mu/min. Simulation of response to a 100 gram oral glucose tolerance test, under these conditions.

Figures 93-94 Intravenous insulin infusion of 20 mu/min. Simulation of response to a 100 gram oral glucose tolerance test.

Figures 95-97 Pulsed intravenous insulin infusion after each meal. Simulation of response to two 100 gram glucose tolerance tests at five-hour intervals.

Figures 98-103 Continuous intravenous insulin infusion regulated by continuous feedback from a glucose sensor. Simjlation of response to two 100 gram oral glucose tolerance tests at five-hour intervals.

Figure 104 Continuous intravenous infusion based on a proportional-plus-derivative controller and feedback from a glucose sensor. Simulation of response to two oral glucose tolerance tests at five-hour intervals.

Figure 104.1 Simulated response of a normal man to two oral glucose tolerance tests at five-hour intervals.

Figures 105-109 Continuous intravenous infusion based on a proportional-plus derivative controller and feedback from a glucose sensor. Simulation of response to two oral glucose tolerance tests at five-hour intervals.

Figures 110-115 Insulin delivery with diffusional delay in glucose measurement and insulin secretion. Simulation of response to a 100 gram oral glucose tolerance test.

Figures 116-121 Pancreatic insulin secretion based on measurement of peripheral (i.v.) glucose concentration. Simulation of response to a 100 gram oral glucose tolerance test.

Figures 122-127 Pancreatic insulin secretion via the peripheral rather than portal circulation. Simulation of response to a 100 gram oral glucose tolerance test.

Figures 128-132 Pancreatic insulin secretion via the peripheral circulation based on measurement of peripheral (i.v.) glucose concentrations. Simulation of response to a 100 gram oral glucose tolerance test.

Figures 133-138 Pancreatic insulin secretion via the peripheral circulation based on measurement of peripheral tissue glucose concentrations. Simulation of response to a 100 gram oral glucose tolerance test.

Figures 139-143 Five-minute delay in the glucose signal to the pancreas. Simulation of response to a 100 gram oral glucose tolerance test.

Figures 144-147 Ten-minute delay in the glucose signal to the pancreas. Simulation of response to a 100 gram oral glucose tolerance test.

I. INTRODUCTION

This review will cover mathematical models of glucose homeostasis. The flow of glucose between the body's organs and the metabolism of glucose by these organs is subject to modulating influences by pancreatic, pituitary, adrenal and gastrointestinal hormones. Insulin, a hormone secreted by the beta cells of the pancreas, is the prime signal in the regulation of glucose metabolism. Insulin regulates the storage and utilization of body fuels thereby keeping blood glucose concentrations within relatively narrow limits.

In the area of glucose metabolism, three classes of models have been developed: 1) compartment, 2) flow-limited, and 3) control models. In developing a compartment model various regions of the body are represented by a compartment in which all property variations can be ignored (Bischoff and Brown, 1966). In addition perfect mixing within each compartment is assumed. The compartments in most cases have no physiological significance. If intercompartmental transfer is assumed to take place by a linear law (representing mass flow or diffusion), the balances have the form:

$$\frac{dC}{dt} = \sum_{j=1}^{n} K_{ij} C_j \quad (i=1,\ldots n)$$

For constant K_{ij}, the solution for concentration as a function of time is a series of exponentials:

$$C_i = \sum_{j=1}^{n} A_{ij} e^{jt}$$

Therefore, a curve fitting procedure is necessary to find the constants of the exponentials that will fit the experimental data. If the rate constants are functions of concentration, $K_{ij}(c)$, (e.g. to represent Michaelis-Menton Kinetics) a set of nonlinear differential equations result. Because of the difficulty in finding the parameters for a nonlinear model, most models of glucose homeostasis have been linear. The most common use of these models is to determine the parameters of a sufficient number of compartments to fit the plasma insulin and blood glucose concentration curves following an intravenous glucose tolerance test (IVGTT). This type of analysis is analagous to dose-response curves for a drug, which are widely used in the pharmacokinetic literature to predict concentrations of a drug following intravenous administration (Wagner 1976). The advantage of these models is that individual parameters for each subject can be determined. The coefficients can then be used to characterize and compare the response of normal and diabetic subjects to an IVGTT and the sensitivity of parameters. Even though these models can often give a reasonable fit to the data, the interpretation of model parameters with respect to the underlying physiology is often ambiguous. In addition, these models can only be used for empirical projections of experiments for which they have been designed, and are of no predictive value in other situations.

Flow-rate limited models also employ a lumped compartment approach, but with the important restriction that the compartments represent actual body regions. Bishoff pioneered the initial formulation of models of this type for describing the distribution of drugs in the body and has prepared a very complete review (Bischoff, 1975) on the

distribution of drugs in the body and has prepared a very complete review (Bischoff, 1975) on the considerations underlying the design of flow-limited models. The term "flow-rate limited" arises from the assumption that membrane permeability is so large that any molecules that flow into a region have an easy time moving through space. Thus, the part of the process that determines the concentration in each region, is how much drug was able to flow in from the blood pool. Each compartment is well mixed, and the blood circulating at an effective volumetric flow rate Q, leaves each compartment in equilibrium with it. For each anatomical region, one writes a mass balance equation. Fig. 1 shows a flow-rate limited model for methotrexate pharmacokinetics. (Bischoff et al, 1971). A typical mass balance on the plasma compartment would be:

$$V_P \frac{dC_P}{dt} = Q_L \frac{C_L}{R_L} + Q_K \frac{C_K}{R_L} + Q_M \frac{C_M}{R_K} - (Q_L + Q_K + Q_M)\, C_P$$

(see Fig. 1 for definition of terms). It is important to note that no empirical relations parameters are included in the prediction, which is made from prior experimentally measured parameters: organ volumes, equilibrium between various tissues, and kinetics of metabolism and elimination. The success of this approach depends on careful examination of both anatomy and metabolism. In contrast to compartment models, the advantage to this approach is that the model design is based on an understanding of the physiology, and simulations can yield insight into the physiological processes. In addition, the model can be used to simulate a variety of dynamic situations, and is not restricted to one experiment. The drawbacks to models of this type is that the resulting

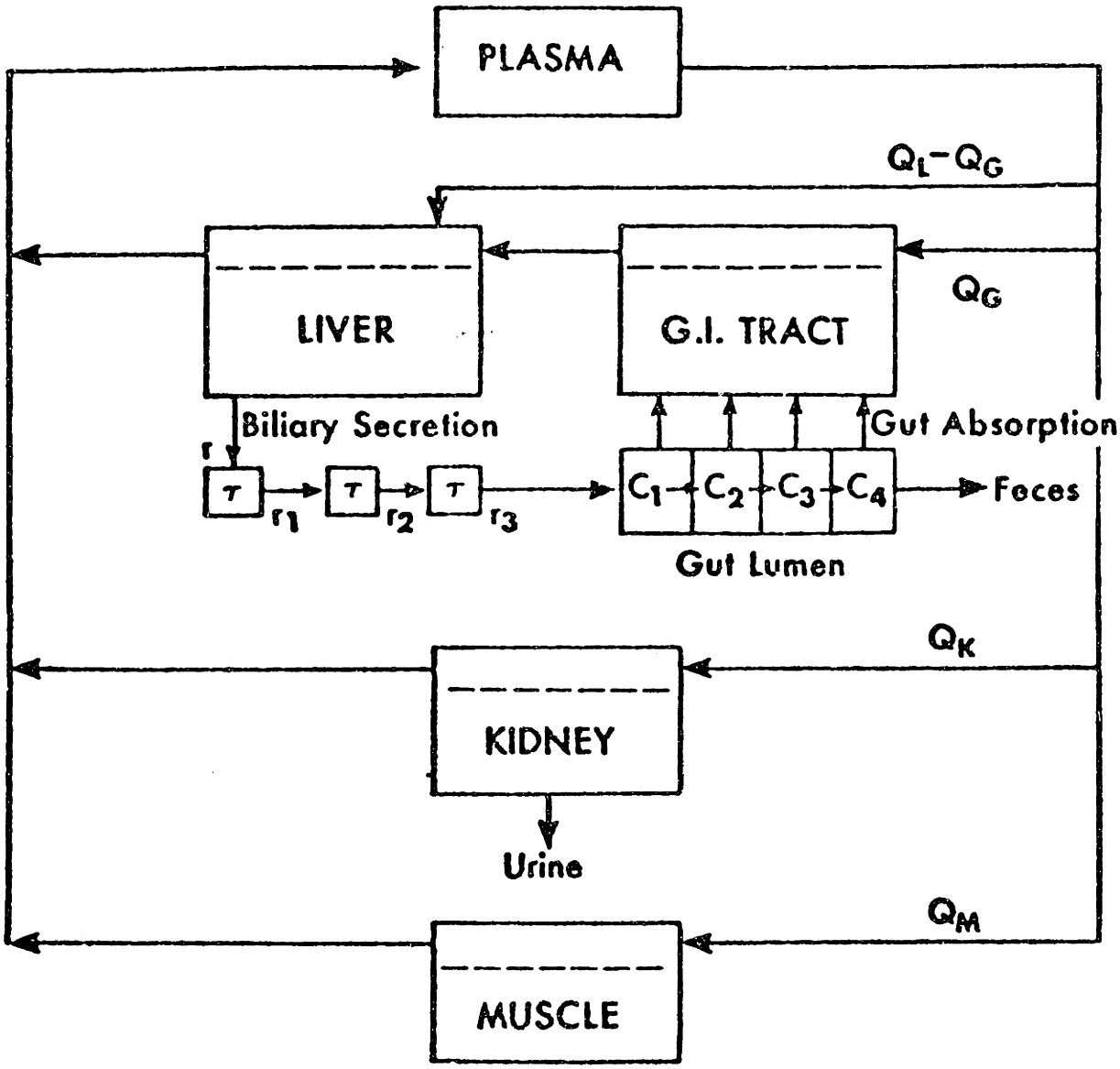

Figure 1

Compartmental model for methotrexate distribution.

curves are by necessity average values, and cannot account for the variability among individuals. In addition, the assumption of a constant blood flow rate throughout an experiment, may not be acceptable in all cases.

Control models involve the design of an algorithm that will maintain glucose levels within a certain range by specifying the pattern of insulin secretion. In other words a model to describe the rate of secretion of insulin by the pancreas is sought. In the development of these models it is therefore assumed that insulin is the most important factor in the control of blood glucose levels. Benedek (1973,1974) has shown that the physiological control system for glucose can be characterized by a proportional-plus-integral-plus-derivative (PID) controller. The rate at which the body's control system can supply or remove glucose is given by:

$$\frac{dQ}{dt} = K_D \frac{d}{dt}(C) + K_p (C_s - C) + K_I \int (C - C_s)\, dt$$

Q is the total mass of glucose present in the blood. C is the concentration (in mass per unit volume) of glucose at time t. C_s is the set point against which the body's sensor measures increases or decreases in glucose concentration. The first term is the contribution from derivative control. If the concentration rises at a rate $\left(\frac{dC}{dt}\right)$, the control system will respond by removing glucose at a rate $K_D \left(\frac{dC}{dt}\right)$. K_D is the coefficient of proportionality for derivative control, in units of volume. Derivative control is indicated by experiments by Grodsky (1972) which show that part of the insulin release is proportional to (dC/dt).

The second term represents the proportional removal of glucose. If the concentration of glucose falls below the set point, the control system supplies glucose at a rate $K_p(C_s-C)$, which is proportional to the deviation from the set point concentration. The units of K_p, the coefficient for proportional control, are volume/time. The origin of this term is the fact that when the concentration exceeds C_s the release of insulin does not occur and glycogen stores in the liver are broken down rapidly into glucose and delivered to the blood. The third term is the long-term average rate at which glucose is added or removed. When the concentration is greater than the set point the process of fat storage (lipogenesis) occurs. When the concentration is below the set point, new glucose production (gluconeogenesis) occurs. The response time for this control term is very long, on the order of seven hours.

The control algorithms developed to date mimic the physiological control system in that they are PID controllers. The advantage of these control models is that they provide a simple algorithm for the temporal pattern of insulin administration to normalize blood sugar. However, the models are based on the assumption that glucose is the only stimulus for insulin secretion, and that insulin concentrations are the only determinant of glucose utilization. With this simplification the algorithms may not offer the control needed on a day-to-day basis.

Several functions are served by the dynamic models of glucose homeostasis described above: 1) they represent a compact generalization about the body of experimental data they simulate; 2) they allow for the simulation of physiology and the design of new experiments; 3) they serve as a method for investigating mechanisms leading to abnormal

physiology; and 4) they can be used to specify the acceptable parameters for an insulin-secretory device for use in diabetics, such as lag time, threshold, and maximum limit of response of insulin secretion to glucose levels.

II. CURRENT CONCEPTS CONCERNING MANAGEMENT OF DIABETES

The predominant clinical diagnostic tests of glucose homeostasis in man are the intravenous and oral glucose tolerance tests. The intravenous glucose tolerance test (IVGTT) generally consists of a single glucose injection of 0.5 gm/kg body weight as a 50% solution following an overnight fast and a 300 gm carbohydrate diet for three days prior to the test (Soeldner, 1971). The k-rate, defined as $K = \frac{0.693 \times 100}{t\ 1/2}$ is used to characterize the exponential decay of plasma glucose concentrations. In normal subjects blood glucose concentration rises from a fasting level of 80-90 mg/dl, the upper limit of the fasting level is 120 mg/dl and anything above this usually indicates diabetes. Fig. 2 illustrates that the insulin response in normal subjects occurs within a few minutes after the termination of the rapid glucose infusion. Mild diabetic individuals with a normal fasting blood glucose but some significant impairment of the rate of glucose utilization during the IVGTT show an insulin response that is diminished particularly in the early phases of the test. The lower left panel shows the corresponding glucose and insulin levels in individuals with moderate diabetes. It can be seen that there is no significant increase of insulin levels until approximately the 20 minute time interval. It seems, therefore, that the hallmark of diabetes is first a diminished early insulin response and a significant delay in achieving the maximum insulin level.

In the oral glucose tolerance test (OGTT), the subject drinks a glucose enriched drink containing 100 gm of glucose (following an overnight fast). As seen in Fig. 3 the blood glucose concentrations in normal

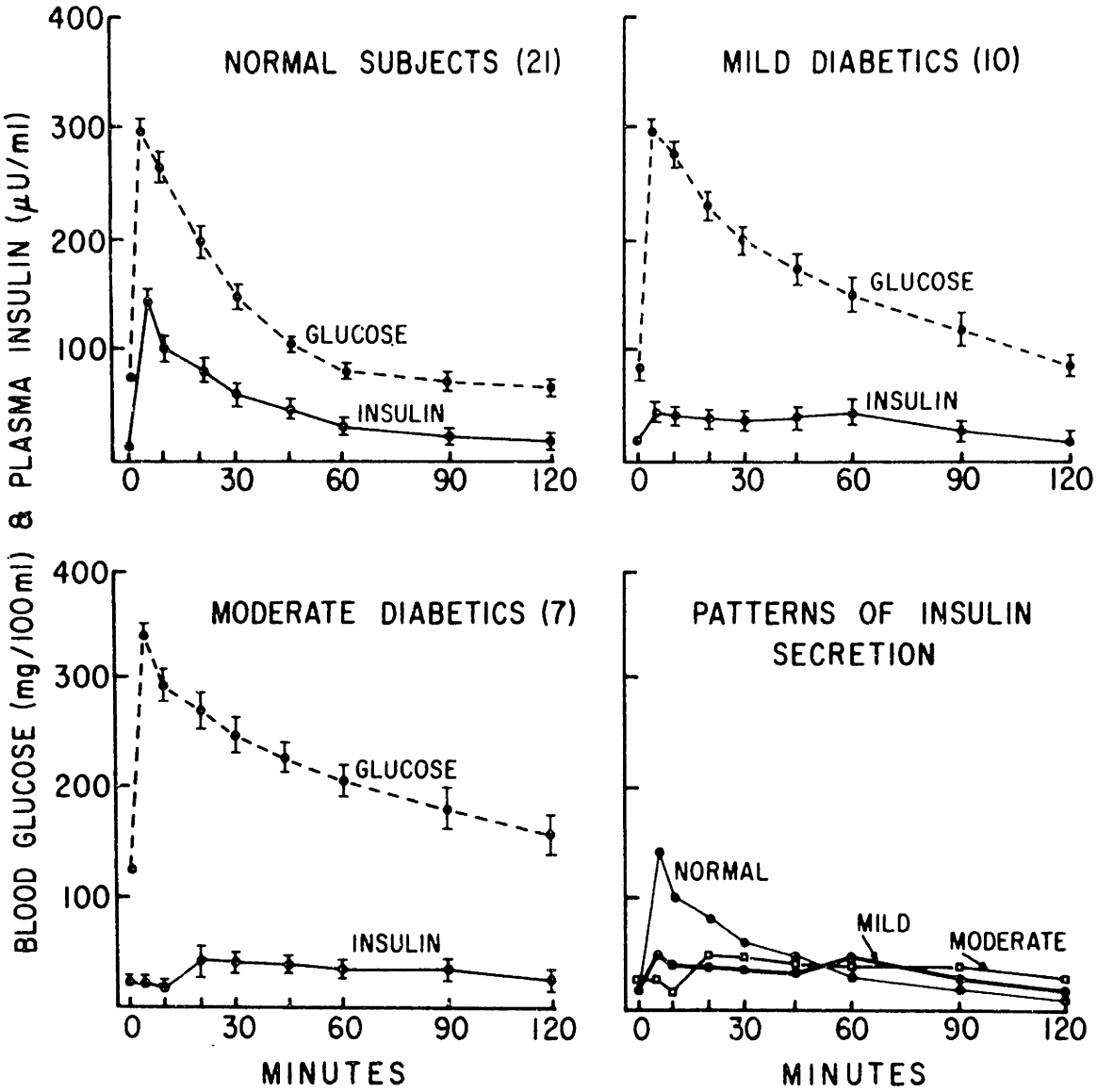

Figure 2

Blood glucose and serum insulin responses during oral glucose tolerance tests in normal subjects and in mild and moderate diabetics (from Seltzer et al, 1967).

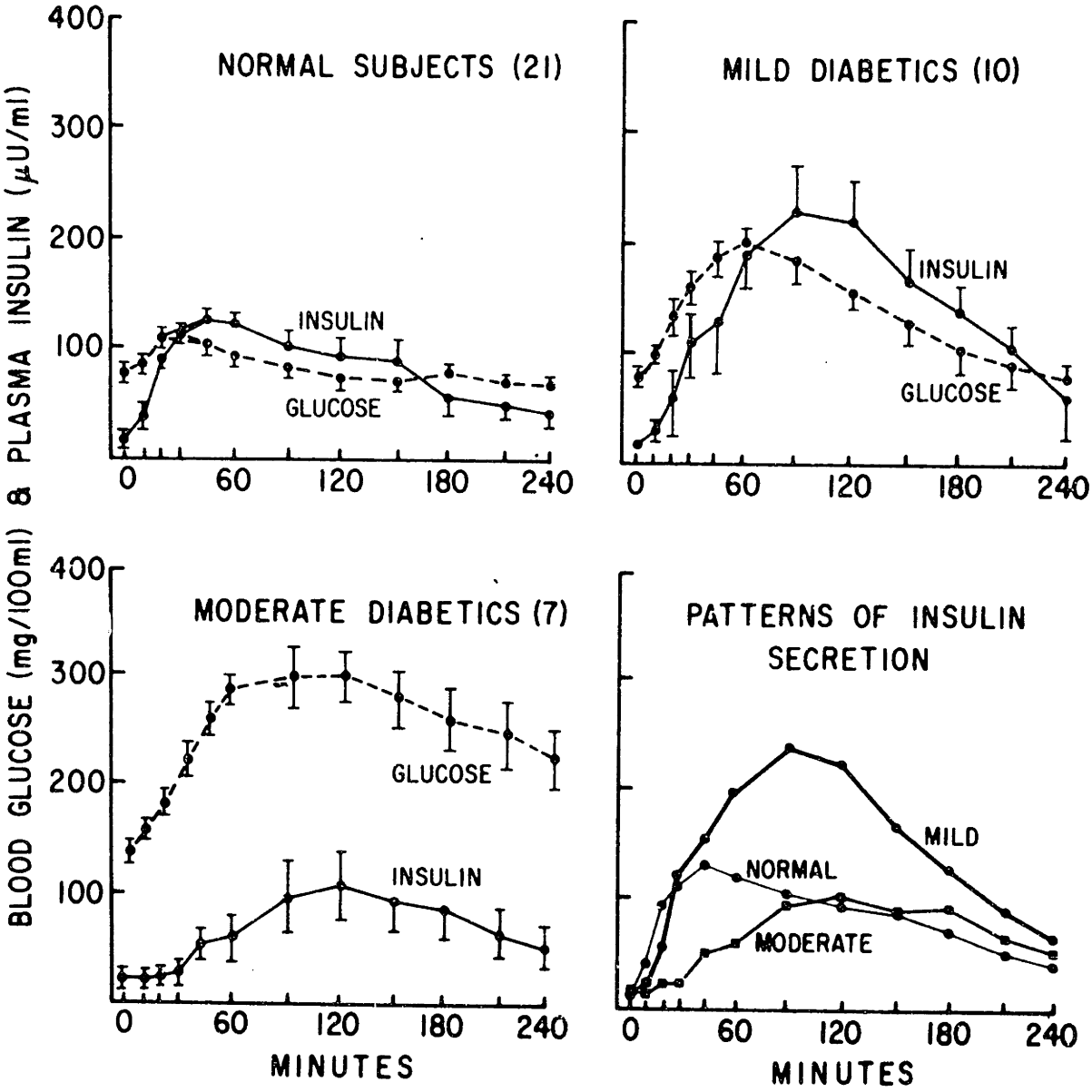

Figure 3

Blood glucose and serum insulin responses during oral glucose tolerance tests in normal subjects and in mild and moderate diabetics (from Seltzer et al, (1967).

subjects rise from a fasting level of 80-90 mg/dl and fall back to normal within three hours, while a moderate diabetic shows a slow rise in blood glucose concentration over 2-3 hours, falling back to control levels (of around 120 mg/dl) only after 5-6 hours. In normal subjects there is a very rapid elevation of serum insulin in the early phases after the oral administration of glucose. In mild diabetic subjects there appears to be a somewhat slower rate of rise, and the maximum insulin level is significantly delayed compared to that seen in normal subjects. Although it is apparent that the mild diabetics have a significantly higher insulin curve than normal subjects, one has to bear in mind that the mild diabetics had considerably higher levels of glucose throughout the duration of the test. Using an "Insulinogenic Index" (an estimate of the insulin to glucose relationship), Seltzer (1967) has shown that these mild diabetics have a significantly reduced insulin to glucose relationship when compared to normal subjects. This has been used to indicate that although the absolute insulin levels are elevated in the milder diabetic, there is a relative insulin deficiency. Examining the insulin curve in the moderate diabetics, it is clear there is a marked reduction in the rate of rise of insulin in the early phases of the test, and that there is an even greater displacement in time of the maximum insulin level.

Clearly, neither the IVGTT or OGTT represent the experiments necessary to determine the steady-state relationship between insulin and glucose, although they have served as the basis for most models to date. Fig. 4 demonstrates another problem in interpretation of the data, namely the large statistical variation in response in a well-defined group of subjects.

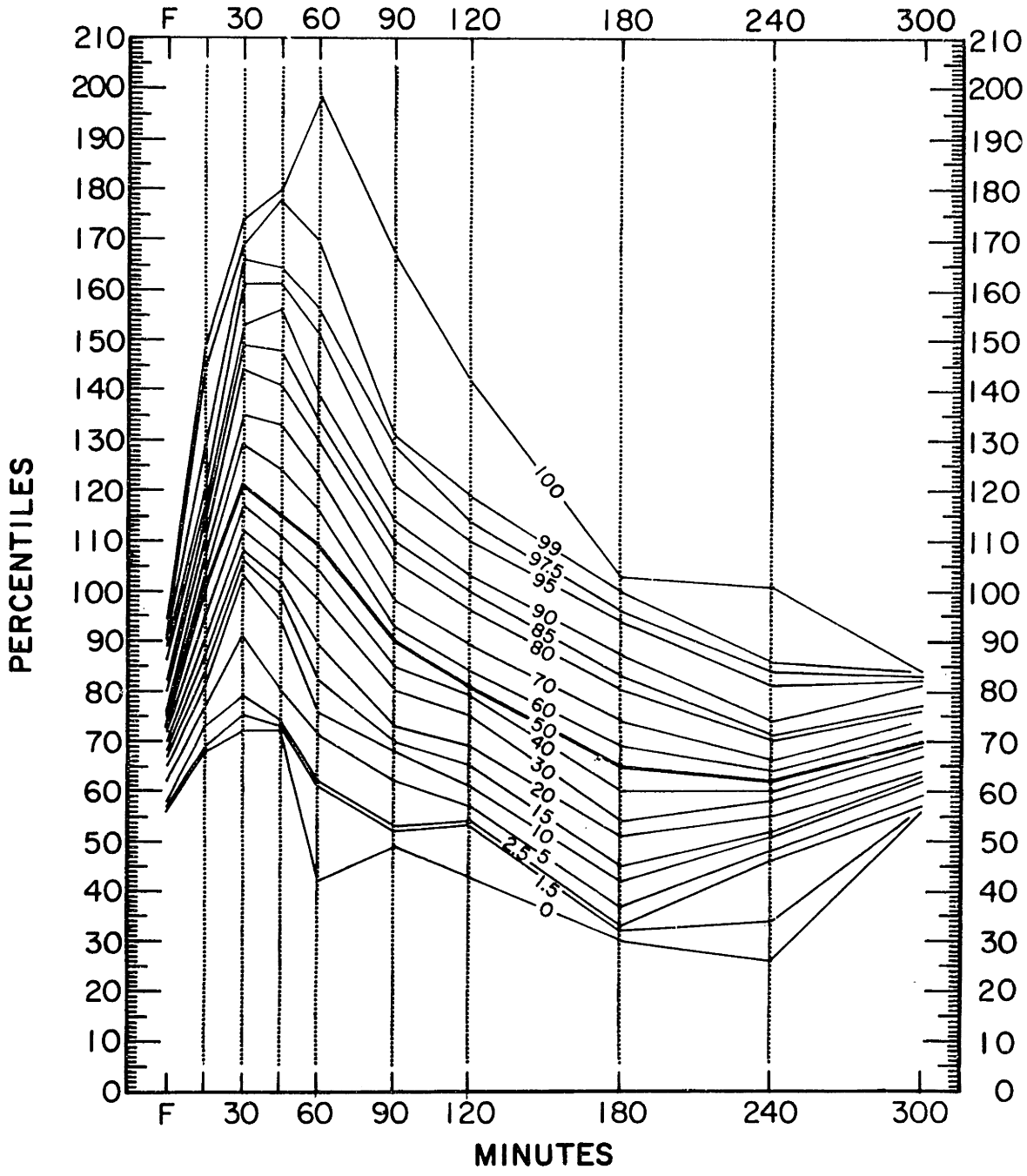

Figure 4

Blood glucose concentrations in normal subjects during oral glucose tolerance tests.

Diabetes mellitus, which is the predominant clinical dysfunction of glucose homeostasis, is comprised of two major syndromes, the juvenile-onset (insulin dependent, ketosis prone) and the maturity-onset (nonketotic) forms. Juvenile-onset diabetes is characterized by the relative absence of insulin synthesis and secretion in young individuals. This form of diabetes is characterized by hyperglycemia and ketoacidosis associated with extremely low concentrations of immunologically measurable insulin. In maturity-onset diabetes, insulin is present, but impairment of secretion is indicated by the delayed appearance of insulin following glucose administration. Impairment is also indicated by the fact that less insulin is secreted at any glucose concentration, leading to hyperglycemia.

The belief that better control of blood glucose concentrations in patients can significantly reduce the serious late complications of diabetes has recently received considerable support in the literature. The American Diabetes Association (Cahill et al, 1976 a,b) has stated that "...a high priority must be assigned to the development of a more physiologic insulin delivery system or to approaches to the correction of the deficient insulin producing mechanism itself." Although clinical studies of the value of careful control have been inconclusive, numerous studies in animals support the notion of careful control. The best planned clinical study to date, a prospective eight-year study known as the University Group Diabetes Program (1970) failed to show any reduction of microvascular lesions in a group whose insulin dosage was adjusted to achieve an almost normal fasting sugar, as opposed to a group given a standard dose of insulin adjusted only for body height and weight. However, even the best clinical control of diabetes falls far short of

the quite precise response to a changing glucose level characteristic of a normal pancreas. The belief that a normal or almost normal insulin response to glucose might present late diabetic complications is still suggested by etiologic and epidemiologic evidence. First, persons with nongenetic diabetes (i.e. diabetes secondary to pancreatitis, pancreatectomy) are subject to the same microvascular disease in the kidney and retina as genetic diabetics (Creutzfeldt and Perings, 1972). Dogs made diabetic by administration of alloxan or growth hormone also develop these complications (Bloodworth, 1972; Engerman and Bloodworth, 1965). The etiology of defective basement membranes in kidney glomerular capillaries of diabetics has been investigated biochemically. A characteristic abnormality was found involving increased glycosylation of lysine-hydroxylysine residues in the basement membrane protein. When glycosylated, these residues cannot perform their normal function of cross-linking adjacent peptides, which ordinarily helps to bind the entire basement membrane into a tight web. The activity of a specific enzyme in the glycosylation sequence was found to be elevated in alloxan-diabetic rats; it returned to almost normal when rats were maintained under very tight control with insulin (Spiro, 1973).

The common neuropathy and somewhat rarer cataracts of diabetes have a well-established etiology. Elevated blood glucose levels cause an abnormal accumulation of sorbitol and fructose in the Schwann cells of nerve or the cells of the lens, which lead to damage and eventual destruction of the cells (Gabbay and O'Sullivan, 1972). A small but prospective study of randomly assigned patients with well-controlled diabetes showed less retinopathy (Job et al, 1975). Recently, glycosylated

hemoglobin has been found in man and laboratory animals in the presence of persistent and prolonged hyperglycemia (Bunn et al, 1975).

Several approaches for the control of blood glucose have been proposed. They can be grouped into two categories which include transplantation of tissue containing functioning beta cells and the use of electromechanical devices designed to imitate beta cell function. Treatment of diabetes has traditionally been related to the control of glucose levels by the subcutaneous injection of insulin. Insulin preparations are divided into three categories according to promptness, duration, and intensity of action following subcutaneous administration (See Fig. 5). Because of the desire to reduce patient noncompliance and error in administration, most diabetics inject a single dose of insulin daily, usually before breakfast, and are instructed to maintain careful control of their diets. As shown in Fig. 6, this is a very poor approach to normalizing blood glucose levels.

Transplantation techniques for the normalization of blood glucose levels have been reviewed by Matas et al (1976). Clinically, whole organ transplantation has been successful in establishing normal glucose homeostasis, but prolonged survival of both graft and patient has rarely been achieved because of both technical and immunological problems.

The transplantation of islet cells is perhaps a more preferable alternative, since only a small percentage of the total islet cell mass is required to maintain normal carbohydrate metabolism. Successful isolation of viable pancreatic islet cells has been achieved by several groups although the yields are low. Najarian et al (1975) has performed islet transplants in immunosuppressed patients who had previously

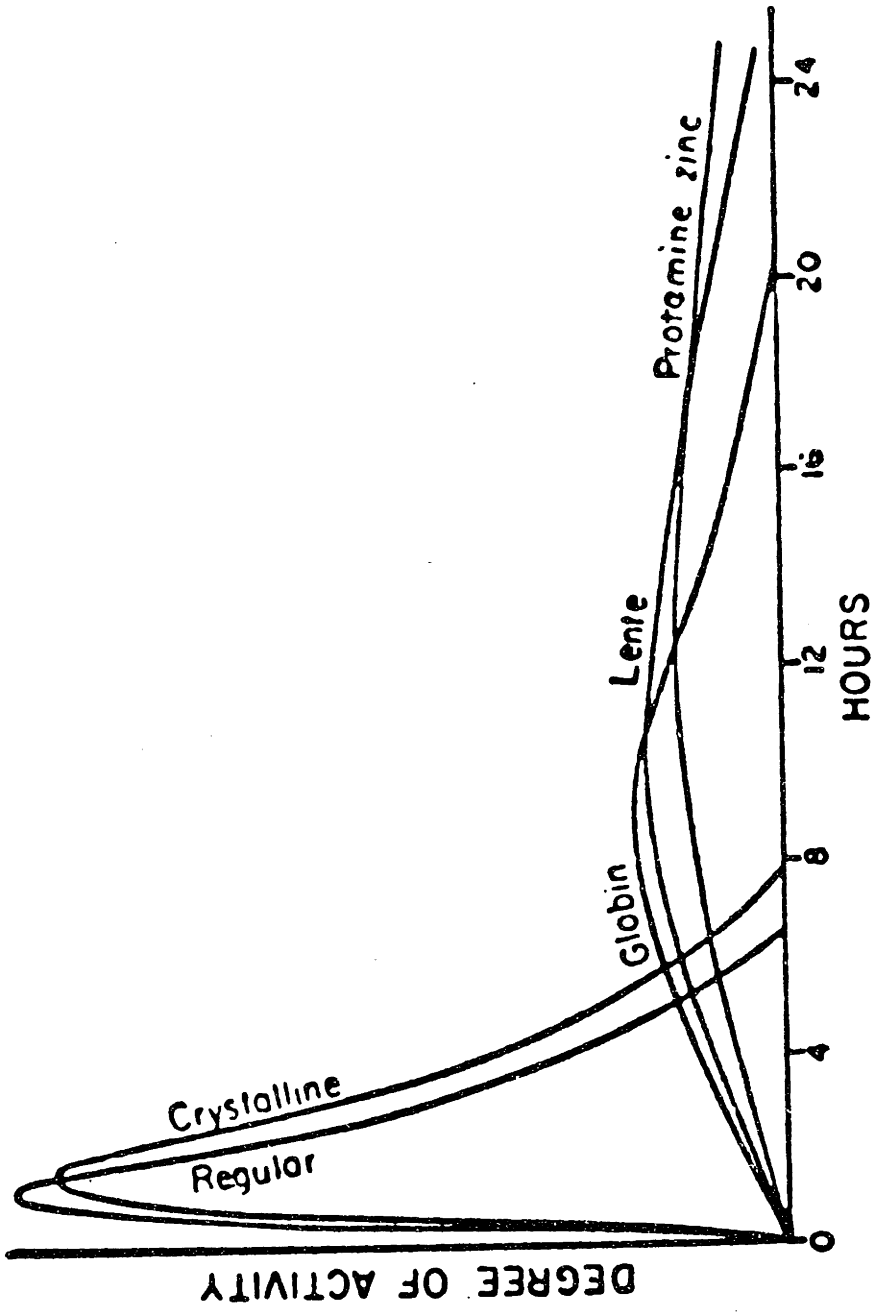

Figure 5

Properties of different preparations on insulin following subcutaneous injection (from Guyton, 1961).

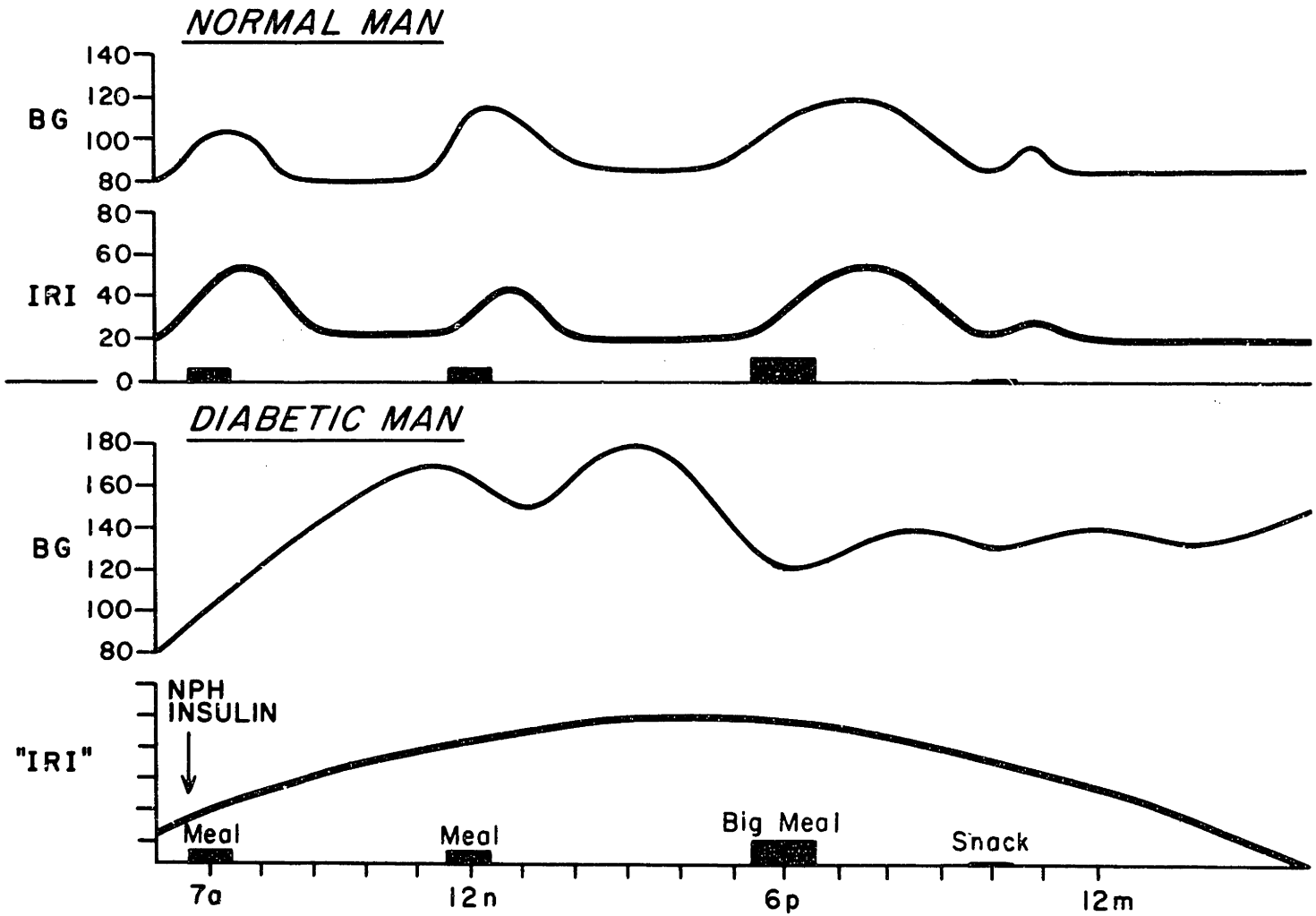

Figure 6

Blood glucose and serum insulin patterns contrasting a stylized normal man to a diabetic treated with intermediate acting (NPH) insulin (from Soeldner et al, 1973).

received a renal allograft. Small quantities of islet tissue were transplanted intramuscularly, intraperitoneally, or into the portal vein. Although no rejection of the previously transplanted kidneys occurred and there were no complications of the islet transplant, none of the patients were cured of diabetes. The researchers hypothesize two reasons for this failure: 1) a critical mass of islet cells must be transplanted to cure diabetes, and 2) that greater attention must be taken to prevent a rejection response.

Chick et al (1975) have proposed an approach based on the observation that protection of grafted cells with artificial membranes prevents immune rejection. The devices consist of beta cells grown on the outside of bundles of hollow fibers (See Fig. 7). The fibers are permeable to both insulin and glucose, but essentially impermeable to larger molecules such as gamma globulin. The results indicate that beta cells could be successfully cultured on these fibers and that the quantity of insulin released could be modulated by altering the glucose concentration in the perfusate (See Fig. 8). However, a major problem in designing the device, which is to be implanted as a shunt in a vascular system, is that of biocompatibility with respect to blood clotting. In addition, a larger device than is presently available is necessary to release insulin within the range estimated for human daily insulin requirements, which is approximately 20 units.

The development of an electromechanical pancreas has been proposed by Soeldner et al (1973) and Bessman (1972). A complete electromechanical system would have to contain the following elements (See Fig. 9): 1) a program that expresses the rate and duration of insulin release to

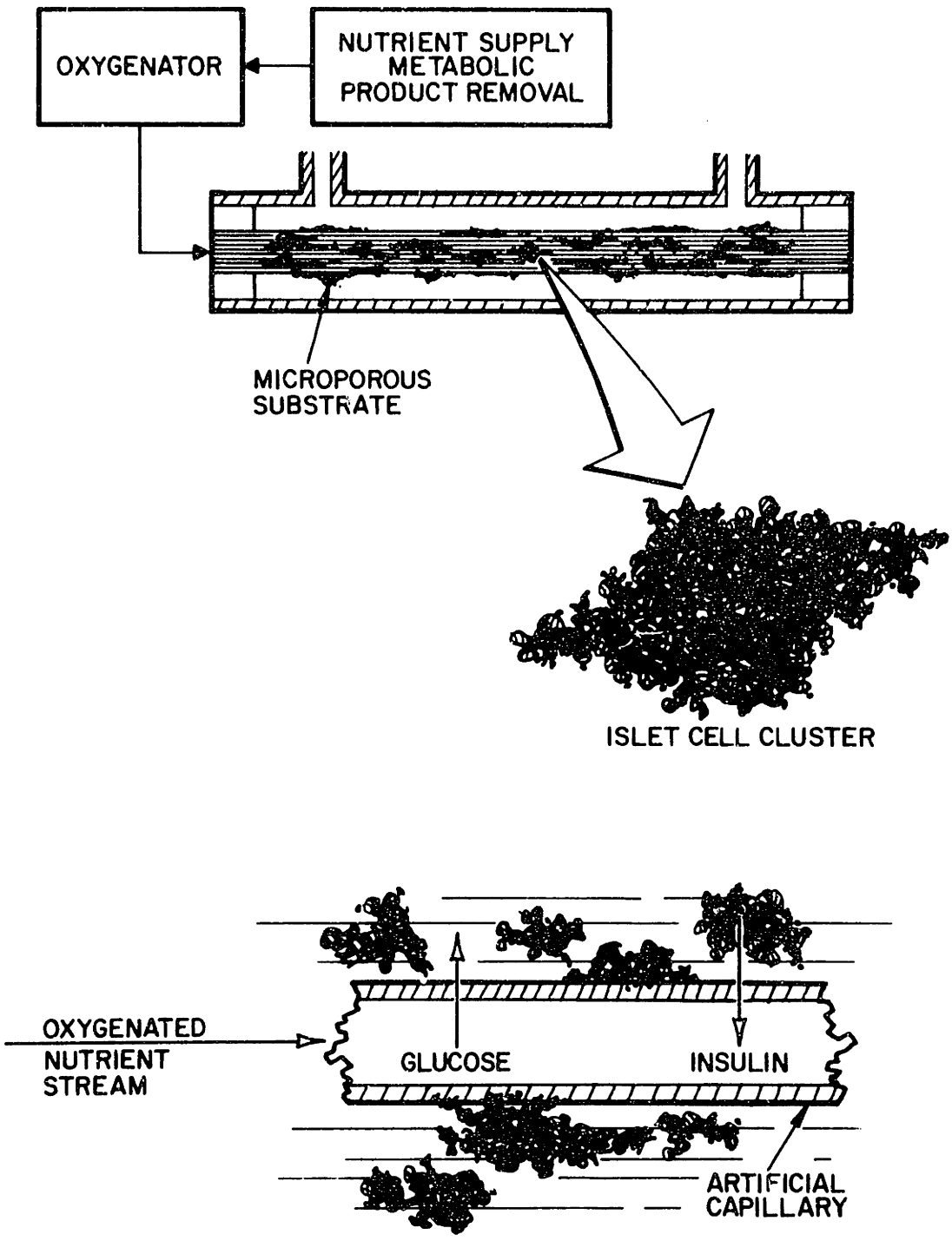

Figure 7

Beta cell culture on hollow fibers (from Chick et al, 1975).

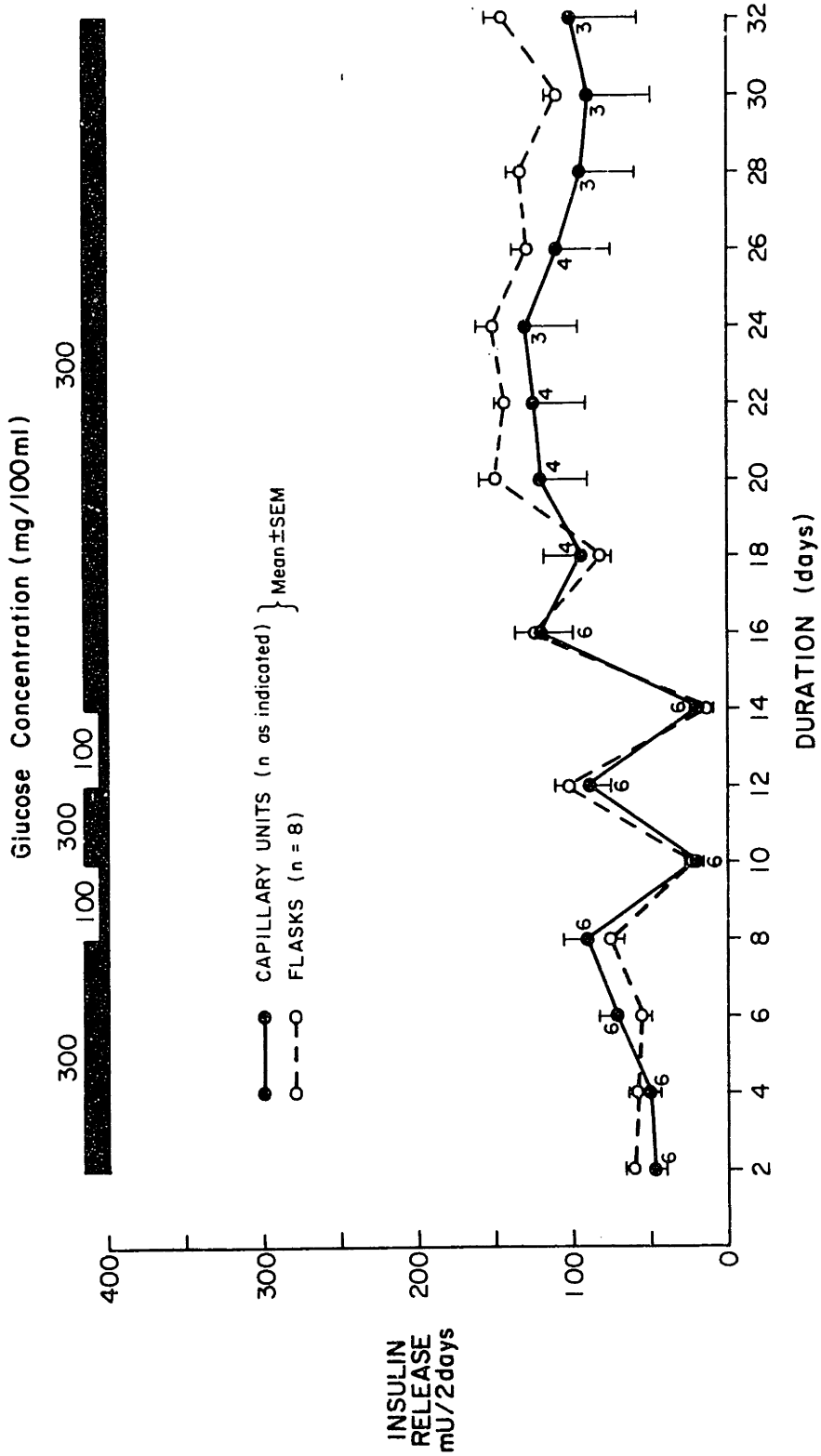

Figure 8

Insulin released into the medium for a representative unit consisting of 100 small bore (200 U I.V.). (from Chick et al, 1975).

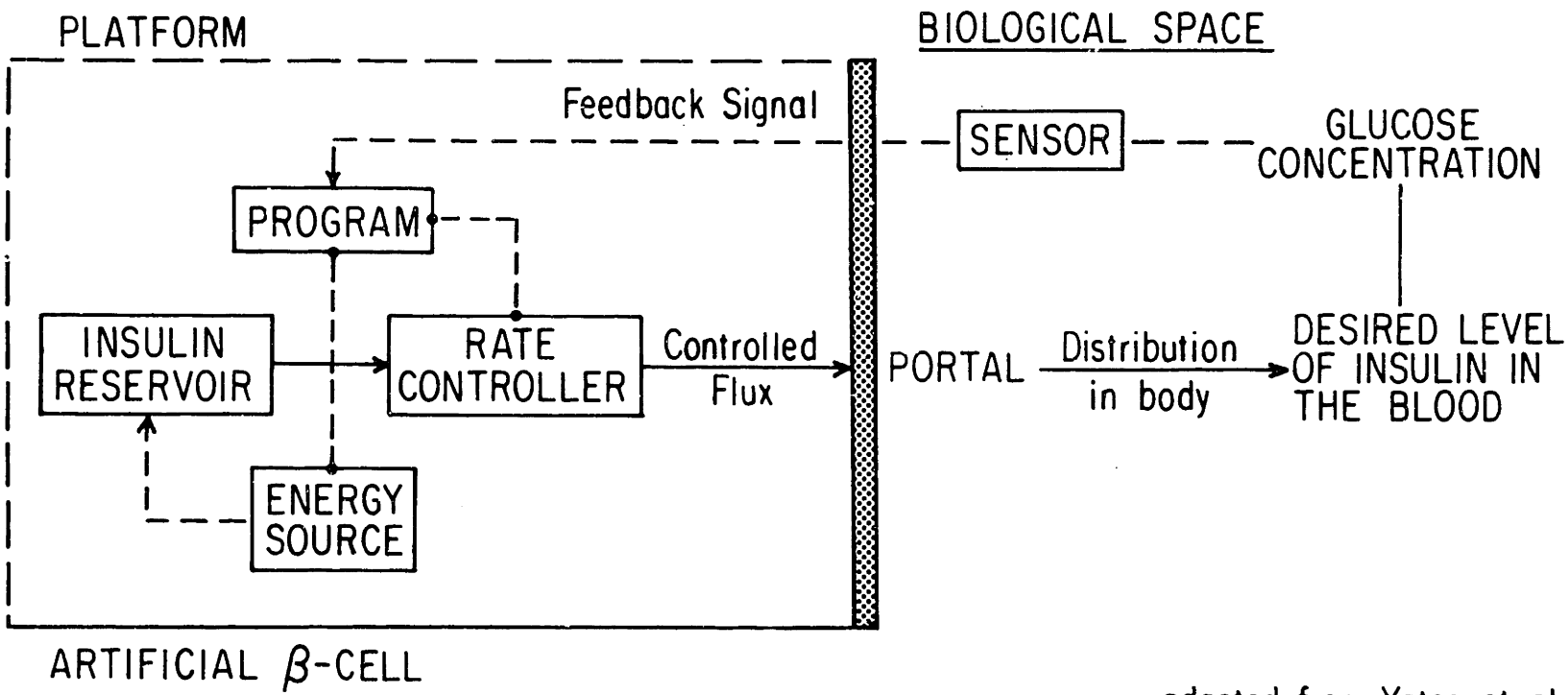

Figure 9

Schematic representation of the components
of an artificial pancreas (adapted from Yates et al, 1975).

maintain glucose levels within normal bands, 2) an insulin reservoir whose function is to store enough insulin for execution of the program and to protect it from interaction with the body, 3) a rate controller that establishes and maintains the prescribed pattern of insulin administration, 4) an energy source that effects the transfer of insulin from the reservoir to the delivery portal, 5) a delivery portal through which the insulin leaves, and 6) a glucose sensor which provides information to the program so it can adjust the pattern of administration. In order to demonstrate the feasibility of an electromechanical pancreas in normalizing blood glucose levels in diabetics, Albisser et al (1974) and Pfeiffer et al (1976) have developed a system consisting of a modified glucose analyzer, a minicomputer, and a set of infusion pumps. Fig. 10 shows Albisser's system, which illustrates the basic design of both systems. Mirouze et al (1977) have developed a similar system with the exception that the minicomputer is replaced by a set of potentiometers which control an insulin infusion pump (See Fig. 11). The control algorithms used in each system will be discussed in a later section. These electromechanical systems are capable of establishing and maintaining normoglycemia in diabetic subjects while restoring glucose tolerance. Insulin secretion patterns, both in pancreatectomized dogs given glucose infusion and in labile human diabetics given usual meals and snacks are shown in Figs. 12 and 13. The large size of the current systems clearly limits their use to physiologic research and clinical investigation.

Other investigators have proposed methods for the control of glycemia without the sophistication of feedback regulation. It is not clear whether these simpler methods would be adequate. Service et al (1970)

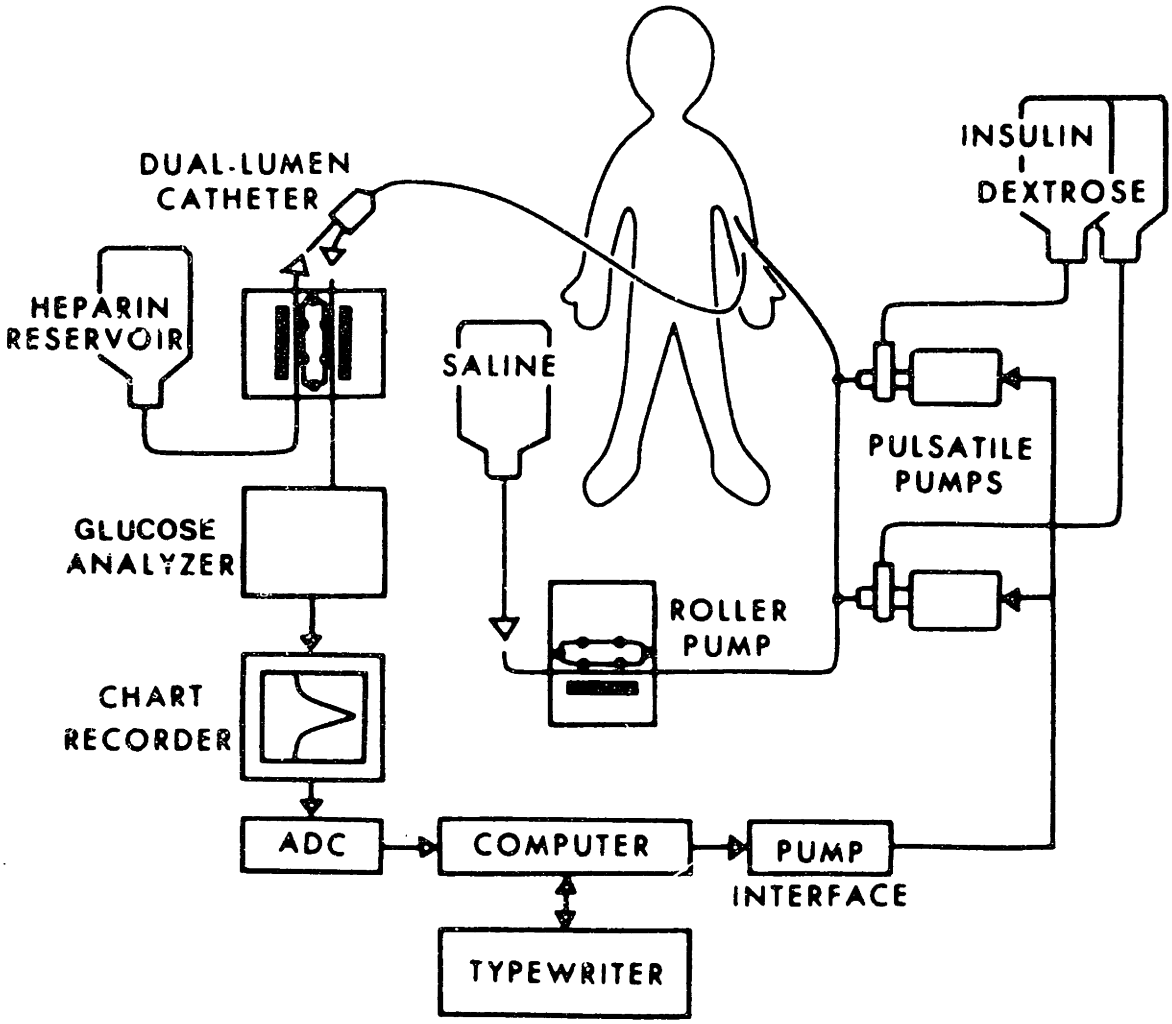

Figure 10

Schematic diagram of apparatus used for monitoring and automatic regulation of blood sugar (from Albisser et al, 1974).

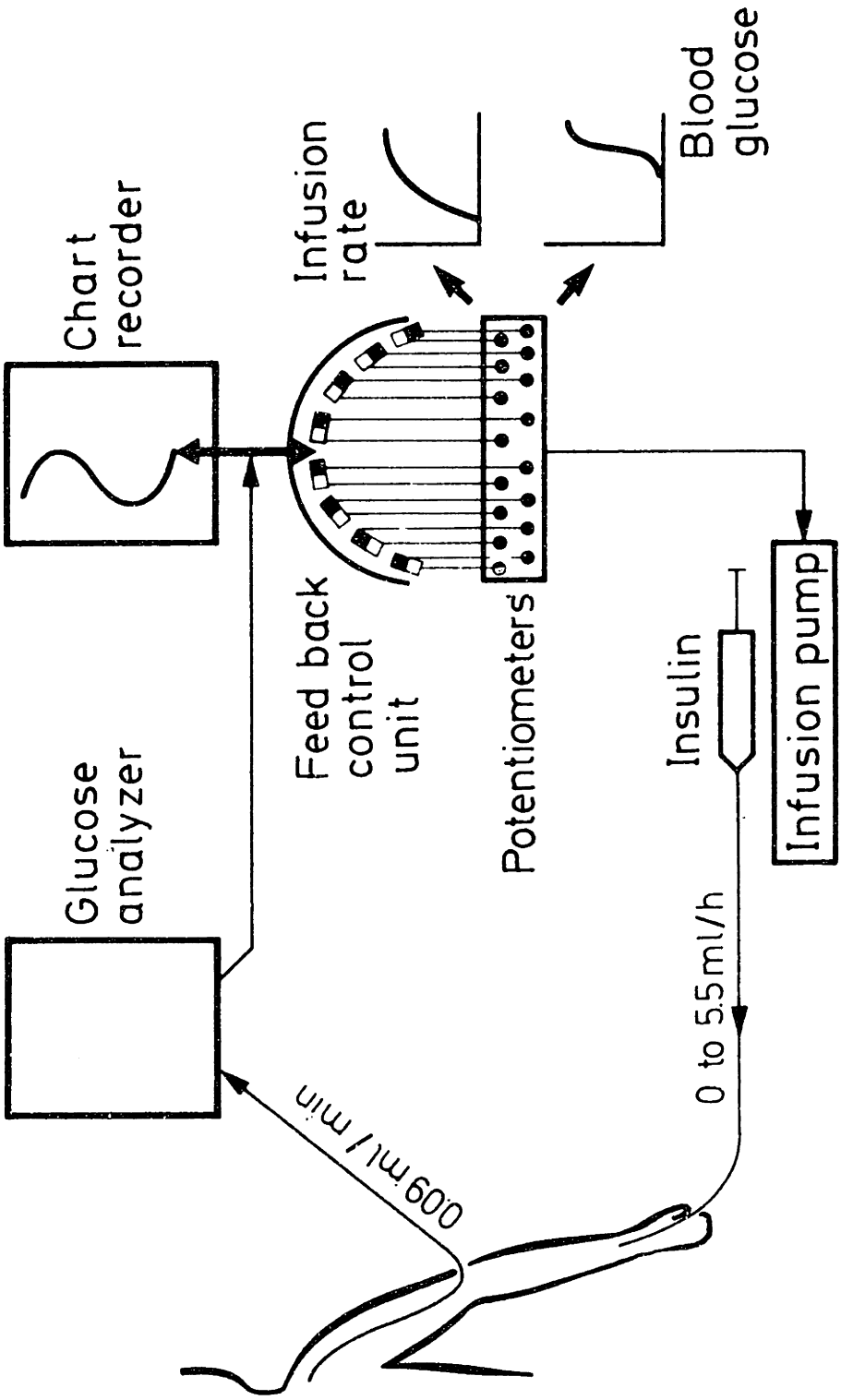

Figure 11

Apparatus used for the automatic regulation of blood glucose (from Mirouze et al, 1977).

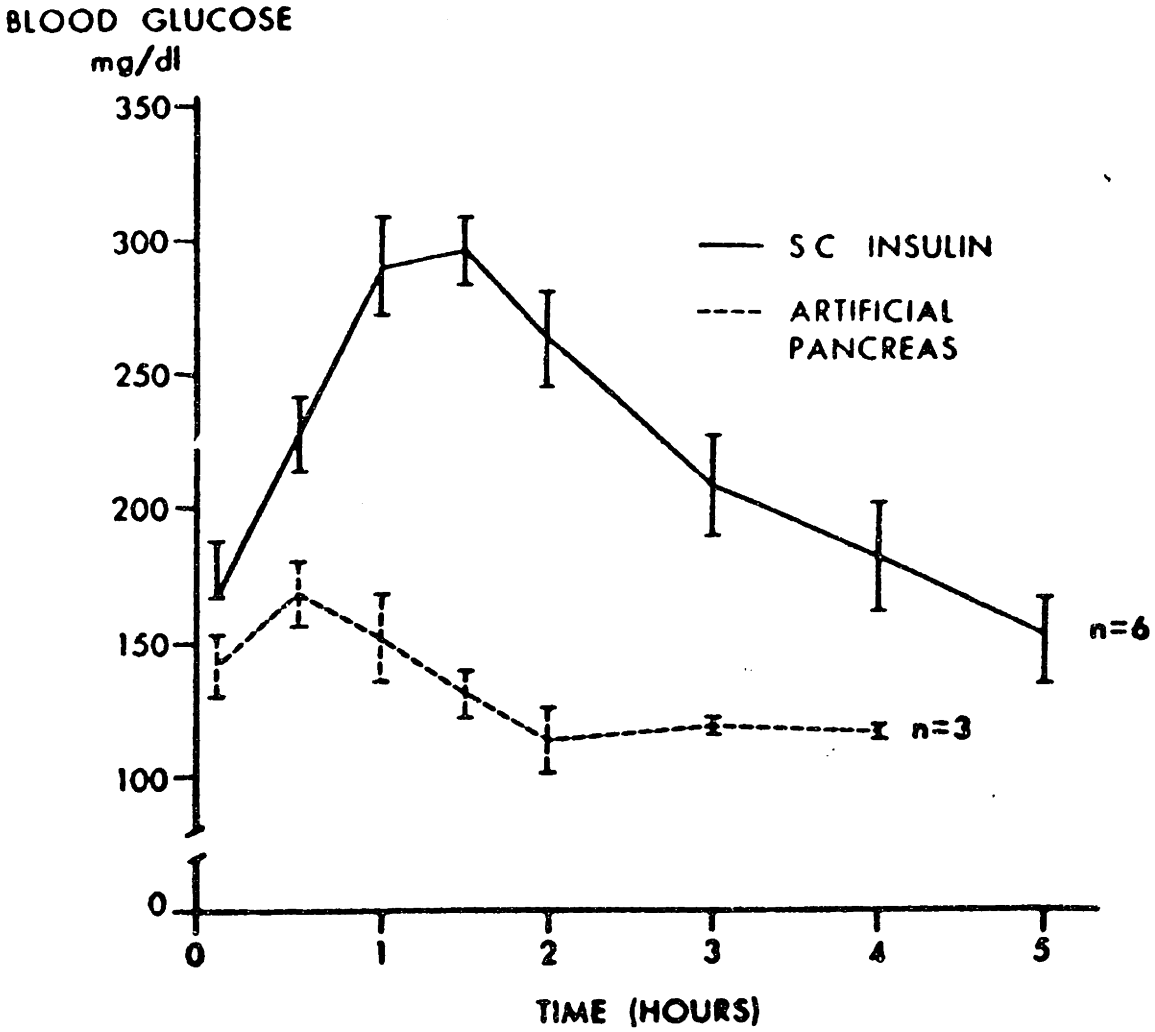

Figure 12

The mean glucose concentrations during an oral glucose tolerance test in diabetics given subcutaneous (S.C.) insulin and controlled by the artificial pancreas (from Albisser et al, 1977).

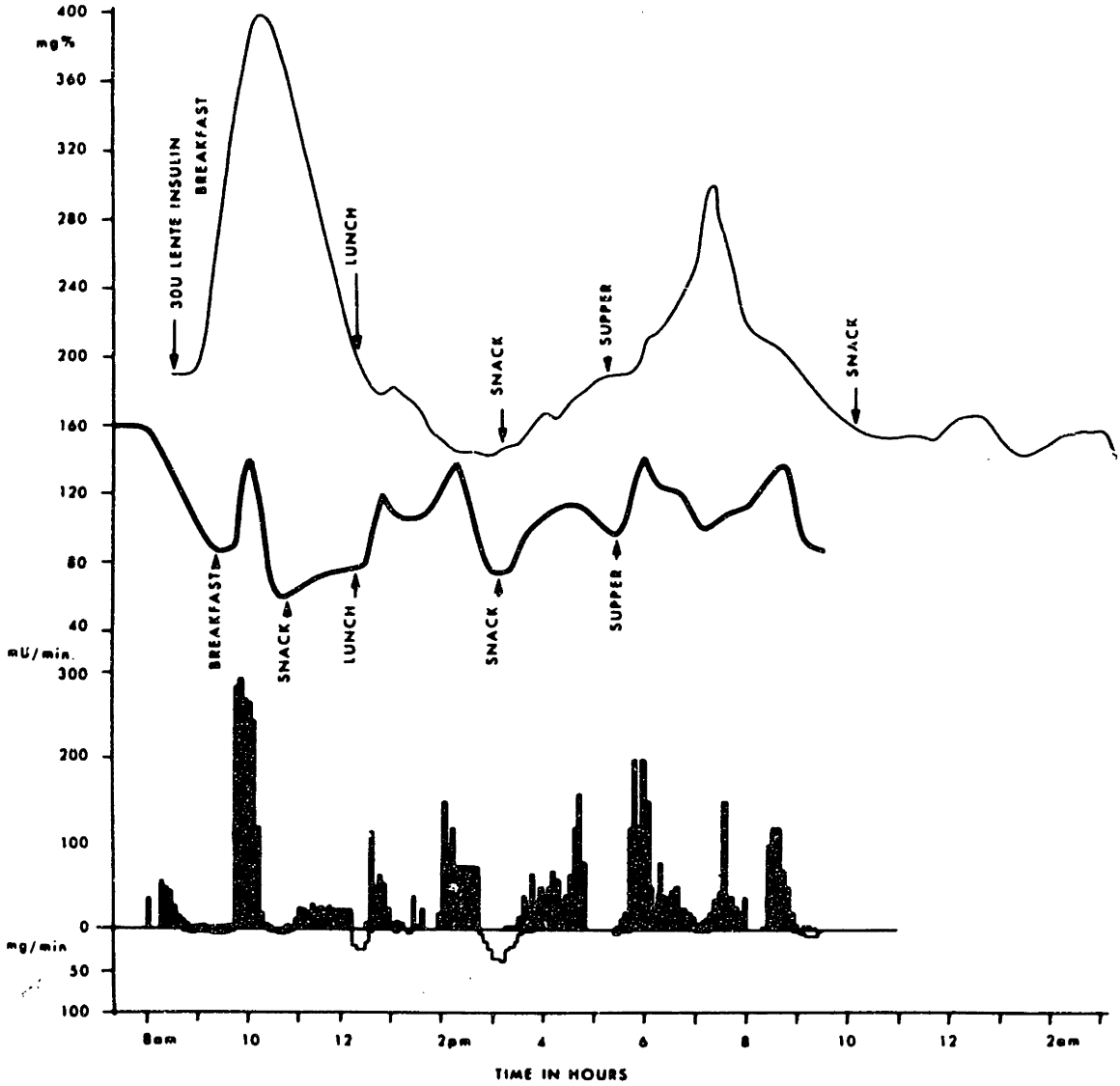

Figure 13

Continuous blood glucose profiles in diabetics sustained by subcutaneous insulin (top curve) and regulated by artificial pancreas (center curve). Infusion patterns (histogram) of insulin (black bars) and dextrose (white) (from Albisser et al, 1974).

administered four insulin injections subcutaneously daily to "unstable diabetics" but still found marked fluctuations. Slama et al (1974) used constant intravenous insulin infusions of 1.5 U/hr with increases to 20 U/hr for 20 to 30 minutes at the start of each meal, for a period of one to five days. With this type of regimen, diurnal mean blood glucose levels ranged from 56 to 138 mg/dl, compared to levels of 46 to 158 mg/dl when the same subjects received multiple subcutaneous injections.

Genuth and Martin (1977) developed a pre-programmed intravenous insulin delivery system that provided five-hour pulses of insulin with each meal such that a normal diurnal pattern of insulin was attained. Each pulse was designed to elevate insulin concentrations five to tenfold above basal at its peak which occurred 45 minutes after the onset of each pulse (See Fig. 14). Between meals and during overnight fasting, a constant basal rate of insulin was maintained. Fig. 15 shows the glucose levels during the course of a day. Plasma glucose was maintained within a range of 66 to 125 mg/dl. This represents a feasible approach, although the potential for overdosing a patient exists in this open-loop control system.

In addition to the question of the temporal pattern of administration of insulin, there is the question of the site of administration of insulin (Felig, 1974a). The pancreas releases insulin into the portal vein. Under physiologic circumstances the concentrations of insulin in the portal vein is three to ten times greater than in peripheral blood (Blackard and Nelson, 1970). This portal-peripheral gradient may account for the fact that the liver is the main storage site for action. In normal man, the major portion of a 100 gm oral glucose load is retained

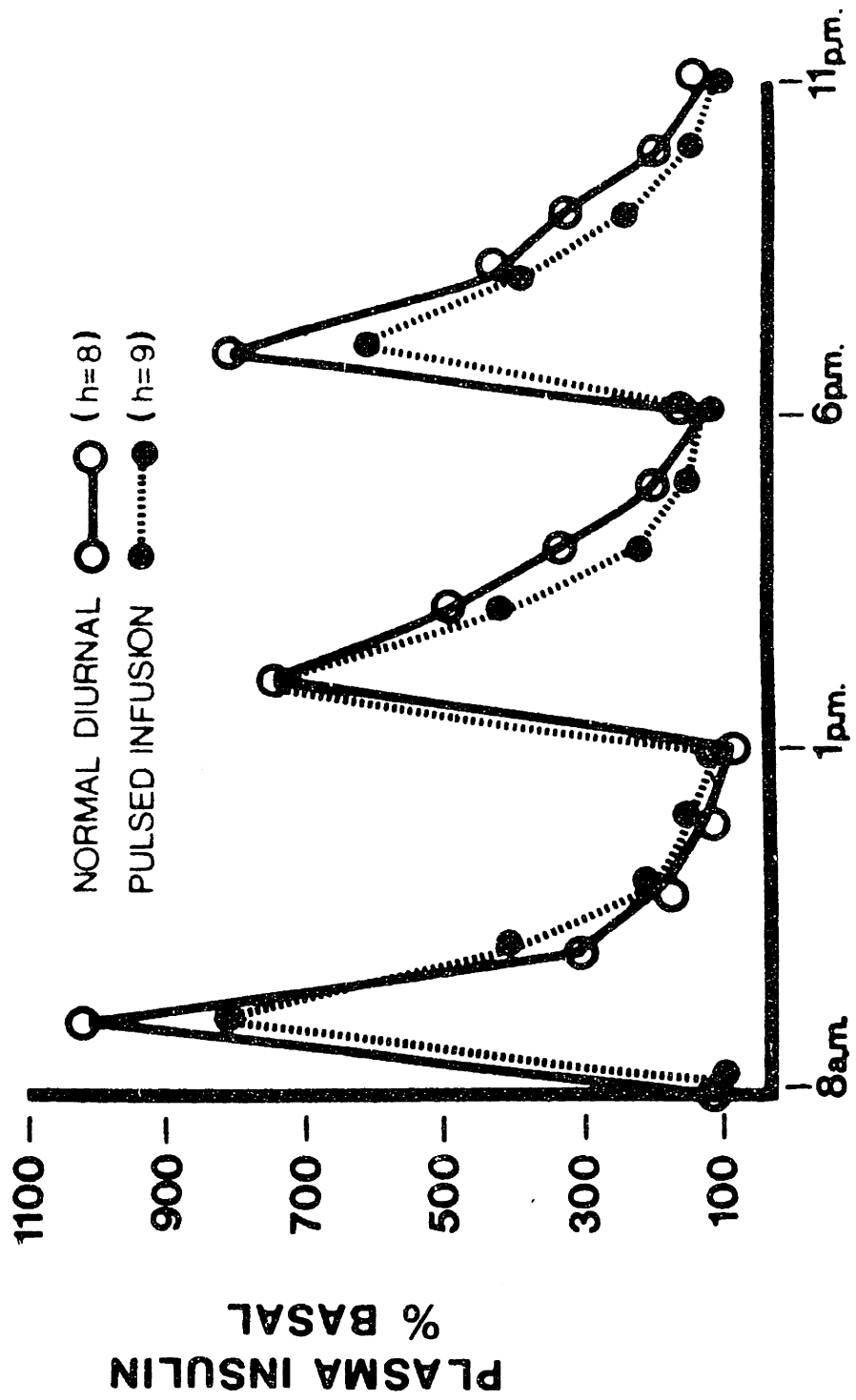

Figure 14

Plasma insulin in nine diabetic subjects during continuous treatment with the pulsed insulin-delivery system (closed circle) compared with plasma insulin in eight normal subjects receiving identical meals at 8:00 a.m., 1:00 p.m., and 6:00 p.m. (from Genuth and Martin, 1977).

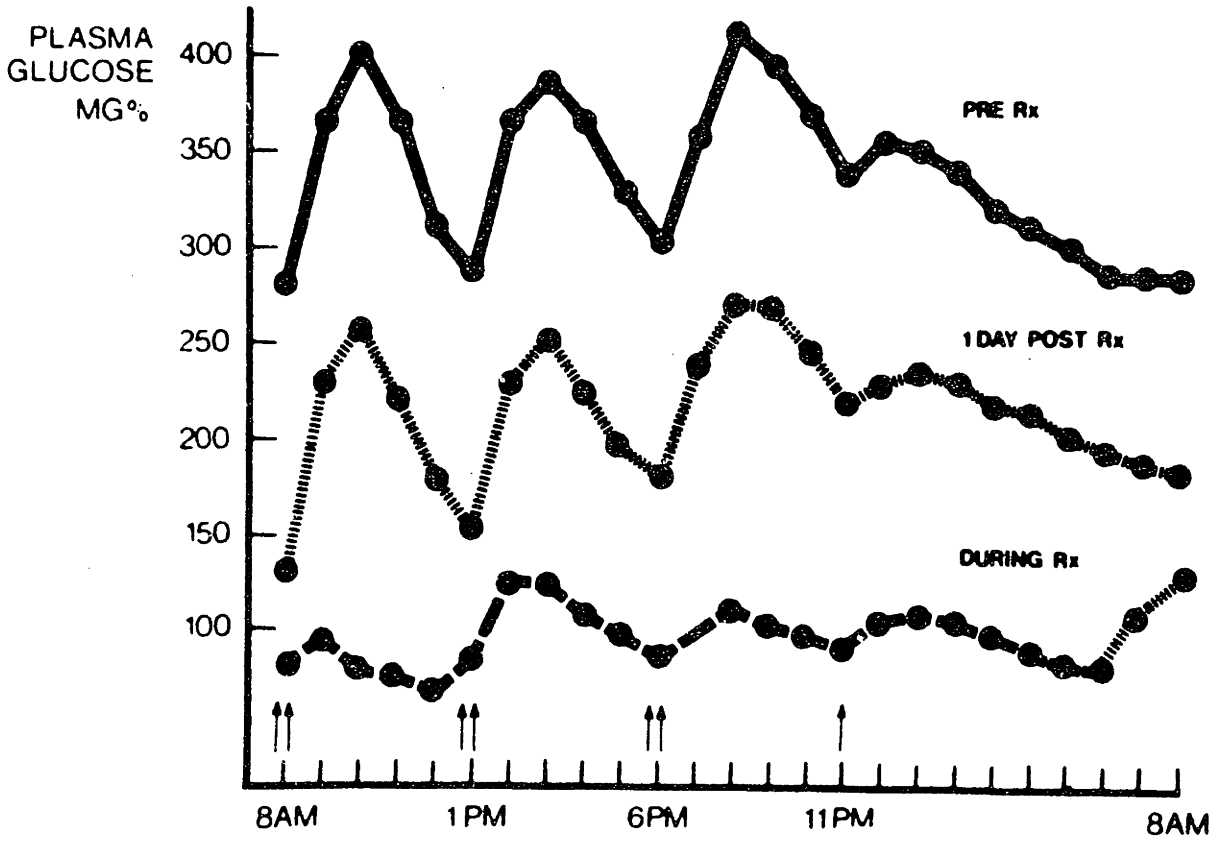

Figure 15

Mean plasma glucose in nine diabetic subjects prior to treatment (solid line), during pulsed insulin delivery (interrupted line), and during the first day of treatment (hatched line) (from Genuth and Martin, 1977).

by the liver whereas only 15 percent is utilized by fat and muscle tissue (Felig et al, 1974b). However, in insulin-deficient diabetics, uptake of glucose by the liver is decreased and glucose production pathways (gluconeogenesis) are stimulated (Wahren et al, 1972). Thus, optimal normalization of diabetics may require restoration of peripheral-portal gradients to achieve the proper balance between hepatic and peripheral effects of glucose. This hypothesis is supported by the observation that transplantation of pancreatic islets to the thigh or peritoneum of inbred diabetic rats reduces hypoglycemia but fails to restore blood glucose to normal (Ballinger and Lacy, 1972). Complete normalization is obtained when the islet cells are transplanted in the portal vein (Kemp et al, 1973).

However, portal and peripheral infusions have been found to be equally good in experiments in dogs by Botz et al (1976) and in the only direct comparison in unanesthesized man by Erwald et al (1974). Botz et al, infused intra-portal glucose at a rate of 10 mg/kg/min for 60 minutes in anesthesized normal and pancreatectomized dogs. During computer-controlled insulin administration, normal glucose tolerance was restored by both portal and peripheral rates of insulin delivery. In addition, there were no significant differences in peripheral glycemic patterns, peripheral insulin levels, and total insulin requirements between the two rates. Erwald et al infused insulin at a rate of 0.05 U/kg for 30 minutes into the portal vein and antecubital vein (i.e. peripheral) of several normal unanesthesized subjects. They found that insulin infusions at either site resulted in the same degree of hypoglycemia in peripheral venous blood.

A final point for consideration is that diabetics receiving insulin develop anti-insulin antibodies which may render exogenous insulin variably inactive in different individuals or the same individuals at different times (Pfeiffer, 1976). Until this effect is quantitated, it is difficult to compare experiments in pancreatectomized animals and diabetics receiving insulin for the first time with diabetics who have taken insulin for long periods of time.

III. RELEVANT PHYSIOLOGY OF GLUCOSE HOMEOSTASIS

A. Physiological Role Of Insulin

Glucose homeostasis involves the regulation of glucose utilization and production. Man can maintain mixed venous glucose concentrations within the limits of 60-120 mg/dl during the course of a day. Although there are numerous control mechanisms to insure this regulation, insulin appears to be the dominant hormone involved (Cahill 1971). Cahill (1976c) has termed insulin man's "fed" signal since after a meal insulin levels rise signaling the body's tissue to take up and store fuel not necessary for metabolic needs. In contrast, a low level of insulin, such as occurs during fasting, tells the body that no fuels are entering and the body's storage sites should be released back into the blood.

Fig. 16 shows the fuel utilization of a typical man, during a fast of at least 12 hours. In the fasted state, liver glucose production is about 125-150 mg/min or 180-220 gm/hr (Cahill and Owen 1968). Liver in normal man contains only 75 grams of glucose stored as glycogen. Between meals, glucose levels can be maintained by glycogenolysis (Nilsson et al 1973) but during more prolonged periods of caloric deprivation hepatic gluconeogenesis must be initiated to maintain adequate glucose concentrations. The main substrates needed by liver to maintain gluconeogenesis are amino acids derived from muscle protein. Glycerol, from triglyceride lypolysis in adipose tissue and lactate and pyruvate from glycolytic tissue (Cori Cycle) provide the other source. The signal which initiates these processes is a drop in circulating insulin levels to an average basal

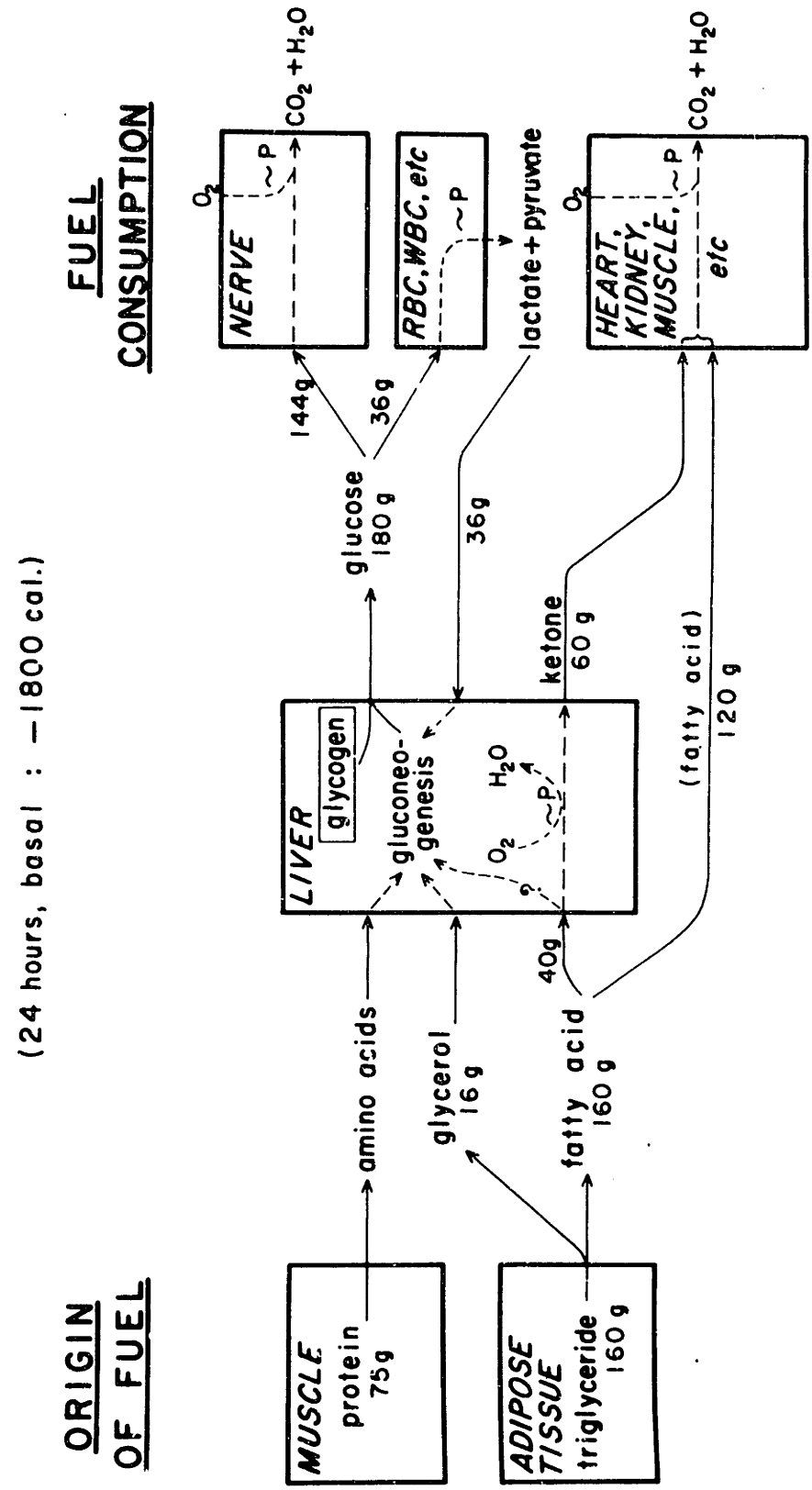

Figure 16

Daily substrate flow in a normal fasted man (from Cahill, 1971).

level of 10 μU/ml. The central nervous system utilizes about 140 grams of glucose per day. The remaining fraction is utilized by tissues such as red blood cells, bone marrow, renal medulla, peripheral tissue, platelets, and leucocytes (Cahill et al 1966).

The fuel requirements of heart, liver, renal cortex, and skeletal muscle during fasting are all satisfied by free fatty acid metabolism. The longer chain free fatty acids derived from adipose tissue are partially oxidized to acetyl CoA. They are then condensed and released by the liver as the ketone bodies, acetoacetate and β-hydroxybutyrate. Ketone bodies are utilized by muscle as fuel and their rate of production by liver closely approximates their usage (Owen and Reichard 1971). This permits less gluconeogenesis and less catabolism of muscle protein. Fig. 17 shows the sequence of metabolic events that occur during fasting.

After a meal, an increase in insulin levels initiates a series of metabolic events in liver (Madison 1969) and peripheral tissue (Morgan et al 1961) depending on the degree of increase. If the meal is small, or glucose is infused at low rates, the metabolic effect of an increase in insulin is to suppress the basal rate of liver glucose production needed to satisfy the requirements of the brain. Glucose, given at 100 gm/min closely approximates the energy needs of the brain for gluconeogenesis or glycogenolysis (Exton 1972). (At blood glucose concentrations of 120 mg/dl the liver shows no net release or uptake of glucose). The body shuts off the liver by increasing the circulating insulin concentrations to approximately 25 μU/ml. This concentration of insulin is not enough to allow muscle and adipose cell uptake of glucose.

When glucose is administered at rates greater than needed to supply the brain, the glucose concentration stimulates a higher insulin concentration.

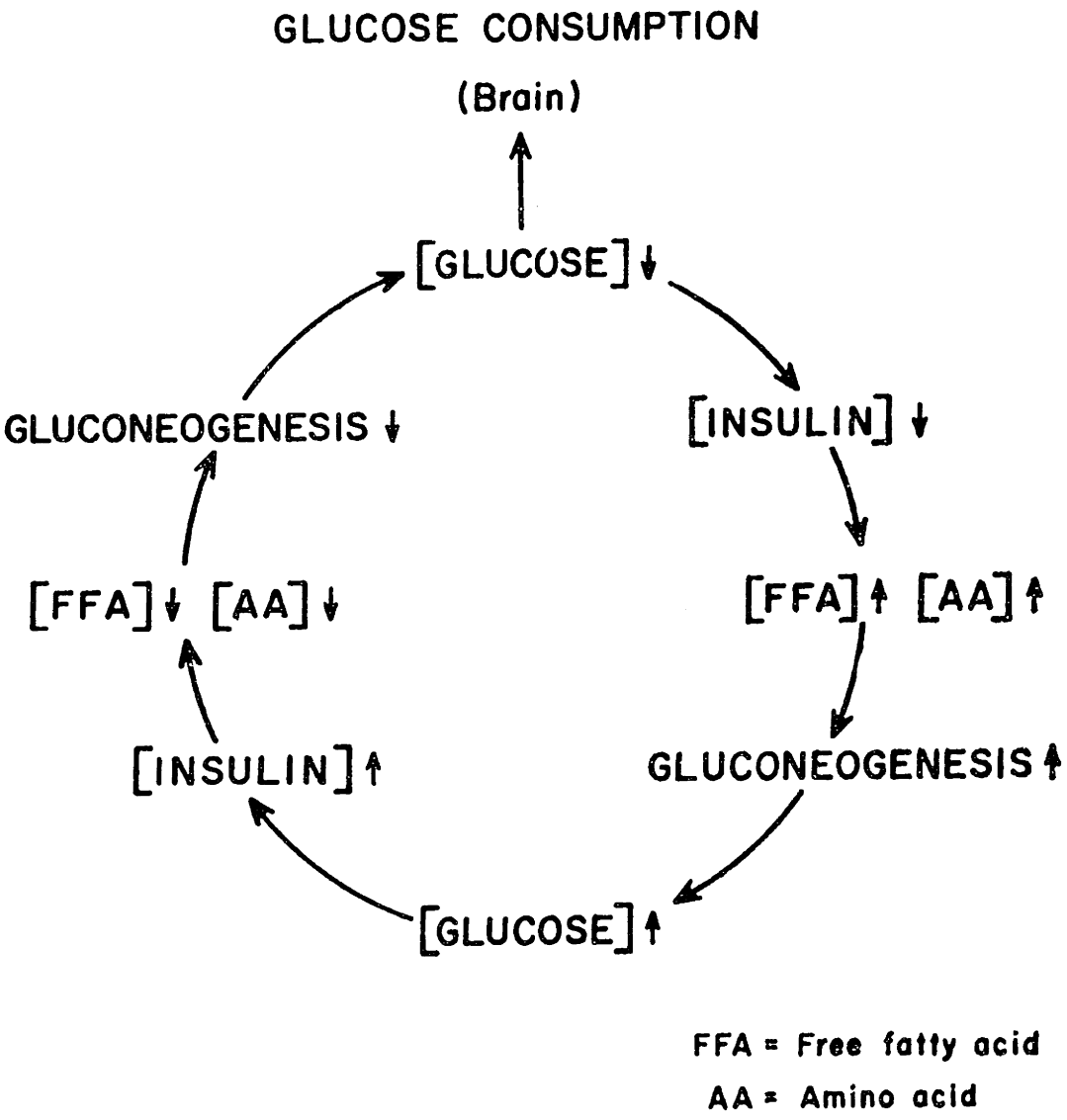

Figure 17

Cycle of glucose homeostasis in a fasting man after liver glycogen has been depleted (from Cahill, 1974).

For example, if glucose is given intravenously at a rate of 300 mg/min, the insulin levels rise to approximately 75 μU/ml (O'Connell et al 1974). Muscle and other tissues utilize glucose, and fatty acid levels fall due to the suppression of their release from adipose tissue. Fig. 18 shows the fuel utilization following a hypothetical mixed meal. Glucose, galactose, and fructose are phosphorylated by the liver and incorporated into glycogen or metabolized for its own energy needs by fat synthesis. In muscle, glucose is also phosphorylated and used for glycogen synthesis about 7-8 minutes after the rise in insulin (Neely and Morgan 1974). Glucose is also metabolized to lactate or pyruvate to meet the muscle's energy needs. If the glucose concentration in the plasma exceeds 200 mg/dl the renal absorption capacity is exceeded and glucose is secreted into urine (Robinson 1967).

The amino acids ingested are taken up directly by tissues, especially muscle (Mortimore 1972). Insulin has been demonstrated to increase the transfer of certain amino acids across the muscle membrane. Insulin also acts on muscle to increase protein synthesis inside the cell, the net effect being increased muscle protein.

The fat or triglycerides absorbed are partially hydrolyzed in the gut lumen and absorbed by the mucosa, where the triglycerides are resynthesized and incorporated into particles or chylomicrons. Most of the chylomicrons are taken up by adipose tissue (Avruch et al 1972). A high concentration of insulin is necessary for this to occur.

In summary, the plasma glucose concentration of normal man is regulated within a narrow zone above the minimum required by brain, but well below that saturating the renal absorption capacity. Insulin plays

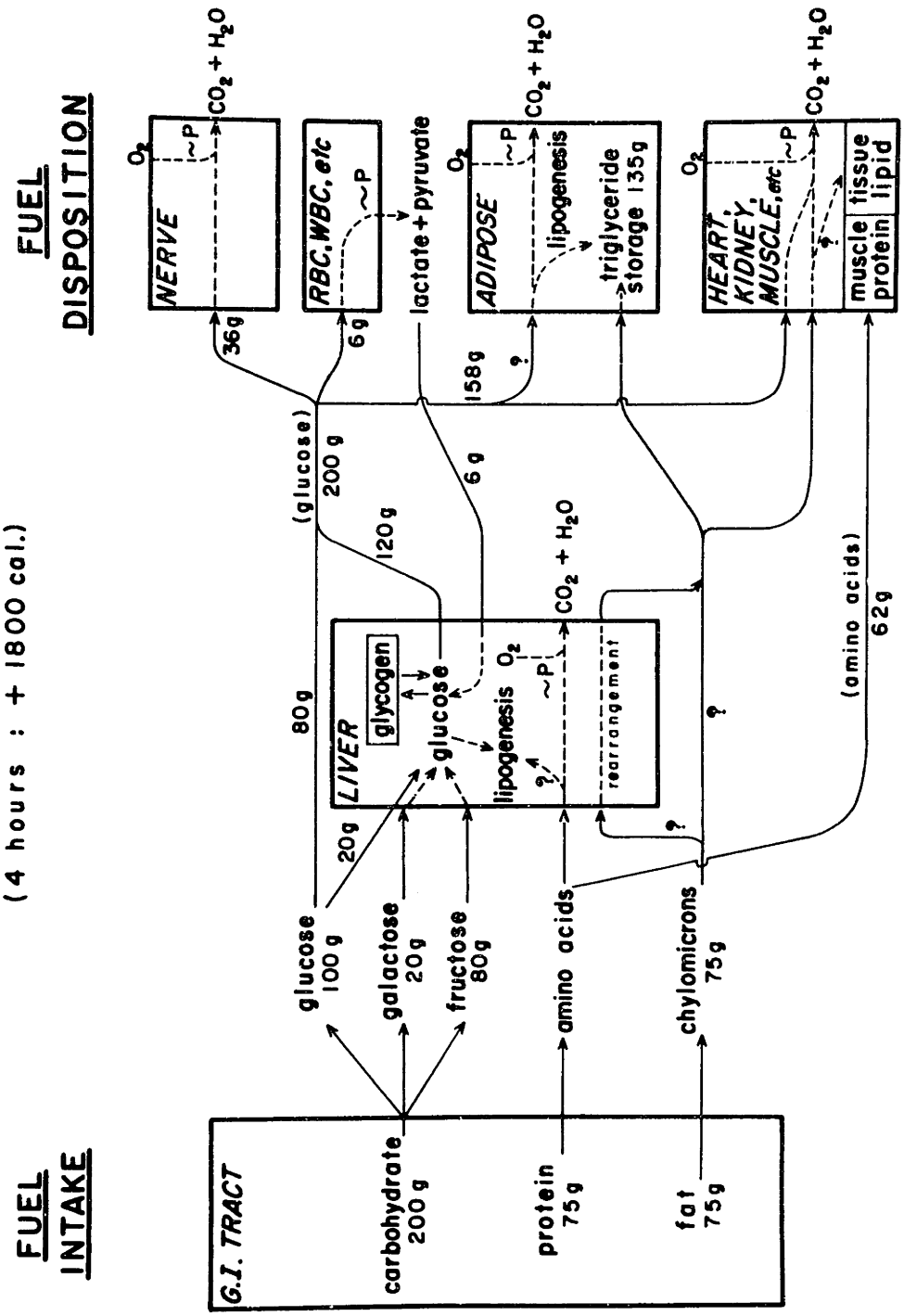

Figure 18

Substrate flux following a mixed meal consisting of carbohydrates, amino acids and lipids (Courtesy of G. F. Cahill, Jr.).

the dominant role in maintaining glucose in this range. Fig. 19 shows the spectrum of glucose metabolism modulated by insulin. All tissues are capable of utilizing glucose, and do so when ample levels are present in the diet (when the blood insulin is high). However, most tissues, especially fat and muscle, do not utilize glucose when insulin levels are low. Instead, they consume fat in the form of free fatty acids released from adipose tissue.

B. Insulin Synthesis And Secretion

Insulin synthesis occurs within the beta cell of the pancreas. As shown in Fig. 20, its synthesis begins on the ribosomes of the rough endoplasmic recticulum (RER). Insulin is formed as a single-chain polypeptide, proinsulin. The conversion of proinsulin to insulin occurs by proteolytic cleavage which reduces it from a protein of molecular weight 9000 to two amino acid chains, insulin (m.w. 6000) and "connecting" peptide (m.w. 3000). This conversion occurs at the time of the transport of proinsulin to the Golgi apparatus where it is packaged into granules. Insulin is then complexed with zinc and stored. Beta cell granules are stored until a stimulus for insulin secretion such as glucose occurs. The early change in the release process is the movement of the beta cell granule to the plasma membrane of the beta cell. The walls of these granules fuse with the plasma membrane of the beta cell and rupture, which release the granules into the extracellular space. The granules rapidly disappear from the extracellular space, undergoing rapid dissolution. The entire process described above has been visualized using electron microscopy (Unger and Orci 1976).

The insulin release process from beta cells has been shown to require extracellular calcium (Lacy et al 1968). The rate of insulin

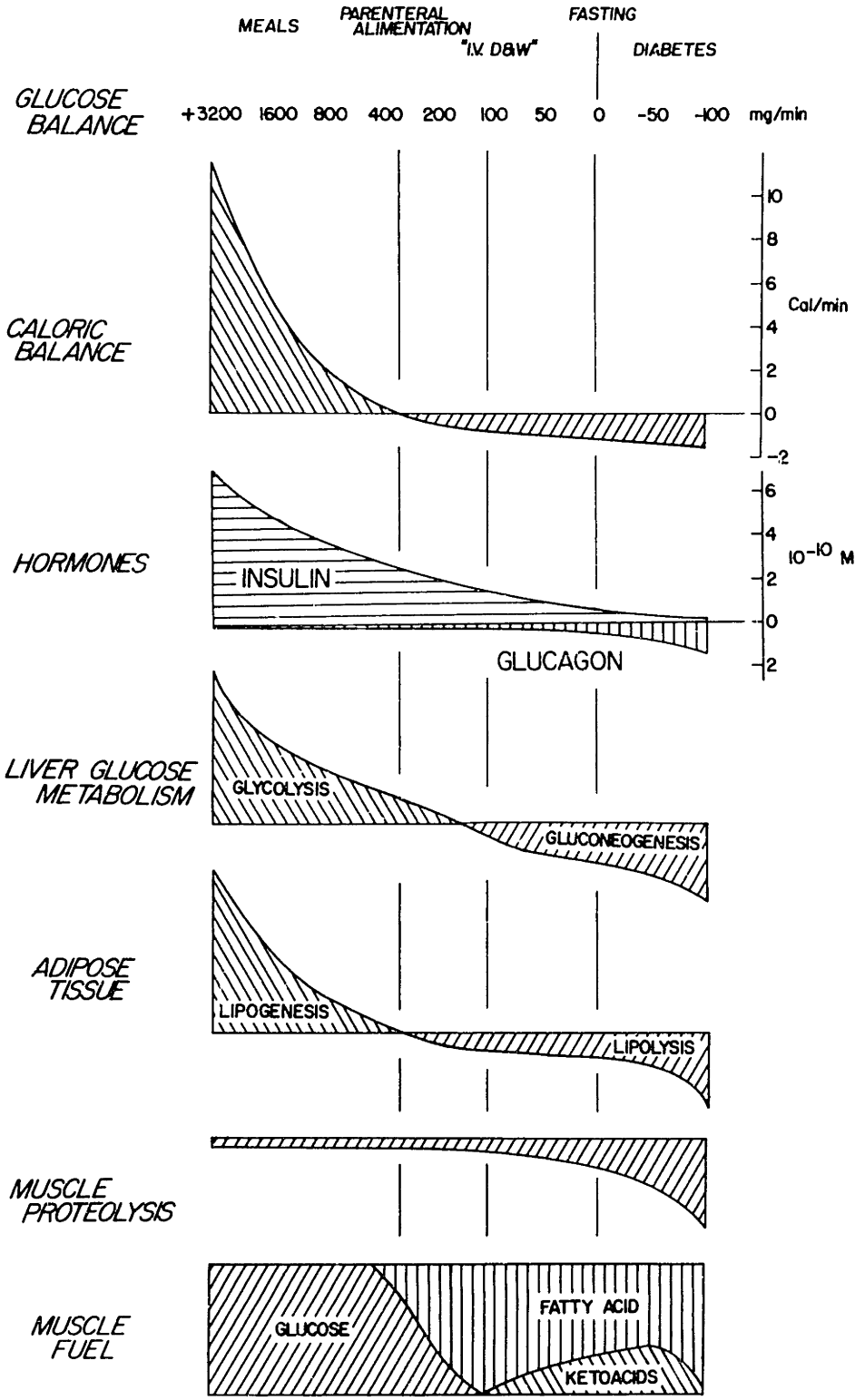

Figure 19

Spectrum of glucose metabolism, which ranges from (left to right) large glucose meals of 3 g/min, infusion of .2 to .5 g/min, infusion of dextrose and water at 0.1 g/min, and total fasting, to a net carbohydrate deficit as observed in diabetics

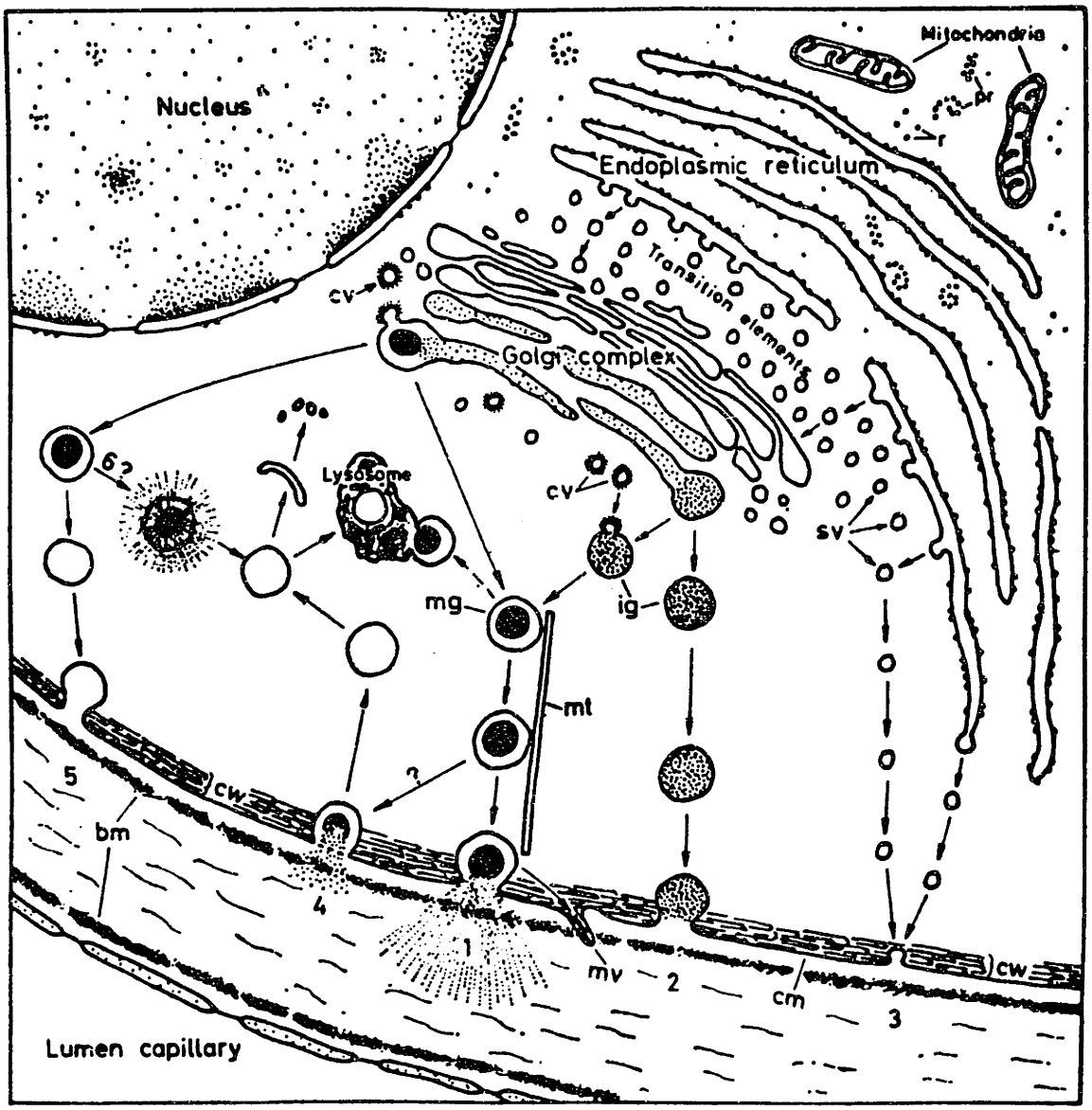

Figure 20

Diagrammatic representation of the morphologic events of the secretory process in an insulin-producing cell (from Renold, A. et al, 1971).

release following glucose administration is correlated with the rate of calcium uptake by the islet. Adenosine 3',5'-monophosphate (cAMP) also has a role in the release process. It appears that cAMP is an important intracellular regulator of insulin secretion and that it modulates the islet cell response to some other primary stimulant or depressant (Cerasi and Luft 1967). This modulation appears to be independent of calcium uptake by the cell. Lastly, ion fluxes may be important in the release of granules. Dean and Matthews (1970) were able to record action potentials in beta cells exposed to glucose, and the number of cells firing were dependent on glucose concentration. They concluded that action potential activity was related to calcium entry and extracellular sodium normally represses this influx.

Insulin release is controlled by the coordinated interaction of the availability of nutrient carbohydrates (amino acids and lipids), neural stimuli and hormones (e.g., intestinal hormones). The best studied and probably most important stimulus for insulin secretion is glucose. Glucose affects several beta cell processes. It increases proinsulin synthesis, Golgi activity, and granule formation as well as stimulating release of insulin granules. As seen in Fig. 21, little stimulation is produced by glucose concentrations below about 4 mmol/liter (72 mg/dl); above this threshold value the rate of release increases rapidly with glucose concentrations up to about 12 mmol/liter (480 mg/dl), and at greater concentrations reaches a plateau. Experiments with an isolated perfused rat pancreas preparation (Curry et al 1968) and in vivo (Porte and Pupo 1969) demonstrate that when the pancreas is presented with a sudden increase in glucose concentrations above 100 mg/dl, there is an

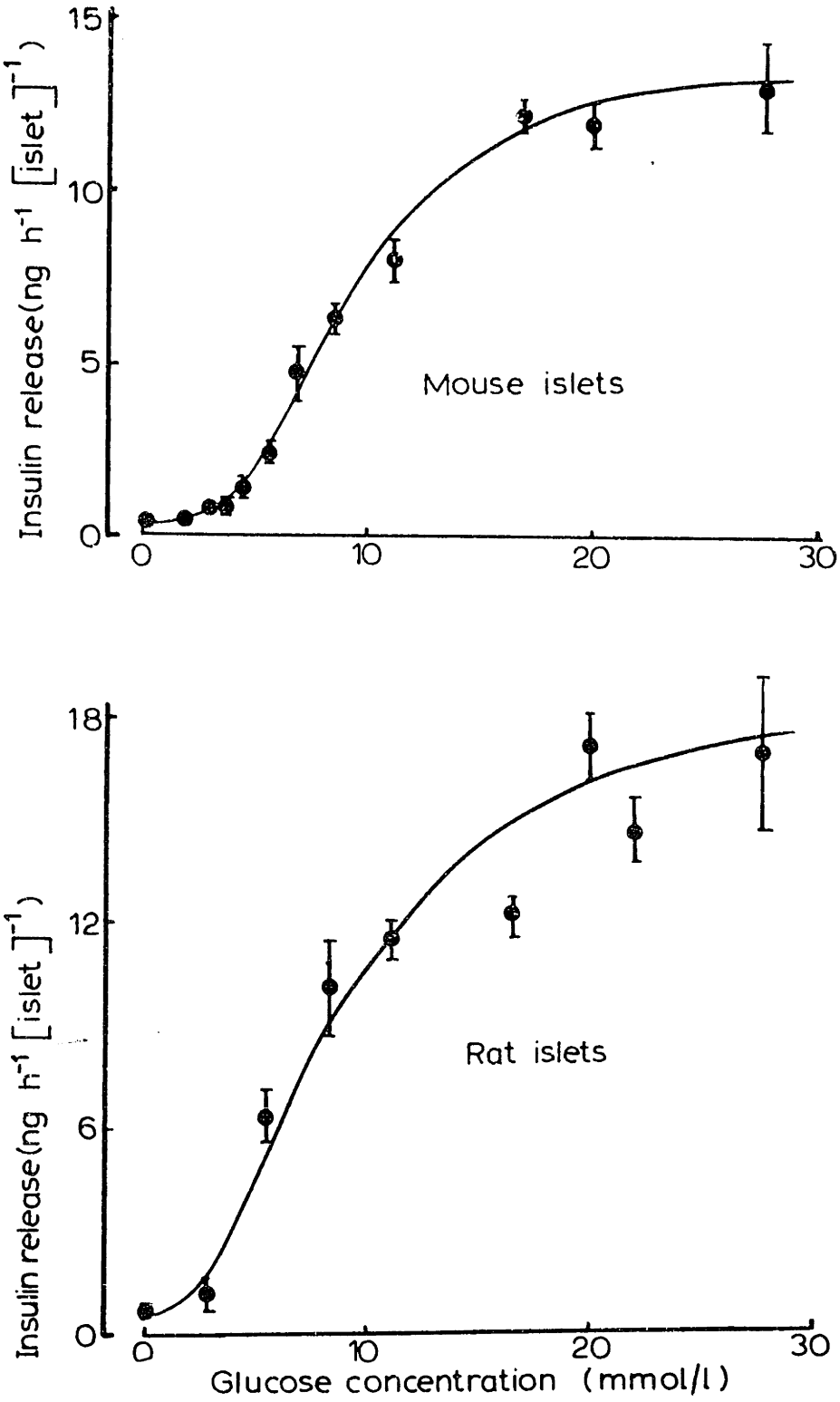

Figure 21

Effect of glucose on insulin release from mouse and rat islets (from Ashcroft, 1976).

insulin secretion (within 30 seconds) which rises and falls within 3-4 minutes. The amount of insulin released during the initial spike is greater with increasing glucose concentration, but at all concentrations the qualitative character of the spike is similar (see Fig. 21A). Even at high glucose concentration, the total amount of insulin released in the first phase is less than 1-2 percent of pancreatic insulin content. This indicates that the response is not a result of total depletion of stored insulin. If a constant glucose infusion above 100 mg/dl is maintained, following this initial phase of secretion is a second phase of secretion. This second phase of secretion starts at a rate of about two times the nonstimulated rate and gradually increases during the course of the infusion. Prolonged glucose stimulation of one hour or more, even when followed by a brief rest, results in a pancreas hypersensitive to further secretion (Grodsky et al 1969), thus prolonged stimulation potentiates the release mechanism.

Additional information about the insulin response to glucose is available from other stimulatory patterns tested on an isolated perfused pancreas preparation. When glucose is administered as a series of continually increasing steps (staircase function) each step elicits an additional spike, as seen in Fig. 22 (Karam 1974; Bergman and Urquhart 1971). Such studies emphasize that insulin release is not determined by the absolute increment in glucose in a linear fashion, since the amount of insulin secreted differed for each step although the glucose increments were the same. Fig. 23 shows the insulin secretion rate when glucose is presented as constantly increasing concentrations (ramp function). This experiment demonstrates another feature, namely that the multiphasic character of insulin release depends on the rate of glucose presentation.

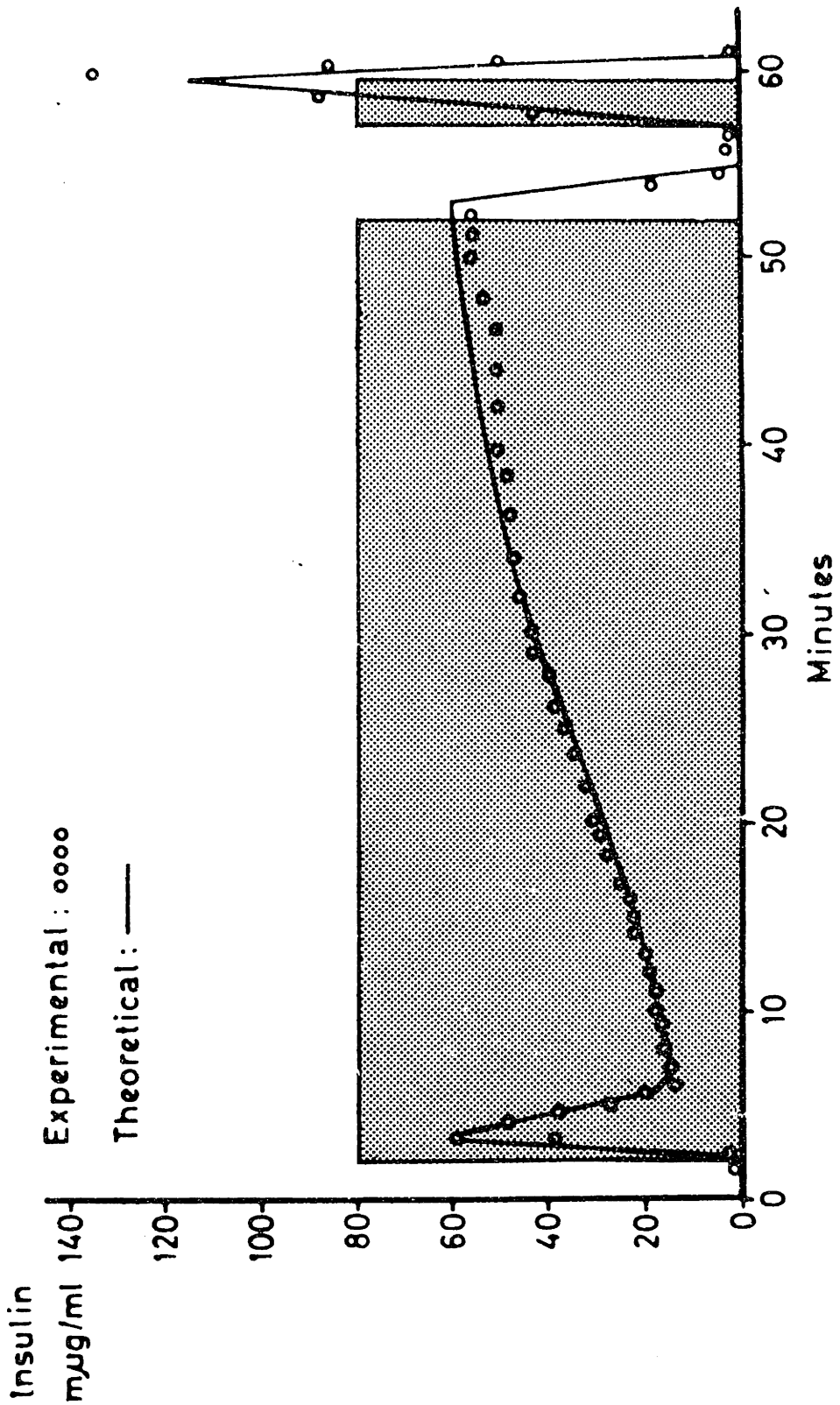

Figure 21A

Effect of prolonged glucose infusion and restimulation on insulin secretion from the in vitro perfused pancreas of the rat (from Curry et al, 1968).

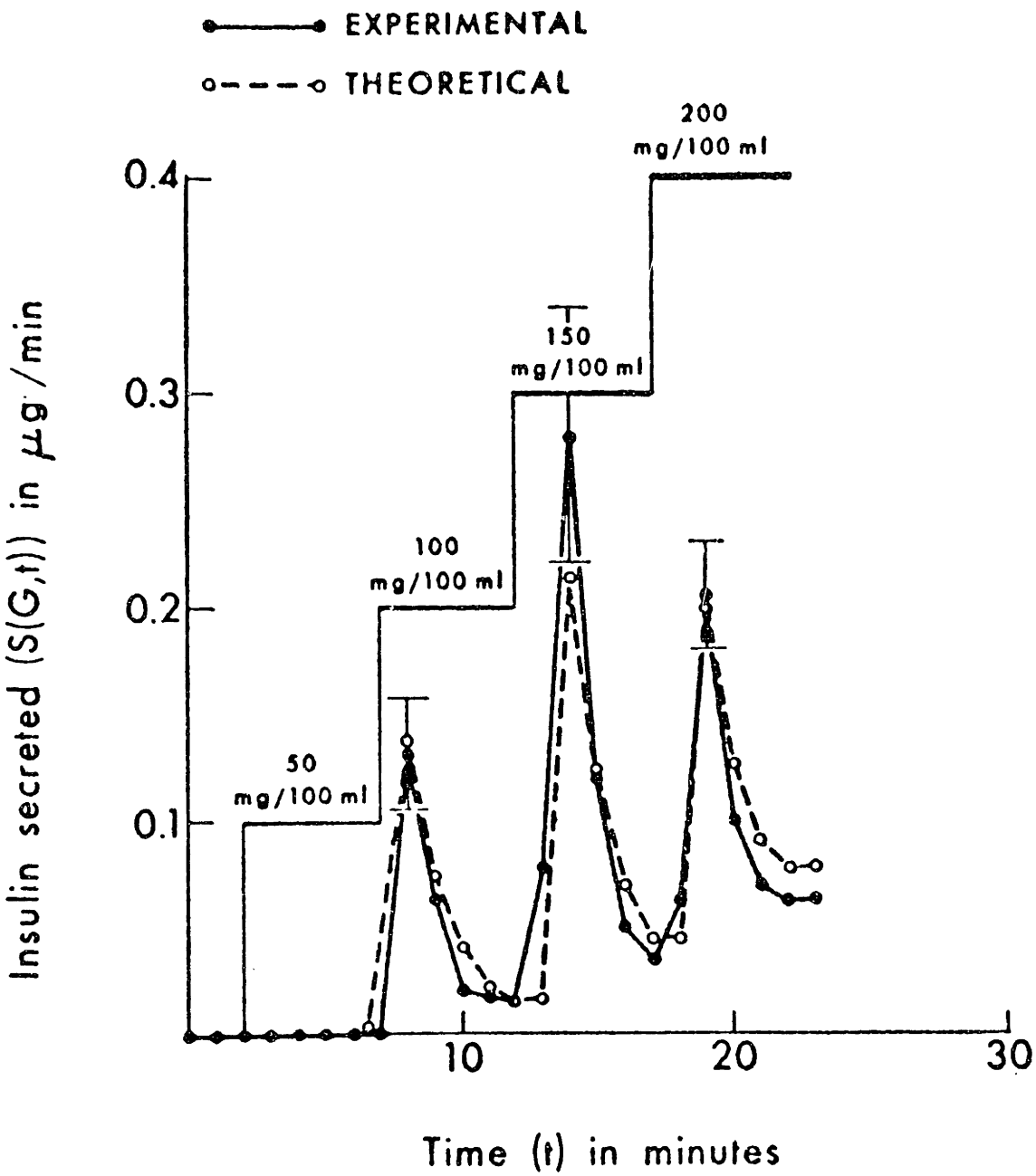

Figure 22

Insulin secretion during staircase stimulations with 50 mg/100 ml increments of glucose (from Grodsky, 1972).

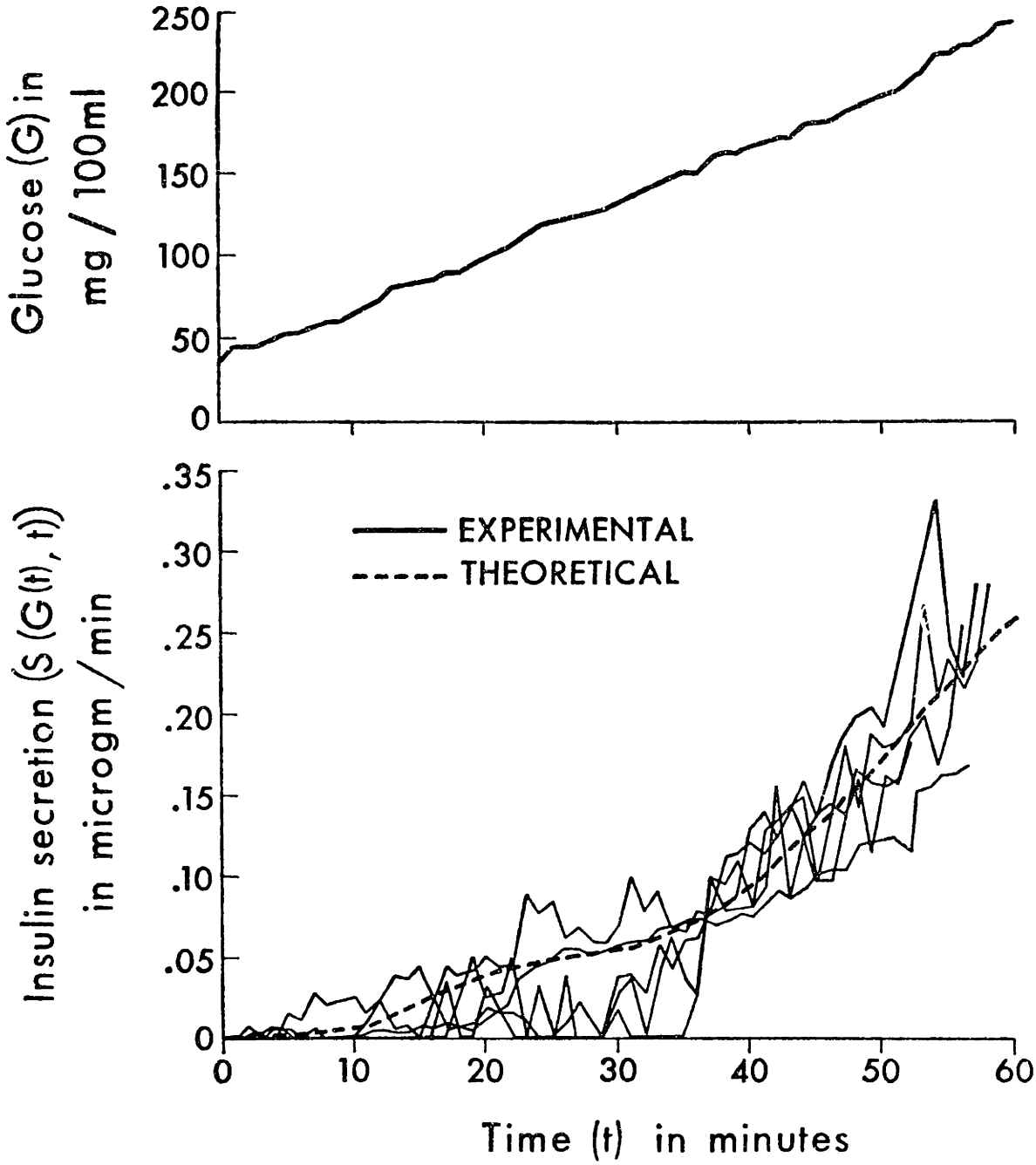

Figure 23

Effect of gradually increasing glucose concentration on insjlin secretion from the in vitro perfused pancreas of rat (from Grodsky, 1972).

The slower the rate, the less discernible the first phase appears (O'Connor et al 1977). Lastly, under conditions when glucose concentration is suddenly reduced, a short refractory period or inhibition of insulin release can be produced (Grodsky et al, 1967).

In summary, the insulin secretion rate is not a simple linear function of glucose concentrations in the pancreatic blood. Available data seem to indicate that the pancreas responds to the glucose concentration and rate of change of glucose concentration in a nonlinear fashion.

Amino acids also stimulate the release of insulin. In man, arginine, lysine, and leucine are the most potent inhibitors of insulin release (Fajans and Floyd 1972). In vitro and in the absence of glucose arginine and other amino acids stimulate monophasic insulin release. Addition of small amounts of glucose (70-80 mg) results in a multiphasic release of insulin. However, at physiological concentrations, amino acids generally have little effect on insulin release when compared to glucose. This is evident from both the relative magnitude of insulin responses to each substrate and the observed lower K_m for glucose-stimulated release (9-10mM) compared with that of arginine (12-14mM) (Gerich et al 1974).

Free fatty acids, β-hydroxybutyrate and acetoacetate all affect insulin secretion but their magnitude is small, and results from experiments contradictory (Balasse and Ooms 1973).

The recognition that the systemic glycemic stimulus to insulin secretion cannot by itself account for the elevation of insulin in the blood after ingestion of glucose in man (McIntyre et al 1965) suggested a role for gastrointestinal hormones in the regulation of insulin secretion. Perley and Kipnis (1967) have quantitated this observation. Glucose was

administered intravenously by means of a infusion system designed to produce glucose concentrations comparable to the ones seen in normal controls after the oral administration of 100 grams of glucose. Figure 24 demonstrates that insulin concentrations are 30-40% higher (for comparable glucose concentrations) when glucose is administered orally rather than intravenously. The mechanism mediating this differential response is probably the release of one or more gastrointestinal hormones as carbohydrate is absorbed. The gastrointestinal hormones secretin, "gut" glucagon, gastrin, cholecystokinin-pancreozymin (CCK-Pk), and gastric inhibitory polypeptide (GIP) have been implicated as possible candidates. Although it is far from clear whether any individual factor is involved, studies with GIP are the most promising. GIP is the only one of these hormones that can be given at physilogic doses and evoke insulin secretion. Experiments by Brown et al (1975) in which GIP is infused (1.0 mg/min) along with I.V. glucose (0.5 gm/min), demonstrate that the insulin response is 3 times as great as that after an I.V. glucose infusion alone. In fasting subjects, GIP administration does not affect glucose concentrations or cause insulin release. In addition, within 45 minutes of a mixed meal, GIP concentrations rise to about six times their fasting concentration, and remain elevated for about three hours. The increased levels of GIP correlate with the rise in glucose levels and precede the peak of insulin release following a 100 gram OGTT. These experiments are complicated by the fact that gut lumen concentrations of glucose, which presumably act as the stimulus for GIP secretion, have never been measured.

Indeed, in spite of the vast literature on the subject of gastrointestinal absorption of carbohydrates, a quantitative estimation of gastric and intestinal concentrations, transit times, and rates of absorption of glucose following

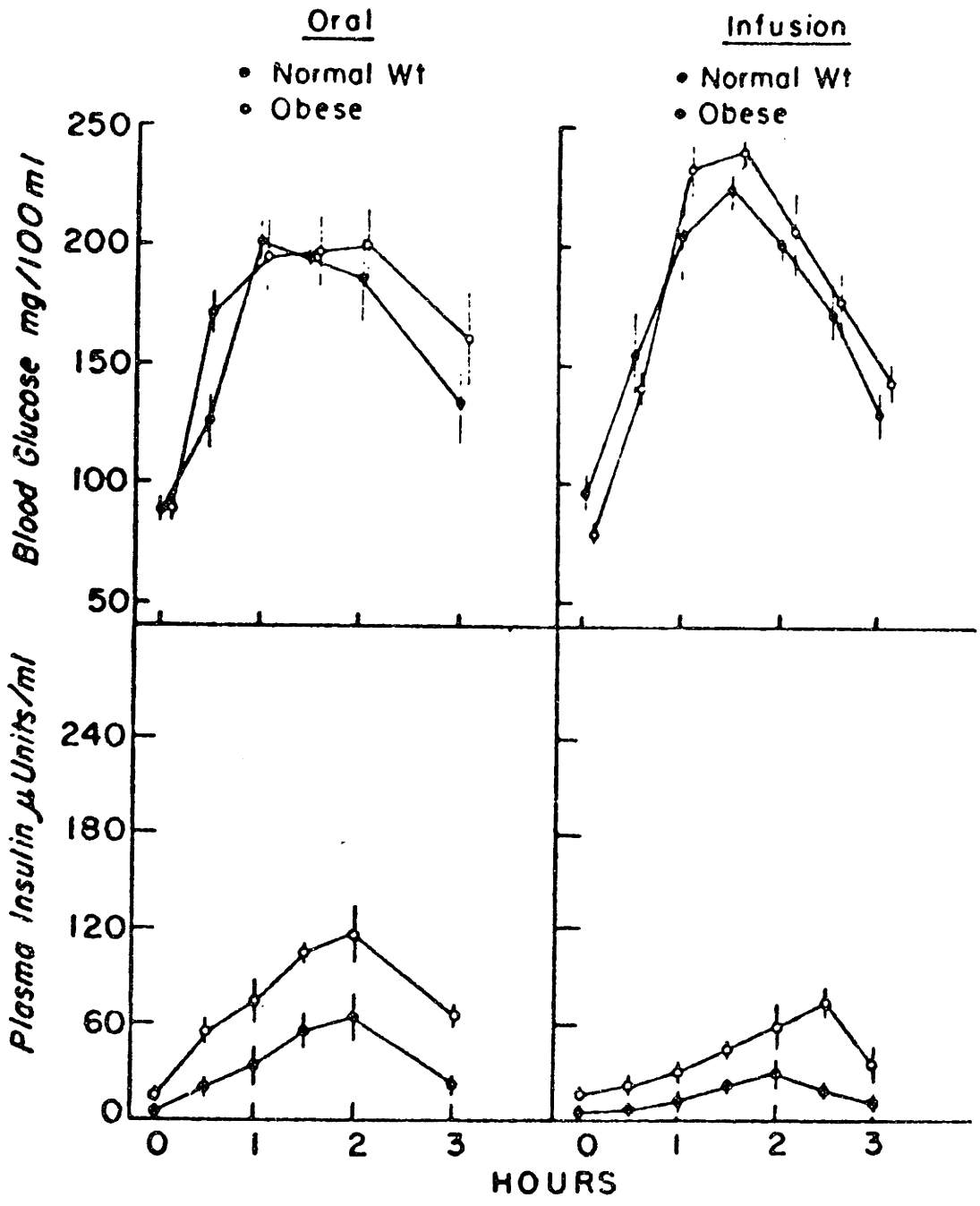

Figure 24

Plasma insulin responses of 12 normal weight and 12 obese diabetic subjects to an oral glucose tolerance test (100 gm) infusion maintained glucose profile (from Perley and Kipnis, 1967).

an oral glucose food is difficult. Following ingestion, glucose must traverse the esophagus, stomach, duodenum, jejunum, and illeum in order for absorption to occur. Glucose is then directly absorbed into blood vessels draining the stomach and small intestine. These vessels ultimately lead into the portal vein. Therefore the concentration of glucose in the portal vein can serve as a measure of the rate of glucose adsorption. Shoemaker et al (1963) measured the portal vein glucose concentration in dogs following a 40 and 50 gram glucose dose. The profile of the portal glucose concentration as a function of time appears to be the same as the commonly measured peripheral glucose concentration, with the exception that the portal concentration is between 5-25% higher.

The main factors that influence gastrointestinal absorption have been studied by Lagerlof et al (1976). It appears that even at high glucose loads, gastric emptying is the single most important determinant of total glucose absorption. The absorptive capacity of the stomach is readily saturated, and at high glucose loads (i.e. greater than 100 mg) the proportion of glucose absorbed by the stomach will be small.

Three processes occur in the active absorption of glucose by the small intestine: (1) diffusion through an unstirred layer of intestinal contents overlying the cell membranes which comprise the lumen wall, (2) A carrier mediated transport across the cell membranes, and (3) extrusion from the cell into the interstitial fluid (Wilson, 1962; Csaky, 1975). Diffusion through the unstirred layer, J_1, can be described by

$$J_1 = D/\ell \ (C_2 - C_2)$$

where D = diffusion coefficient

ℓ = thickness

C_1 = bulk glucose concentration

C_2 = glucose concentration at the cell membrane

Again, the unstirred layer constitutes a diffusion barrier for solutes that are required to make contact with the interstitial surface for hydrolysis or transport to occur. Although the thickness of the unstirred layer is unknown, it has been estimated to be as much as 1 mm. Quantitative estimates for D have not been reported. The carrier-mediated transport across the cell membrane, J_2, can be described by Michaelis-Menton kinetics:

$$J_2 = \frac{V_{max} C_2}{K_m + C_2}$$

where V_{max} = maximum absorption rate

k_m = Michaelis constant

Lastly, sugar accumulates in the cells at high concentrations and is extruded by simple diffusion.

Once within the cell some glucose is utilized by cellular metabolism. Experiments in which ^{14}C-glucose absorption was measured in a vein draining the small intestine in dogs, showed that 90% of the glucose ingested can be found as either glucose or lactate. About 65-80% was absorbed as glucose, and 7-17% was absorbed as lactate (representing cellular metabolism) (Atkinson et al, 1957).

In work by Lagerlöf et al (1976) the highest absorption rates were recorded within one hour after ingestion of glucose. The maximum absorption rate, V_{max}, was calculated to be 12.0 ± 2.8 mg/min/cm. This is within the range estimated by Holdsworth et al (1964) and Fordtran et al (1962) with

perfusion studies. This maximum rate does not appear to be the actual upper limit of saturation, but is the maximum that is attained under physiologic conditions. The reasons for this will be discussed below. It has been found (Wiseman, 1964) that a glucose load is normally completely absorbed in the first 100 cm of small intestine. (This then corresponds to a maximum V_{max} of 1200 $\pm$ 280 mg/min). In addition, Lagerlöf et al (1976) has noted that absorption of a 100 gm glucose load is complete within 3-4 hours.

In the normal gut, the rate of absorption of carbohydrates is mainly governed by two factors : the load per unit time and the time available for absorption, the mean transit time (related to flow rate through the region). The load per unit time entering the gut is governed by the stomach. In general, the rate of glucose absorption increases very little with increasing glucose load. As a glucose load increases, the rate of gastric emptying is delayed which prevents a corresponding increase in intestinal glucose load. Therefore, glucose is delivered to the small intestine at a rate which remains within its absorptive capacity (Reynell's Spray, 1956). It appears that after a short period of imbalance during which the hyperosmotic contents of the stomach are rapidly spread through the intestine, the emptying is adjusted to protect the intestine from high osmolarity. As the meal is successively diluted in the stomach, the volume emptied increases. Gastric secretion proceeds at a constant rate as long as the stomach is emptied. The cells excreting gastrointestinal hormones have microvilli which are triggered by the absorption of food.

During the first time after ingestion of a meal the load is high and the mean transit time short. A considerable portion of the emptied food

constituents are therefore propelled to lower parts of the intestine. By the increased area available the absorption rate is thereby increased. During the later phases after ingestion, the load is relatively small and the mean transit time is high. Food is then absorbed over a shorter length.

The plasma half-life of insulin is less than nine minutes in man (Soeldner and Slone 1965). While insulin can be detected in urine, the kidney filters and reabsorbs the hormone, and renal excretion is not a major rate of elimination. The liver and kidney are of primary importance in degrading insulin produced per day. The remaining insulin is lost via binding and inactivation by peripheral tissues such as muscle and fat.

C. Physiology of Glucagon and Somatostatin

The discussion so far has centered on the metabolic consequences of altered insulin levels. The pancreas also contains alpha and delta cells, which secrete the hormones glucagon and somatostatin, respectively. There is still much controversy over the metabolic effects of altered glucagon and somatostatin levels in affecting glucose homeostasis.

The ingestion of a carbohydrate meal in a normal individual is followed by a prompt increase in insulin as well as a decrease in glucagon. Unger (1975) proposed that this bihormonal response indicates that the insulin: glucagon ratio is the major determinant of glucose homeostasis. Felig et al (1976a) have proposed two criteria to test this hypothesis, namely, "(1) is glucose normally disposed of in an organ that is sensitive to glucagon and insulin, and (2) if normal suppresion of glucagon is prevented (by infusion of glucagon) will glucose homeostasis be affected?"

As previously discussed, liver, muscle, and fat tissues are all able to respond to insulin-modulated stimulation of glucose utilization.

In contrast, glucagon affects glucose disposal in only the liver (Felig and Wahren 1975a). Therefore, the concept of a bihormonal influence on glucose uptake assumes that the liver is the major site of glucose disposal. This assumption is supported by experiments which demonstrate that 60 percent of an oral glucose load is retained within the splanchnic bed and utilized by the liver (Felig et al 1975b).

Sherwin et al (1976) examined the response to continuous infusions of glucagon resulting in two to three-fold increases in the plasma level of glucagon. When an oral glucose load was administered, the usual fall in glucagon was prevented. But despite the hyperglucagonemia, glucose tolerance was no different than that observed during a control study in which insulin was infused. Furthermore, in studies with patients with glucagon levels of 1,000-2,000 pg/ml (the basal level of glucagon is 100 pg/ml), glucose intolerance is mild and inconsistent (Mallinson et al 1974). These findings suggest that insulin is the primary determinant of glucose tolerance and that the insulin:glucagon ratio provides no more meaningful an index of glucose homeostasis than the absolute concentration of insulin. This point is further established by the relative sensitivity of alpha and beta cells to small increments in glucose concentration. When glucose is infused into normal sugjects at a rate of 150 mg/min, blood glucose rises by 15 mg/dl, serum insulin levels rise by 60-80 percent and liver glucose output falls by 85 percent (Felig and Wahren 1971). However, arterial glucagon concentrations are unchanged.

Although glucagon is not important in the disposal of glucose loads, it has been shown to prevent hypolgycemia during noncarbohydrated-mediated stimulation of insulin secretion. As previously discussed, proteins are

capable of inducing insulin secretion. A rise in insulin would normally suppress hepatic glucose output and result in hypoglycemia. However, splanchnic glucose output does not fall after a protein meal (Wahren et al 1976). Glucagon has been shown to overcome the suppressive effects of small increments in insulin on hepatic glucose output (Felig et al 1976b).

Somatostatin is an inhibitor of both insulin (Albert et al 1973) and glucagon secretion (Gerich et al 1974). Administration of somatostatin results in a fall of blood glucose at a rate of 0.5-1.0 mg/dl/min. This decline only persists for 60-120 min. When somatostatin is increased beyond two hours, blood glucose levels return to hyperglycemic concentrations (150 mg/dl). This rise is due to the consequences of insulin supression - a progressive rise in hepatic glucose production as well as a decline in glucose utilization. If the infusion is ceased, or insulin is infused, glucose concentrations return to fasting levels.

In addition to its effects on fasting glucose concentrations, somatostatin has been shown to decrease the blood glucose rise following a carbohydrate-containing meal in diabetics (Gerich et al 1974). It appears to act by decreasing and or delaying carbohydrate absorption or by decreasing blood flow to the liver.

In normal man, glucose homeostasis is primarily determined by secretion of insulin rather than inhibition of glucagon. Somatostatin appears only to affect glucose disposal only through its inhibition of gastrointestinal absorption of carbohydrate.

D. Metabolic Consequences Of Diabetes

Fig. 25 shows the substrate metabolism in man with severe insulin deficiency. This type of insulin deficiency is characteristic of juvenile

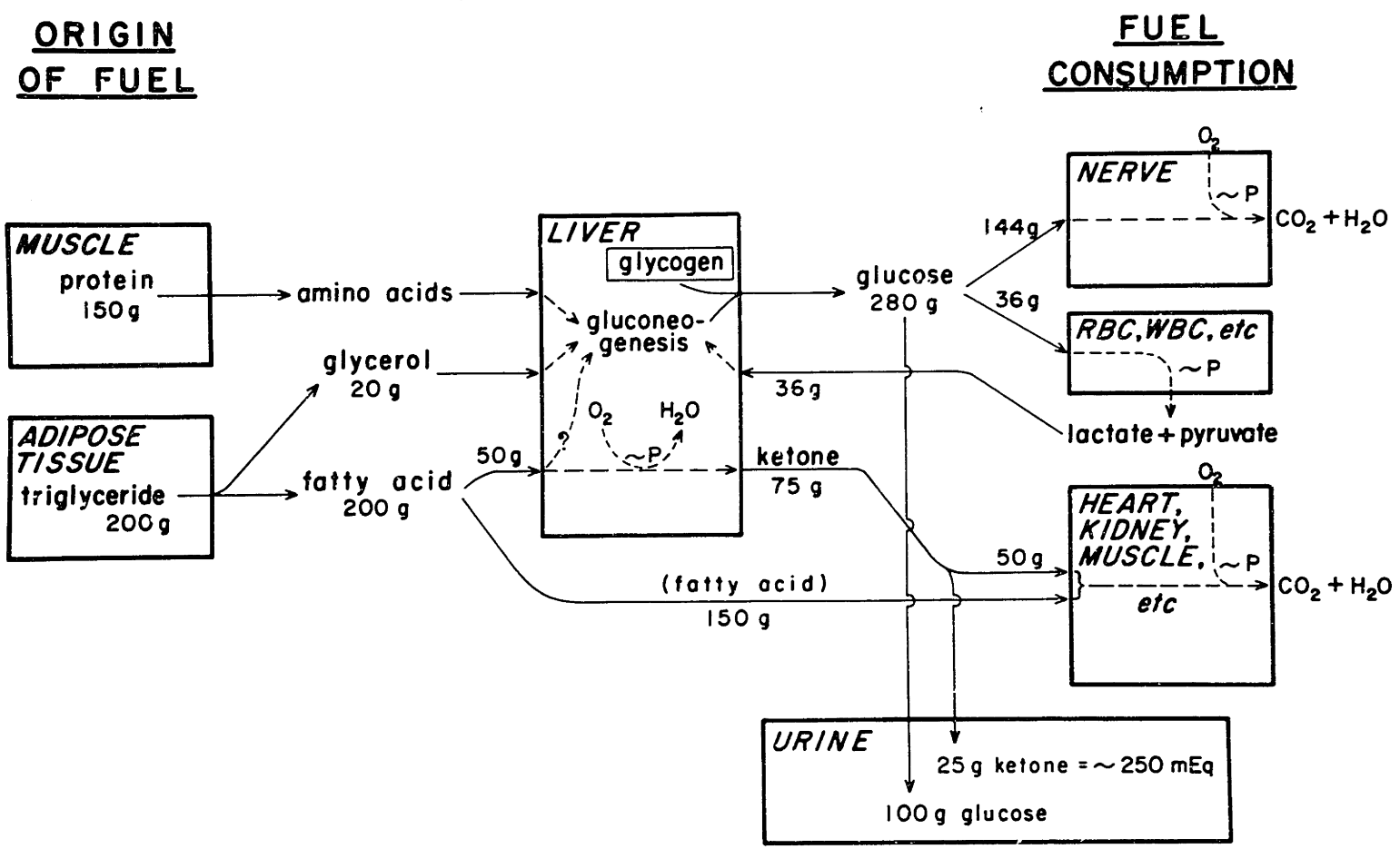

Figure 25

Substrate flow in a diabetic man (Cahill and Soeldner, 1969).

diabetes, in which the insulin response to stimulation with glucose or other stimuli is absent. In maturity-onset diabetes, response is usually delayed. Also, plasma insulin response to glucose is almost always less in persons with maturity-onset diabetes than in normal persons.

Whenever basal plasma insulin levels become inadequate, mobilization of free fatty acids from adipose tissue and amino acids from muscle proteins occur. Gluconeogenesis in the liver is greatly increased. Since there is no compensatory increase of glucose utilization, hyperglycemia and glycosuria (glucose loss in urine) result. In addition, there is an increase in keto acid production and the balance between production and utilization is disturbed. The more severe the insulin lack, the more disrupted the normal homeostatic mechanisms become. In its most severe case, insulin insufficiency will result in overproduction of fuel substrates in blood, excessive ketogenesis and gluconeogenesis, ketonuria, glycosuria and dehydration.

IV. MODELS OF GLUCOSE

A. Compartment Models

A one-compartment model for the distribution of insulin and glucose was developed by Bolie (1961) and will serve as a basic illustration of compartment models. Two first order differential equations describe the concentrations of insulin and glucose respectively:

$$V_1 \frac{dI}{dt} = U_1(t) - F_1(I) + F_2(G) \tag{1}$$

$$V_2 \frac{dG}{dt} = U_2(t) - F_3(I,G) - F_4(I,G) \tag{2}$$

Equation (1) states that the rate of accumulation of insulin equals the rate of injection, $U_1(t)$, minus the rate of destruction, plus the rate of production. V_1 is the volume of the insulin compartment. The rate of destruction of insulin, F_1, is assumed to be a function of insulin concentration, while the rate of production of insulin, F_2, is assumed to be a function of glucose concentration. Equation (2) states that the rate of accumulation of glucose equals the rate of injection, $U_2(t)$, minus the rates of glucose disappearance. Note there is no term for glucose production (via gluconeogenesis or glycogenolysis). The rate of glucose disappearance is assumed to occur at two independent rates, F_3 and F_4, both dependent on glucose and insulin concentrations. The two rates are supposed to represent the rate of liver accumulation of glucose and the rate of peripheral utilization, respectively. The rate of kidney excretion, as well as utilization of glucose by other tissues is not considered. The assumption is then made that these four rates, F_1,

F_2, F_3, and F_4 are all linear functions of glucose and/or insulin concentrations and the equations are rewritten as:

$$\frac{dI}{dt} = \frac{U_1(t)}{V_1} - k_1 I + k_2 G \tag{3}$$

$$\frac{dG}{dt} = \frac{U_2(t)}{V_2} - k_3 I - k_4 G \tag{4}$$

where k_1, k_2, k_3, and k_4 are constant coefficients. Equations (3) and (4) therefore represent two first-order linear differential equations whose solution is given by:

$$I = -k_3 \frac{D_1}{V} te^{-k_5/2t} \tag{5}$$

$$G = \frac{D_2}{V} \left[(k_5 - 2k_1)t/2 \right] e^{-k_5/2t} \tag{6}$$

$$k_5 = 16k_2^2 k_4^2 + 2k_1 \tag{7}$$

In equations (5) and (6), $U_1(t)$ and $U_2(t)$ are taken to be injections of D_1 units of insulin and D_2 grams of glucose, respectively. For convenience, a new variable k_5 has been defined by (7). The constant parameters in (5) and (6) are chosen so that the glucose and insulin concentrations following an intravenous glucose tolerance test (IVGTT) are approximated. The calculated glucose tolerance curves are able to fit experimental data, but the calculated insulin tolerance curves do not reproduce the biphasic experimental curves (see Fig. 2) following an IVGTT.

A review of compartment models of glucose homeostasis was done by Charette et al (1969) and serves as a complete summary of modeling

efforts up to 1969. Atkins (1970) has simulated these models and analyzed the number of compartments and mathematical functions for glucose and insulin production and disappearance that will fit an OGTT. As the reader can imagine, almost an infinite number of combinations can be used to reproduce the experimental curves. Furthermore, it is almost impossible to relate the rate constants to the known physiology.

Cerasi et al (1974) have developed a model with the necessary complexity to simulate accurately the glucose and insulin concentrations following an intravenous glucose infusion. However, this model is not necessarily the minimal model, i.e., the model with the minimum number of parameters that can fit the data. The model is significant because several of the parameters can be interpreted in terms of known physiology. The glucose concentration is given by a nonlinear one-compartment equation:

$$V_G \frac{dG}{dt} = u(t) - k_1(G-200) + k_2(G_o-G) - k_3 \left[(I_L+I_o)(G+G_o) - I_oG_o\right] \qquad (8)$$

The first term on the right hand side of equation (8) represents the rate of infusion of glucose. The second term represents the rate of urine excretion of glucose (which occurs only when glucose concentrations are above 200 mg/dl). The third term, which is included only when glucose concentrations fall below the fasting value G_o, compensates for hypoglycemia. The last term represents "peripheral glucose uptake" (actually total body glucose uptake) as a function of glucose concentrations and interstitial insulin concentrations, I_L. The glucose model does not include the rate of glucose production by liver, and it does not separate glucose utilization by various organ groups.

The distribution of insulin is represented by a three-compartment model:

$$\frac{dI_p}{dt} = -k_4 I_p - k_5(I_p - I_L) + k_6 I_R \tag{9}$$

$$\frac{dI_L}{dt} = -k_7(I_p - I_L) - k_8(I_L - I_t) \tag{10}$$

$$\frac{dI_t}{dt} = k_9(I_L - I_3) - k_{10} I_t \tag{11}$$

Where I_p is interpreted to represent the concentration of insulin in the plasma and I_L the concentration of insulin in interstitial fluid. The interpretation of I_t as the concentration of insulin in "the tissues where insulin is utilized and degraded" is somewhat obscure.

The insulin secretion rate, $k_6 I_R$ is determined by a set of five differential equations:

$$\frac{dp_1}{dt} = k_{11} p_1 + k_{12} f(g) \tag{12}$$

$$\frac{dp}{dt} = k_{13}(p - p_1) \tag{13}$$

$$\frac{db_1}{dt} = k_{14} b_1 + k_{15} I_R \tag{14}$$

$$\frac{db}{dt} = k_{15}(b - b_1) \tag{15}$$

$$I_R = e^{p-b} f(g) \tag{16}$$

where p is a dimensionless potentiator variable which represents the effects of a prolonged glucose stimulation; b is a dimensionless inhibitory

variable which represents negative feedback of insulin secretion, while p_1 and b_1 are intermediate variables. The nonlinear function f(g) which determines the influence of varying glucose concentrations on insulin secretion rate (see Fig. 26) was determined empirically in order to fit experimental data of the effect of glucose on insulin release (see Fig. 21). Therefore, the insulin secretion rate $K_6 I_R$ is determined by three multiplicative factors: f(g) and e^p which increase the insulin secretion rate, and e^{-b} which decreases it. Blood glucose concentrations act directly on f(g) and e^p.

All the parameters in the model except for k_1, k_3, k_6, k_{12}, k_{15}, and V_G were given fixed values. These six parameters were determined by fitting curves from 10 minute and 60 minute glucose infusions. In particular the parameter K_6 was shown to be significantly less in diabetes than in normal subjects, indicating a reduced ability to secrete insulin. The model is hard to justify physiologically because of the oversimplifications made in the model for glucose distribution (e.g., no term for the production of glucose via gluconeogenesis or glycogenolysis was included) and the complexity of the rate of insulin secretion.

Gatewood et al (1968) have developed the only compartment model to date that simulates an oral glucose tolerance test. The model equations represent one compartment for the distribution of glucose and insulin and are given by equations (3) and (4). However, $U_2(t)$, the rate of glucose intake was chosen to be a function of the form:

$$U_2(t) = R \left[u(t) - u(t-t_a)(1-\exp\{ -\beta(t-t_a)\}) \right] \qquad (17)$$

Equation (17) represents a constant maximum glucose rate of infusion, R,

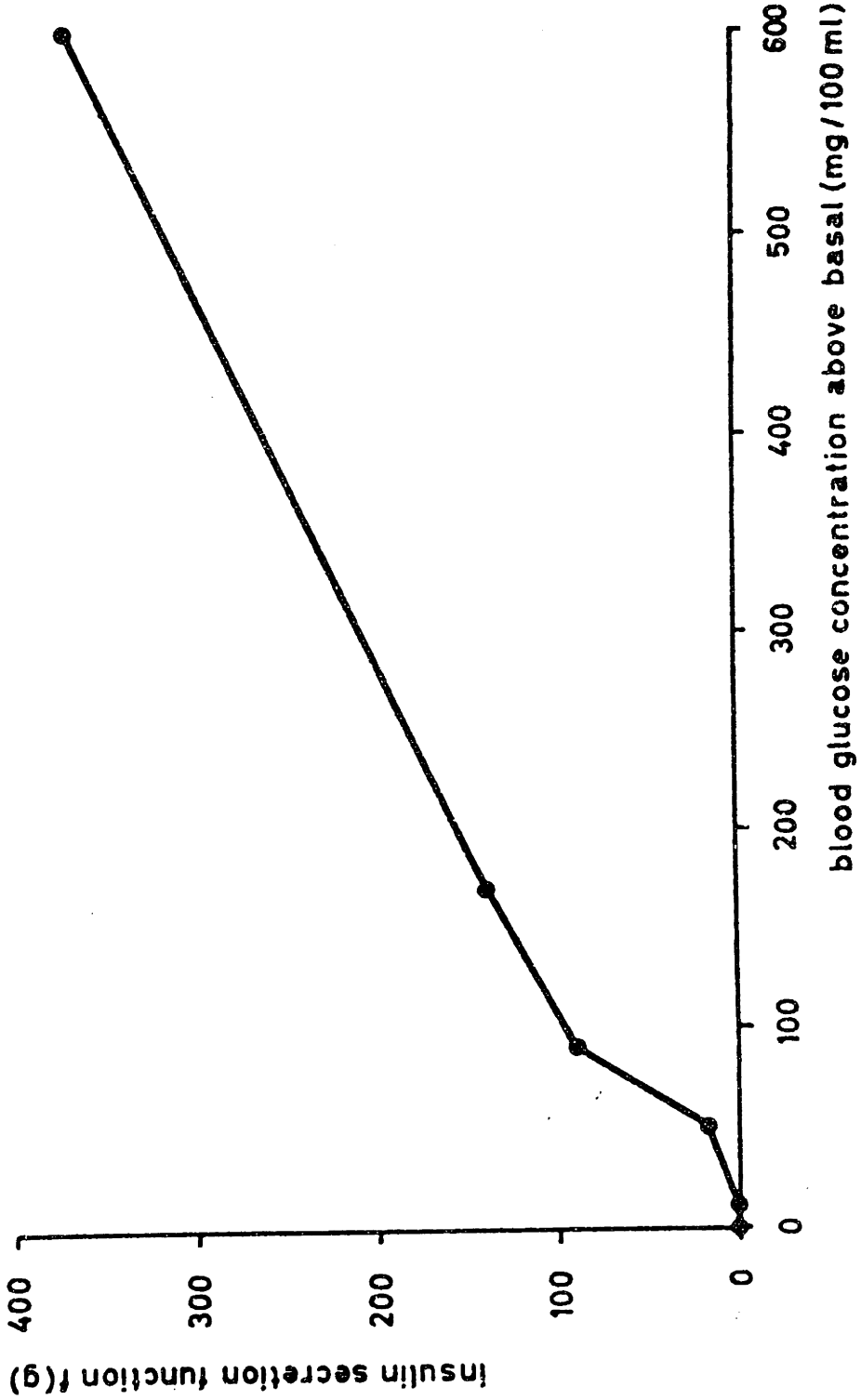

Figure 26

The nonlinear function relating the glucose concentration to the rate of insulin secretion (from Cerasi et al, 1974).

until time, t_a, when the glucose infusion begins to exponentially decay. The reciprocal of β represents the time constant for total absorption of glucose. u(t) represents a unit step. This approximation of the rate of absorption of glucose is a reasonable one physiologically. Gatewood et al chose t_a to be 30 minutes and β to be .04 minutes^{-1}. Glucose absorption is known to occur by a carrier-mediated process, which can be represented by Michaelis-Menton kinetics (the rate of glucose absorption is a sigmoidal function of gut lumen glucose concentrations). At the initial concentrations at which glucose is given during an OGTT (33 gm/dl), the carrier is saturated, until a time t_a, when glucose concentrations begin to decline, thereby decreasing their rate of transport. However, there is considerable uncertainty as to the time constants (see Section III.C). Their model as a whole was inaccurate for the same reasons discussed above, namely a one-compartment linear model is not sufficient to fit the OGTT curves.

A variety of compartment models have been developed for use in conjunction with experiments using ^{14}C-glucose as a tracer in studies of glucose metabolism (Spencer et al 1971; Shames et al 1971; Malmendier et al 1974). After ^{14}C-glucose is injected intravenously, blood and breath samples are taken and analyzed to determine the specific activity of blood ^{14}C-glucose and breath $^{14}CO_2$. Most models are based on the assumption that ^{14}C-glucose injected intravenously traverses one or more compartments before leaving the breath as $^{14}CO_2$. Insulin is not included in these oxidative models of glucose metabolism.

A model developed by Spencer et al (1971) is representative of this type of analysis, and is shown in Fig. 27. The equations describing the

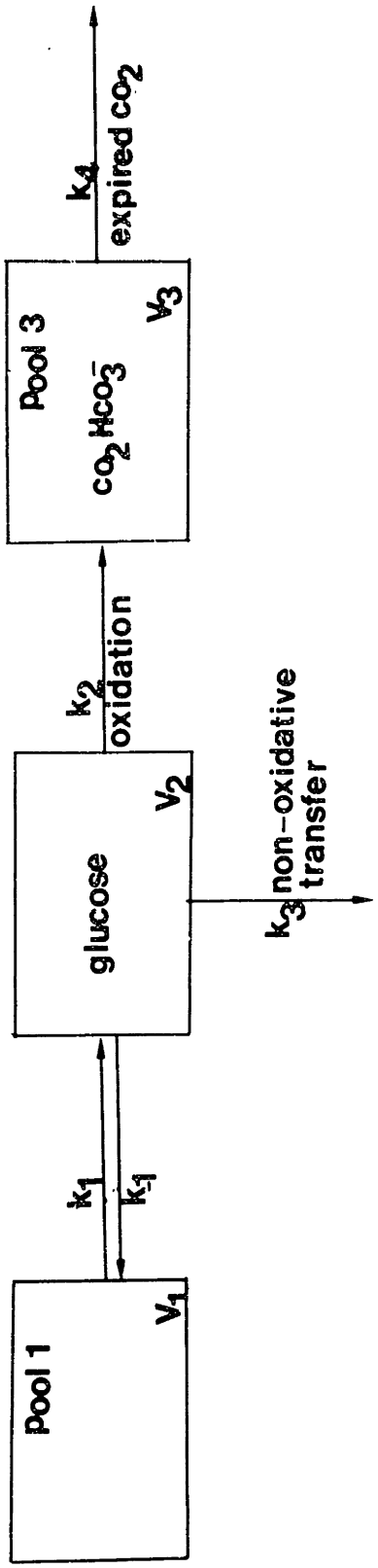

Figure 27

Model of oxidation glucose metabolism (from Spencer et al, 1971).

oxidative and nonoxidative metabolism of glucose are:

$$V_1 \frac{dC_1}{dt} = k_1(C_2-C_1) \tag{18}$$

$$V_2 \frac{dC_2}{dt} = k_1C_1 - (k_1+k_2+k_3)\ C_2 \tag{19}$$

$$V_3 \frac{dC_3}{dt} = k_2C_2 - k_4C_3 \tag{20}$$

Equation (18) states that the accumulation of carbon species produced from glucose, $\frac{dC_1}{dt}$, equals the rate of breakdown of glucose minus the rate of production of glucose. In other words, compartment one represents the carbon in species produced from glucose and convertible to glucose, namely, glycogen, amino acids and lipids. However, the assumption that the rate constant, k_1, is the same for glucose production from other carbon species (e.g., glycogenolysis, gluconeogenesis) and for glucose conversion to other species (e.g., glycogen synthesis) is not consistent with the physiology. Equation (19) states that the rate of accumulation of glucose, $\frac{dC_2}{dt}$, is equal to the rate of production of glucose minus the rate of disappearance of glucose via conversion to other carbon species (k_1C_2), via oxidative metabolism to CO_2 (k_2C_2), and via nonoxidative metabolism to lactate and pyruvate (k_3C_2). Equation (20) states that the rate of accumulation of CO_2 (either as CO_4, HCO_3 or other compounds), $\frac{dC_3}{dt}$, is equal to the rate of production of CO_2 from glucose, minus the rate of expiration of CO_2. The constant coefficients k_1, k_2, k_3, and k_4 are determined by fitting the blood ^{14}C-glucose and breath $^{14}CO_2$ specific activity data from the experiments described above. A three-compartment model gives an excellent fit to the data and the coefficients

can be used to quantitate the changes in distribution of injected ^{14}C-glucose in patients in various different metabolic states.

A novel set of experiments by Insel et al (1974, 1975) have led to the development of a compartment model for insulin and glucose to analyze the control of glucose metabolism by insulin. Insulin, in the upper physiological range (40 mU/m^2/min) was given as a continuous infusion followed by an infusion of ^{14}C-glucose the magnitude of which was the amount necessary to maintain basal glucose levels. The experiments lasted for 170 minutes, during which time blood glucose and insulin levels were measured. The rationale behind this experimental protocol was that insulin markedly reduces endogenous glucose production and therefore the glucose infusion would closely approximate the utilization of glucose.

The insulin model is a three-compartment model (see Fig. 28). The combined mass of the three compartments is equivalent to insulin space (15.7% body weight). Compartment 1 is apparently the plasma space (M_1 = 4.5%). The other two compartments are extravascular; compartment 2 is small (M_2 = 1.7%) and equilibrates rapidly with plasma, and comparment 3 is larger (M_3 = 9.5%) and equilibrates slowly with plasma. The size of each compartment and rate of transfer between compartments (assumed to be linear) were fitted with pulse-injection and continuous infusions of insulin in patients. During the infusions, blood glucose concentrations were kept constant, according to the protocol described above, allowing the assumption that endogenous insulin secretion was a constant, basal rate of secretion.

The glucose model is also a three-compartment model (Fig. 29)

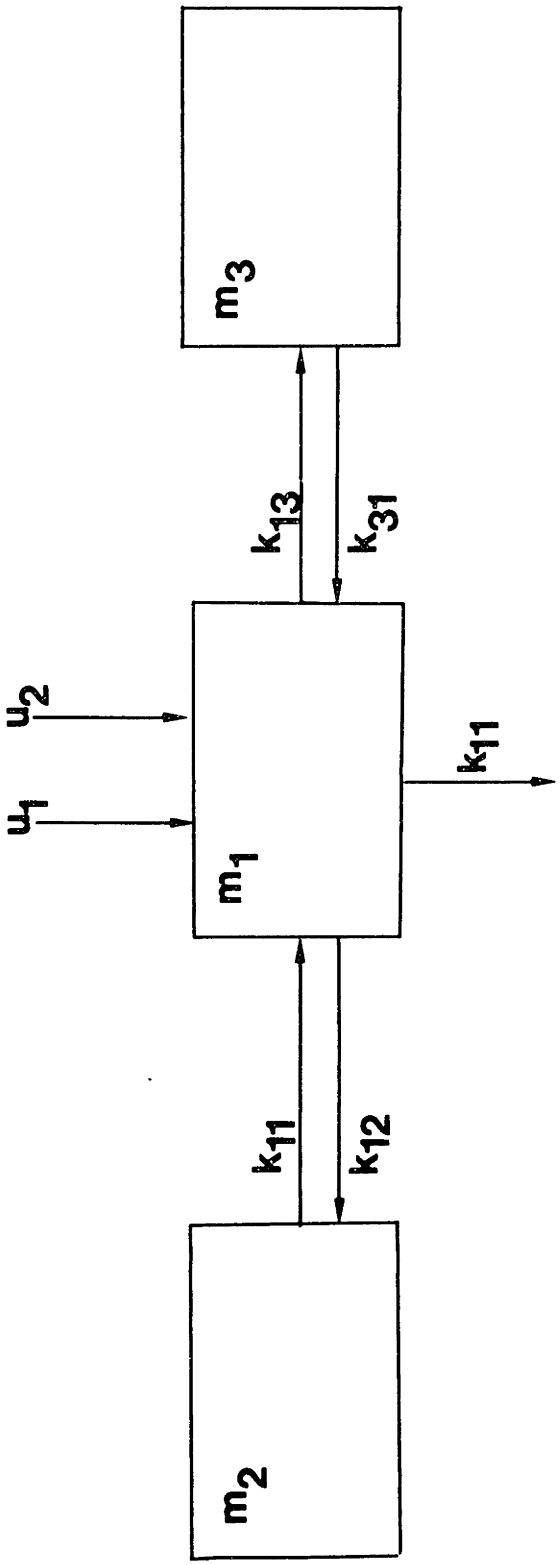

Figure 28

Three compartment model for insulin distribution (from Insel et al, 1975).

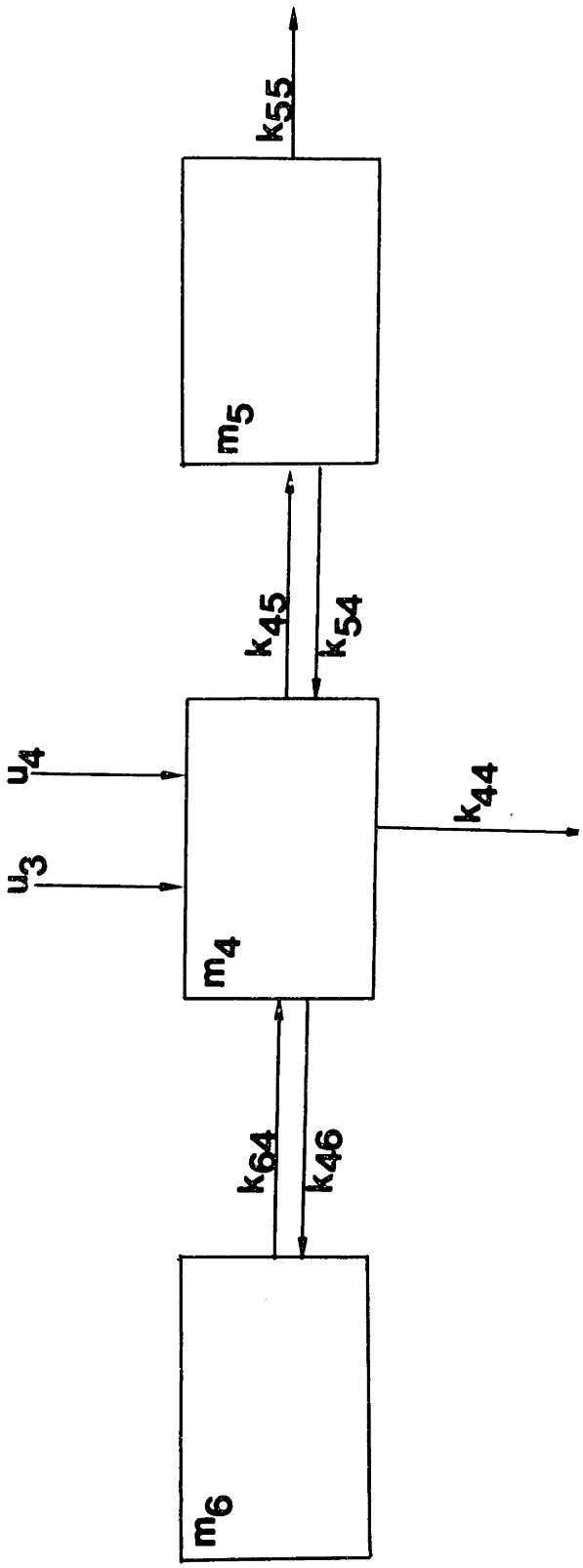

Figure 29

Three compartment model for glucose distribution (from Insel et al, 1975).

consisting of a central compartment (M_4 = 68 $\pm$ 7 mg/kg) in rapid equilibrium with a smaller compartment (M_5 = 50 $\pm$ 17 mg/kg) and in slow equilibrium with a larger compartment (M_6 = 96 mg/kg). Two rates of loss of glucose were postulated. One is a zero-order (insulin and glucose independent loss) from the central (blood) compartment, k_{44}. The magnitude of k_{44} was estimated to be equal to the rate of glucose uptake by the central nervous system. Under conditions of the experiments, where blood glucose was held constant at basal concentrations, this is a valid assumption. The other rate of loss is an insulin-dependent loss, k_{55} that was made proportional to a change in insulin concentration in compartment 3, in an attempt to explain the effect of insulin on glucose utilization.

Recall that the experiment is predicated on the assumption that the rate of glucose utilization is approximated by the rate of infusion necessary to keep glucose levels constant during the course of the experiment. In terms of the model, the total rate of glucose utilization is given by:

$$R = R_c + k_{55} M_5 \tag{21}$$

where R_c is the constant rate of utilization by the central nervous system. If k_{55} is made proportional to the insulin concentration in compartment 3, as suggested by Insel et al

$$k_{55} = A + BI_3 \tag{22}$$

where A and B are constants. Substituting (21) into (22) yields

$$R = R_c + (A + BI_3) M_5 \tag{23}$$

Noting that at steady-state (when the rate of utilization is compensated by the rate of infusion of glucose)

$$-M_5(k_{45} + k_{55}) + M_4(k_{45}) = 0 \tag{24}$$

$$M_5 = \frac{M_4(k_{45})}{k_{45} + k_{55}} = \frac{M_4(k_{45})}{k_4 + (A + BI_c)} \tag{25}$$

Finally substituting (23) into (25) yields

$$R = R_c + \frac{k_{45}(A + BI_3)M_4}{k_4 + (A + BI_3)} \tag{26}$$

which gives the dependence of the rate of glucose utilization on insulin concentrations and parameters determined from fitting experimental data. This index has been suggested by Insel et al to characterize this dependence in a variety of metabolic states. The model clearly illustrates the design of a compartment model which can be used for meaningful interpretation of parameter variability among patients and parameter sensitivity in various metabolic states.

Foster et al (1973) have developed a very unique compartment model for glucose homeostasis. Fig. 30 shows the design of the model. The glucose model is a three-compartment model representing a central glucose compartment (GG), a liver glycogen compartment (GLYLIV), and a peripheral glycogen comparment (PGS). The rate of accumulation of glucose in the central comparment (GG) equals the rate of gluconeogenesis (GLUNEO), plus the rate of glycogenolysis (GLYO), and uptake of lactate (LULAC), minus the rate of urine loss (U), nervous system uptake (NSU), red blood cell uptake (RBCU), adipose tissue utilization (ATU) and muscle uptake (MU)

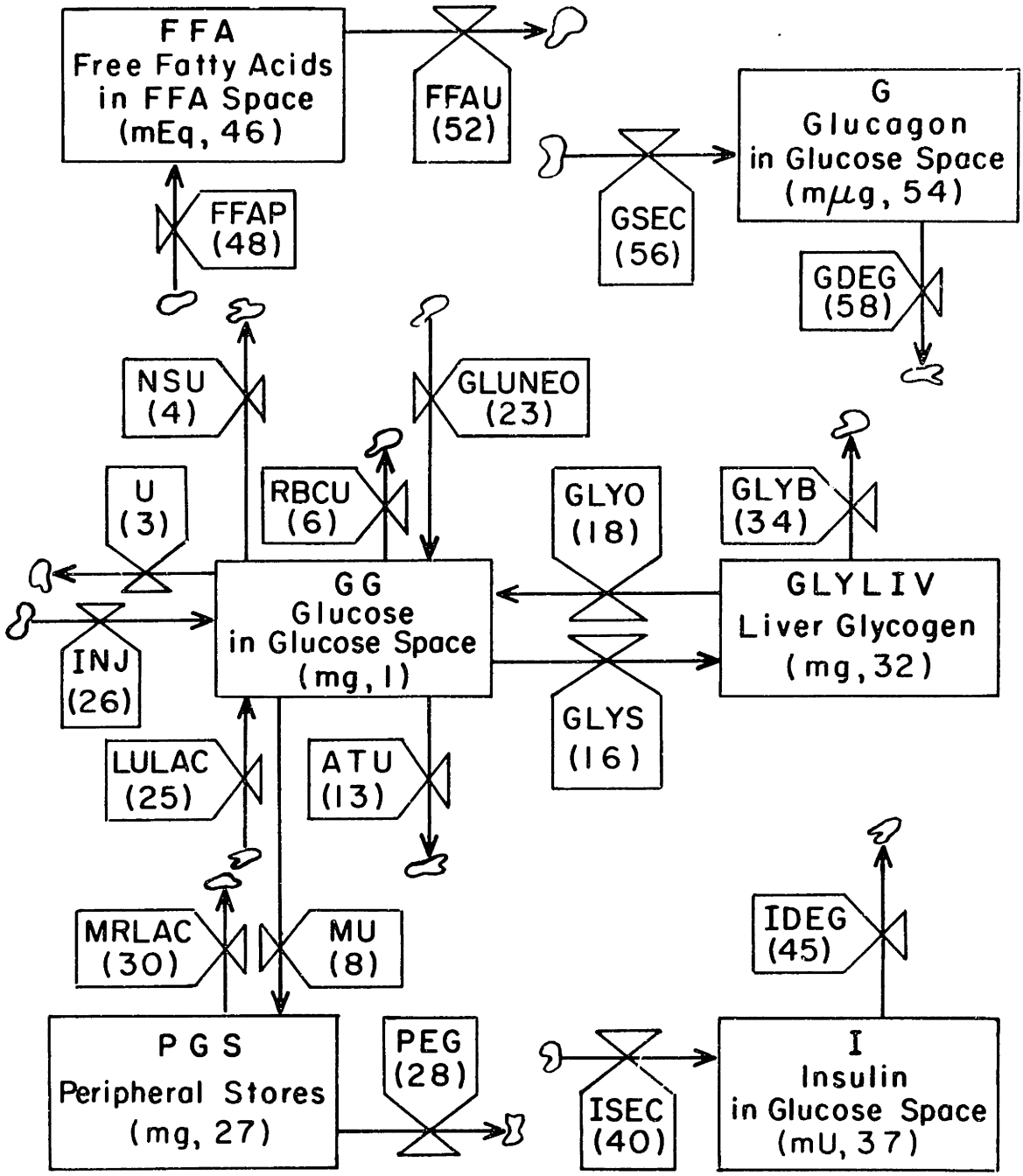

Figure 30

Model for glucose homeostasis (Foster et al, 1973).

The rate of accumulation of glucose (stored as glycogen) in the peripheral compartment (PGS) equals the rate of muscle uptake of glucose (MU), minus the rate of muscle utilization of glucose (PEG), and muscle release of lactate (MRLAC). This model specifies all the relevant physiological dynamics. A one-compartment model for insulin and glucagon represent the rate of accumulation of each hormone as the rate of secretion, (ISEC) and (GSEC) respectively, minus the rate of degredation, (IDEG) and (GDEG) respectively. Finally, there is a one-compartment model for free fatty acids (FFA) which represents the rate of accumulation of FFA as the rate of production (FFAP), minus the rate of utilization (FFAU).

The unique feature of Foster's model is that each rate is determined based on the best estimate available from the literature. In other words, there is no curve-fitting procedure used to fit the data. Foster recognized that several of the rates depend on the concentrations of glucose and/or insulin in the blood, and many rates are nonlinear. For example, the rate of nervous system uptake of glucose is a function of glucose concentration. The concentration of glucose determines the "effect of glucose concentration on nervous system uptake of glucose" (see Fig. 31). This effect, when multiplied by the fasting rate of glucose uptake by the nervous system, will yield the rate of glucose uptake by the nervous system (NSU) under all conditions. Insulin secretion is a function of glucose concentrations, free fatty acid concentrations and the rate of change of glucose concentrations in Foster's model. Each of these factors (see Figs. 32,33) has a nonlinear effect on insulin secretion and when multiplied together times the basal insulin secretion rate will yield the insulin secretion rate (ISEC). Each of the 22 rates in the model is represented in a similar manner as the rates that have been described.

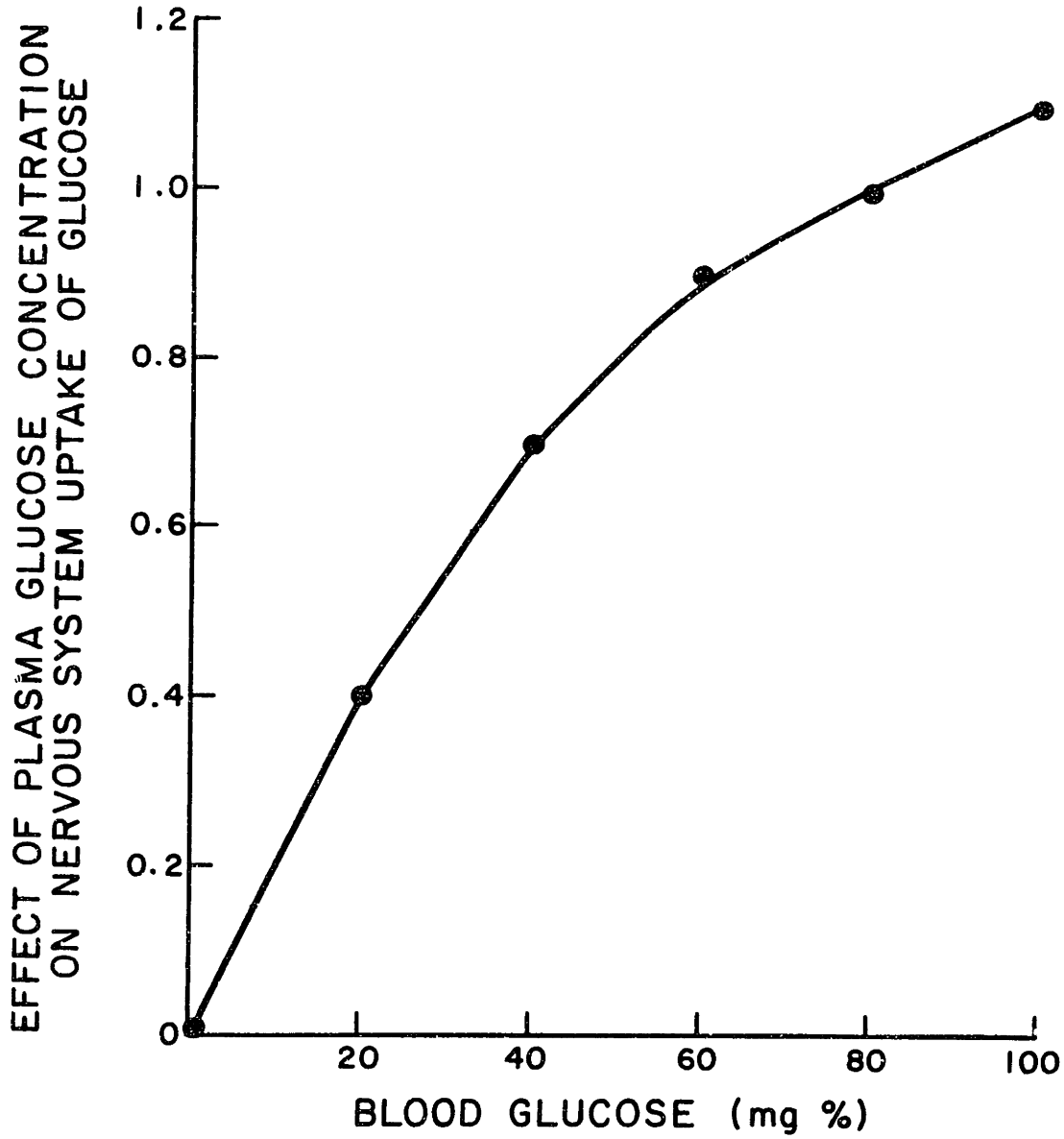

Figure 31

The quantitative relationship between the blood glucose concentration and the nervous system uptake of glucose (NSU) (from Foster et al, 1973).

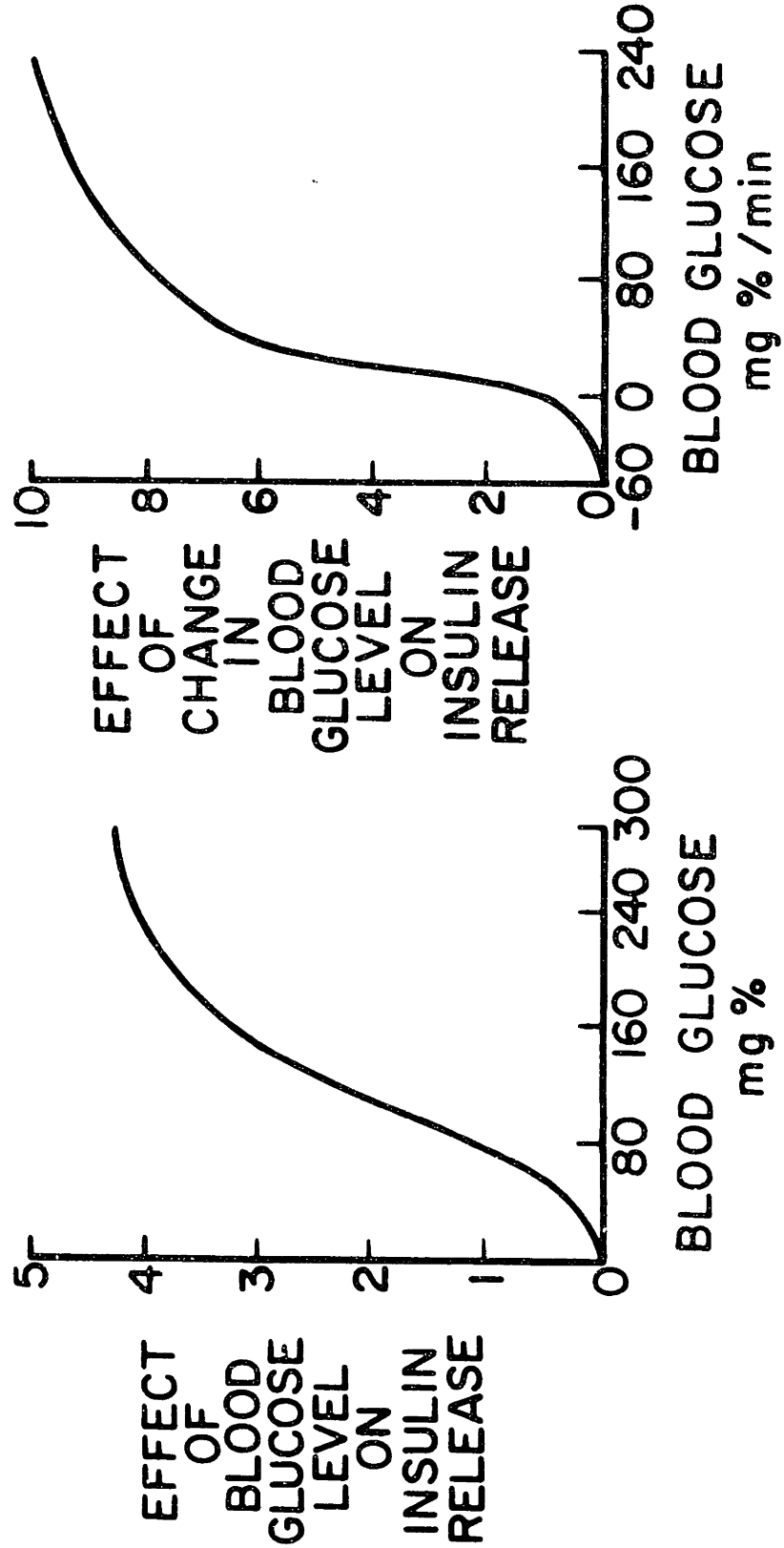

Figure 32

The influence of blood glucose concentration and rate of change of blood glucose concentration on insulin secretion (from Foster et al, 1973).

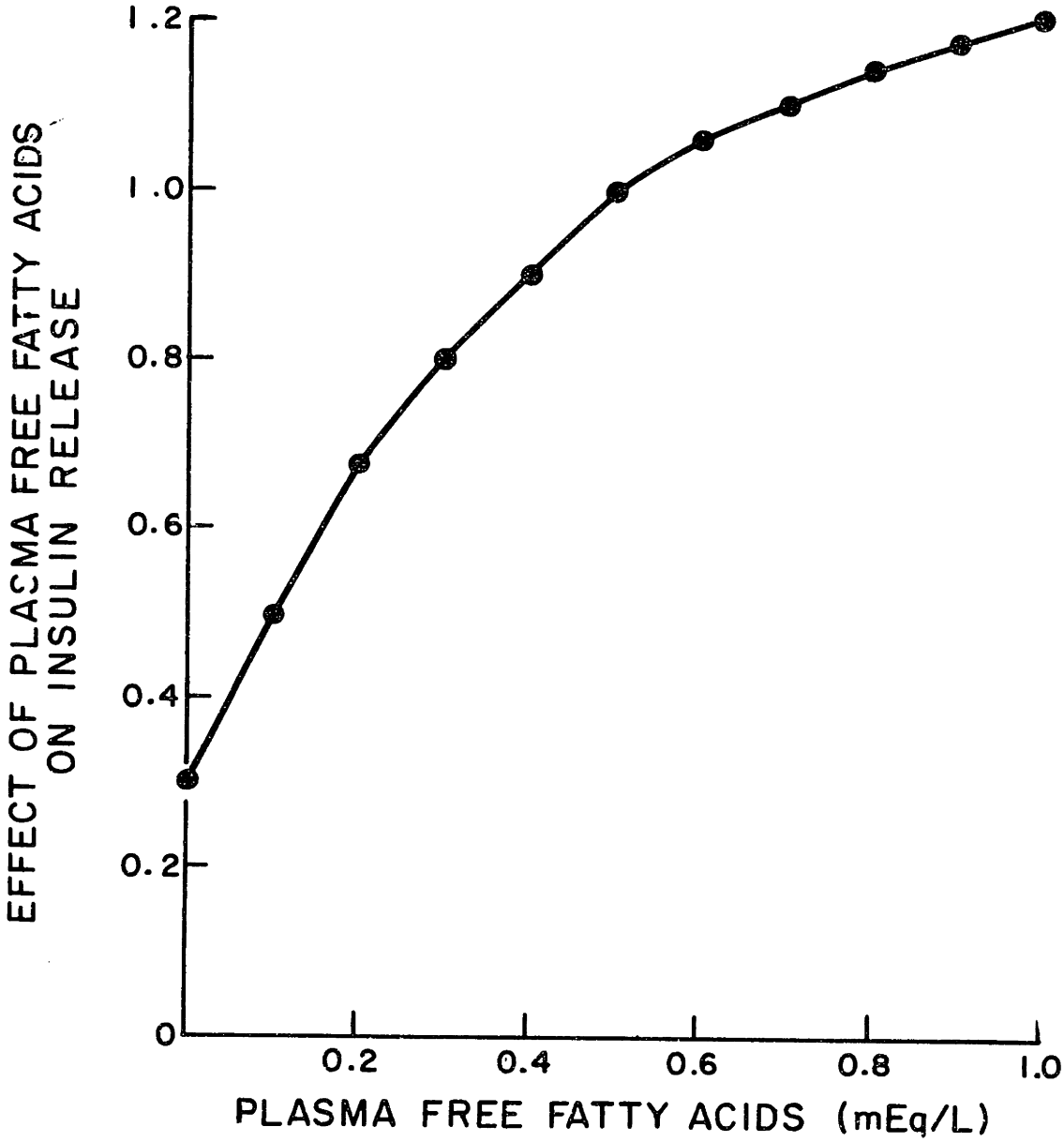

Figure 33

The influence of plasma free fatty acid concentration on insulin secretion (from Foster, 1973).

The model is capable of simulating the response of an "average" man to an IVGTT. The model only simulates an "average" man since the model parameters were determined based on average values from the literature. Several of the rates were modified to test the sensitivity of overall response to various rates. For example, reducing the effect of glucose concentration on insulin secreation by 50 percent led to model behavior which was qualitatively like the observed behavior of prediabetics to an IVGTT. Fixing the total insulin secretion rate as a constant led to the same qualitative response or that of a juvenile diabetic to an IVGTT. Therefore, the model allows the testing of various theories regarding mechanisms of diabetes.

However, the model does not correctly simulate a response to dynamic stimuli other than an IVGTT. This suggests that the underlying structure of the model has several defects and its usefulness is clearly limited.

B. Blood-flow Limited Models

The model to be presented in this thesis is a flow-limited model for glucose distribution and metabolism based on the work of Guyton (1977). It is based solely on the dynamic changes of glucose and insulin concentrations alone. While the restriction to glucose and insulin interactions represents a simplification of all the physiologic processes that can affect glucose homeostasis, from the review of glucose homeostatis presented, it is clear that (1) insulin is the most important determinant of glucose homeostatis, and (2) glucose concentrations are the main stimulant for insulin secretion.

The concept of 'flow-limited' conditions, as defined by Bischoff (1975), means "that the membrane permeability (in an organ) is so large that any molecule that flows into the region has an easy time moving throughout the space." Thus, the concentration of a substance in an organ is determined by the amount that was able to flow in from the blood pool. In addition the concentration is identical throughout the region.

The circulatory design of the model for glucose distribution is shown in Fig. 34. Table 1 shows the blood flow, organ volumes and the transmembrane equilibration times used in the simulation. The central organ compartment (to be referred to as heart) may be considered to represent rapidly mixing blood and fluid spaces in the heart, lungs, arteries and nonhepatic splanchnic organs. The peripheral compartment (to be referred to as muscle) includes skeletal muscle and adipose tissue. Although the fluid volumes of the liver and kidney are small, their blood flows are large and they are important sites of glucose metabolism.

Glucose equilibrates rapidly between vascular and extravascular spaces in liver and kidney (Cahill et al 1958), which justifies considering these organs as single compartments according to the above criteria. As can be seen from Table 1, the transmembrane (blood-tissue) equilibration time in the head, heart, and muscle compartments is the same order as the blood-flow rates into the organs. This suggests a membrane resistance to transport, and each of these organs is represented by a blood and tissue (interstitial and intercellular) compartment.

The calculation of these transmembrane equilibration times is

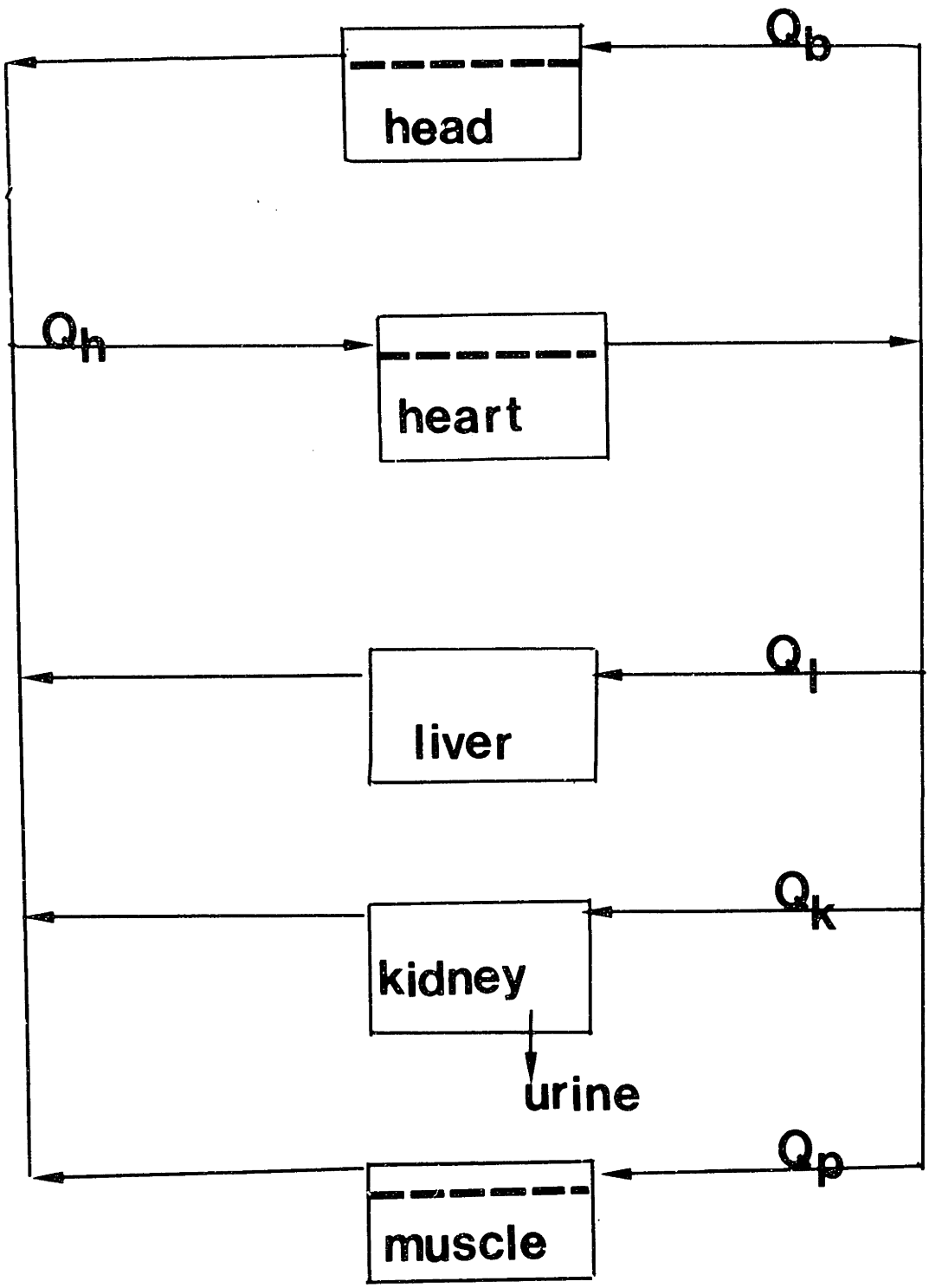

Figure 34

Diagram of Guyton's model for glucose distribution in a normal man.

TABLE 1

GLUCOSE MODEL PARAMETERS FOR A NORMAL (70Kg) MAN

Organ	Blood Volume[a] (liters)	Fluid Volume of Tissue[a] (liters)	Blood Flow Rate[b] (liter/min)	Transmembrane Equilibration Time (T_M) (min)
Heart, lung, central vessels and viscera	2.2	3.5	-	1.0
Central nervous system	0.2	0.2	0.7	0.2[c]
Skeletal muscle, adipose tissue	2.4	7.0	2.4	5.0
Liver	0.8	0.4	1.5	0[d]
Kidney	0.4	0.2	1.2	0[d]
Total	6.0	11.3	5.8	-

[a] From Reichard et al, 1961; Ikkos and Luft, 1957

[b] From Wade and Bishop, 1962

[c] From Cahill and Soeldner, 1969

[d] From Forbath and Hetenyi, 1966

difficult because of the lack of good experimental data, and one is forced to make estimates for heart and muscle. The muscle transcapillary equilibration times is one of the most crucial in the model because periphery accounts for almost two-thirds of the body's interstitial volume. Tiran et al (1975) estimated a muscle transmembrane equilibration time of seven minutes, while our estimate is five minutes.

A mass-balance equation is written for each compartment in the model. The equations for glucose distribution are:

$$\frac{V_B dC_B}{dt} = Q_B(C_H - C_B) + K_B A_B(C_{BT} - C_B) - r_{\substack{RBC \\ uptake}} \quad (2$$

$$\frac{V_{BT} dC_{BT}}{dt} = k_B A_B (C_B - C_{BT}) - r_{\substack{brain \\ uptake}} \quad (2$$

$$\frac{V_H dC_H}{dt} = Q_B C_B + Q_L C_L + Q_k C_k + Q_M C_M - Q_H C_H + k_H A_H(C_{HT} - C_H) - r_{\substack{RBC \\ uptake}} \quad (2$$

$$\frac{V_{HT} dC_{HT}}{dt} = k_H A_H (C_H - C_{HT}) - r_{\substack{heart \\ uptake}} \quad (3$$

$$\frac{V_k dC_k}{dt} = Q_k(C_H - C_k) - r_{\substack{RBC \\ uptake}} - r_{excretion} \quad (3$$

$$\frac{V_L dC_L}{dt} = Q_L(C_H - C_L) - r_{\substack{RBC \\ uptake}} + r_{\substack{glycogen \\ breakdown}} + r_{gluconeogenesis} - r_{\substack{glycogen \\ synthesis}} \quad (3$$

$$\frac{V_M dC_M}{dt} = Q_M(C_H - C_M) + k_M A_M(C_{MT} - C_M) - r_{\substack{RBC \\ uptake}} \quad (3$$

$$\frac{V_{MT} dC_{MT}}{dt} = k_M A_M (C_M - C_{MT}) - r_{\substack{muscle \\ uptake}} \quad (3$$

where:

Q = blood flow rate

kA = transmembrane glucose transport rate

C = glucose concentration

V = volume of compartment

r = rate of metabolism, uptake, excretion; each of these rates are discussed subsequently,

and the subscripts H, L, k, and M define the heart, liver, kidney and muscle blood respectively; the subscripts HT, MT, and BT define the heart, muscle, and brain tissue respectively. The resulting set of differential equations are solved simultaneously to simulate the concentration of glucose in each organ as a function of time. It should be emphasized that the simulation is based on an a-priori design of the model and experimentally determined organ volume, blood flow rates, transmembrane transport rates and rates of metabolism.

The transmembrane transport rate, $k_H A_H$, is calculated from blood, flow, capillary permeability and interstitial fluid volume (see Fig. 35) and has the units of volume/time:

$$\left(\frac{k_H A_H}{V_H}\right) = \frac{1}{T_M}$$

where T_M = transmembrane equilibration time (from Table 1).

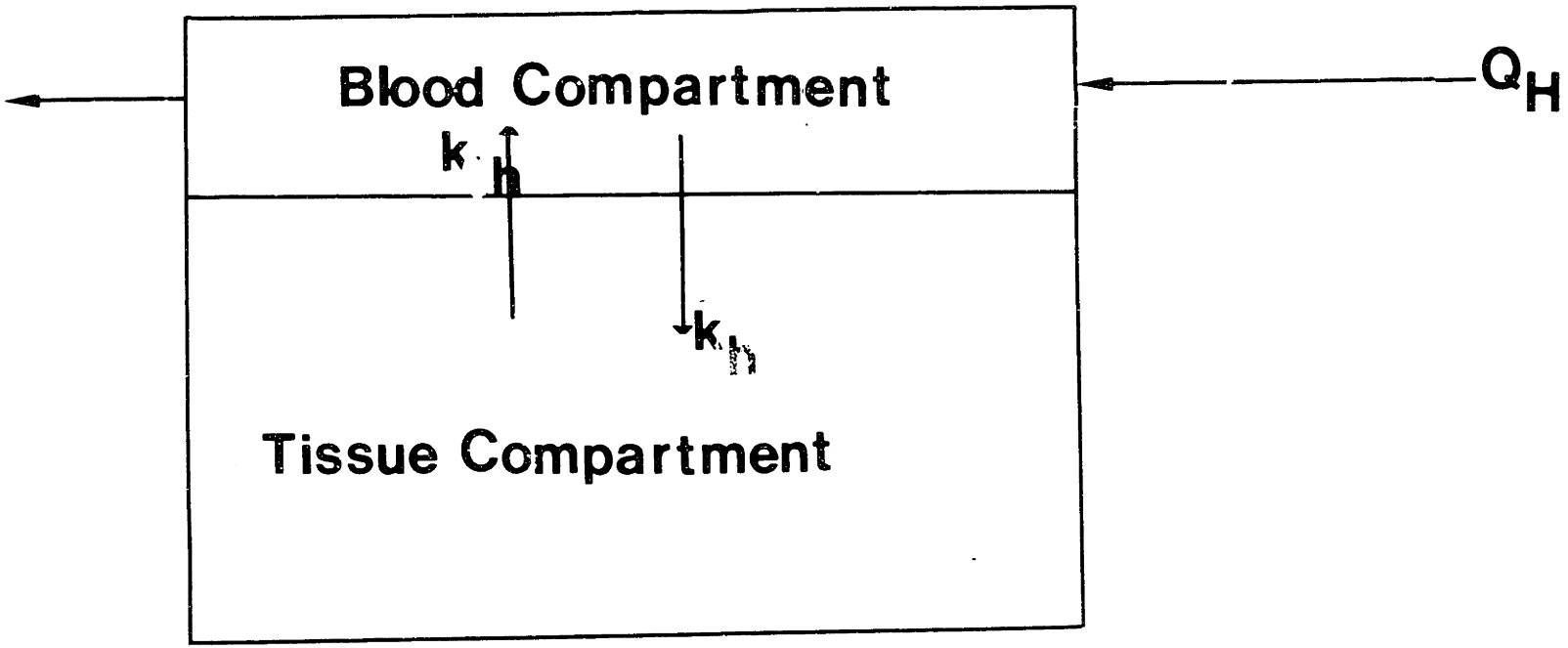

Figure 35

Diagram of a compartment (heart) in which blood and tissue regions are represented.

These are calculated similarly for the muscle and head compartments.

Table 2 presents the glucose flux (mg/min) in the basal postabsorptive state (after an overnight fast). The rate of red blood cell uptake of glucose, r_{RBC} assumed constant at 10 mg/min and for each organ is calculated by

$$r_{\substack{RBC \\ utilization}} = 10 \text{ mg/min} \times \frac{V_H}{V_T}$$

where V_T is the total blood volume, and V_H is the volume of the organ (in this case the heart).

Both the heart and brain rate of utilization of glucose, $r_{heart\ uptake}$ and $r_{brain\ uptake}$, are variable under certain conditions, however their absolute change is small enough that in the model they are considered constant (see Table 2).

The rate of glucose excretion by kidney, $r_{urinary\ excretion}$, is a function of the renal blood glucose concentration. In agreement with known physiology, the urinary excretion in the model begins at 180 mg/dl and increases linearly 230 mg/min for every 180 mg/dl rise in renal glucose concentration.

The rate of muscle glucose uptake in equation (42) is a multiplicative function of (a) the effect of muscle glucose concentration on muscle glucose uptake (EGMGU), (b) the effect of muscle insulin concentration on muscle glucose uptake (EIMGU). In addition, the decrease in muscle glucose uptake that occurs during hypoglycemia (c) is represented by a function dependent on heart glucose concentrations. At heart glucose concentrations below fasting (80 mg/dl) this function (EHGMGU) acts to decrease muscle glucose uptake. To determine the rate of muscle uptake

TABLE 2

GLUCOSE PRODUCTION AND UPTAKE IN THE BASAL POSTABSORPTIVE STATE

	Glucose Flux (mg/min)	Reference
Liver glucose production	160	Forbath and Hetenyi, 1966
Central nervous system uptake	100	Kety, 1957
Red blood cell uptake	10	Prankerd, 1961
Peripheral uptake	30	Zierler and Rabinowitz, 1963
Heart and central visceral uptake	20	

of glucose, the basal rate of glucose uptake (30 mg/min) is multiplied by (a),(b), and (c) which are found from Fig. 36, 37, and 38, respectively. In other words these effects are multiplicative factors which increase or decrease the rate of muscle glucose uptake depending on the glucose and insulin concentrations. Instead of fitting an analytic function to these nonlinearities, the factors are found by linear interpolation of the curves. The functions are derived from experiments using human forearm preparations (Rasio et al 1972; Morgan et al 1961, Wick et al 1953). The experimental data also indicates that EIMGU and EHGMGU act via a three-minute time delay. Therefore:

$$r_{\substack{\text{muscle}\\ \text{glucose}\\ \text{uptake}}} = 30 \text{ mg/min} \times U(t - 3.0)(EIMGU \times EHGMGU) \times EGMGU$$

where $U(t - 3.0)$ represents a three-minute transport delay.

From equation (32), the rate of accumulation of glucose in the liver is equal to the rate of flow of glucose into the liver, plus the rate of glycogen breakdown, plus the rate of gluconeogenesis, minus the rate of red blood cell uptake and glycogen synthesis. The rate of red blood cell uptake has already been discussed. The model assumes that total liver glycogen content in a normal man after an overnight fast averages 35 grams (Sokal and Gerasi 1959). The basal rate of glycogen breakdown averages 100 gm/min. Insulin is the primary signal that is responsible for turning off glycogen breakdown and allowing glycogen synthesis to occur.

In the model, the rates of glycogen synthesis, glycogen breakdown, and gluconeogenesis are functions of the liver insulin concentration

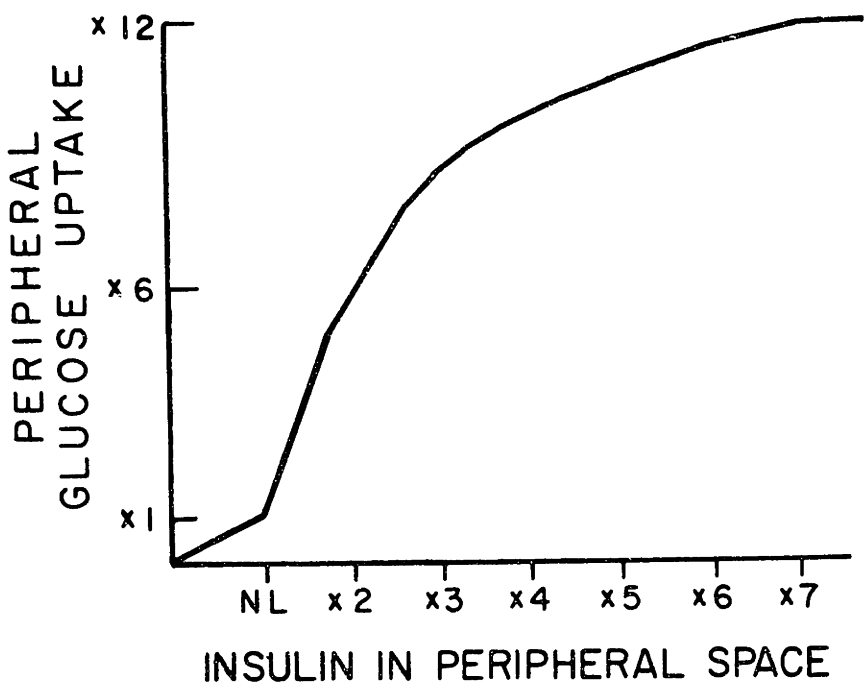

Figure 36

Peripheral glucose uptake as a function of insulin concentrations.

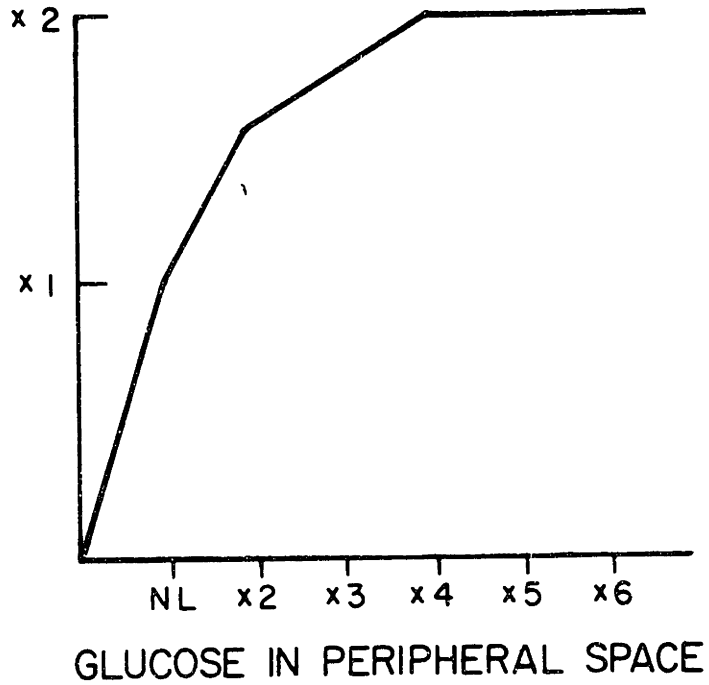

Figure 37

Peripheral glucose uptake as a function of glucose concentrations.

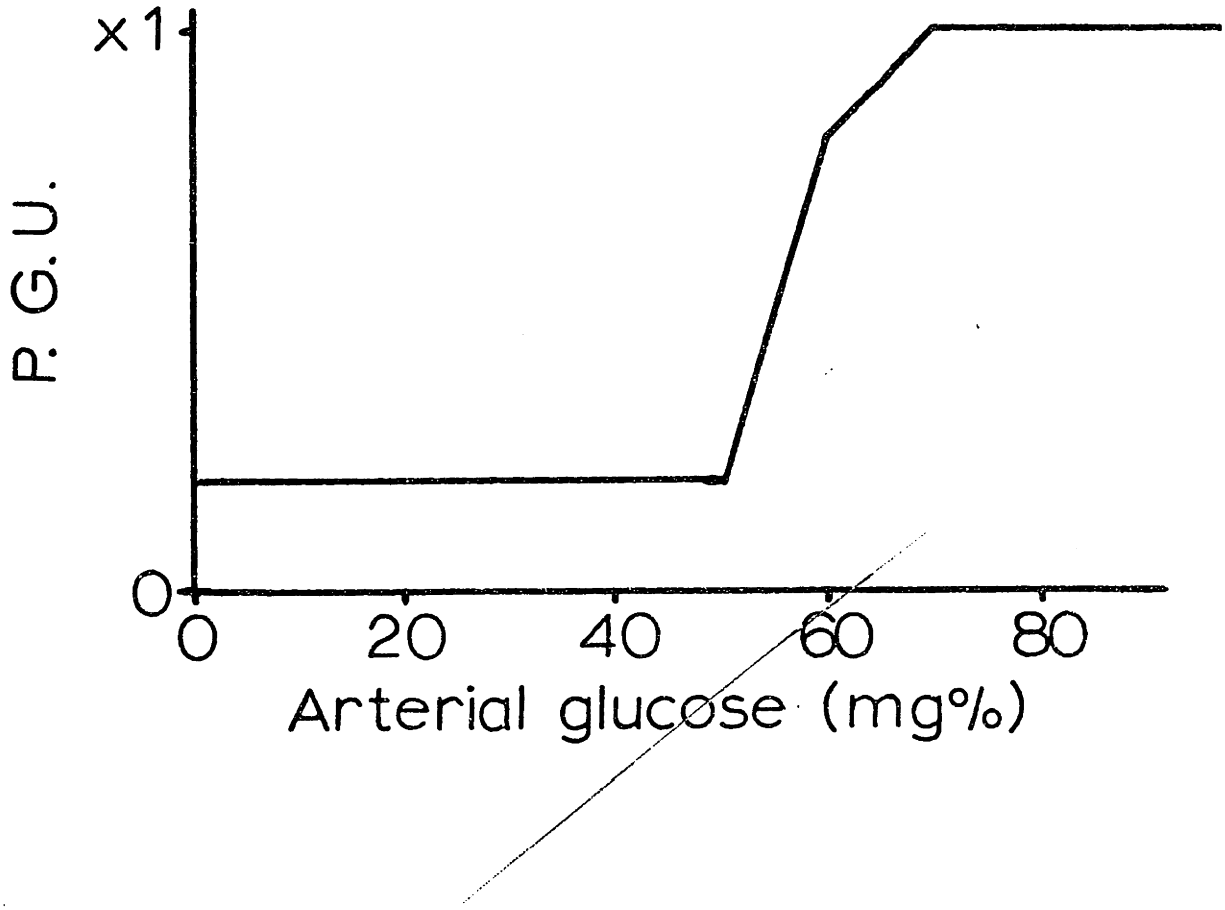

Figure 38

Peripheral glucose uptake as a
function of heart glucose concentrations.

(see Figs. 39-43). In addition to the effect of liver insulin concentration on liver glucose metabolism, the decrease in glycogen synthesis and increase in glycogen breakdown and gluconeogenesis that occurs during hypoglycemia are represented by a function dependent on heart glucose concentrations. At heart glucose concentrations less than fasting, this function increases glycogen breakdown and gluconeogenesis and decreases glycogen synthesis. Once glycogen synthesis occurs, it can be augmented up to two-fold by liver glucose concentrations (see Fig. 44). There is a three-minute transport delay in the action of glucose and insulin on all these rates.

The circulatory design of the model for insulin distribution is shown in Fig. 45. Table 3 lists the plasma volumes and transmembrane equilibration times used in the simulation. Because the central nervous system is not a major site for the disposition of insulin (as is the case with glucose) it has been included in the central (heart) compartment. As can be seen from Table 3, the transmembrane equilibration times for glucose in heart and muscle are the same order as the blood-flow rates into these organs. The liver and kidney tissue are major sites for the degradation of insulin. Therefore each of these organs is represented by a blood and tissue compartment. The mass-balance equations for insulin are:

$$\frac{V_H dC_H}{dt} = Q_L C_L + Q_k C_k + Q_p C_p - (Q_B + Q_L + Q_k) C_H + k_H V_H (C_{HT} - C_H)$$

$$\frac{V_{HT} dC_{HT}}{dt} = k_H V_{HT} (C_H - C_{HT})$$

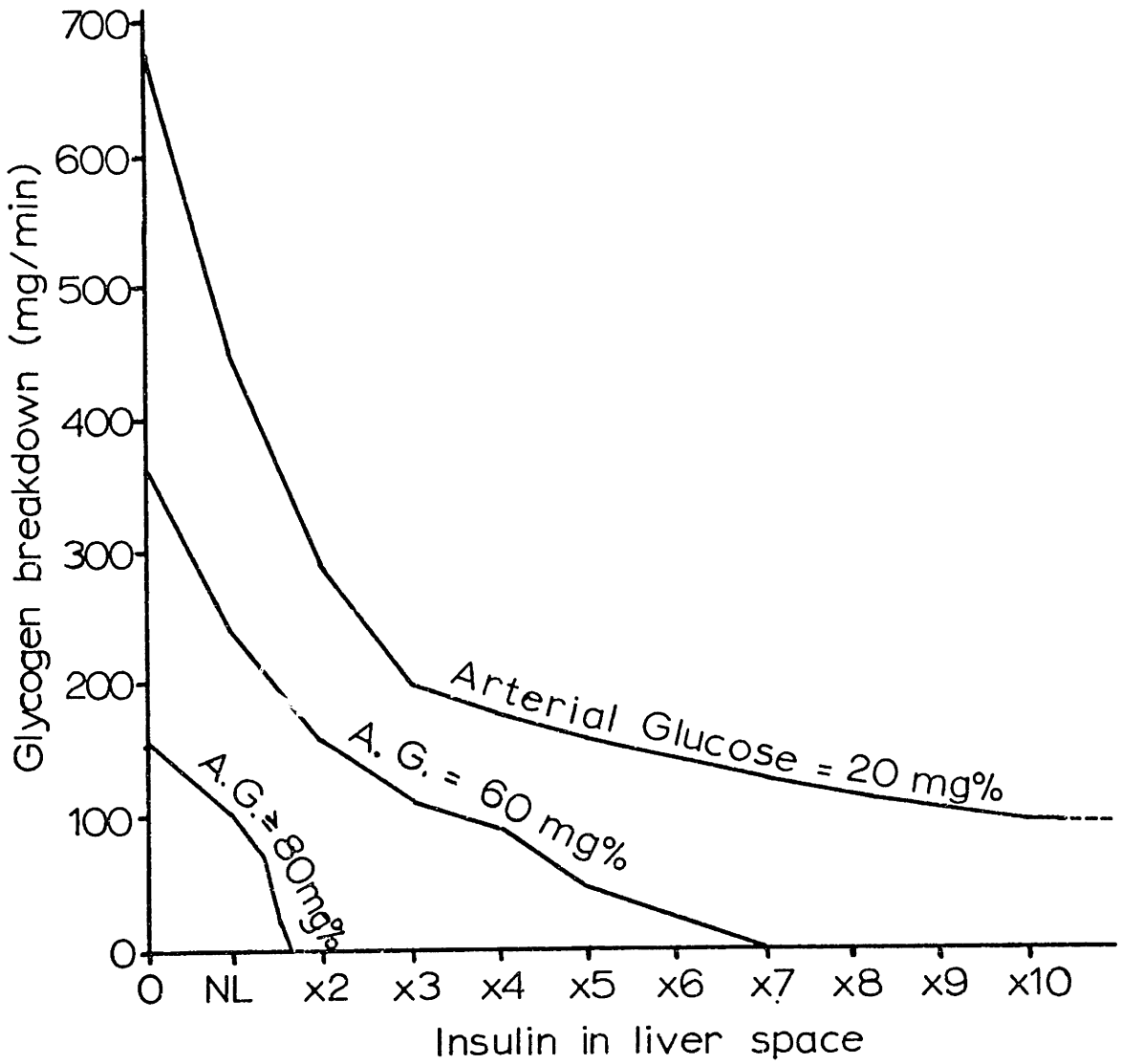

Figure 39

The influence of heart glucose concentration on the rate of glycogen breakdown.

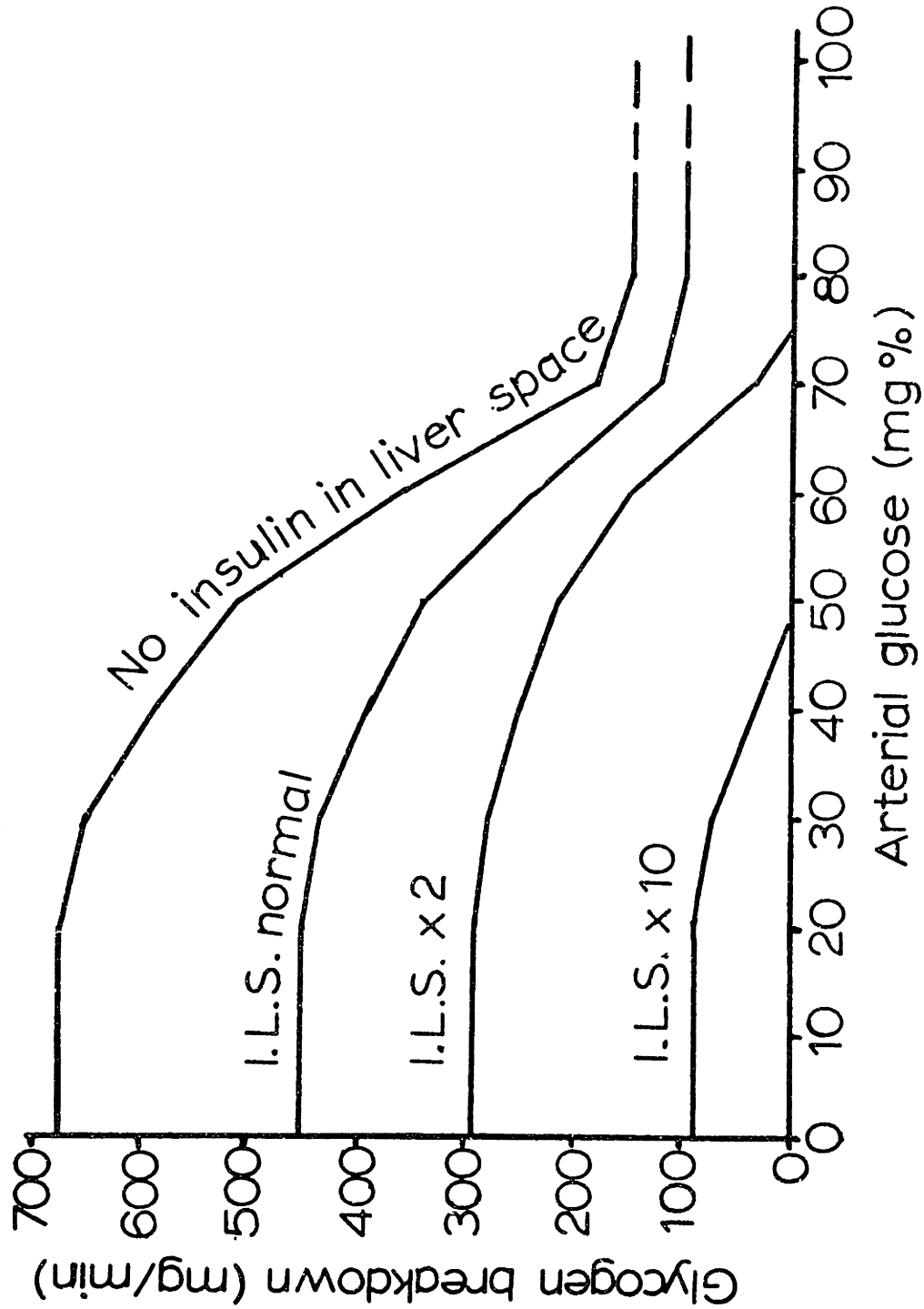

Figure 40

The influence of insulin concentration on the rate of glycogen breakdown.

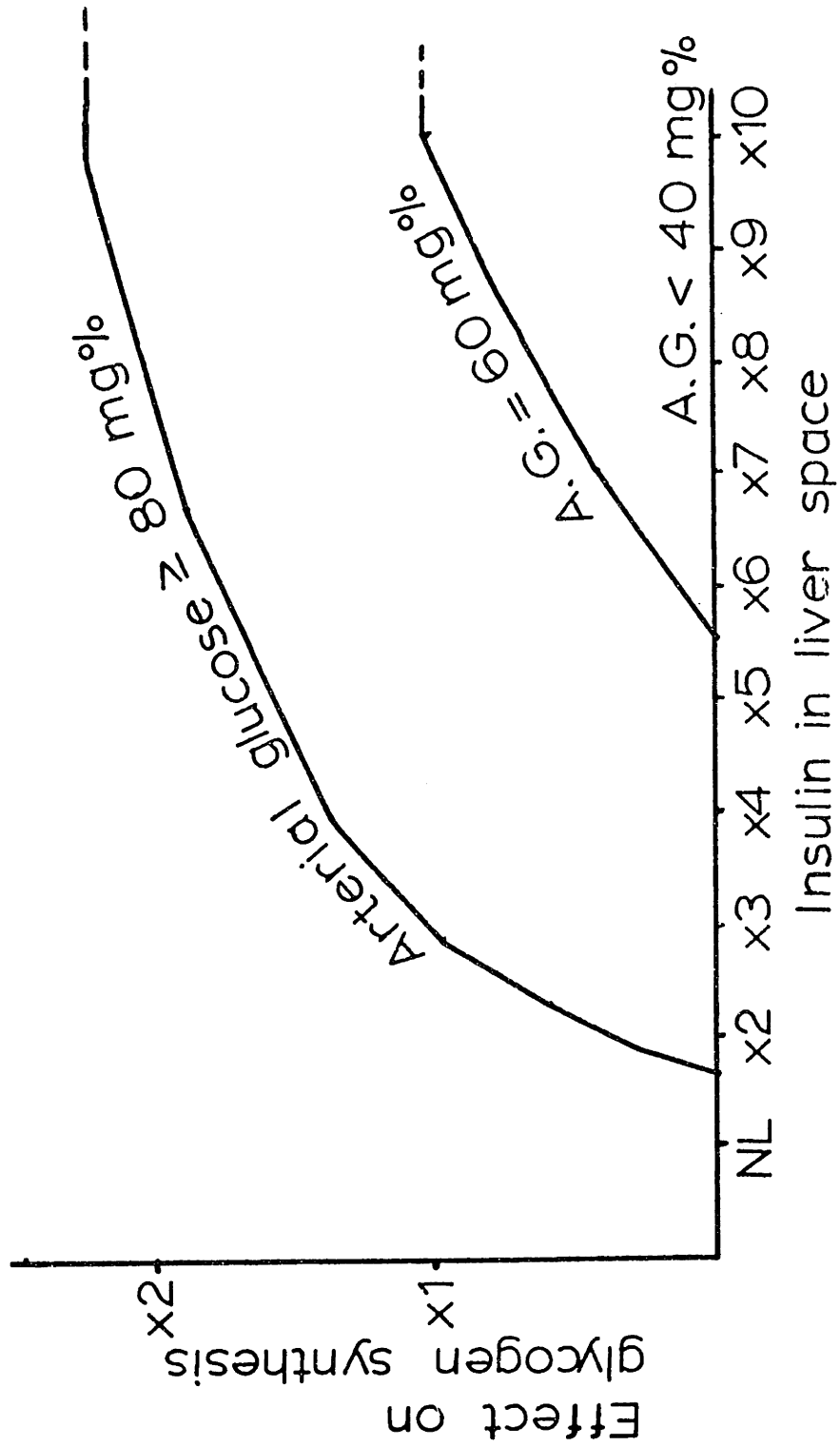

Figure 41

The influence of insulin concentration on the rate of glycogen synthesis.

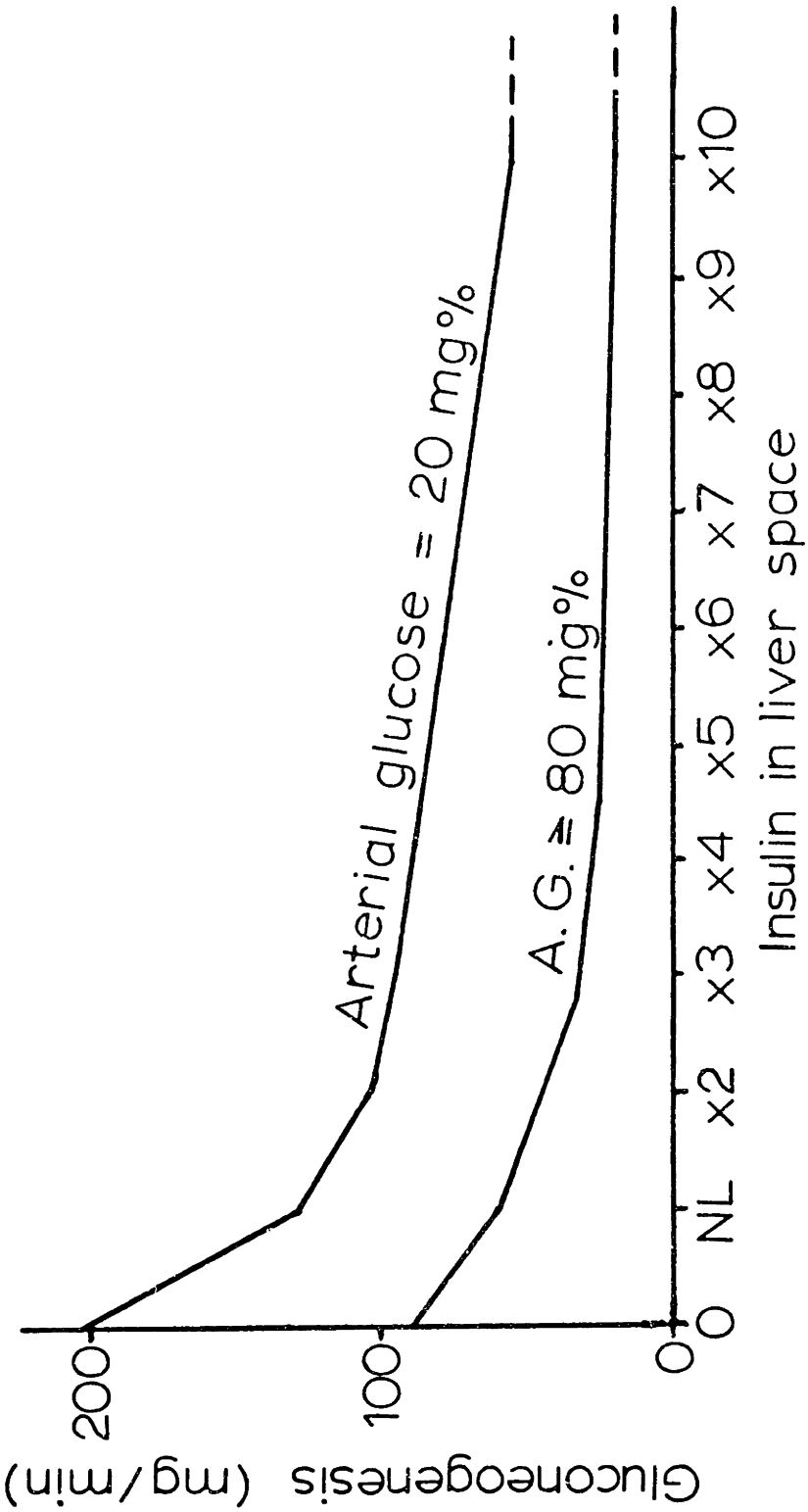

Figure 42

The influence of insulin concentration on gluconeogenesis.

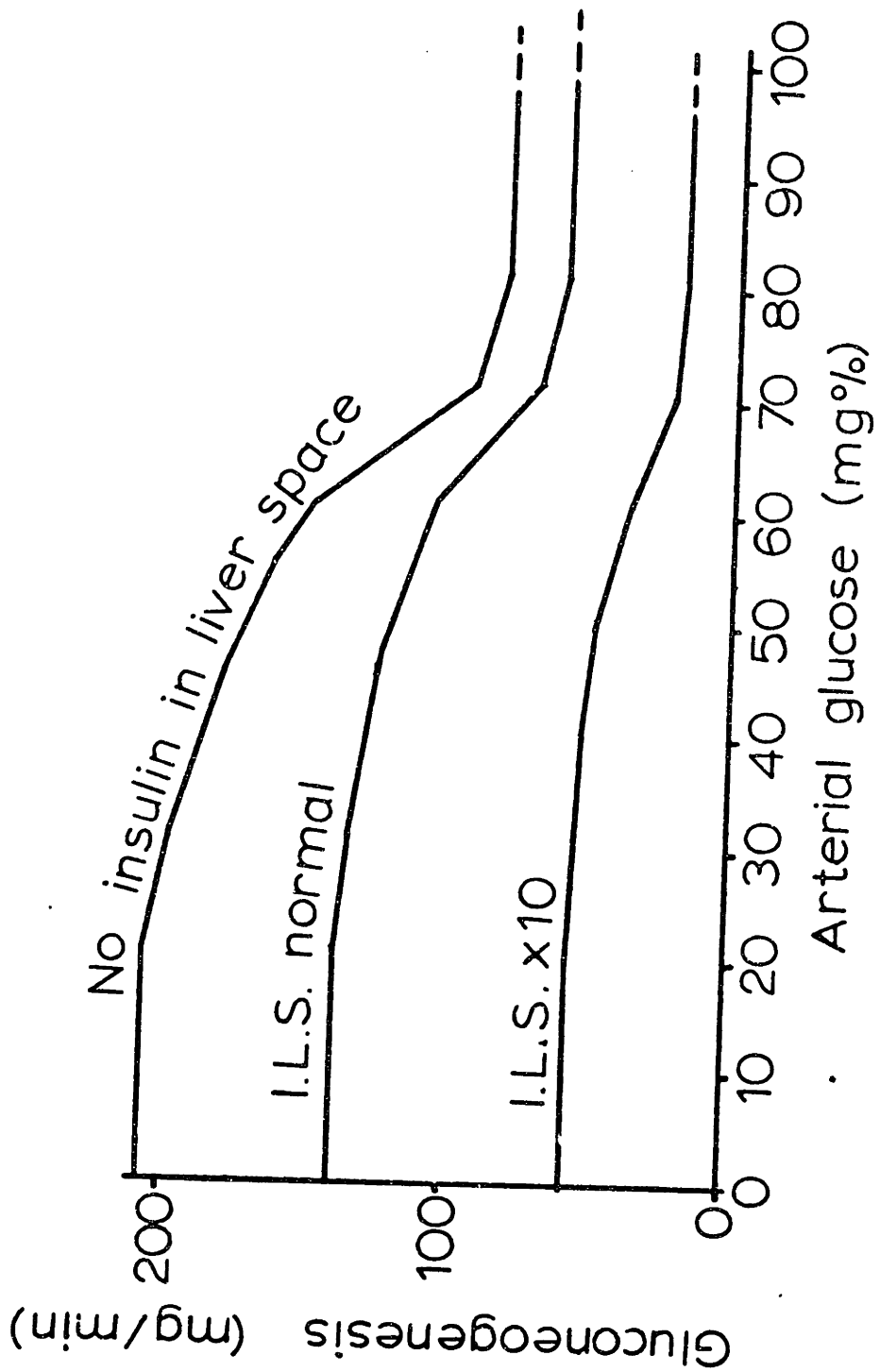

Figure 43

The influence of heart glucose concentration on gluconeogenesis.

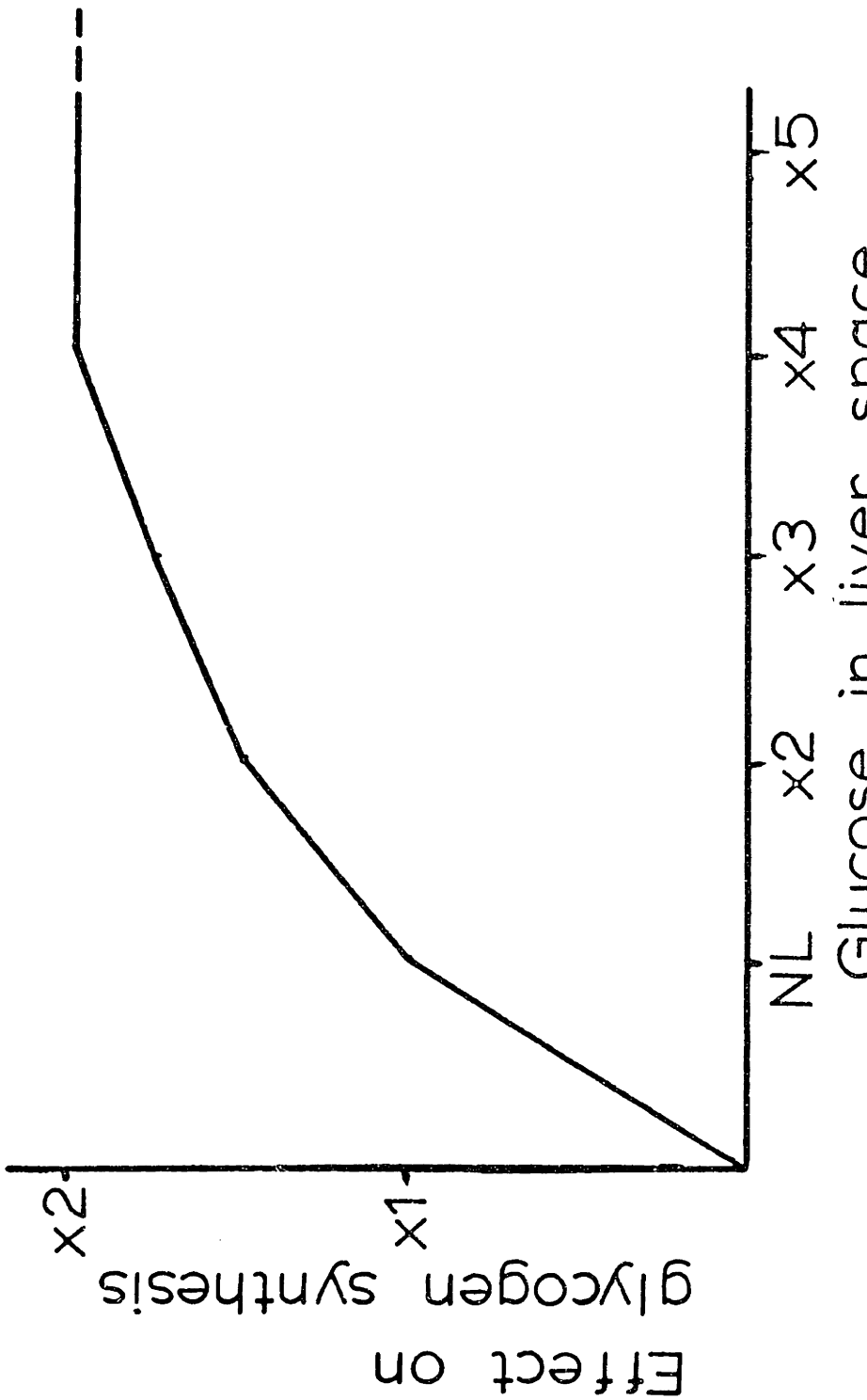

Figure 44

The influence of liver glucose concentration on glycogen synthesis.

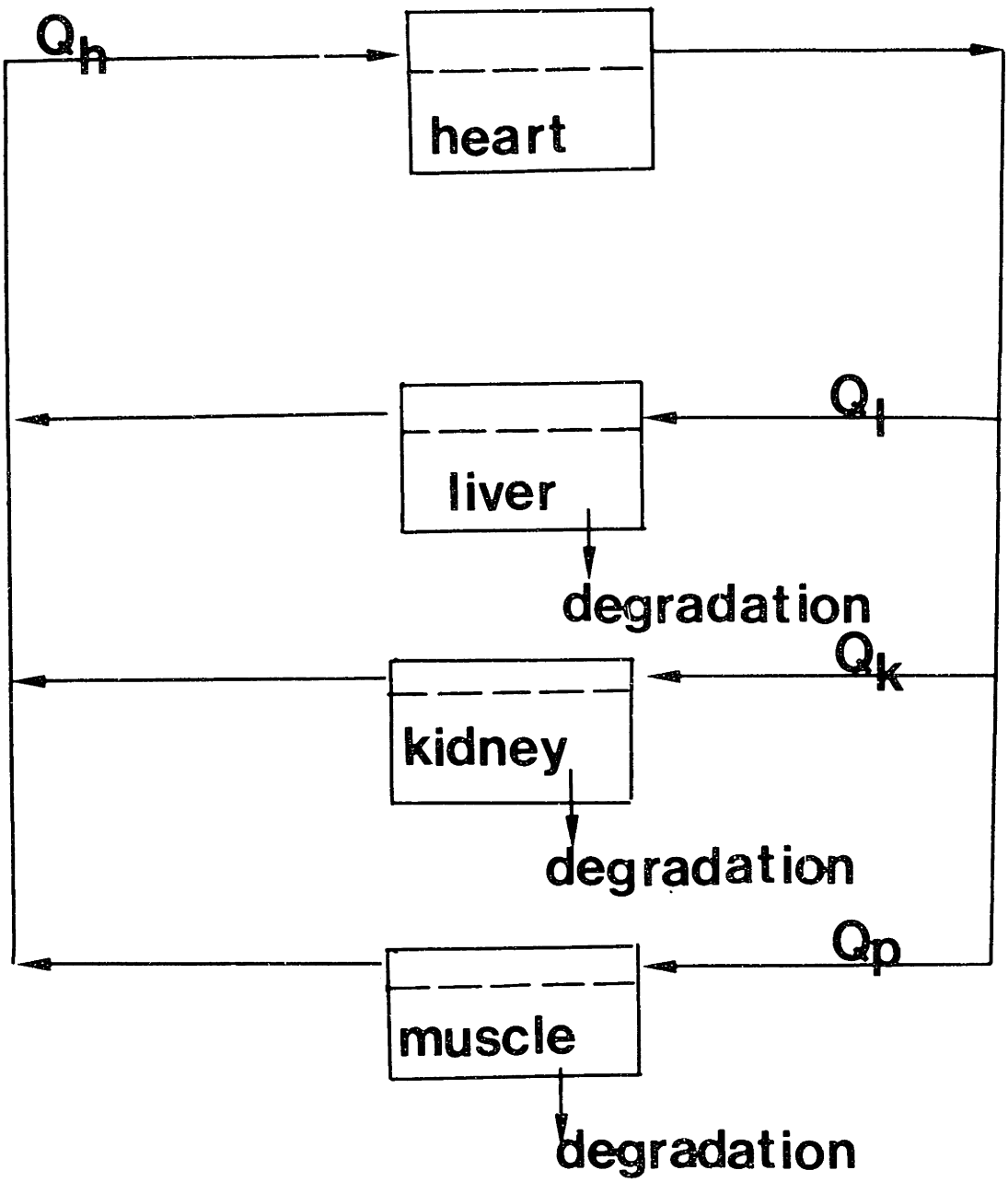

Figure 45

Diagram of Guyton's model for insulin distribution in a normal man.

TABLE 3

INSULIN MODEL PARAMETERS FOR A NORMAL (70 Kg) MAN

Tissue	Plasma Volume (liters)	Transmembrane Equilibration Time (min)
Heart, lung, head, and central vessels	1.44	10.0
Peripheral Tissues	1.44	20.0[c]
Liver	0.48	0.1[d]
Kidney	0.24	0.1[d]
Total	3.60	-

[a] From Wade and Bishop, 1962

[b] From Reichard et al, 1961; Ikkos and Luft 1957

[c] From Orskov and Christensep, 1969

[d] From Genuth, 1972

$$\frac{V_L dC_L}{dt} = Q_L(C_H - C_L) + k_L A_L(C_{LT} - C_L) + (IRR)V_L$$

$$\frac{V_{LT} dC_{LT}}{dt} = k_L A_L(C_L - C_{LT}) - r_{degradation}$$

$$\frac{V_k dC_k}{dt} = Q_k(C_H - C_k) + k_k A_k(C_{kT} - C_k)$$

$$\frac{V_{kT} dC_{kT}}{dt} = k_k A_k (C_k - C_{kT}) - r_{degradation}$$

$$\frac{V_M dC_M}{dt} = Q_M(C_H - C_M) + k_M A_M(C_{MT} - C_M)$$

$$\frac{V_{MT} dC_{MT}}{dt} = k_M A_M (C_M - C_{MT}) - r_{degradation}$$

where Q = plasma flow rate

kA = transmembrane insulin transport rate

C = insulin concentration

V = volume of compartment

r = rate of insulin degradation

IRR = insulin release rate

and the subscripts are defined as for glucose.

In the model, the liver, kidney, and muscle degrade one-half, one-third, and one-sixth, respectively, of the insulin presented to them, regardless of the plasma concentration of insulin. Changes in blood flow would change these fractions, but the model flows are constant. These rates of clearance are consistent with published values (Genuth 1972).

No good quantitative model exists for describing the physiological dynamics of insulin secretion (IRR). Before discussing the model used in Guyton's simulation several other models upon which it is based will be presented.

Bergman and Urquhart (1971) have developed a hypothesis for the secretion of insulin in response to glucose based on the following view of insulin secretion as shown in Fig. 46.

$$\dot{a} = G - .025a$$

$$\dot{I}_p = 0.01a - 0.09I_p$$

$$\dot{b} = .021I_p - .11b$$

$$\dot{I}_g = .02b - (.07 + .02G)I_g + 0.021$$

$$\dot{I}_m = I_g(.015 + .015G) - I_m(1.45 + .75d)$$

$$c = \begin{cases} 4.1G & 0 \leq G \leq .25 \\ 2.3G + .59 & G > .25 \end{cases}$$

$$\dot{d} = 1.6g - 6.0d$$

$$\text{secretion} = I_m(1.45 + .75d)$$

Granular insulin (I_g) is formed via a relatively slow combination of "source" molecules into a precursor molecule, I_p, which is then transformed (via intermediate "b") into I_g, granular insulin. Granular insulin in transformed into insulin in a readily releasable form, I_m. Insulin, I_m, can be released at the cell membrane. Glucose is postulated to have multiple interactions in stimulating the secretion of insulin: (1) Glucose increases the production rate of I_p. The effect is mediated through the production of an intermediate "a," which acts to increase the rate of combination of source molecules into I_p. (2) The rate at

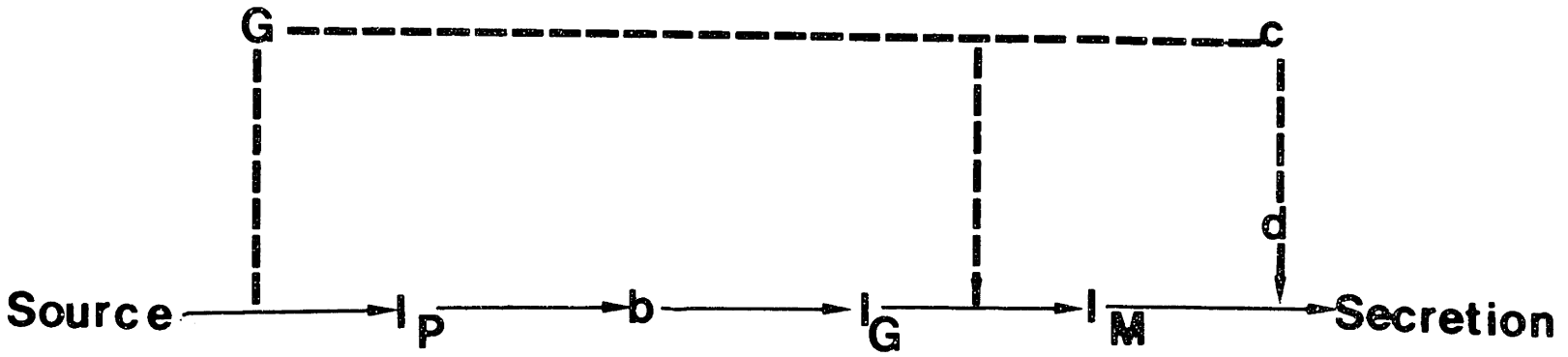

Figure 46

Model of beta-cell secretion of insulin in response to glucose (from Bergman and Urquhart, 1971).

which granular insulin, I_g, is converted to I_m is also glucose dependent. (3) Lastly, glucose stimulates the transport of insulin out of the cell via intermediates "c" and "d." The production of "c" is assumed to follow saturation kinetics. The constants are empirically derived to fit the experimental data from isolated perfused pancreas studies.

The model steps which describe the production of insulin are a reasonable approximation of the known biochemical sequence leading to insulin secretion (see Section IV). However, there is no experimental evidence to substantiate the rates of the steps, which are chosen to fit the data. In addition, the sequence by which glucose stimulates insulin production and secretion is also only speculative. However, the model does accurately simulate experiments in which an isolated perfused pancreas is presented with a variety of glucose stimuli (e.g. ramp function, step function, constant infusion).

Grodsky (1972) and Licko (1973) have proposed a "threshold secretory mechanism" to account for insulin secretion in response to a glucose stimulus. Their hypothesis proposes that insulin is not stored in a homogeneous form, but as packets with a distribution of thresholds to glucose. These packets respond quickly, releasing insulin when their threshold is exceeded.

Grodsky and Licko assume that insulin is stored as a packet, representing a group of insulin molecules. For every packet there is a certain threshold θ; such that a stimulus effectively acts on those packets whose thresholds are below the stimulus concentration, G. In other words, there exists a threshold density function $E(\theta,t)d\theta$, representing the number of packets in a threshold internal $(\theta,\theta+d\theta)$

and therefore the amount of insulin releasable by a shift in glucose concentration from $G = \theta$ to $G = \theta + d\theta$. The total releasable amount of insulin releasable at a given glucose concentration G, is then

$$X(G(t),t) = \int_{o}^{G(t)} E(\theta,t)d\theta \tag{35}$$

The rate of release of insulin in response to a glucose stimulus is

$$\dot{X}(G(t),t) = \int_{o}^{G(t)} \dot{E}(\theta,t)d\theta + E(G(t),t)\ \frac{dG(t)}{dt} \tag{36}$$

Equation (35) indicates that the rate of change of insulin secretion is proportional to the glucose concentration as well as the rate of change of glucose concentration, a fact we know to be true from experiments. However, it represents only a loss term; there must be a mechanism by which insulin packets are refilled and redistributed, $R[G(t),t]$. The complete function for insulin secretion is then:

$$\dot{X}[G(t),t] = \int_{o}^{G(t)} \dot{E}(\theta,t)\ d\theta + R[G(t),t] + E\ [G(t),t]\ \frac{dG(t)}{dt} \tag{37}$$

To determine the functions E and R, Grodsky designed a set of experiments to measure insulin secretion during a single-step continuous infusion at different absolute concentrations. The result is shown in Figs. 47 and 48, in which insulin secretion is plotted as a function of glucose concentration during the early phase (initial spike) and second phase of release. Since G(t) is a constant infusion of magnitude, G, the third term in (37) is zero. To obtain an analytical expression for E, they assumed that during the early phase of insulin release the rate of replenishment was zero and the total amount of insulin release,

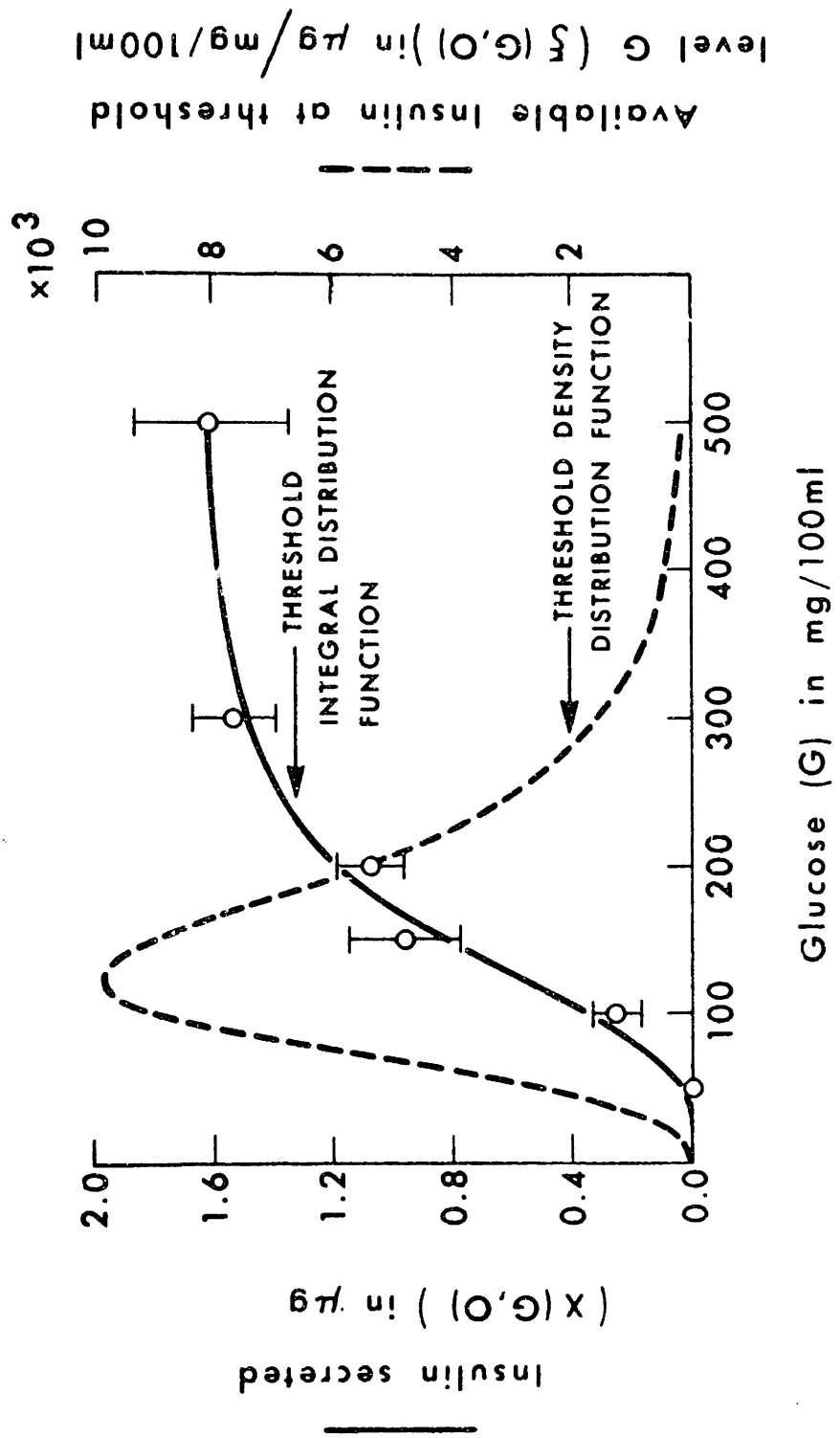

Figure 47

Total insulin secreted during the early phase (min 1-10)
(from Grodsky, 1972).

X(G,t) was given by Fig. 48. The analytical representation of X(G,t) was approximated by:

$$X(G,t) = \int_{o}^{G} E(\theta,t)\, do = -mX_{max} \frac{G^k}{C + G^k}$$

where X_{max} is the maximum amount of releasable insulin (1.65 μg) and m, C, and k are constants: $m = 0.62\ min^{-1}$, $C = 1.51 \times 10^7$, $k = 3.3$. They then assumed that for times greater than ten minutes (the duration of the early phase of insulin secretion), the rate of insulin release was equal to the steady-state replenishment rate, $R(G,\infty)$. The analytical approximated of $R(G,\infty)$ from Fig. 48 was:

$$R(G,\infty) = \frac{0.5\ G^{10}}{8.875 \times 10^{21}\ G^3 + 3.5 \times 10^6\ G^7 + G^{10}}$$

and the rate of replenishment as a function time was assumed to be:

$$R\ (G,t) = (1 - e^{\alpha t})\ R(G,\infty)$$

where $\alpha = 0.034\ min^{-1}$.

Making these substitutions (37) becomes:

$$\dot{X}[G(t),\ t] = \frac{-1.023\ G^{3.5}}{1.51 \times 10^7 + G^{3.5}} + \frac{0.5\ (1 - e^{-0.034t})\ G^{10}}{8.875 \times 10^{21} + 2.25 \times 10^{15}\ G^3 + 3.5 \times 10^6\ G^7 + G^{10}} + \left[\frac{8.22 \times 10^7\ G^{2.3}}{(1.51 \times 10^7 + G^{2.3})^2}\right] \frac{dG}{dt}$$

The rate of change of glucose concentration, $\frac{dG}{dt}$, is determined by the type of stimulus (e.g. ramp, $\frac{dG}{dt}$ = constant). The model accurately simulates experiments in which an isolated perfused pancreas is presented with various glucose stimuli.

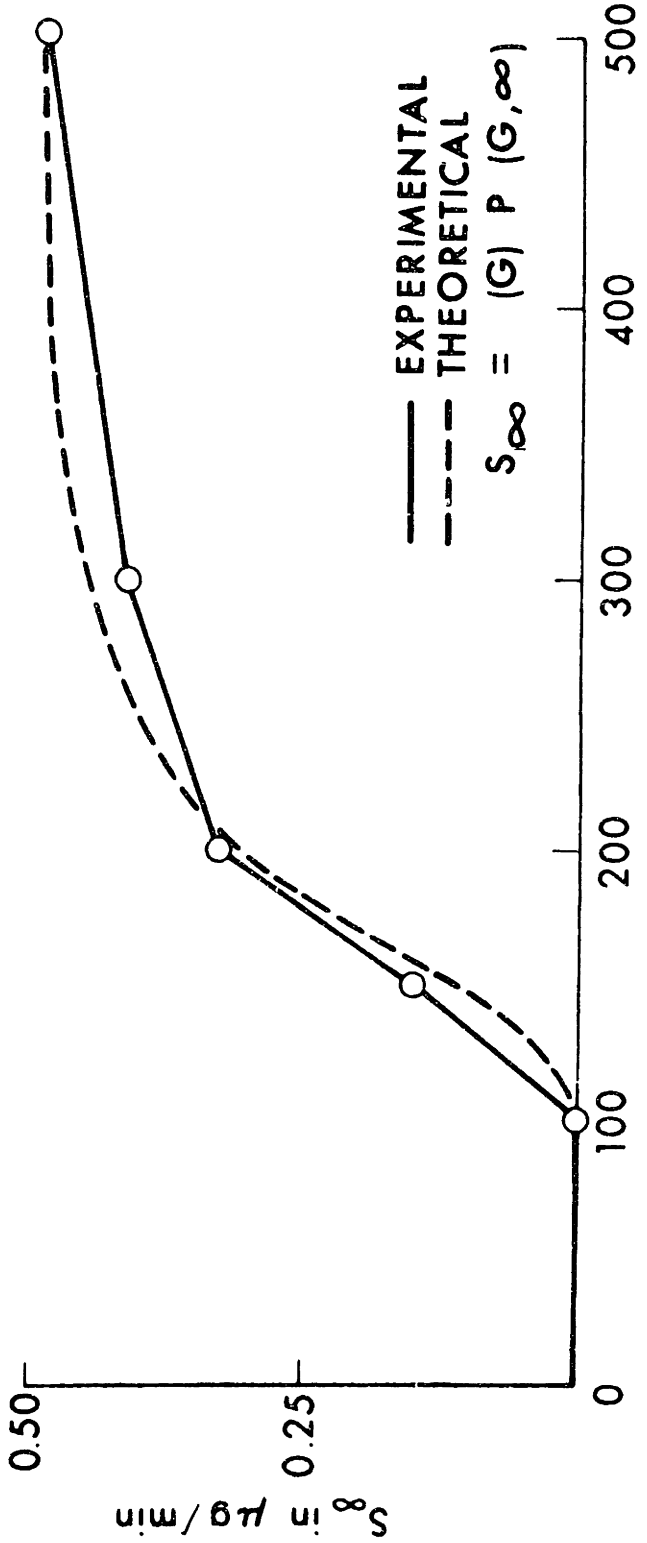

Figure 48

Maximum secretion rate of insulin release during the second phase as a function of glucose concentration.

Guyton has proposed a theory for the synthesis and secretion of insulin which is incorporated in the model. The following equations describe the synthesis and storage of insulin:

$$G = 0.01\ C_H - 102\ G - .5\ G_m$$

$$G_m = 2\ G - 1.5\ G_m$$

$$M_{RNA} = M_{RNA}\ (EGMRNA) - .05$$

$$I_p = Source - .05\ I_p$$

$$I_G = .05(I_p - I_G)$$

$$I_S = .05I_G - (EGID)\ ISTF + \frac{(HSI + RSI)}{TDEG}$$

(The terms are defined in Fig. 49. The units for insulin and glucose concentrations are μU/ml and mg/dl, respectively.)

As shown in Fig. 49, proinsulin, I_p is formed from "source" molecules (i.e. amino acids) and transformed in the Golgi apparatus to I_g, insulin. Insulin, I_g, is then transported out of the Golgi apparatus and stored as I_S, in a readily releasable form. The beta cell glucose concentration is postulated to affect insulin secretion by increasing the amount of MRNA available to synthesize proinsulin from source molecules. The effect of glucose on MRNA is shown in Fig. 50. A metabolite of glucose, G_m is included because glucose is postulated to act via an intermediate and not to directly cause insulin release. The release of insulin is described by:

$$\dot{HSI} = \left(\frac{HSE}{HSE+RSE}\right)(EGID)(ISTF + \left(\frac{RSI}{RSI+RSE}\right) MAX(A,0) + \left(\frac{HSI}{HSI+HSE}\right) MIN(0,A) - \frac{HSI}{TDEG}$$

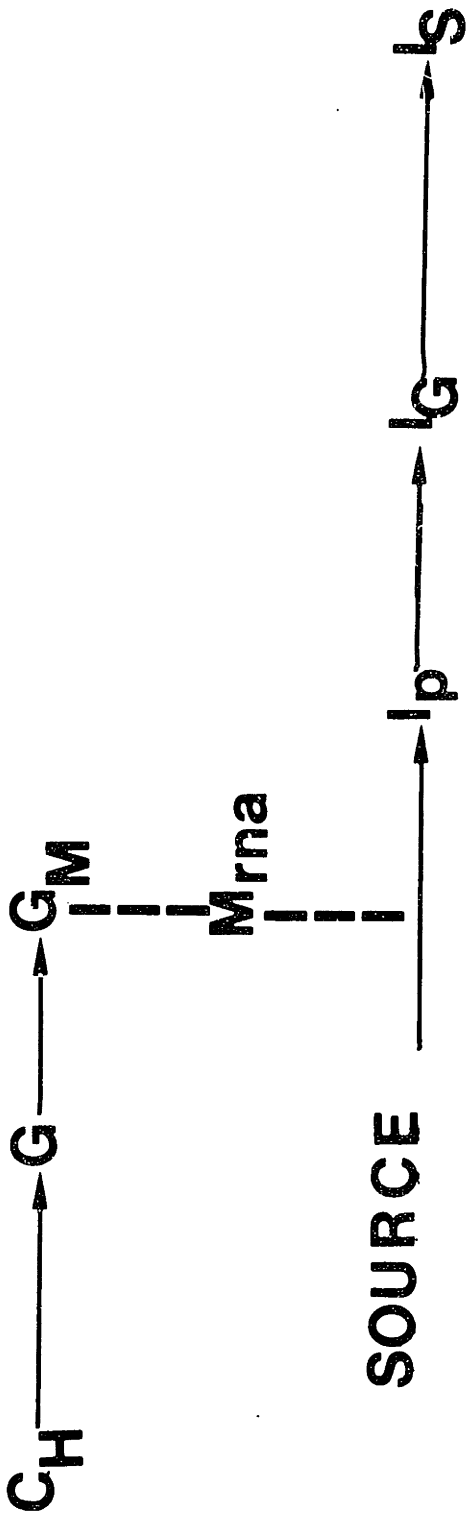

Figure 49

Model of beta-cell synthesis and storage of insulin.

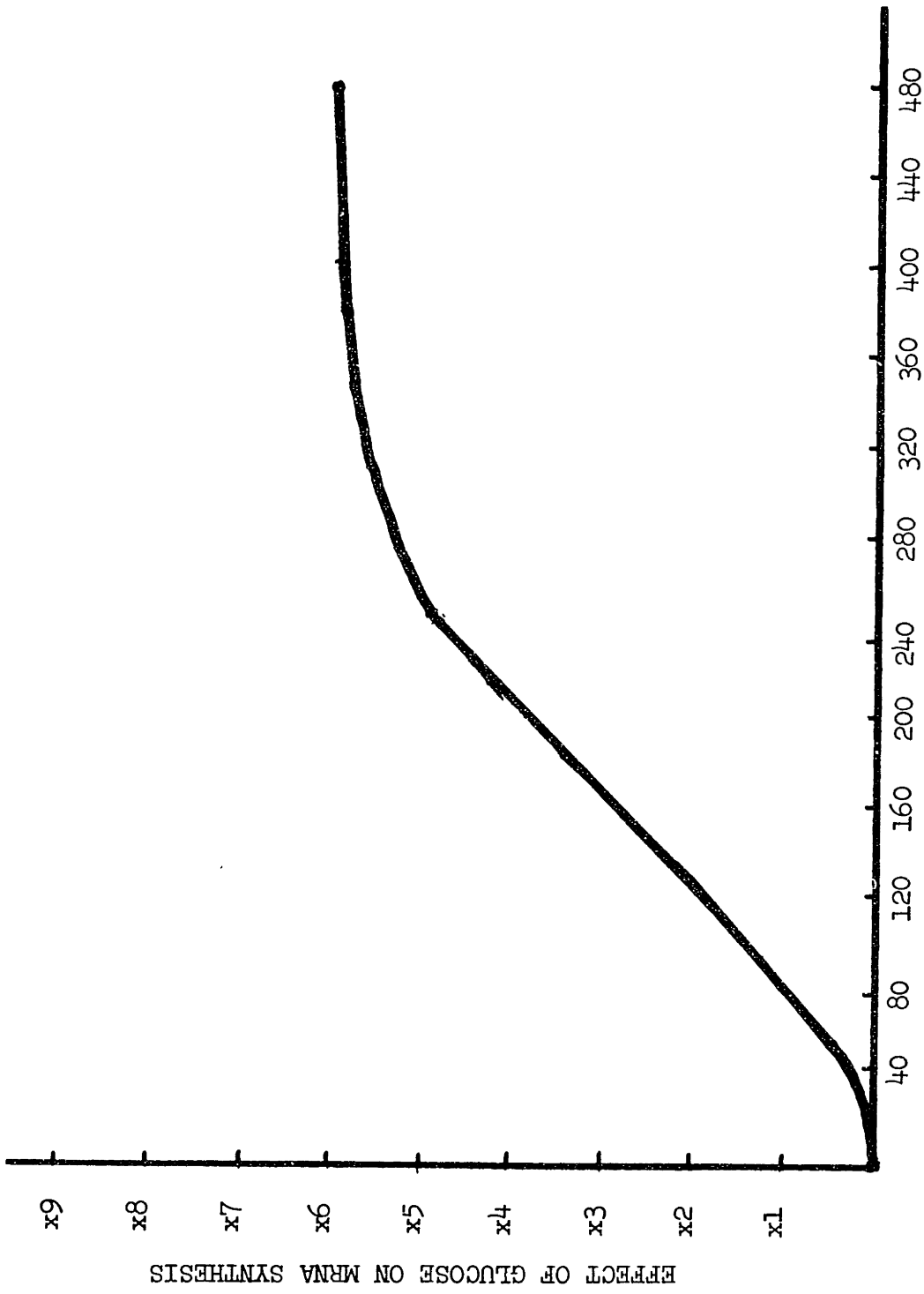

Figure 50

The effect of heart glucose concentrations on the rate of MRNA synthesis.

$$= (HSE+HSI)\ EGID - \left(\frac{HSE}{HSE+RSE}\right)(EGID)(ISTF) + \left(\frac{RSE}{RSI+RSE}\right) MAX(A,O) + \left(\frac{HSE}{HSI+HSE}\right) MIN(O,A) - \frac{HSE}{TDEG}$$

$$= \left(\frac{RSE}{HSE+RSE}\right)(EGID)\ ISTF - \left(\frac{RSI}{RSI+RSE}\right) MAX(A,O) - \left(\frac{HSI}{HSI+HSE}\right) MIN(O,A) \quad \frac{RSE}{TDEG} - IRR$$

$$R = (RSE+RSI)\ EGID - \left(\frac{RSE}{HSE+RSE}\right)(EGID)\ ISTF - \left(\frac{RSE}{RSI+RSE}\right) MAX(A,O) - \left(\frac{HSE}{HSI+HSE}\right) MIN(O,A) - \frac{RSE}{TDEG} + IRR$$

$$A = (RSI+RSE)(1-DISRHS) + HSI + HSE$$

$$IRR = 2.5\ RSI$$

Where: HSI = holding sites insulin occupied

HSE = holding sites empty

RSI = releasing sites insulin-occupied

RSE = releasing sites empty

TDEG = degradation time = 45 minutes

IRR = insulin release rate (μU/ml/min)

and the functions ISTF, DISRHS, and EGID are shown in Figs. 51,52,53 respectively. The model for insulin secretion in response to glucose is based on a modification of Grodsky's threshold theory: The response to glucose is mediated by a set of holding (threshold not reached) and releasing (threshold surpassed) sites for insulin. As glucose concentrations rise, a certain fraction of holding sites are converted to releasing sites, which immediately secrete the insulin contained within them. The function, DISRHS (distribution of releasing-holding sites) determines the fraction of releasing sites converted as a function of glucose concentration. This function was determined by calculating the amount of insulin released during the initial peak of insulin secretion as a function of glucose, during an IVGTT. The function ISTF (insulin

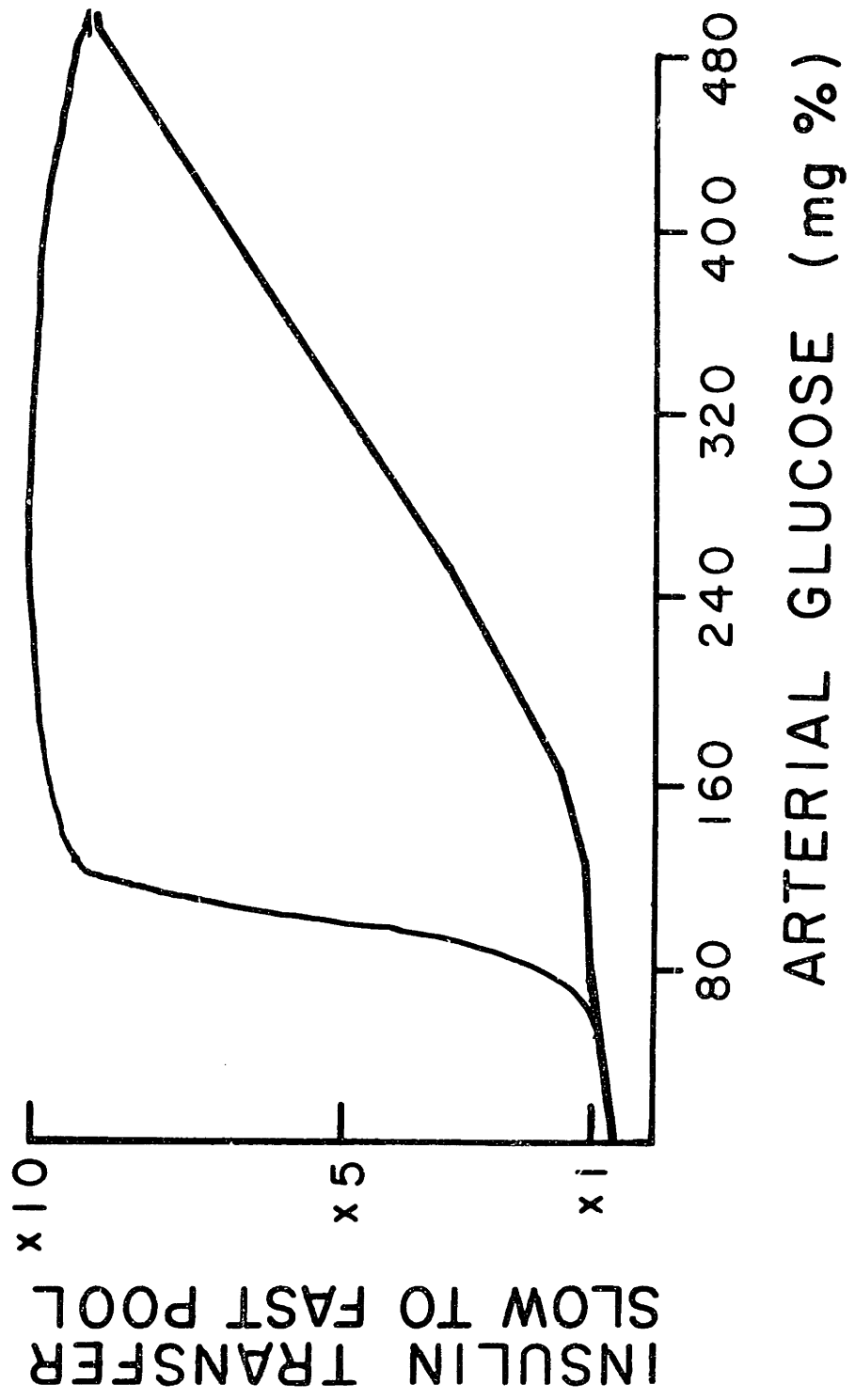

Figure 51

The effect of heart glucose concentrations
on the rate of transfer of stored insulin to releasing-holding sites.

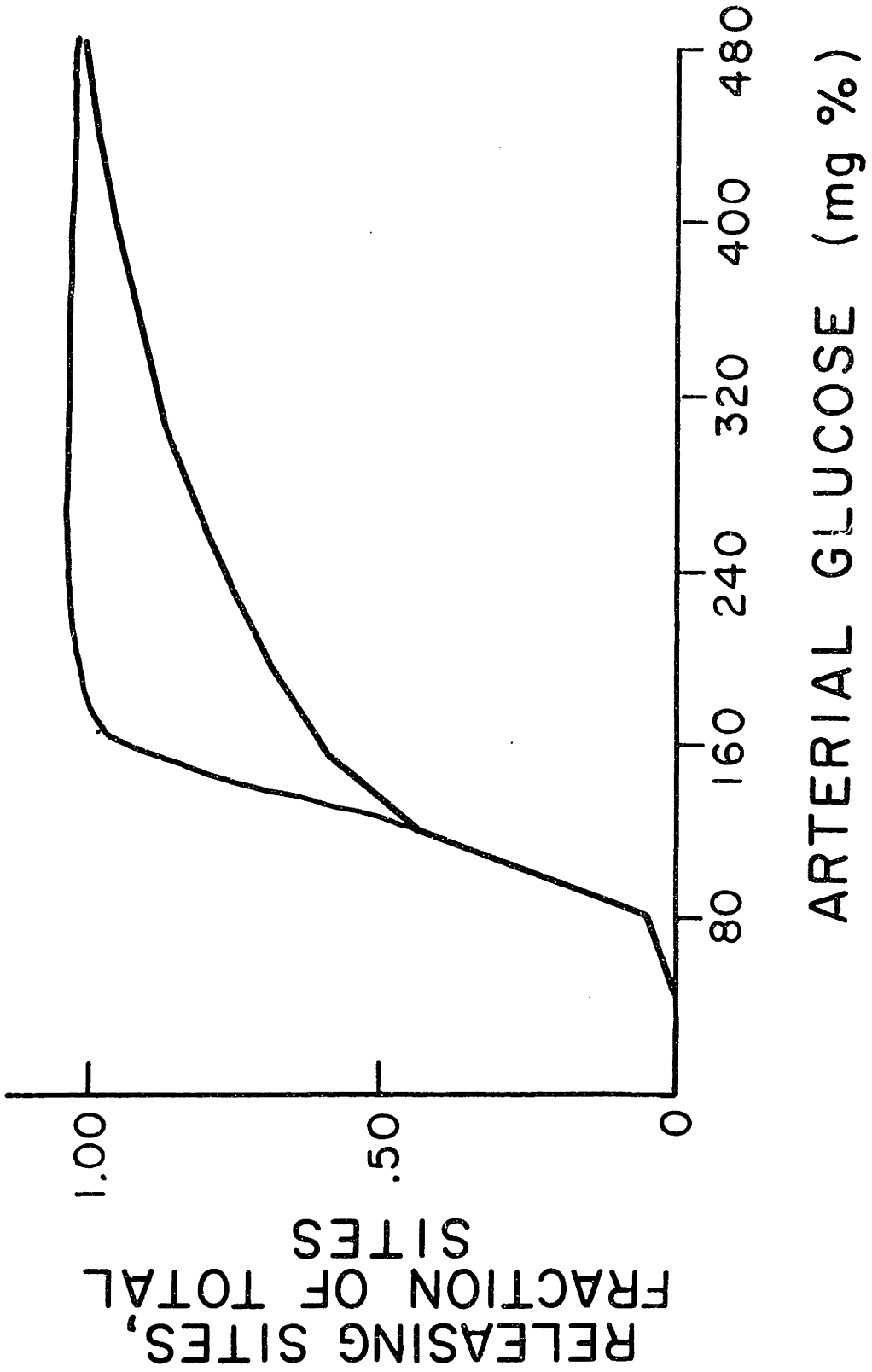

Figure 52

The effect of heart glucose concentrations on the fraction of insulin releasing sites.

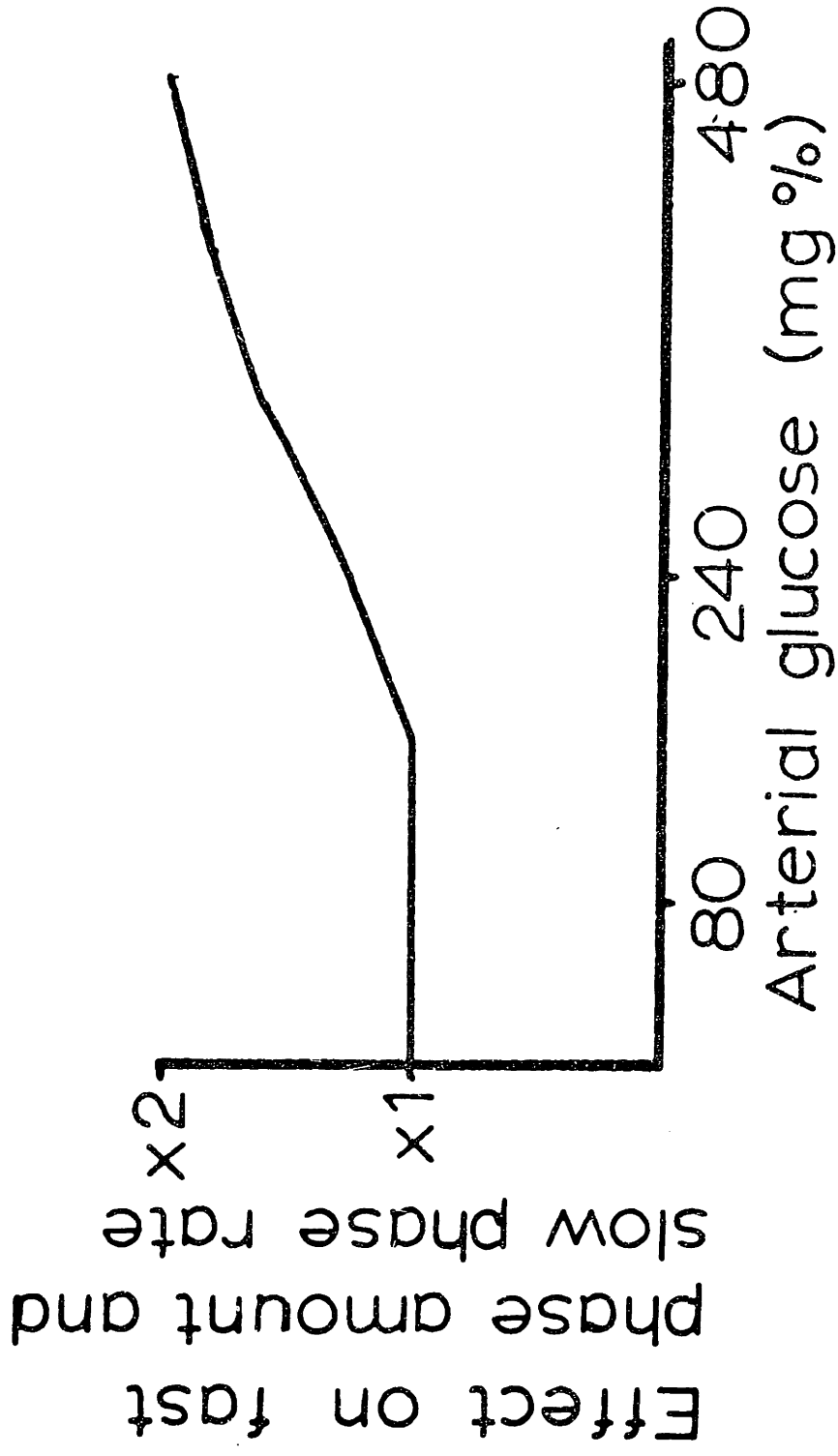

Figure 53

The delayed effect of heart glucose concentrations on the secretion of insulin.

transfer from storage to releasing-holding sites) determines the rate of transfer of stored insulin, I_S, to releasing and holding sites, as a function of glucose concentration. This function was determined from calculating the amount of insulin released during the second phase of insulin release as a function of glucose concentration during an IVGTT. Because it has been demonstrated that the magnitude of fast phase release to a given glucose stimulus can vary according to long-term glucose exposure of the pancreas, the total number of releasing-holding sites in the model have a slow turnover time, TDEG. Lastly, experiments in which glucose is administered as a constant infusion for sixty minutes demonstrate that the second phase of insulin release slowly rises. This is incorporated into the model as EGID, the delayed effect of glucose on insulin release, which acts via a 45 minute transport delay. Fig. 54 shows the response of the pancreas model to a constant infusion of glucose at 300 mg/ml, which agrees with data from isolated perfused pancreas experiments.

The three models for insulin secretion presented each represent an alternative hypothesis for the events that result in the response of the beta cell to stimulation with glucose. While none of the above hypotheses can be substantiated on the basis of current experimental data, they all share one aspect in common; they all accurately simulate the response of the pancreas to a variety of stimuli. The input of glucose into the model was either as an intravenous injection into the heart compartment or oral absorption via the hepatic (liver) compartment. An intravenous injection is easily represented by

$$V(t) = A$$

where the input, V(t), is a constant A (mg/min), for a fixed time period

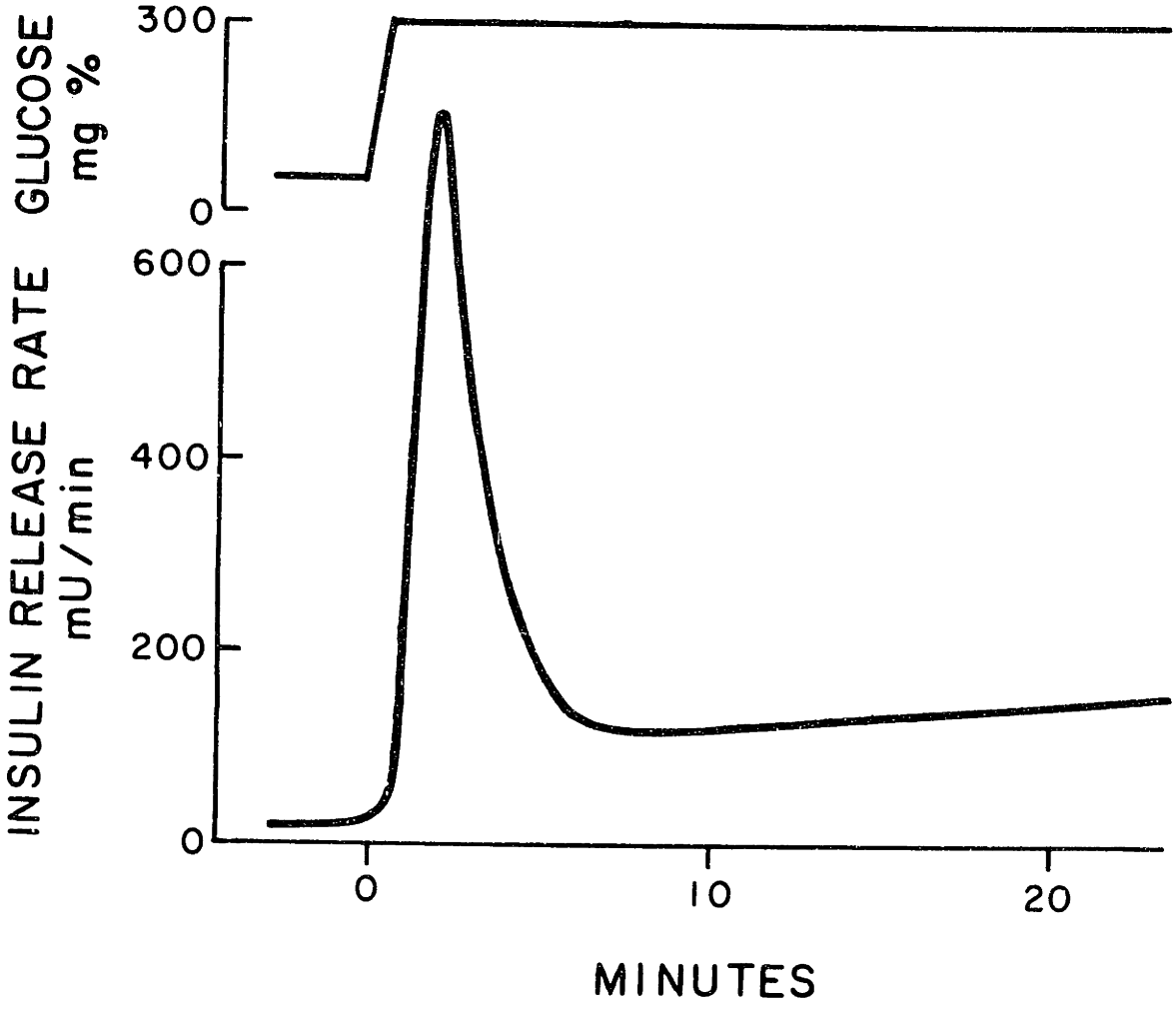

Figure 54

Beta-cell model simulation of response to a constant infusion of glucose at a concentration of 300 mg/dl.

(e.g. A = 11666.67 mg/min for 3 minutes in a standard IVGTT). The representation of the oral absorption of glucose is more difficult. From data at the Joslin Clinic,[1] in which glucose concentrations were sampled at one minute intervals following an OGTT, no rise in peripheral glucose concentrations were observed for six minutes. This data suggests that there is no significant glucose absorption during this period of time and probably represents the transit time to the small intestine. It can be recalled from the discussion of absorption mechanisms that a hyperosmotic glucose concentration will "effectively" saturate the gastrointestinal absorption mechanism. This mechanism will remain saturated for variable periods of time dependent on the load (e.g. it is saturated for 48 minutes following a standard 100 gm OGTT). Therefore, for most glucose loads, the rate of glucose absorption rapidly increases as glucose is delivered to the small intestine and reaches a constant maximum rate where it remains for this entire period (e.g. a typical 100 gm glucose load in 300 ml, saturates absorption for 45 minutes). As the glucose concentration in the gut lumen declines, the rate of absorption decays according to Michaelis-Menton kinetics (ie. the rate of absorption, r equals

$$r = \frac{K_1 C}{K_2 + C}$$

where C is the lumen glucose concentration and K_1 and K_2 are constants). For a 100 gram OGTT, absorption is complete in 240 minutes. Thus, the absorption of glucose can be analytically described as[2]:

---

[1] J.S. Soeldner and M. Tan, personal communication.

[2] The start of an OGTT is considered as minus three minutes.

$$V(t) = \begin{cases} 0 & -3.0 \leq t < 3.0 \text{ minutes} \\ RA \ \{\text{Sin}\left[(T-To)/(T_1 - 3.0)* \Pi/2\right]\} & 3.0 \leq t < T_1 \text{ minutes} \\ RA & T_1 \leq t < T_2 \text{ minutes} \\ RA \ \{\text{Sin}\left[(T-T_2)/(T_{end} - T_2)*\Pi/2\right]\} & T_2 \leq t < T_{end} \text{ minutes} \\ 0 & t \geq T_{end} \text{ minutes} \end{cases}$$

where RA is the rate of absorption (800 mg/min)

To is the onset of absorption (3 minutes)

T_1 is the onset of saturation (minutes)

T_2 is the start of absorption decay (minutes)

T_{end} is the total absorption time (minutes)

for a 100 gm OGTT (T_1 = 10 minutes, T_2 = 30 minutes, T_{end} = 240 minutes). Note that because of the relative magnitude of T_2 and T_{end}, V(t) will not significantly decay for 48 minutes.

The insulin response to an OGTT is greatly enhanced in comparison to the amount of insulin that would be secreted to an equivalent amount of glucose given intravenously. This increase can be calculated from papers by Perley and Kipnis (1966) and Brown et al (1975). Recall that several hormones, the most likely one being GIP were discussed as the agents responsible for this enhancement. In the model, this potentiation is represented by an increase in the transfer of insulin from the storage to releasing-holding (ISTF) sites and an increase in the fraction of releasing sites for a given glucose concentration (DISRMS). This potentiation is only seen for glucose concentrations greater than the basal level of 80 mg/dl. The dotted

lines in figures 51 and 52 show how each of these functions are increased by an unspecified mediator that enhances the rates at each in the model, this is achieved by specific arterial glucose concentration.

C. Control Models

Various control algorithms have been proposed and a few actually have been used for maintaining blood glucose levels in a normal range by the control of insulin and/or glucose infusions. The control algorithms were designed to mimic the body's normal physiological control system which Benedek has shown can be characterized by a proportional-plus-derivative-plus-integral (PID) controller.

Kadish and Little (1970) developed the first such algorithm, although their goal was the control of a glucose infusion to maintain a constant blood glucose concentration following the administration of insulin at various doses. Their algorithm was a PID controller of the form:

$$R_I = K_p(G_p - G_s) + \frac{K_D d(G_p)}{dt} + K_I \int (G_p - G_s)\, dt \qquad (38)$$

In equation (38), R_I is the rate of glucose infusion; G_s is the set point concentration at which the glucose concentration is to be maintained, K_p, K_D, and K_I are the constants of proportionality for proportional, derivative and integral control, respectively. The constants are empirically determined to obtain an acceptable control of blood glucose concentration G_p. The flow system Kadish and Little used to transport blood

continually through a monitoring system introduced a transport delay of five minutes in reporting a glucose concentration to the controller. Therefore, it was necessary to estimate the glucose concentration at $t_p + d$ (t_p = present time, d = delay), G_p ($G_p = G(t_p + d)$). This extrapolation was done by a linear least-squares fit to the current data point and two previous measurements.

Similar methods for maintaining the glucose concentration at a desired concentration have been developed by Norwich et al (1975), Kline et al (1968), and Insel et al (1975). This type of algorithm is useful in the design of experiments to study the effect of insulin on glucose uptake (at constant glucose concentrations) in different metabolic states as discussed in Section V.B.

Albisser et al (1974) have developed an algorithm which controls the rate of infusion of glucose and insulin according to the deviation of blood glucose from a set point and the rate of change of blood glucose concentration with time (proportional-plus-derivative control). The equations describing the rate of infusion of insulin and glucose are:

$$R_I = 1/2\ R_I max \left[1 + \tanh S_1(G_p - B_I)\right] \tag{39}$$

$$R_G = 1/2\ R_G max \left[1 - \tanh S_D(G - B_D)\right] \tag{40}$$

wwhere R_I and R_D are the rates of insulin and glucose infusion, respectively.

Albisser et al have never discussed how these algorithms were developed. However, recall Fig. 21, which is the experimentally determined relationship between the glucose concentration and rate of insulin secretion in isolated perfused beta cell islets. Fig. 56 is the graph

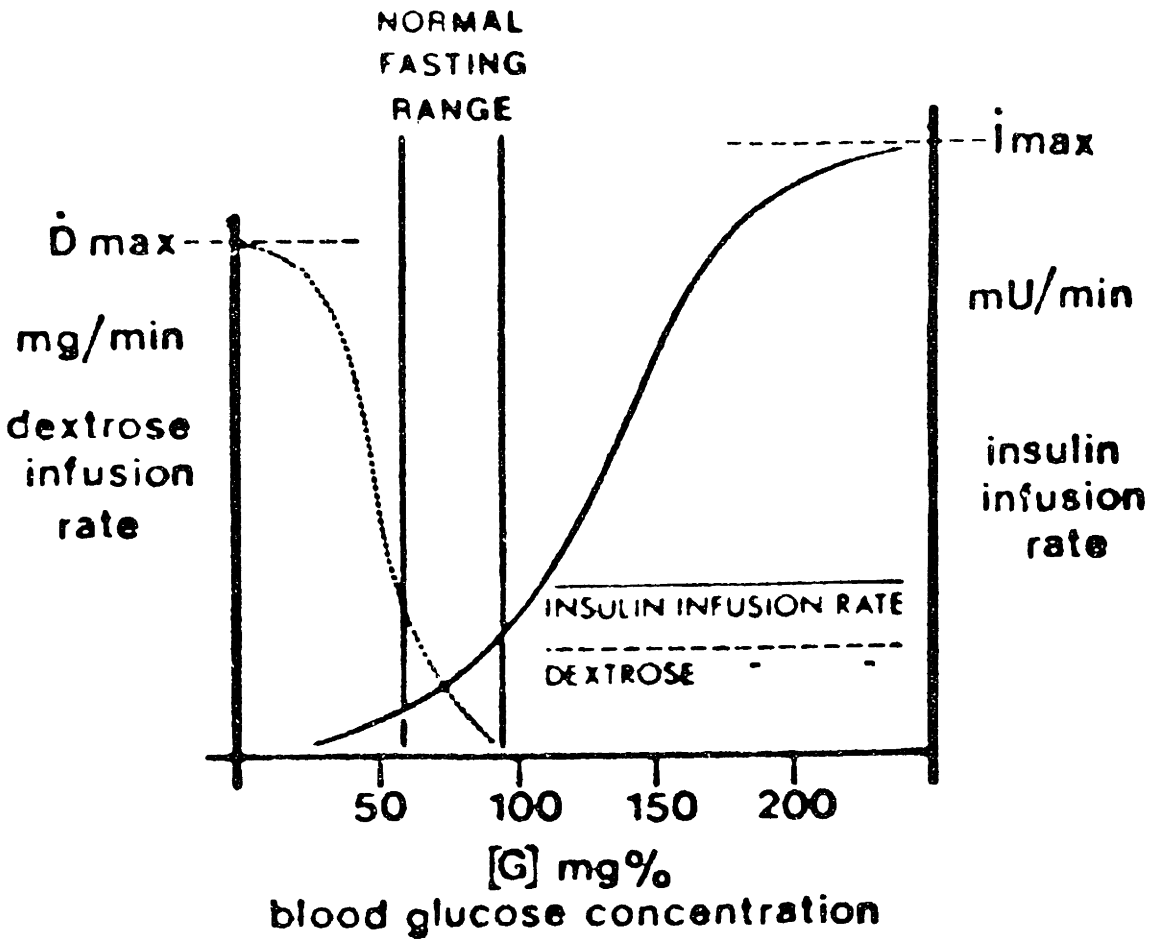

Figure 56

Relationship of blood glucose concentration to insulin and dextrose infusion rates (from Botz, 1976).

of equation (39) which relates the rate of insulin infusion to glucose concentrations. It can be seen that these two figures have the same functional form. This is not surprising since the algorithm has been designed to mimic the behavior of the pancreas.

Furthermore, Charette et al (1969) have shown that a way to mathematically describe the functional form of a "sigmoid curve" is by:

$$Y = Y_o + A \tanh B(X - X_o) \tag{41}$$

$$Y_o = (Y_h + Y_l)/2 \tag{42}$$

$$A = (Y_h - Y_l)/2 \tag{43}$$

where X represents the substrate (glucose) concentration; Y represents the rate of (insulin) secretion; and Y_h and Y_l represent the upper and lower saturation values for the secretion rate. In this case, the lower saturation valve can be taken as zero, and (50) reduces to

$$Y = \frac{Y_h}{2} \; 1 + \tanh B(X - X_o) \tag{44}$$

Therefore a "sigmoid" curve can be represented by the choice of three parameters, Y_h, B, and X_o. By comparing (39) to (44) we see that:

$Y = R_I$ = the rate of insulin infusion;

$Y_h = R_{I_{max}}$ = the maximum insulin infusion rate;

$B = S_I$ = the slope of the curve; and

$X_o = B_I$ = the blood glucose concentration at which half maximum infusion rate is chosen.

The choice of these three parameters must be determined for each patient by trial and error, until an acceptable control of blood glucose concentrations is found. The algorithm for the glucose infusion (Equation 40), is used to compensate for any overshoots.

Although Albisser et al have reduced the time delay between monitoring the glucose concentration and reporting the result to the controller to 90 seconds, they have also developed a method to predict the glucose concentration, G_p at the "present" time, based on the rate of change of glucose

$$G_p = G + DF \tag{45}$$

$$DF = K_1 \ (EXP(A/K_2)) \tag{46}$$

$$DF = K_1 A^3 + K_2 A \tag{47}$$

where DF is the difference factor, G is the glucose concentration and A is the rate of change of glucose concentration (A = dG/dt).

A graph of (46) and (47) are shown in Fig. 57. The constants K_1 and K_2 are empirically determined. Originally (Albisser et al 1974) used (46), but found that as the blood sugar concentration fell, the insulin infusion rate based on G_p resulted in a larger than necessary insulin infusion rate to return the glucose concentration to basal values. Therefore, Equation (40) was adapted to compensate for this "overshoot" by infusing glucose to restore the blood glucose concentration to a baseline value in the first clinical experiments. However, by adapting Equation (47), (Botz et al 1976) which predicts a lower value for G_p, (see Fig. 57) as glucose concentration falls, the need for a

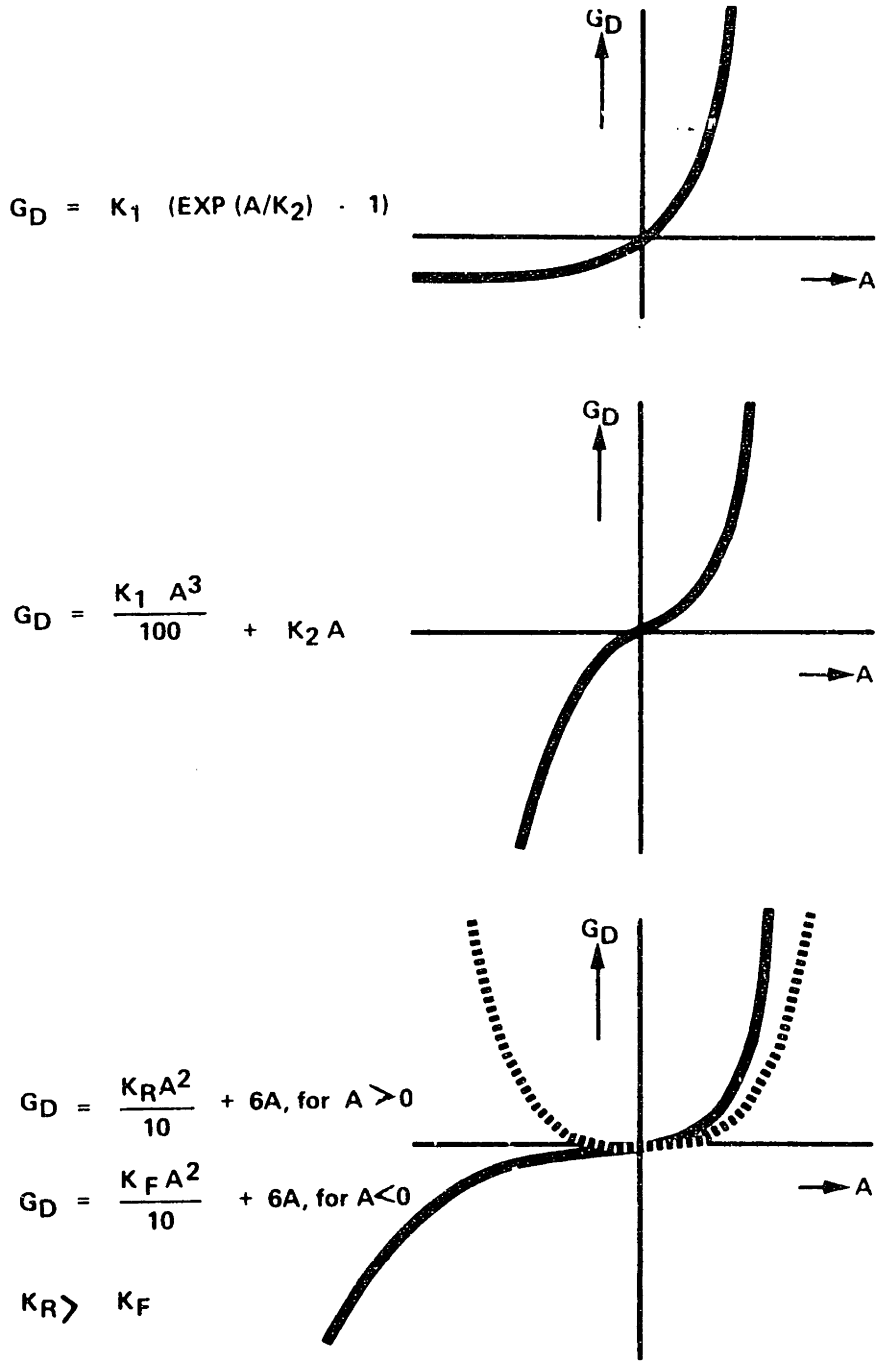

Figure 57

Algorithms for calculation of the "glucose difference" factor, DF (from Clemens et al, 1977).

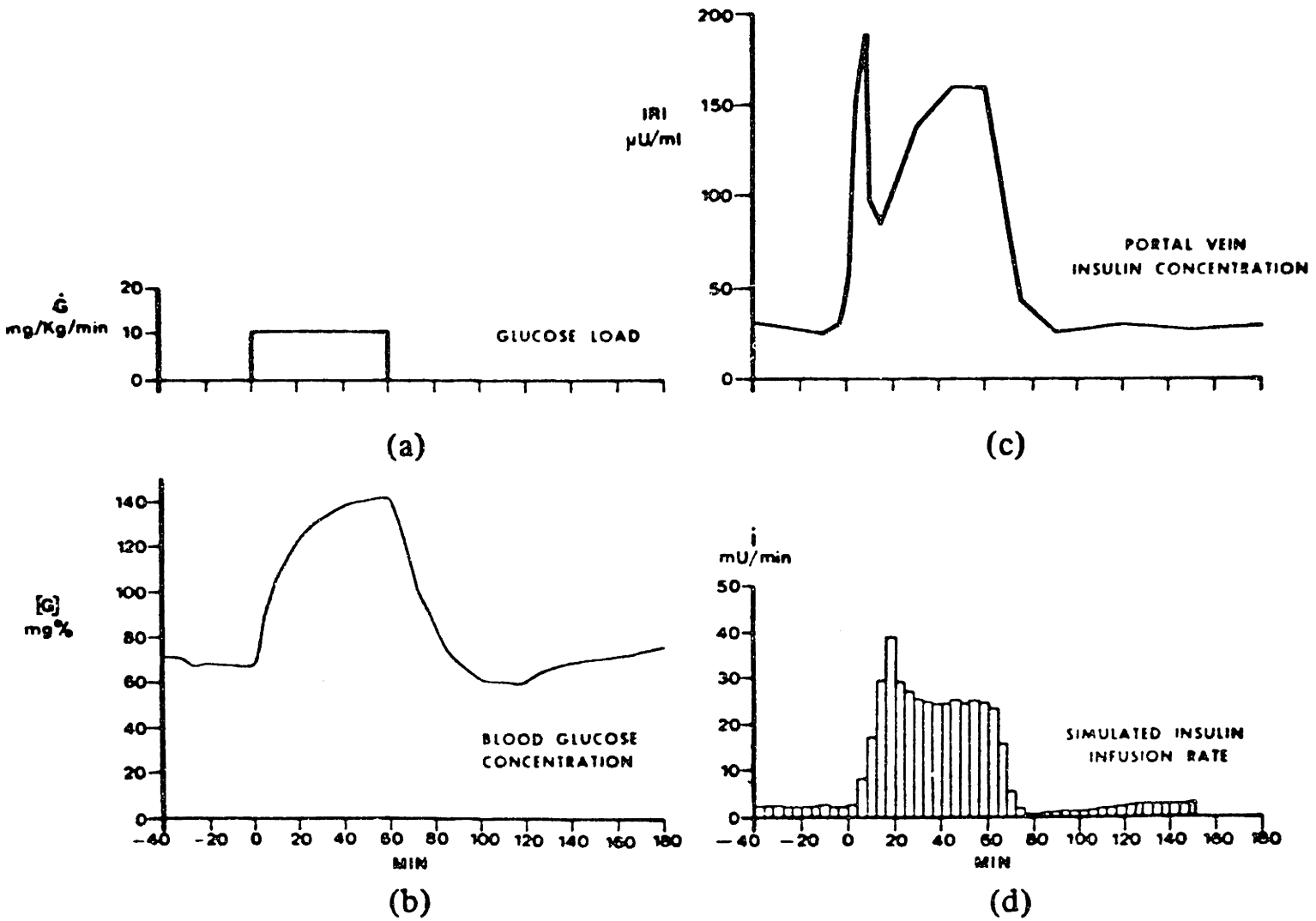

Figure 58

Comparison of normal and simulated insulin/blood glucose relationships in response to 60 min glucose load (10 mg/Kg/min) (from Botz, 1976).

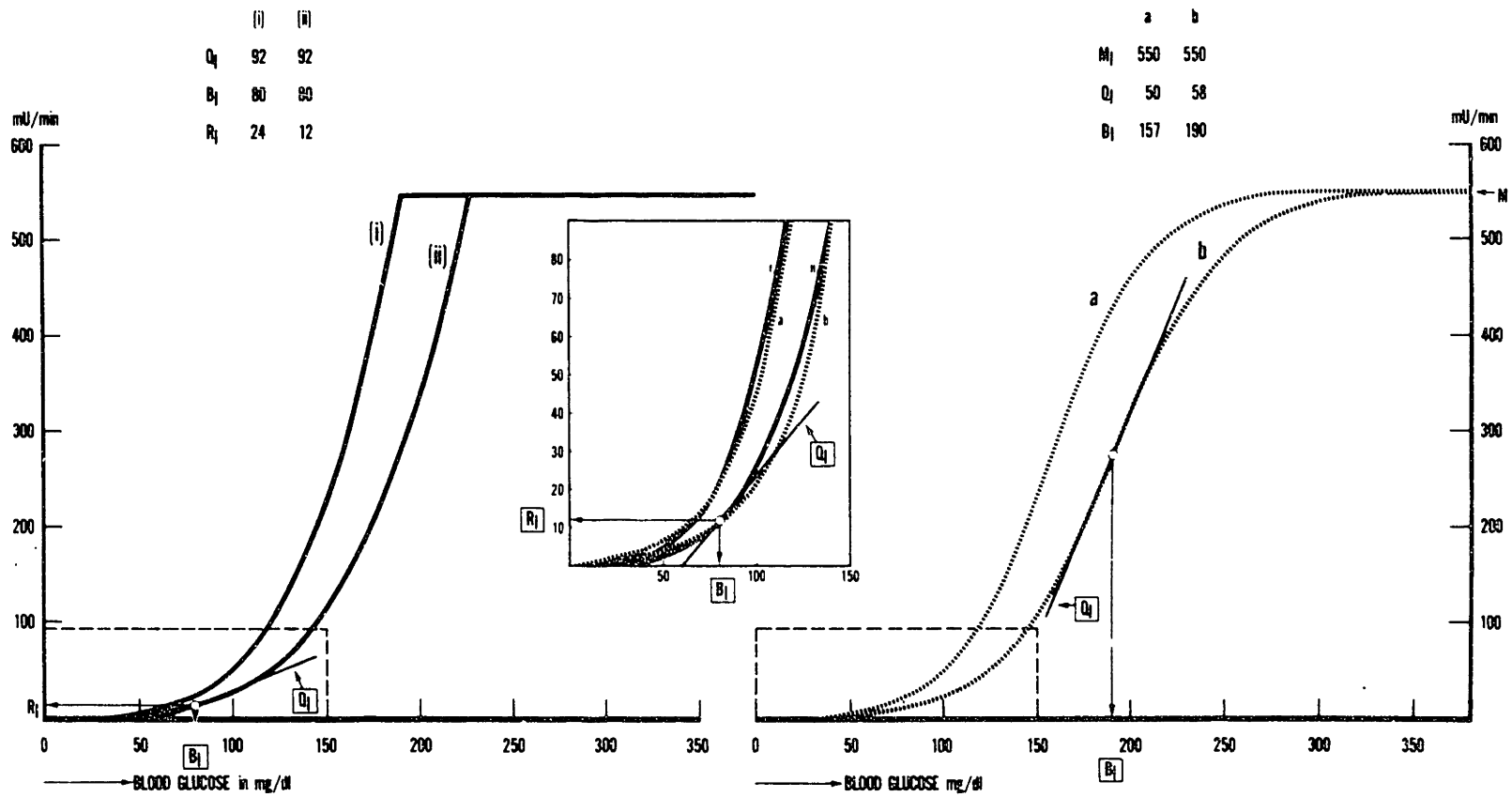

Figure 59

Control algorithm relating blood glucose concentration to insulin secretion rate.

glucose infusion to compensate for overshoots was eliminated. With this modification Albisser et al have succeeded in developing an algorithm to mimic the pancreatic secretion of insulin (see Fig. 58).

Clemens et al (1977) have developed an algorithm which is functionally equivalent to Albisser et al, except that they have chosen to mathematically describe a "sigmoid" curve differently. The equations of their algorithm are:

$$R_I = R_{I\,min}\left[\frac{1 + (G_p - B_I)}{S_I}\right]^4 \tag{48}$$

$$DF = \begin{cases} \frac{K_R A^2}{10} + GA & A > 0 \\ \frac{K_F A^2}{10} + GA & A < 0 \end{cases} \tag{49}$$

Fig. 59 shows a graph of Equation (49). R_I is the minimum rate of insulin secretion; B_I is the set point for the glucose concentration, and S_I is the slope of the curve. Fig. 61 shows a graph of Equation (49) used for calculating the predicted glucose concentration. Equation (49) allows the choice of a different slope between rate of change of glucose concentration and the difference factor (DF) used in calculating the predicted glucose concentration when the rate of change of glucose concentration is falling and when it is rising. In clinical experiments it is difficult to discern any difference between the control action of Albisser's and Clemens' algorithms. Indeed, they both represent proportional-plus-derivative controllers.

Mirouze et al (1977) have developed an analog control algorithm by the use of a set of miscroswitches connected to a potentiometer which

governs the rate of insulin infusion.

The system Mirouze et al developed has a transport delay of three minutes, which is not compensated for in the algorithm. Therefore, as can be expected, this control action of this algorithm is not as accurate as either of the two described above.

In summary, the control algorithms discussed and their clinical implementation, represent the first step in the design of an artificial pancreas that responds to glucose concentrations.

V. RESULTS

The flow-limited model was simulated at the Joint Mechanical and Civil Engineering Computer Facility (Interdata Model 80 Computer) using DYSYS (Dynamic System Simulation). DYSYS is a program which solves a system of first order nonlinear differential equations using a fourth-order Runge-Kutta Integration Scheme. DYSYS must be supplied with a Fortran subroutine called EQSIM (Equation Simulator) in which the model to be simulated is contained. The model is written as a system of equations:

$$\frac{d}{dt} Y_i = F_i\ (t, Y_1, Y_2 \cdots Y_n)$$

where Y_i are the values of the state variables, and F_i their derivatives as a function of time and the states. A printout of the model is presented in Appendix A.

The Runge-Kutta method is based upon a Taylor Series expansion of F in the vicinity of t_o and Y_o. Given Y_o, the value of Y at some time t, say t_o, then the approximate value of the Y vecctor is:

$$Y_{t+\Delta t} = Y_o + \frac{1}{6}\left[K_o + 2K_1 + 2K_2 + K_3\right]$$

where the K's are defined as:

$$K_o = F(t_o, Y_o)\cdot\Delta t$$

$$K_1 = F(t_o + \Delta t/2,\ Y_o + \tfrac{1}{2}K_o)\cdot\Delta t$$

$$K_2 = F(t_o + \Delta t/2,\ Y_o + \tfrac{1}{2}K_1)\cdot\Delta t$$

$$K_3 = F(t_o + \Delta t,\ Y_o + K_2)\cdot\Delta t$$

The Runge-Kutta solution will converge to the true solution as $\Delta t \to 0$.

The validity of the proposed model for glucose-insulin dynamics was tested with data obtained from the Joslin Research Laboratory, Boston.

The data represents the averaged responses of several normal test subjects. In all cases the experiments were conducted after an overnight fast.

Figure 60 shows the simulated and experimental data of a 0.5 gm/kg 3-minute intravenous glucose tolerance test. Figure 61 shows the same amount of glucose infused over 12 minutes rather than 3, and enables one to experimentally distinguish the fast and slow phases of insulin release. Figures 62 and 63 show the result of double pulse glucose studies in which a second 0.5 gm/kg 3 minute pulse of intravenous glucose is given either 30 minutes (6-30-6) or 60 minutes (6-60-6) after the original pulse. Note that the model predicts, and the experiments verify that the fast phase of insulin release is considerably diminished after the second pulse of the G-30-G study.

Figures 64 and 65 show the experimental and simulated peripheral glucose and insulin concentrations following a 100 gram oral glucose tolerance test. The glucose and insulin concentrations in the liver, heart, peripheral and Kidney compartments are shown in figures 66 and 67, respectively. Note that a peak portal-peripheral blood glucose gradient of 50 mg/dl is established. Published data in which portal and peripheral blood glucose concentrations are measured is rare, but available data suggests this gradient is between 50-100 mg/dl (Shoemaker et al, 1971).

Figures 68 and 69 show the rate of glucose absorption and disposition of a glucose load. Experimental data previously cited (Lagerlöf et al, 1976; Shoemaker et al, 1963) indicate that only 70-80% of a glucose load is actually absorbed (the rest presumably being metabolized by cells of

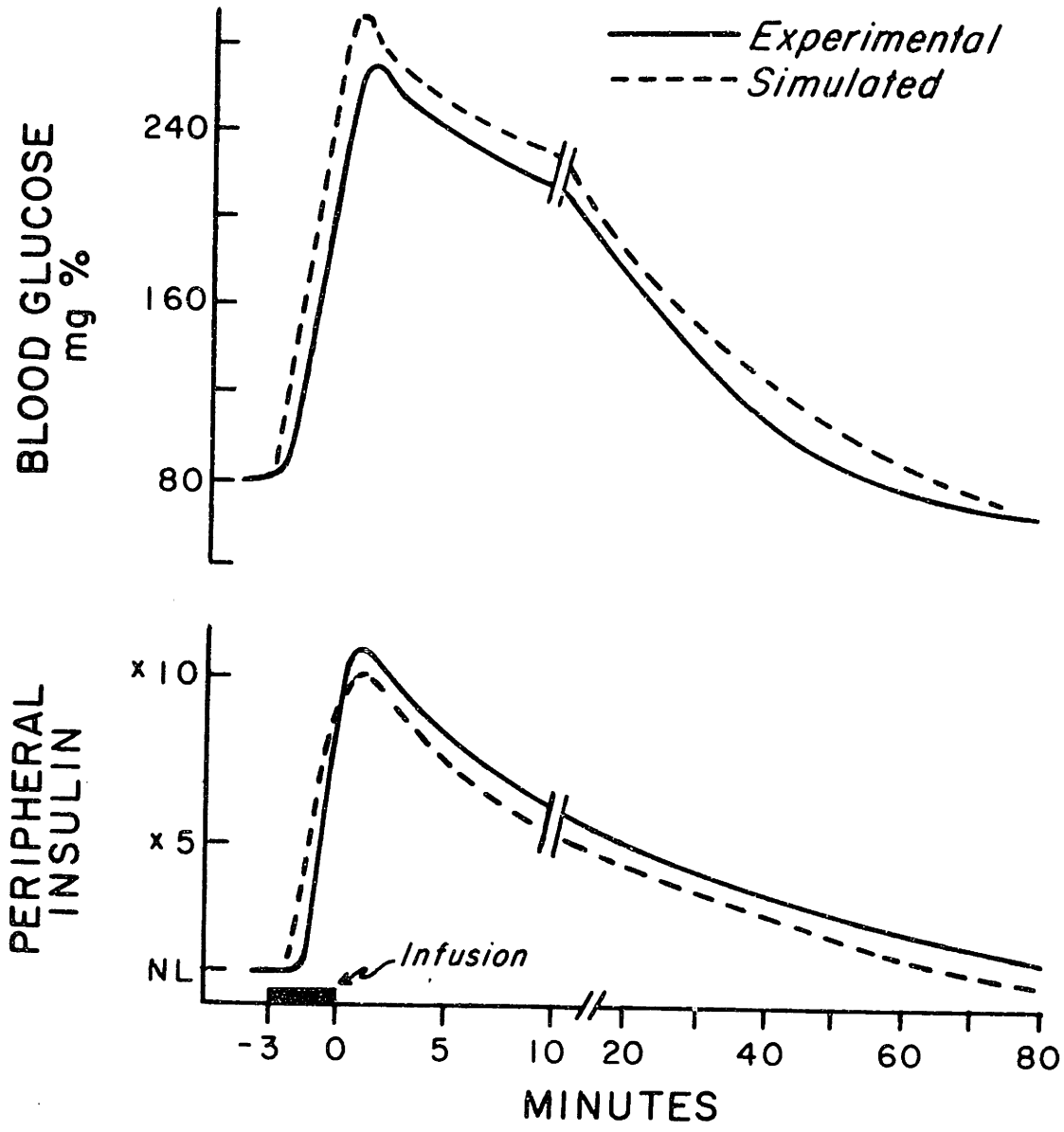

Figure 60

Three-minute, 0.5 GM/Kg IVGTT.
Comparison of model simulation to experimental data.

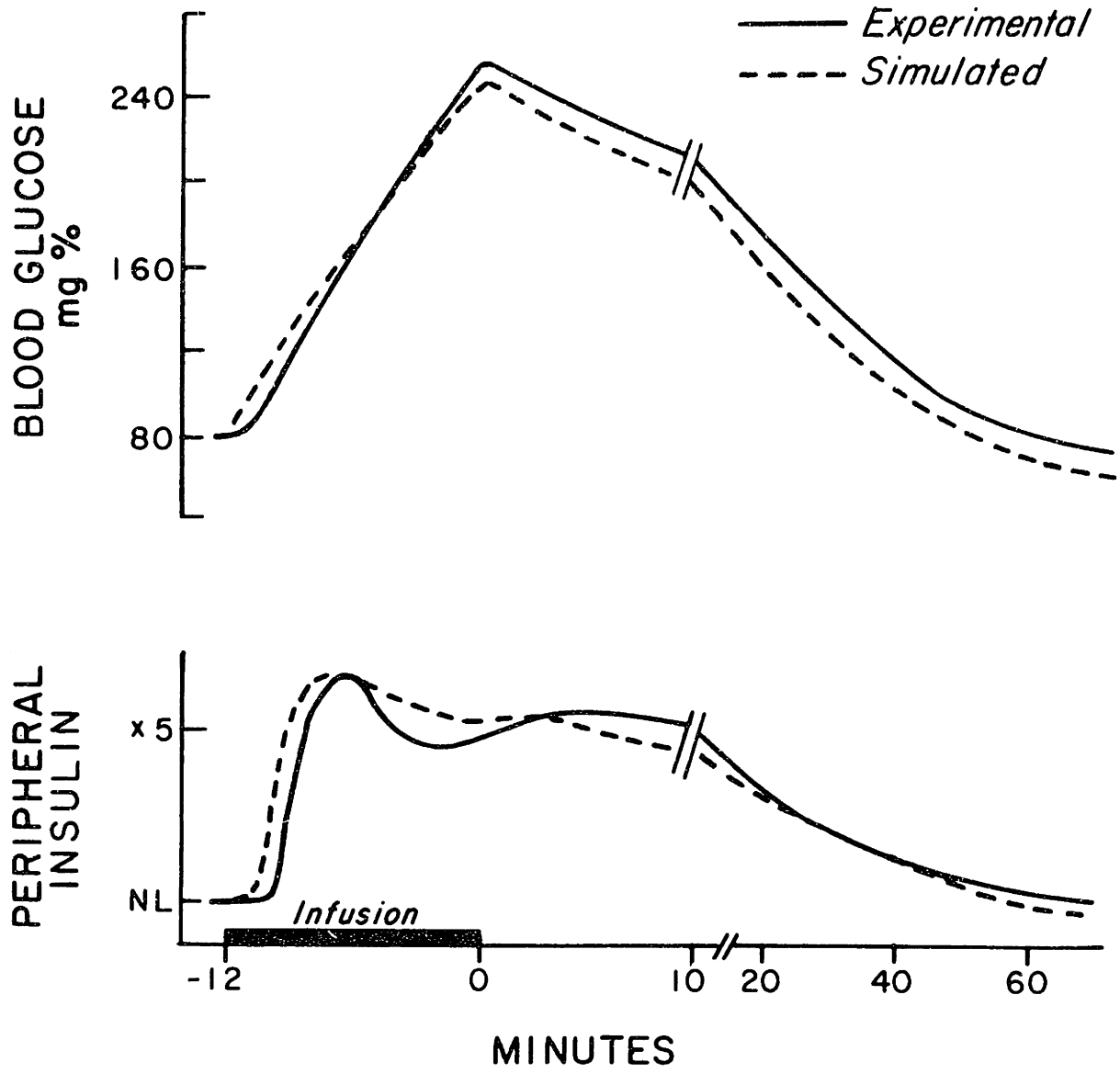

Figure 61

Twelve-minute, 0.5 GM/Kg IVGTT.
Simulated versus averaged experimental result.

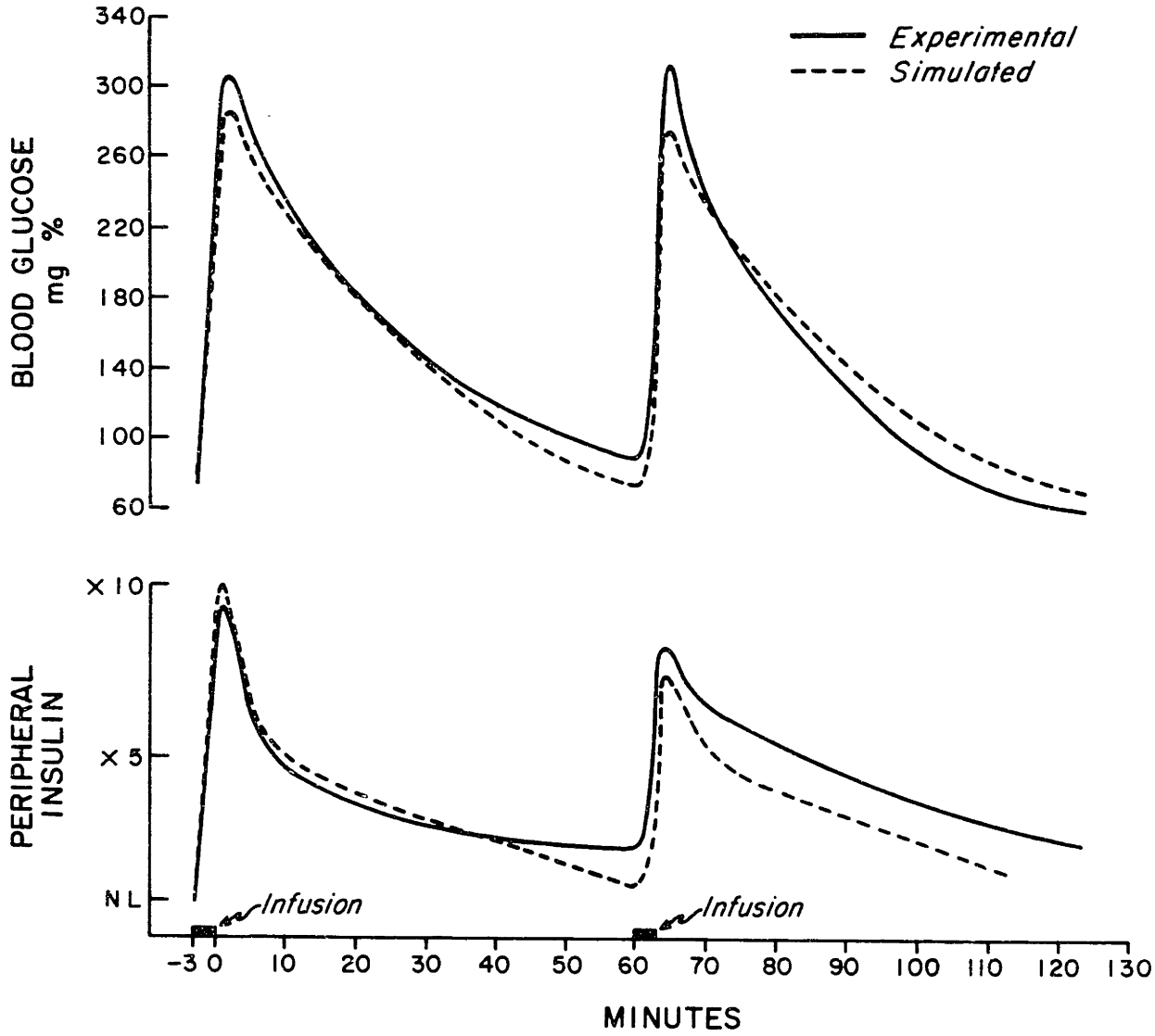

Figure 62

G-30-G double pulse glucose study simulated versus average experimental result.

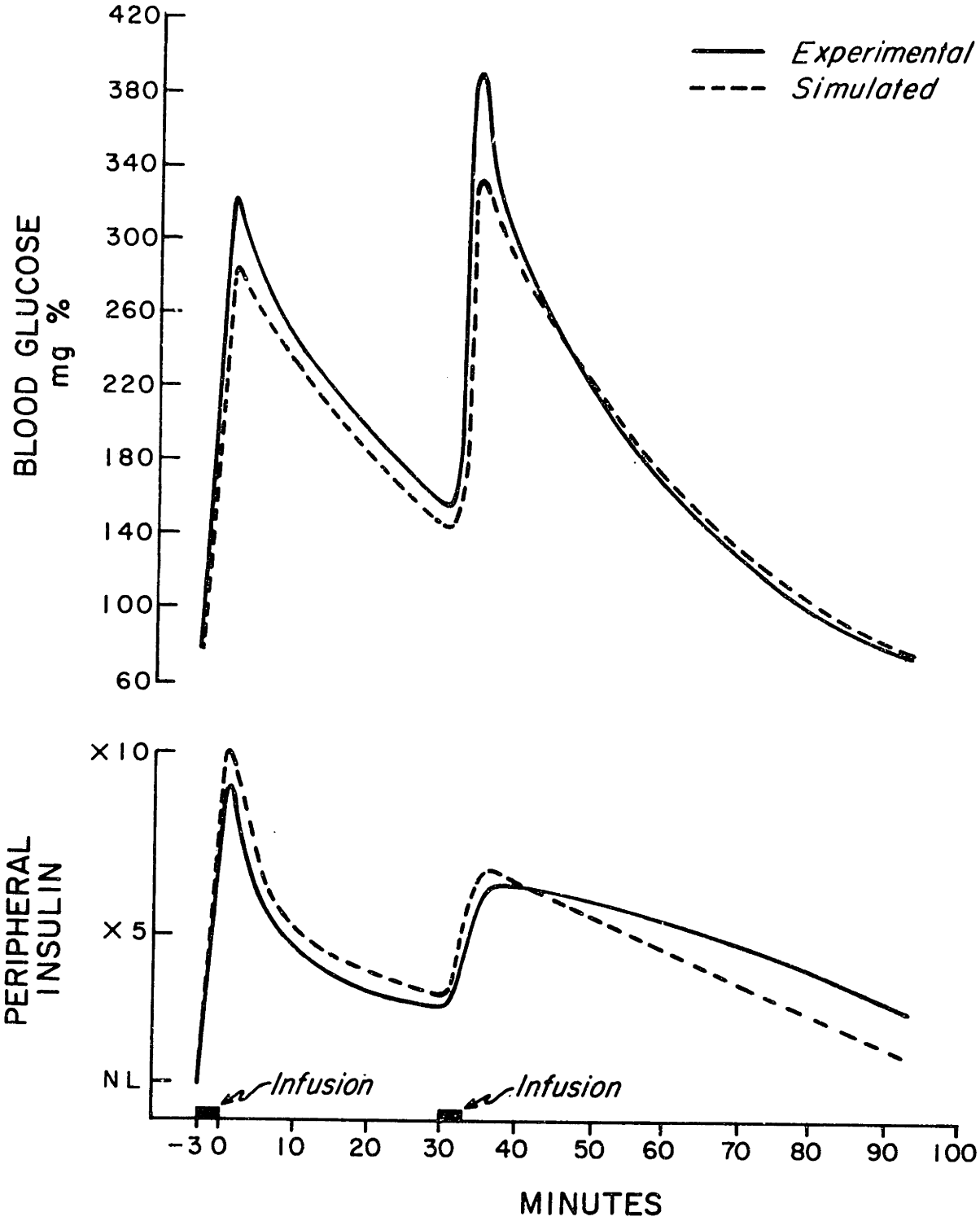

Figure 63

G-30-G double pulse glucose study
simulated versus average experimental result.

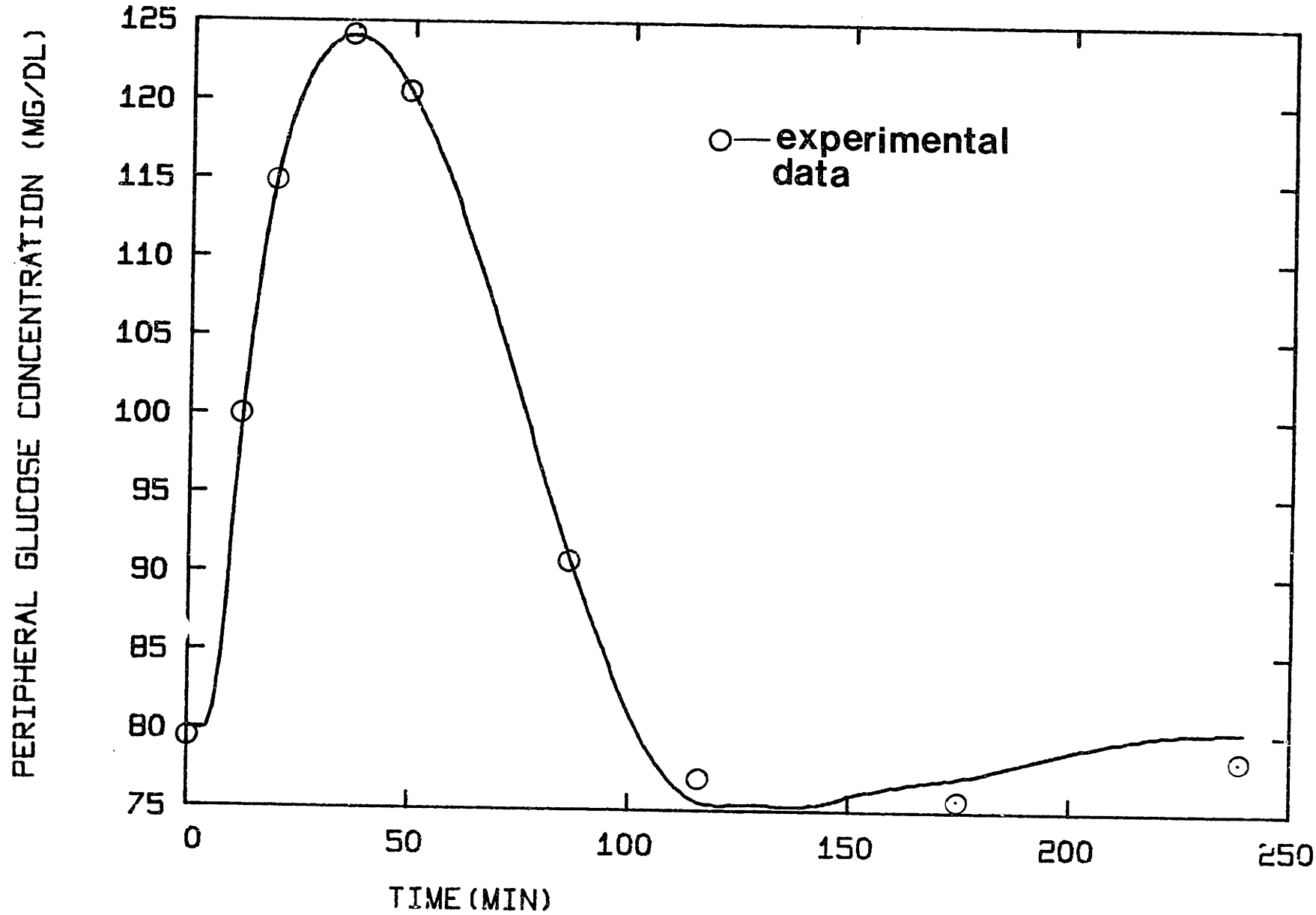

Figure 64

100 gram oral glucose tolerance test.
Simulated versus experimental results.

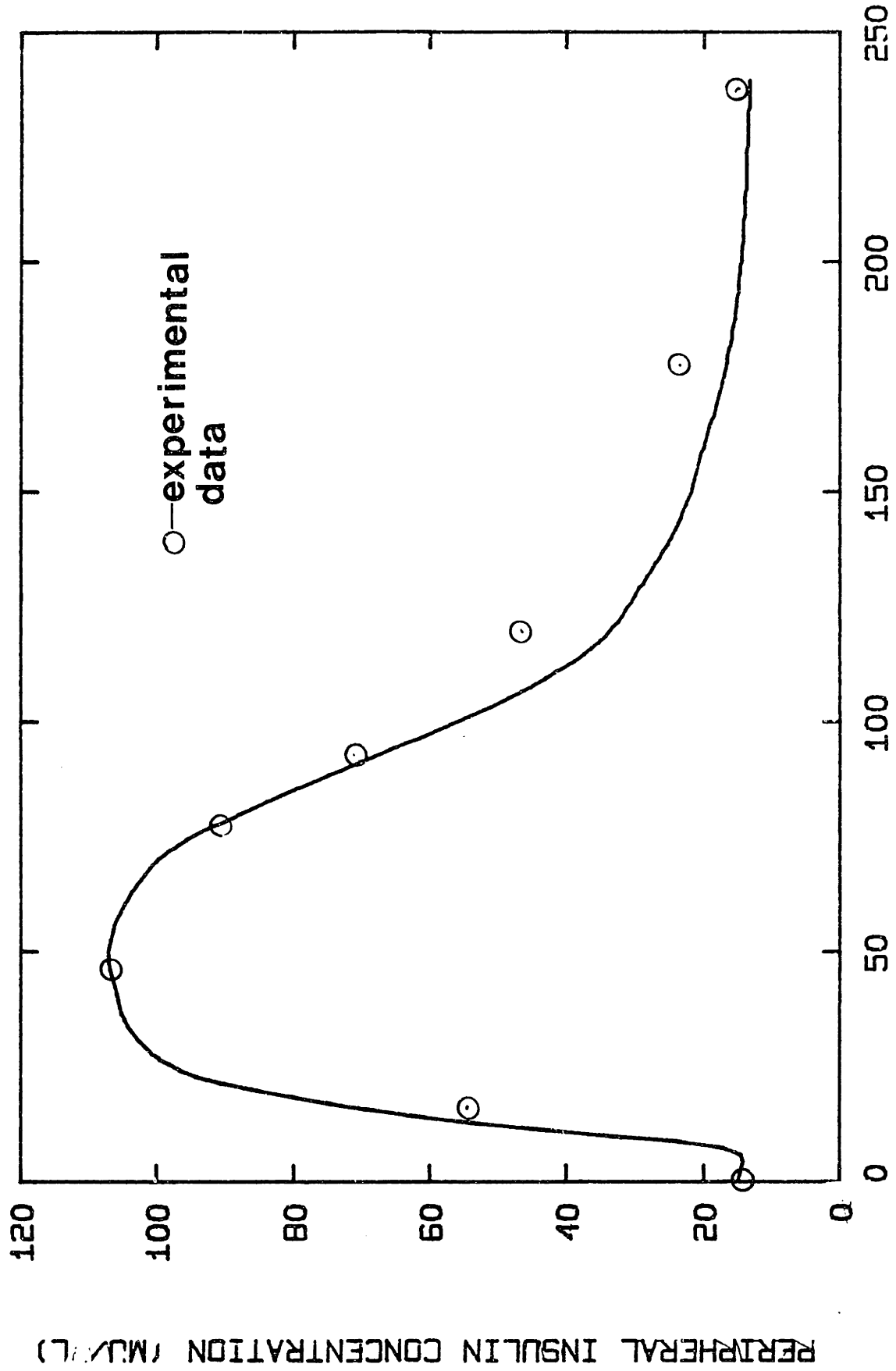

Figure 65

100 gram oral glucose tolerance test.
Simulated versus experimental results.

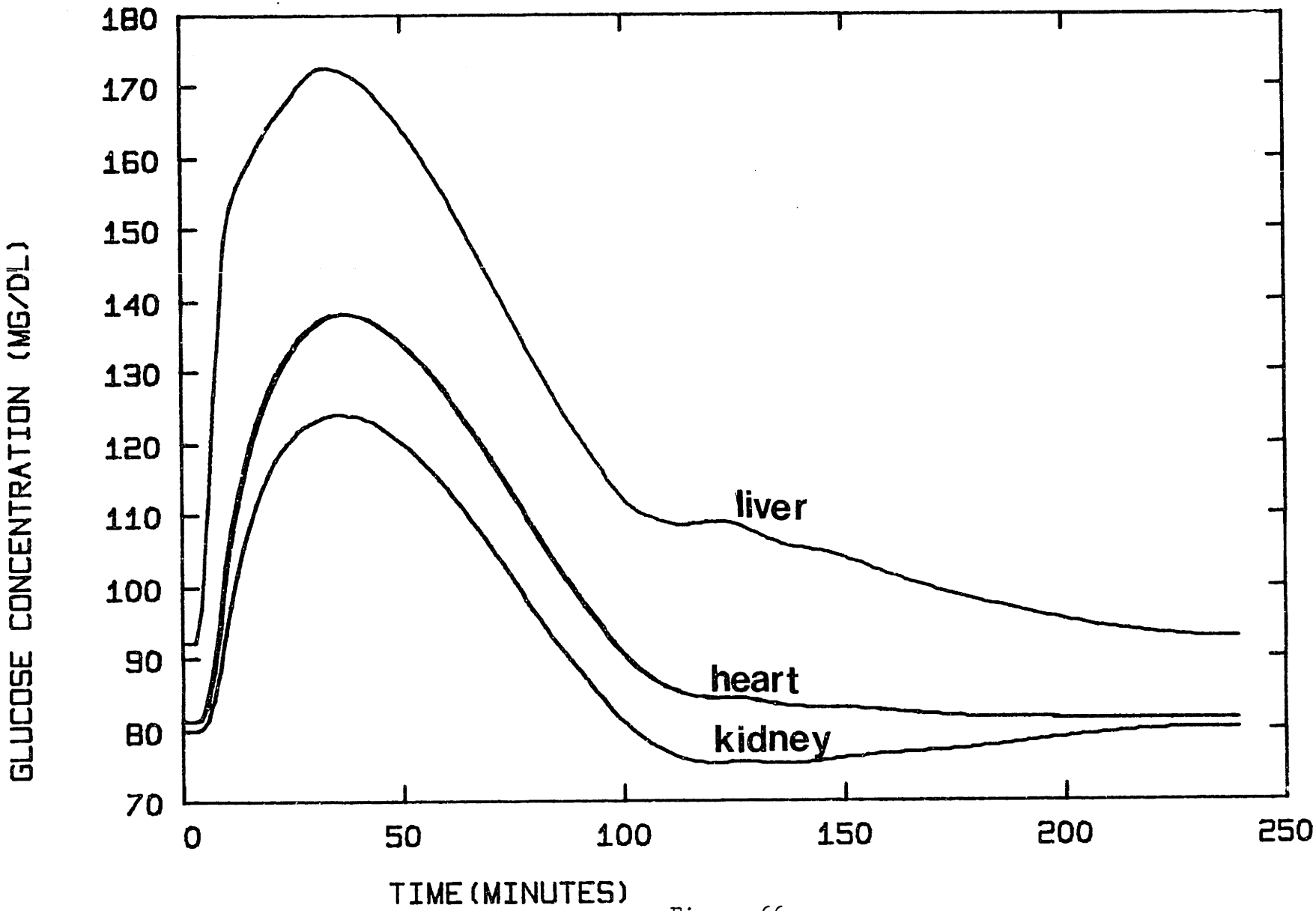

Figure 66

100 gram oral glucose tolerance test.
Model simulation of liver, heart, and kidney glucose conditions.

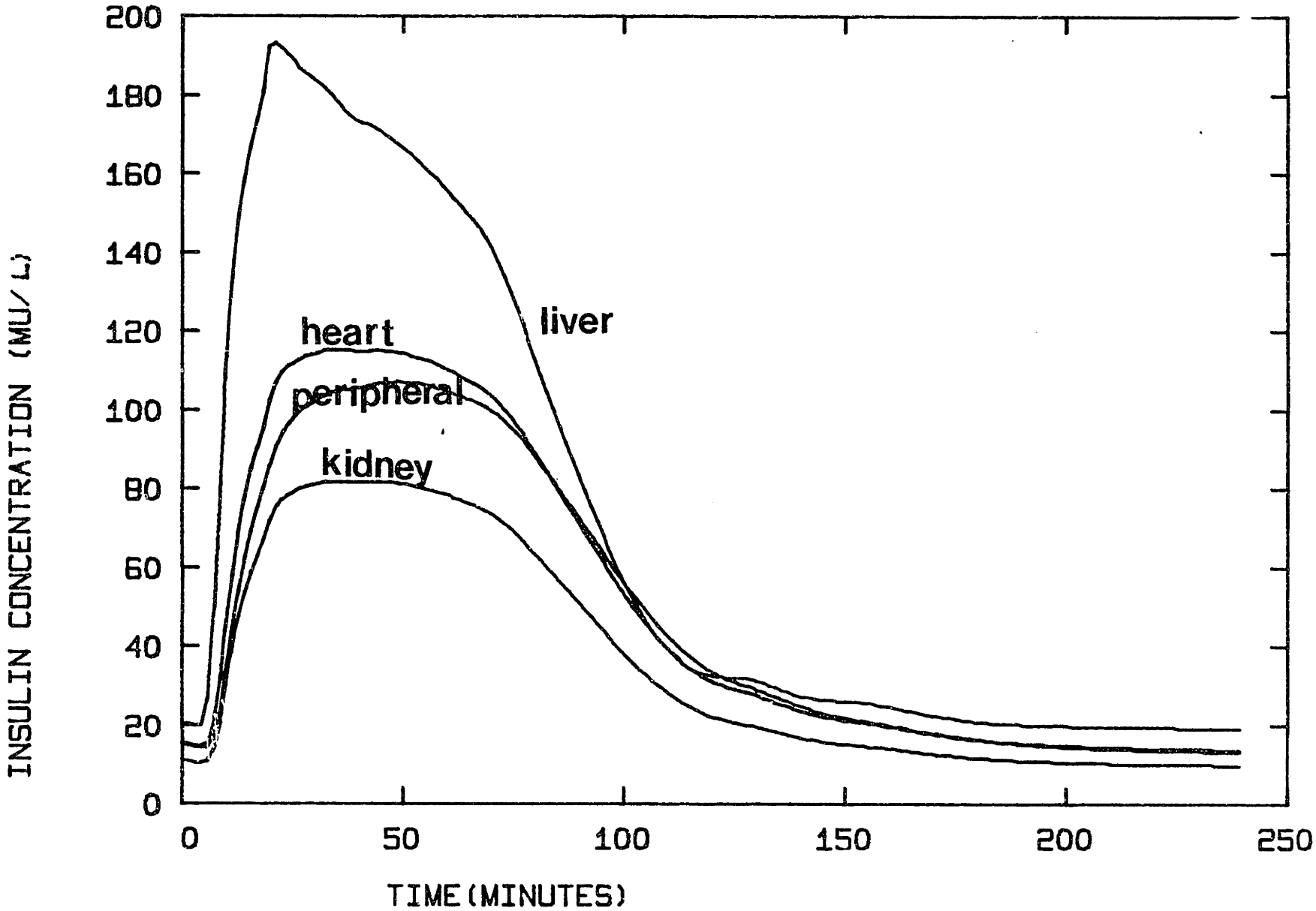

Figure 67

100 gram oral gluclose tolerance test.
Model simulation of liver, heart, and peripheral glucose concentrations.

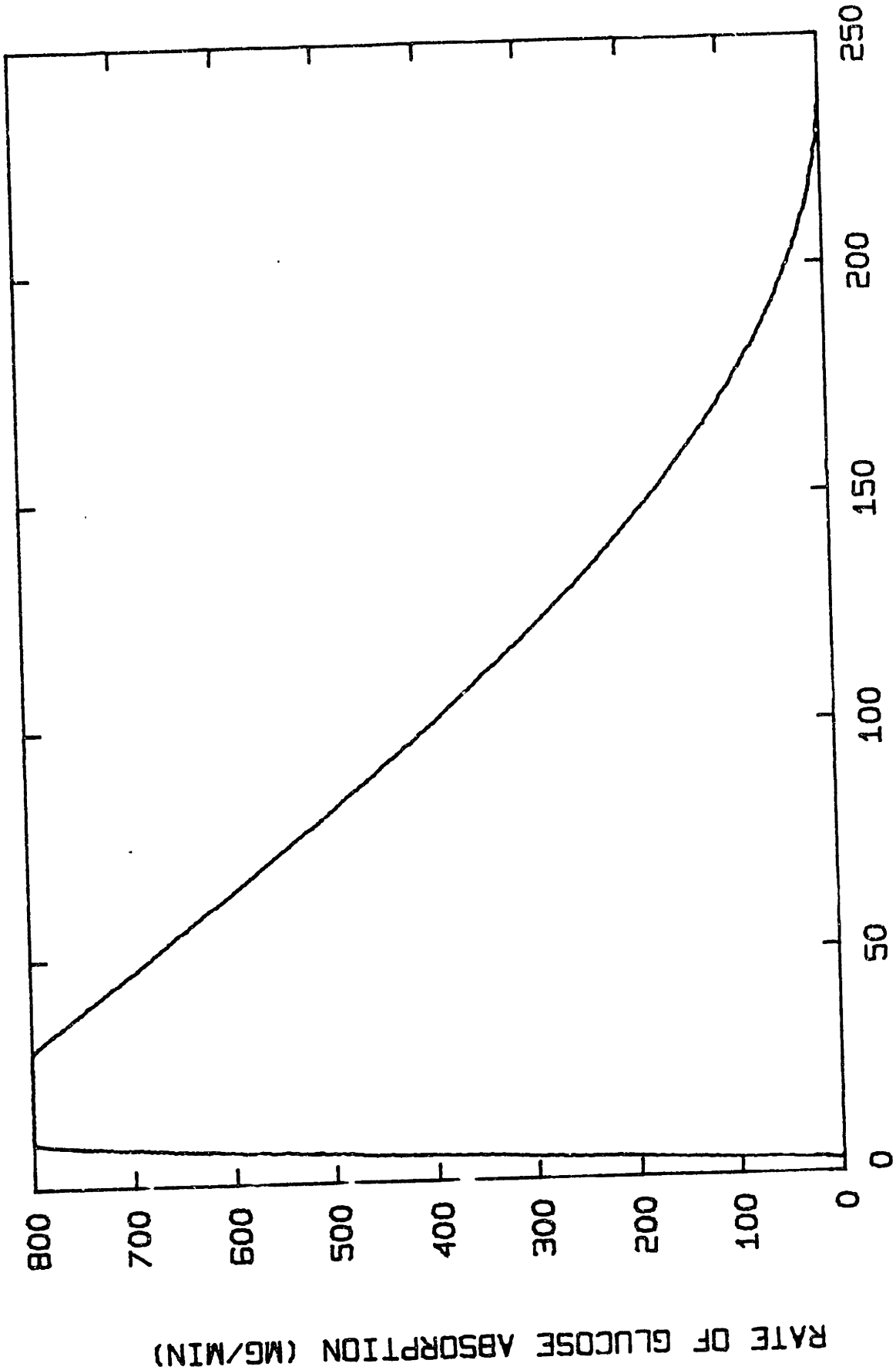

Figure 68

The rate of absorption of glucose following a 100 gram oral glucose tolerance test.

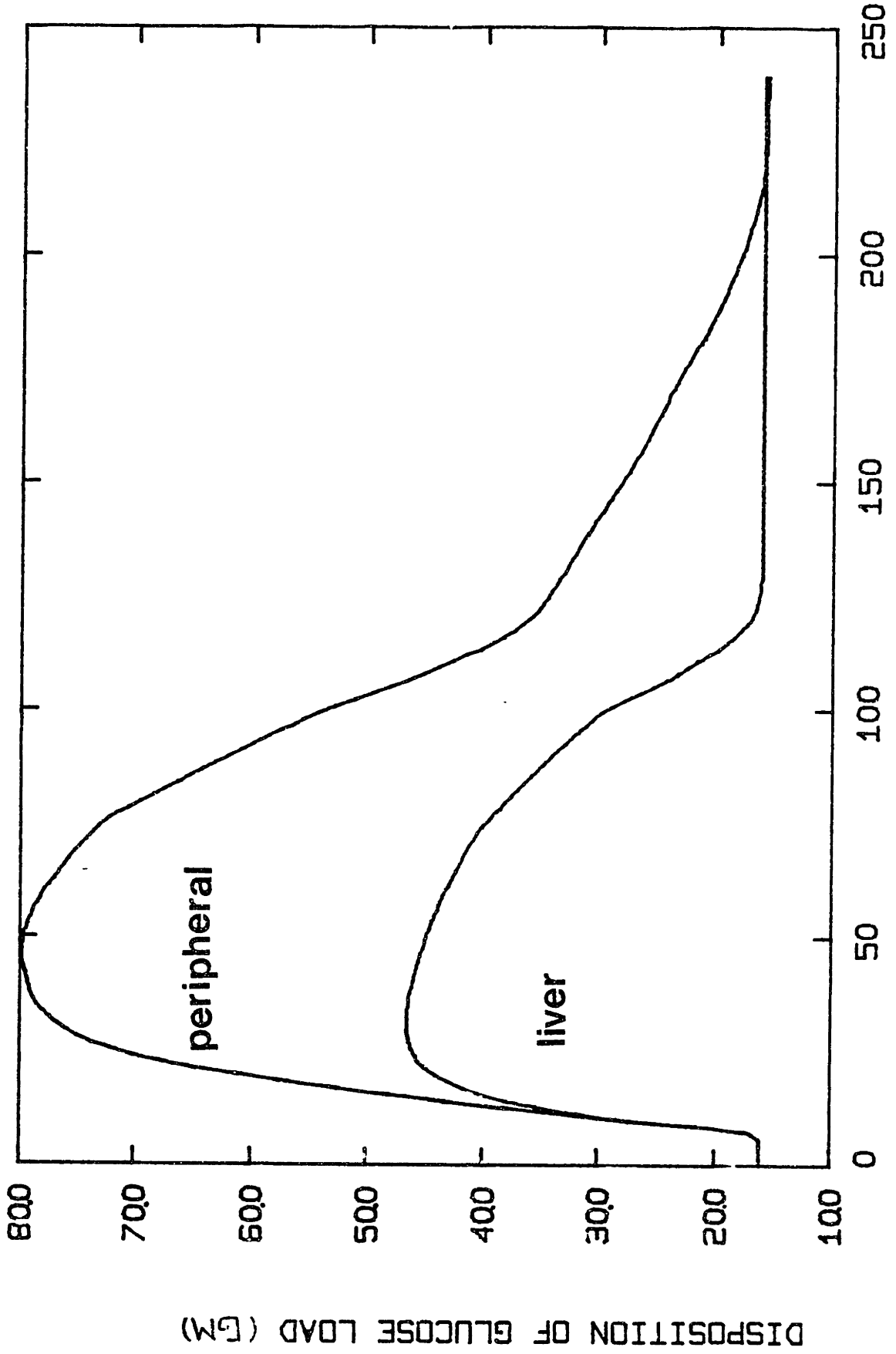

Figure 69

The disposition of a glucose load following a 100 gram oral glucose tolerance test. The area under the lower curve indicates total liver utilization; the area between the upper and lower curve indicates the total peripheral tissue utilization.

the G.I. tract). Therefore, following a 100 gm OGTT, it would be expected that only 70-80 grams would be absorbed. Indeed the model predicts that 80 grams are absorbed. The priamry site for disposition of an oral glucose load is in the liver, where 60% of the glucose absorbed is retained (Felig et al, 1976); the remaining 40% is utilized by peripheral tissues. The model predicts that 56% of the absorbed glucose load is retained by liver while 44% is utilized by peripheral tissues (see Figure 69). It is interesting to contrast this with the disposition of a glucose load following an intravenous glucose tolerance test of 0.5 gm/kg (shown in Figure 70). Although the total load is significantly less, 5% of the glucose is lost in urine. The hepatic retention is 40%, and the peripheral utilization of glucose is about 55%.

Figure 71 shows the rates of peripheral glucose uptake (MGU), glycogen synthesis (GLYS), glycogen breakdown (GLYB), and gluconeogenesis (GNEO) simulated by the model. When the liver is presented with increasing glucose concentrations, glycogen breakdown ceases, although gluconeogenesis occurs at a diminished rate. Simultaneously the rates of peripheral glucose uptake and glycogen synthesis are stimulated. As peripheral glucose concentrations begin to fall, these rates reverse. Specifically glycogen stores are mobilized to maintain peripheral glucose concentrations in the range of 70-80 mg/dl. Gluconeogenesis and glycogen breakdown together must produce enough glucose to meet the needs of the glucose dependent tissues (100 mg/min) namely the blood cells and the brain. Cahill and Owen (1968) have shown that in the fasted state (3-4 hours after a meal) liver glucose production is about 125-150 mg/min; the model reaches a steady state fasting

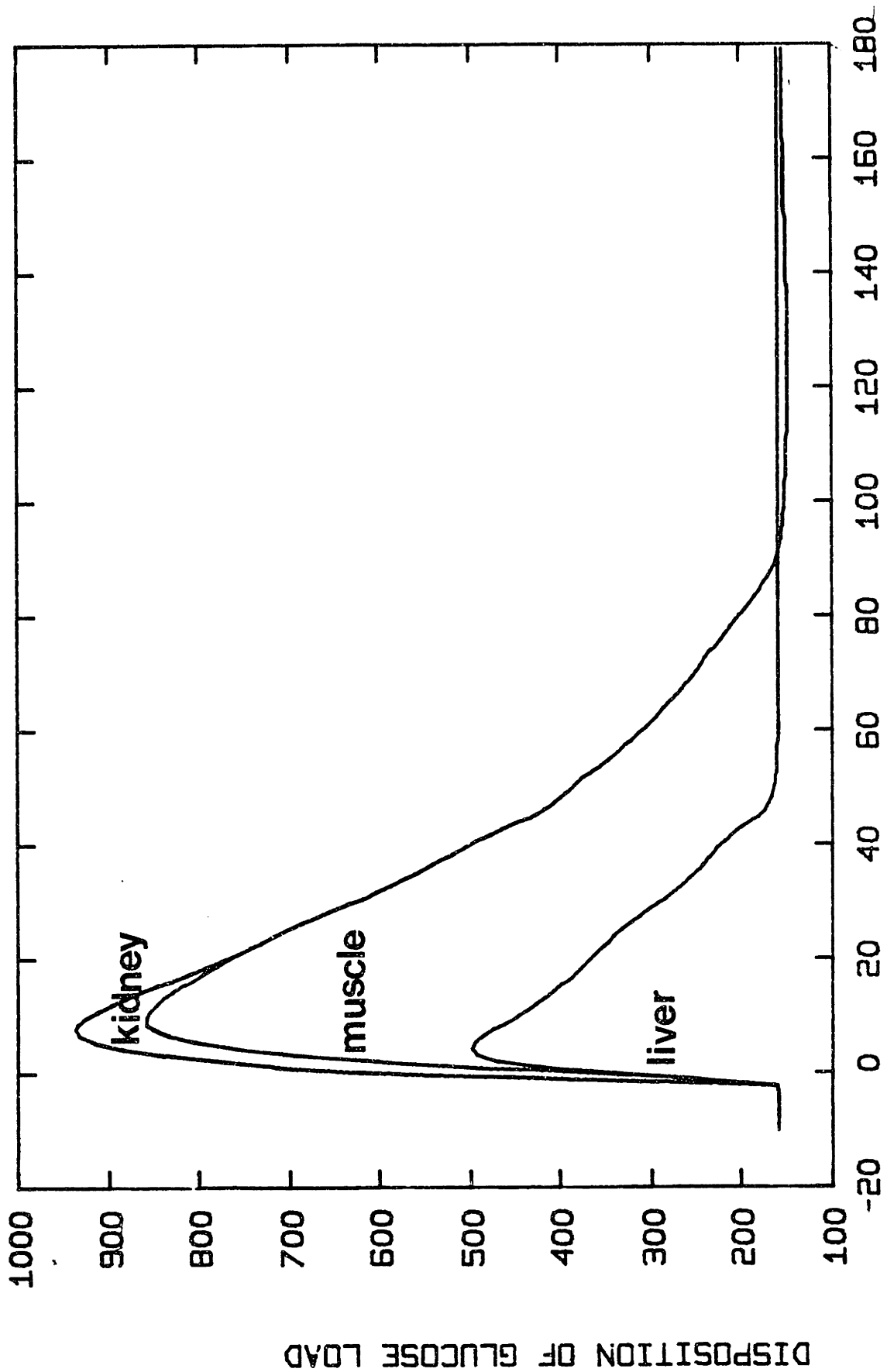

Figure 70

The disposition of a glucose load following a 35 gram IVGTT.

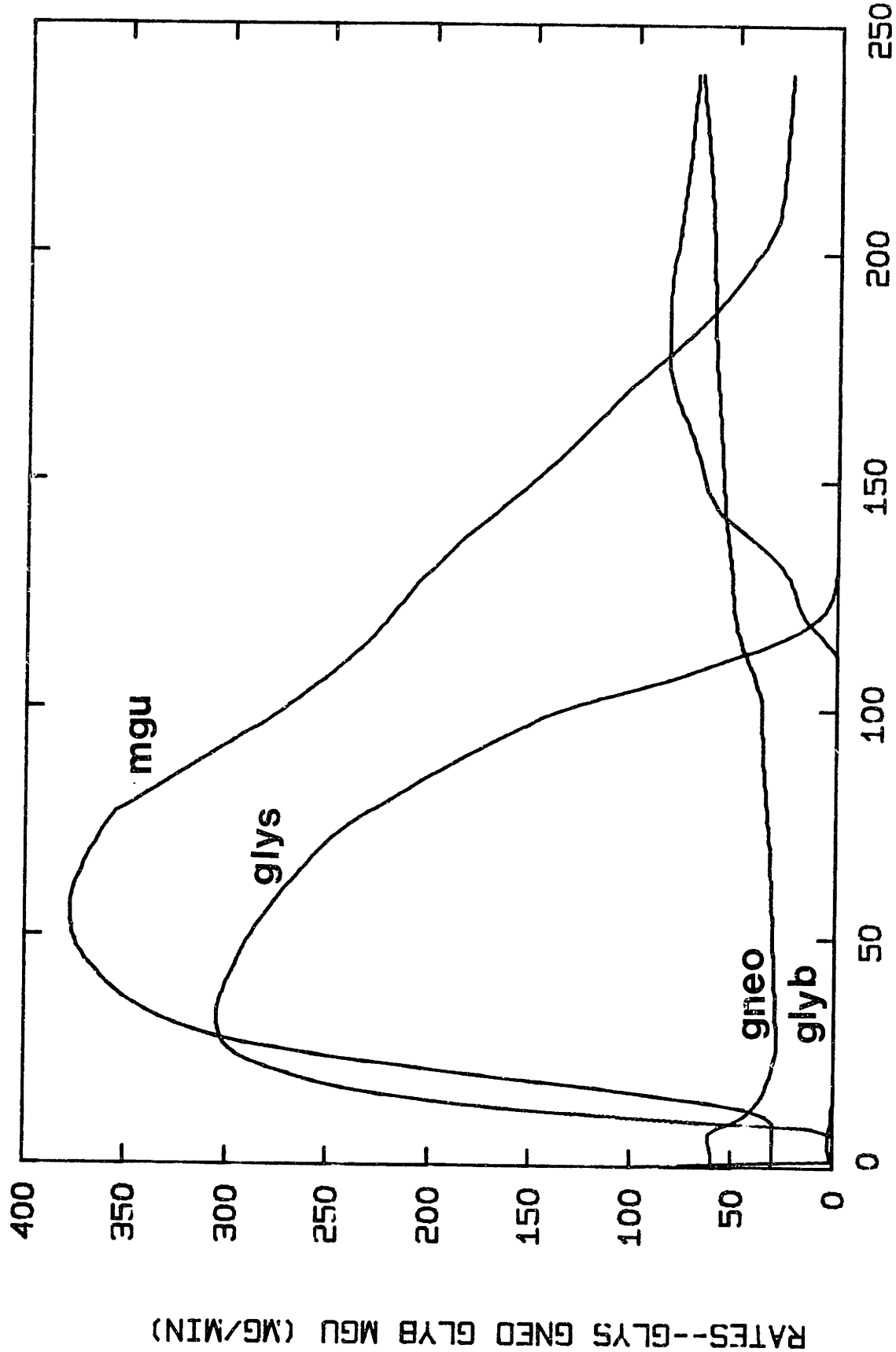

Figure 71

Simulated rates of peripheral glucose uptake (mgu), glycogen synthesis (glys), gluconeogenesis (gneo), and glycogen breakdown (glyb) following a 100 gram oral glucose tolerance test. Note that fasting glycogen stores were taken to be 1/10th of normal.

hepatic production of a glucose of 150 mg/min as seen in figure 71. As glycogen stores are depleted, gluconeogenesis (glucose production from amino and fatty acids) increases to compensate for decreasing glycogen breakdown. Figure 72 shows a simulation in which fasting glycogen stores were taken to be 1/10th normal (i.e. 5 grams). At about 200 minutes, glycogen breakdown begins to decrease, and gluconeogenesis increases. Total liver glucose production remains at the necessary 150 mg/min.

Figure 73 shows the insulin secretion rate. The insulin secretion rate is a function of the total mass of glucose ingested, the rate of glucose absorption, and the gastrointestinal hormones secreted in response to glucose. It is interesting to consider the insulin secretion rate in the absence of any gastrointestinal hormones. Figure 74 shows the result of a simulation, in which the rate of insulin secretion was only a function of glucose. By comparing figures 73 and 74, it is apparent that gastrointestinal hormones potentiate the rate of insulin secretion by 50%. This is in agreement with data reported by Perley and Kipnis (1966). In addition, note that the "second phase" of insulin secretion is significantly diminished. Apparently G.I. hormones affect both the magnitude and duration of both phases of insulin release. Figure 75 demonstrates the relative glucose intolerance that results from such diminished insulin secretion. The peak glucose concentration is delayed to 60 minutes, instead of a peak at 30 minutes observed in normal individuals.

Figures 76 and 77 show the simulated peripheral glucose and insulin concentrations in response to three oral glucose tolerance tests at five hour intervals. Figure 78 presents the rates of peripheral glucose uptake

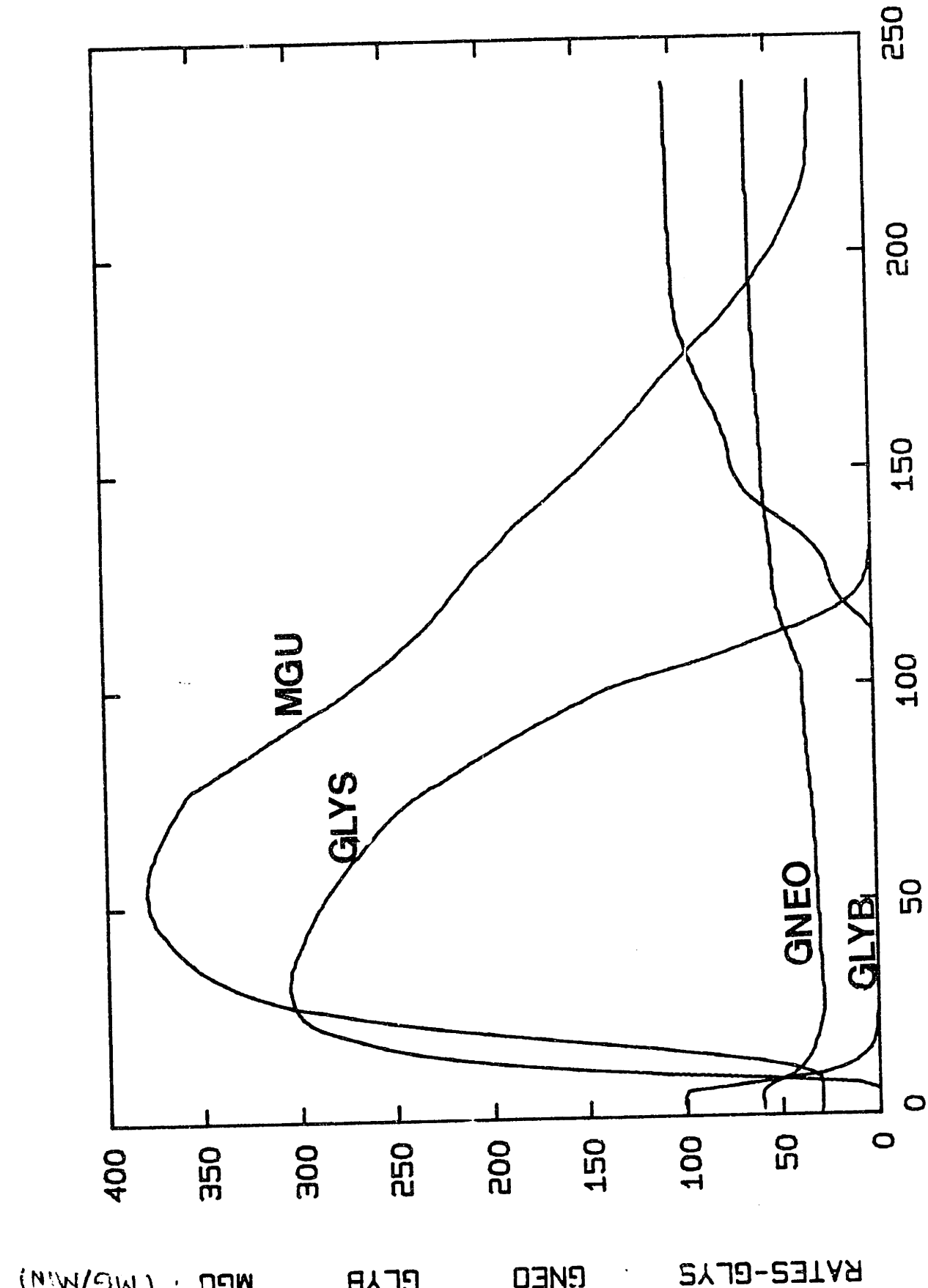

Figure 72

Simulated rates of peripheral glucose uptake (MGU), glycogen synthesis (GLYS), gluconeogenesis (GNEO), and glycogen breakdown (GLYB) following a 100 gram oral glucose tolerance test.

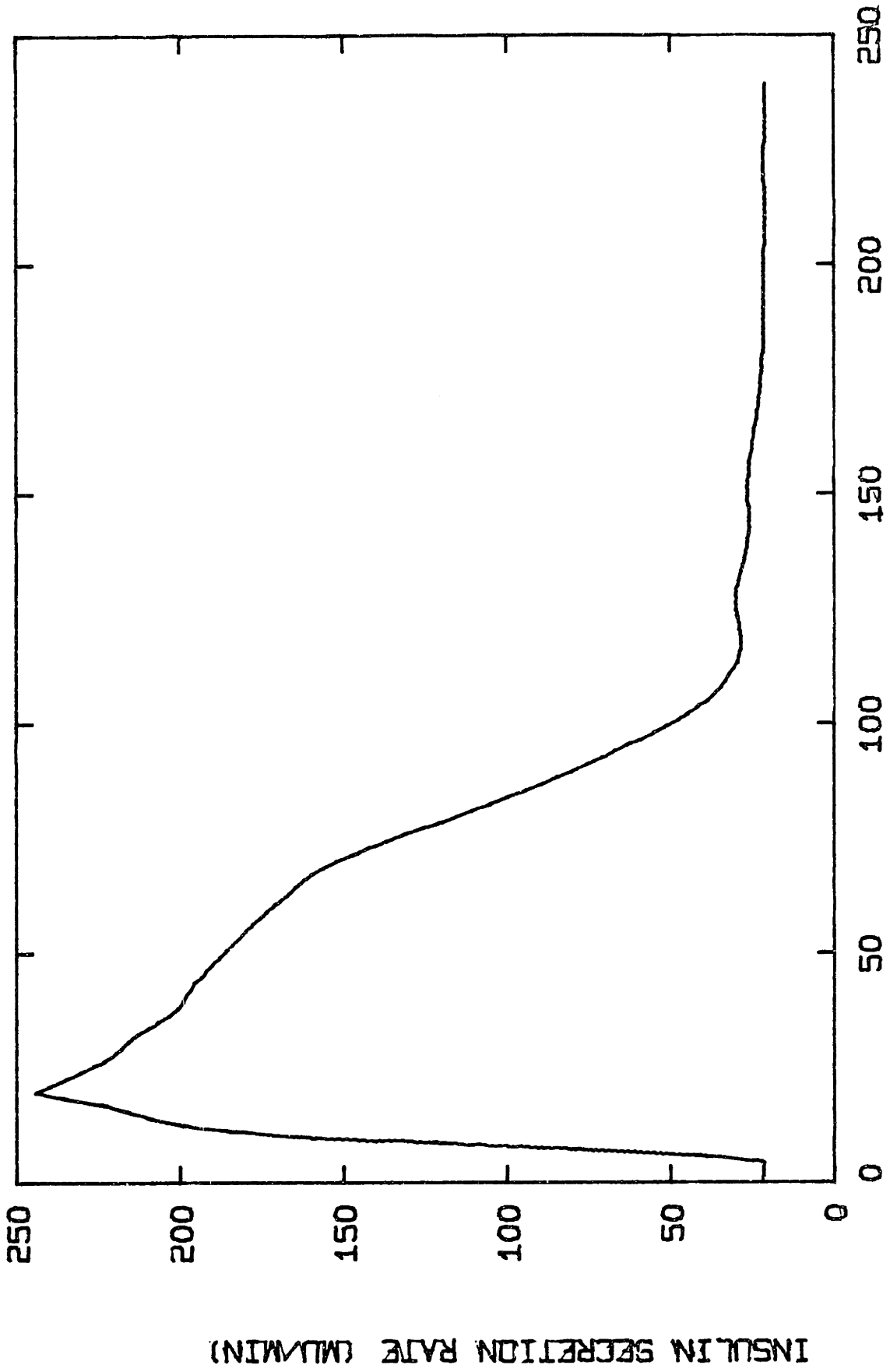

Figure 73

The rate of insulin secretion in response to a 100 gram oral glucose tolerance test.

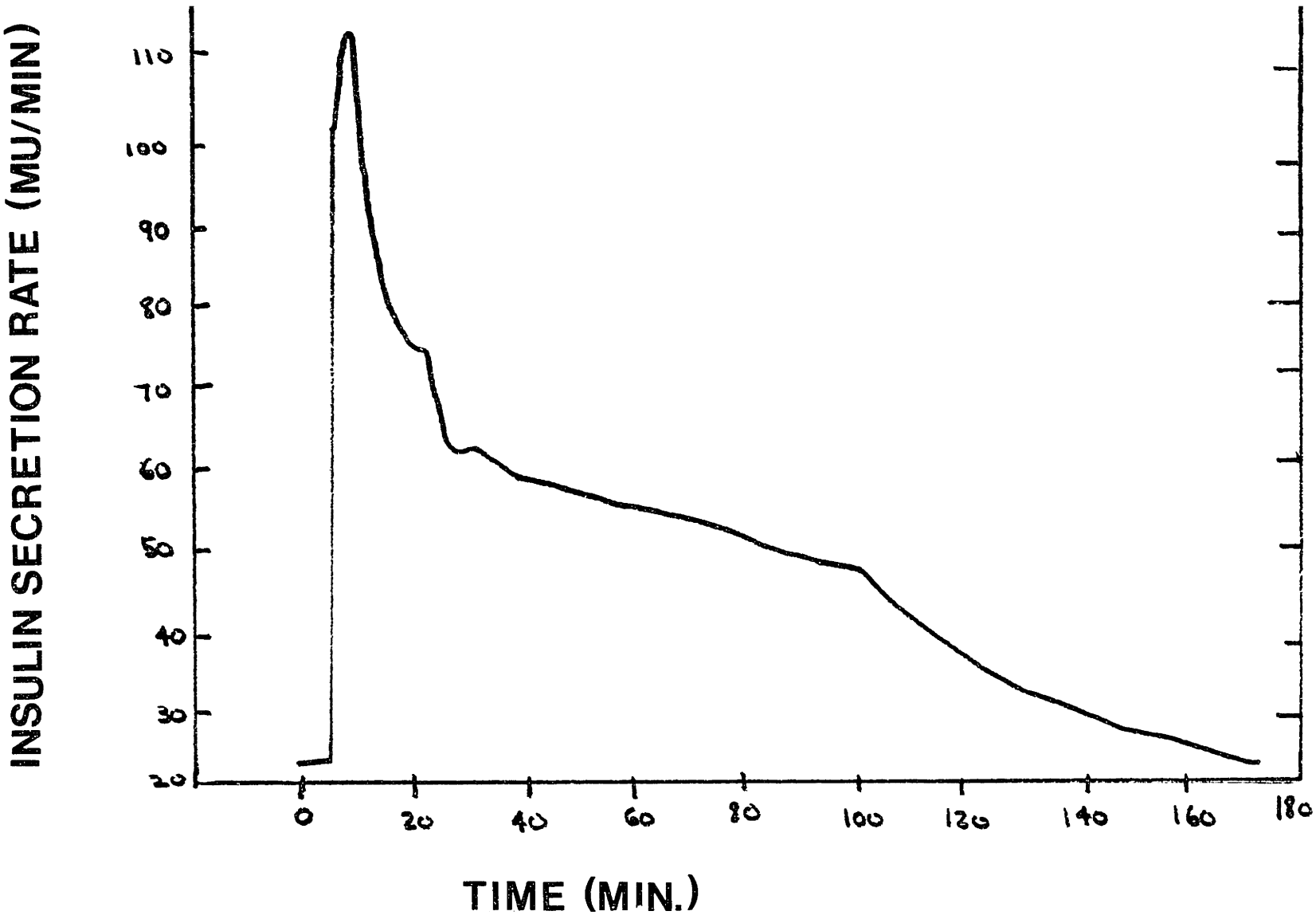

Figure 74

The rate of insulin secretion in response to a 100 gram oral glucose tolerance test. Note that in this simulation, the effect of GI hormones on insulin secretion has been omitted.

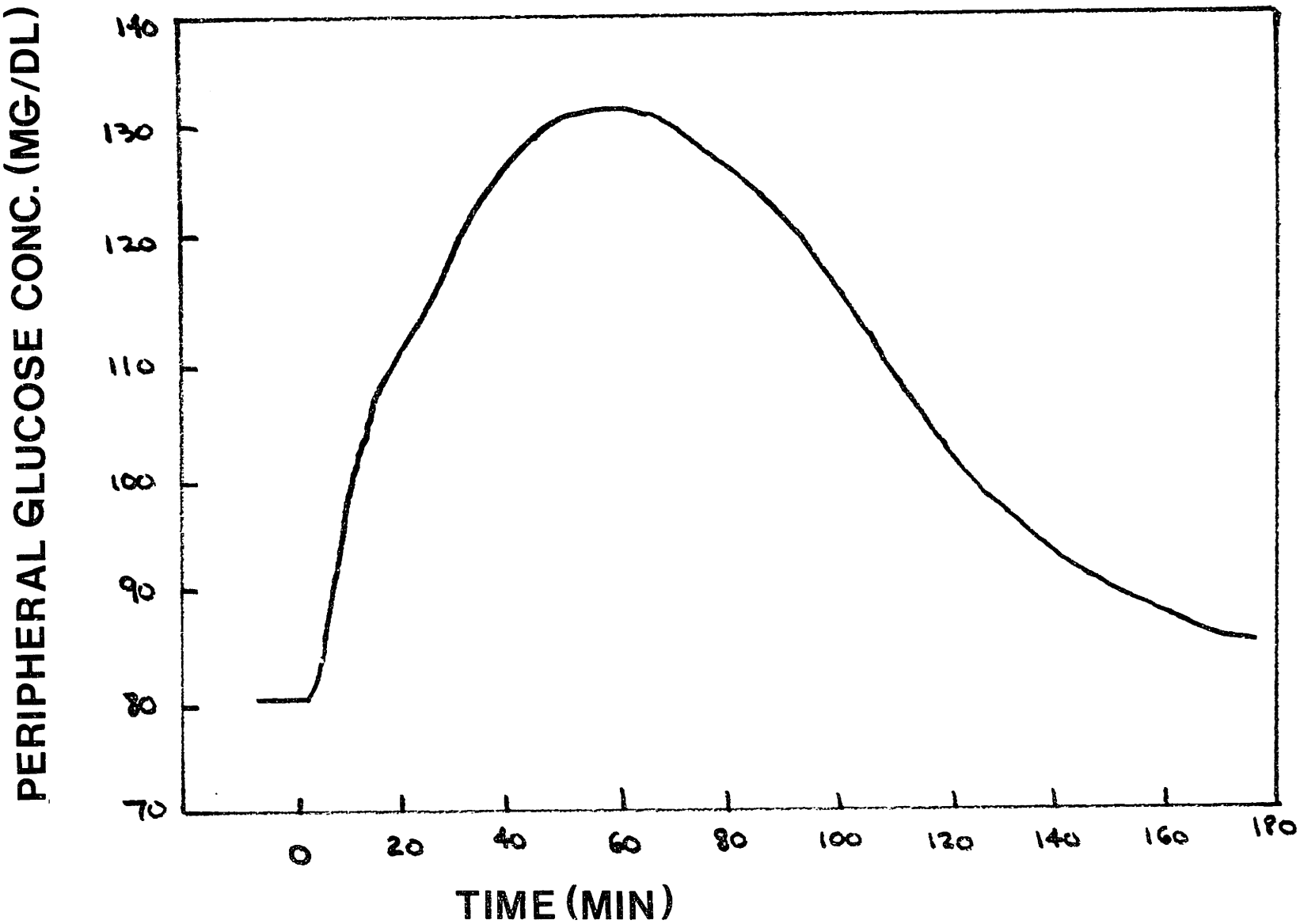

Figure 75

Simulation of the peripheral glucose concentration following a 100 gram oral glucose tolerance test, with diminished insulin secretion.

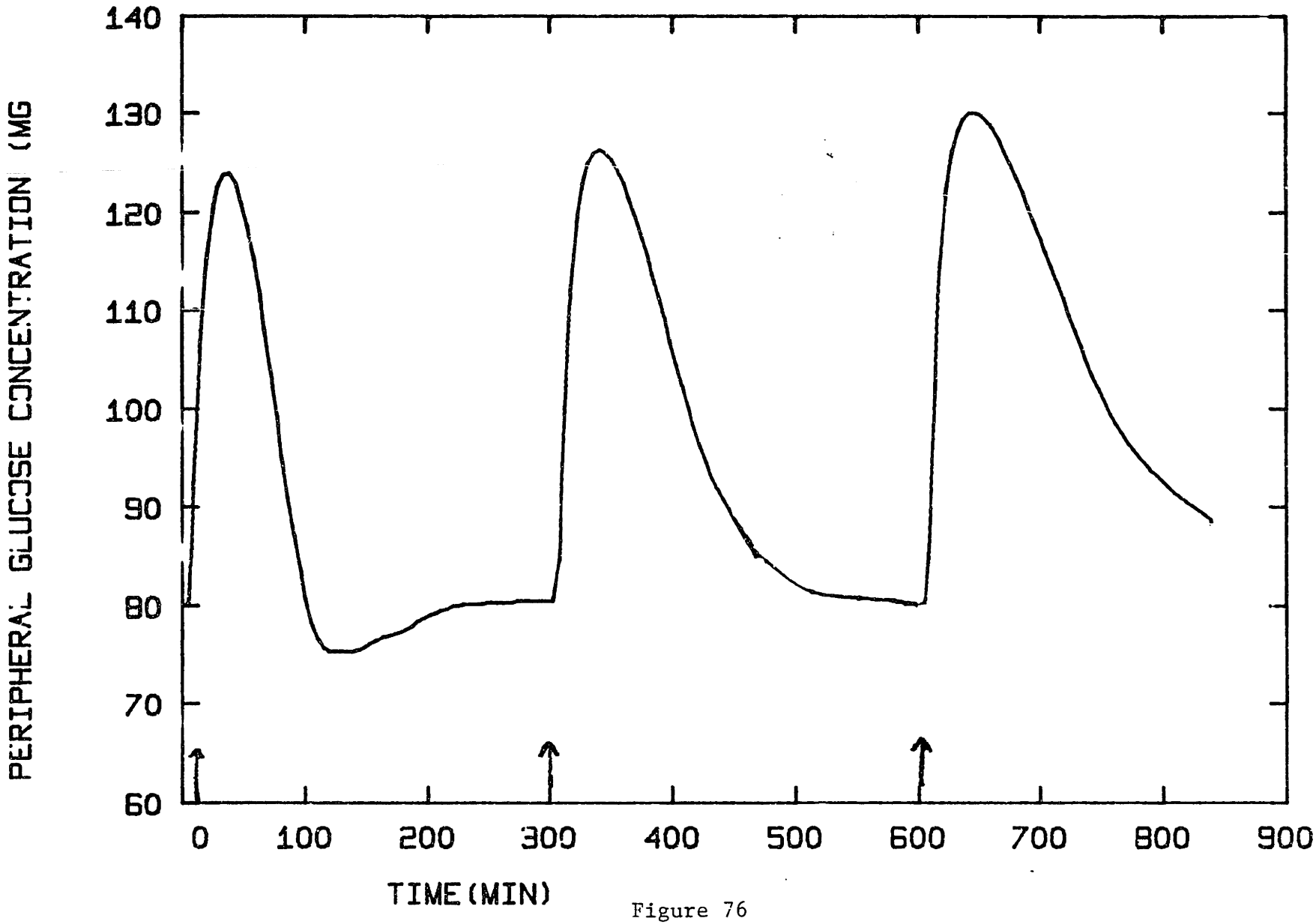

Figure 76

Simulated blood glucose concentration in response to three 100 gram oral glucose tolerance tests at five-hour intervals. (Arrows indicate start of each test.)

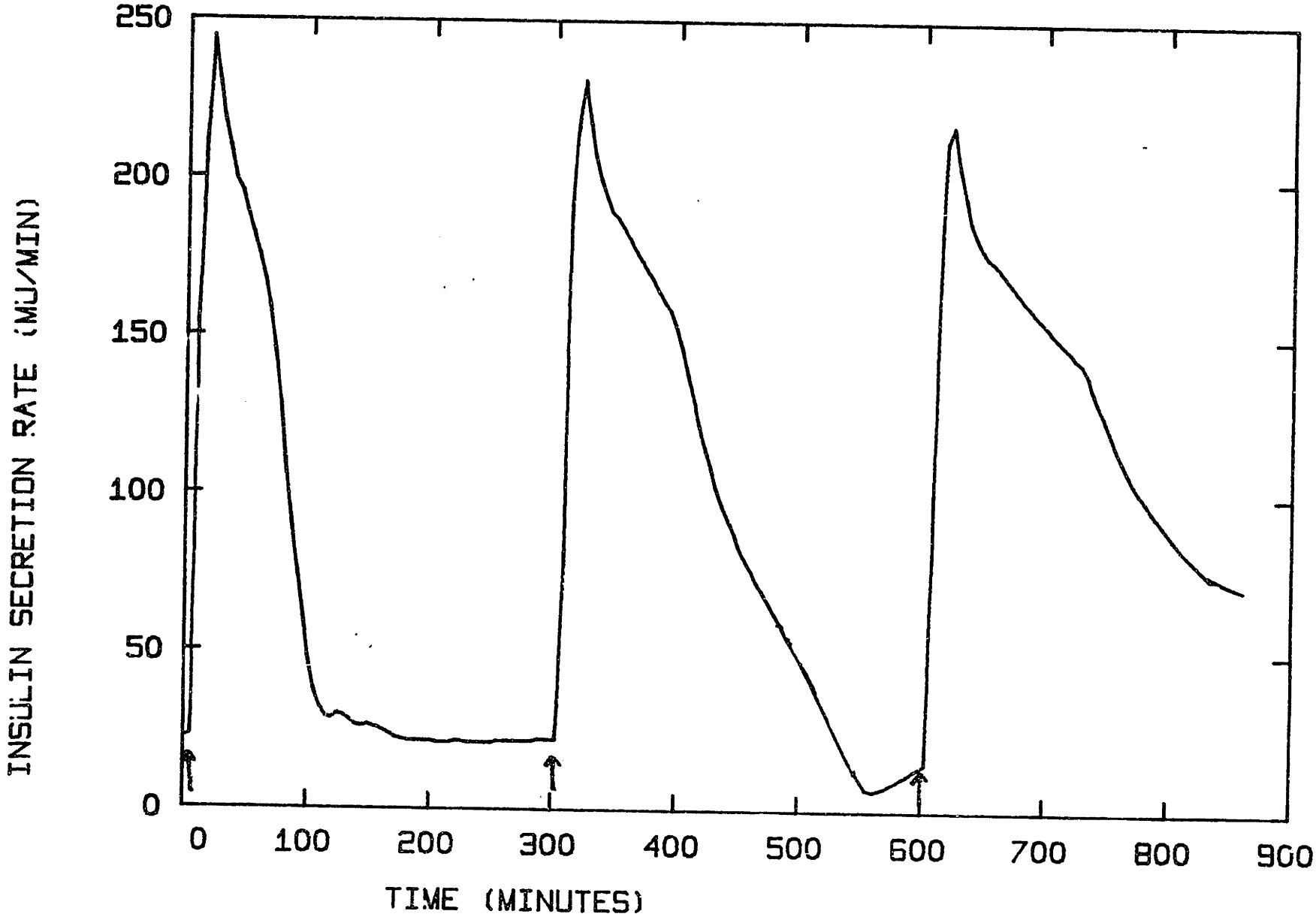

Figure 77

Simulated peripheral insulin concentrations in response to three 100 gram oral glucose tolerance tests at five-hour intervals. (Arrows indicate start of each test.)

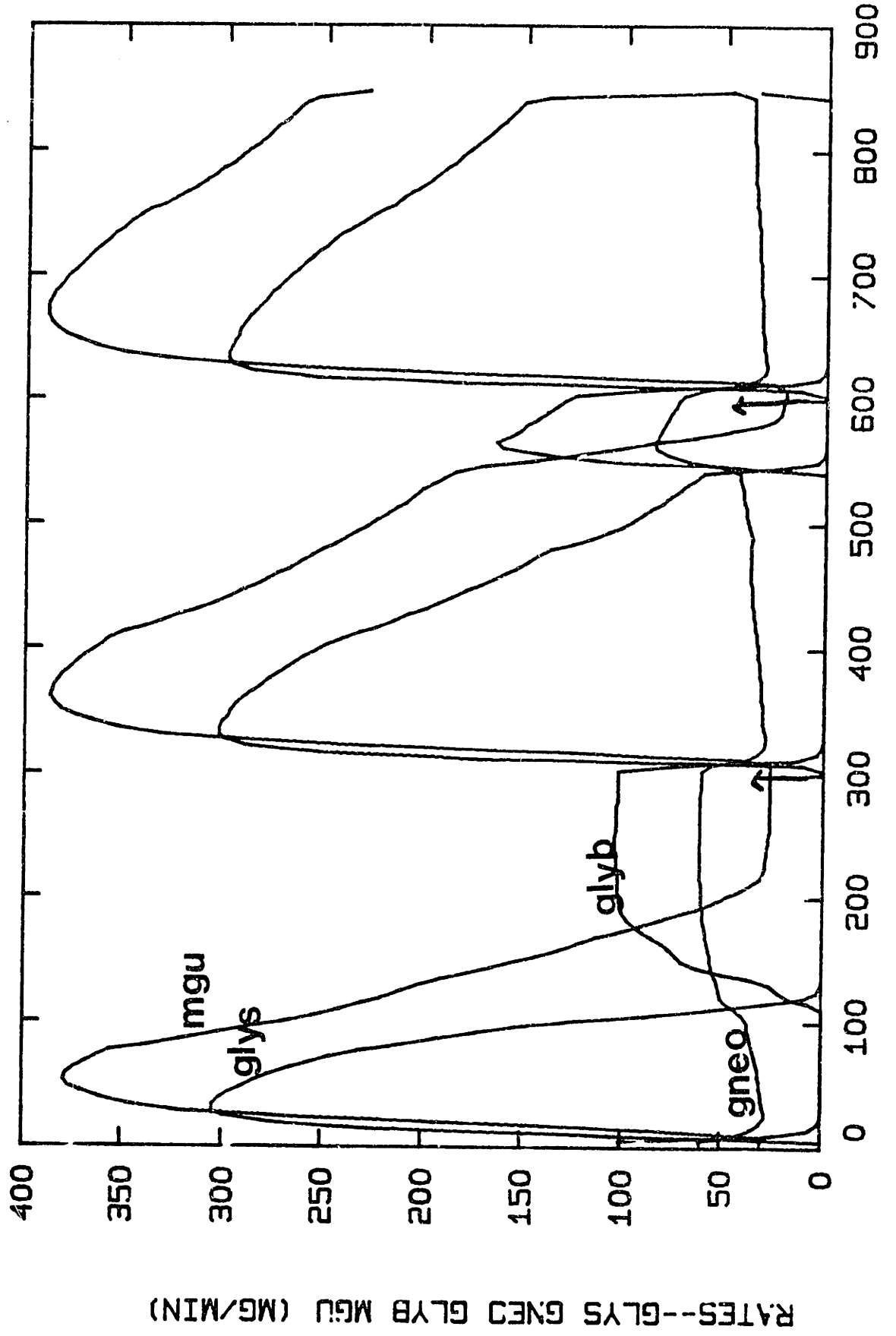

Figure 78

Simulated rates of Peripheral glucose uptake (mgu), glycogen synthesis (glys), glycogen breakdown (glyb), and gluconeogenesis (gneo) in response to three 100 gram oral glucose tolerance tests at five-hour intervals. (Arrows indicate start of each test.)

(MGU), glycogen synthesis (GLYS), glycogen breakdown (GLYB) and glyconeogenesis during this 15 hour period. There is very little data on the continuous monitoring of glucose and insulin concentrations throughout the course of a day (Minuze et al, 1977; Hansen and Johansen,1970; Molner and Taylor, 1972; Malherbe et al, 1969). Direct comparison with data is not possible, although the qualitative shape of curves and their duration is comparable to published studies.

Figures 79 and 80 present phase plots of the simulated peripheral insulin concentration as a function of peripheral glucose concentration following an OGTT and IVGTT respectively. Figures 81 and 82 present phase plots of insulin secretion rate versus pancreatic (arterial) glucose concentrations. These plots will be important in comparing the degree of control achieved by different delivery methods of insulin to diabetics.

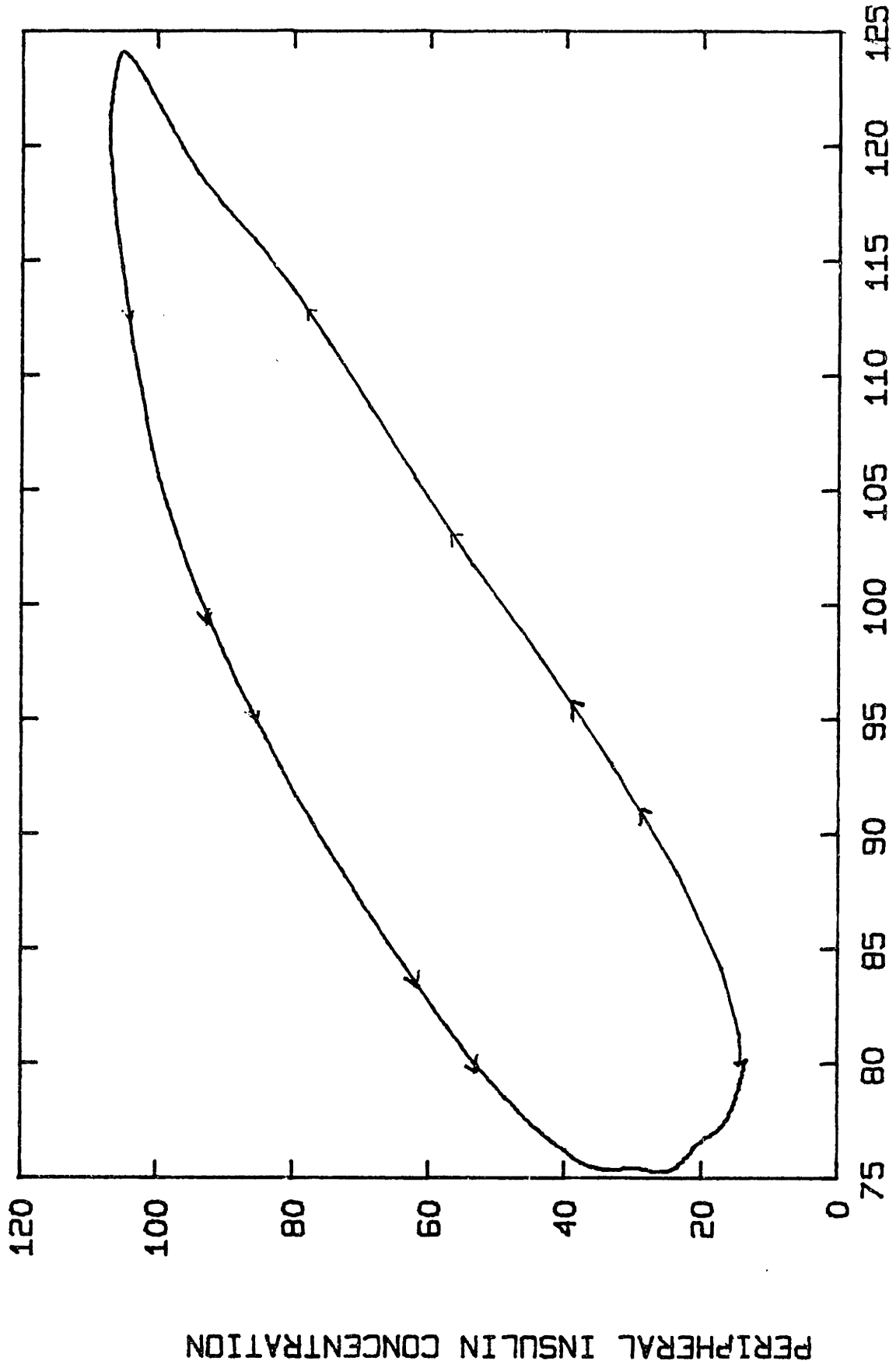

Figure 79

Phase plot of simulated peripheral insulin versus peripheral glucose concentrations following a 100 gram oral glucose tolerance test.

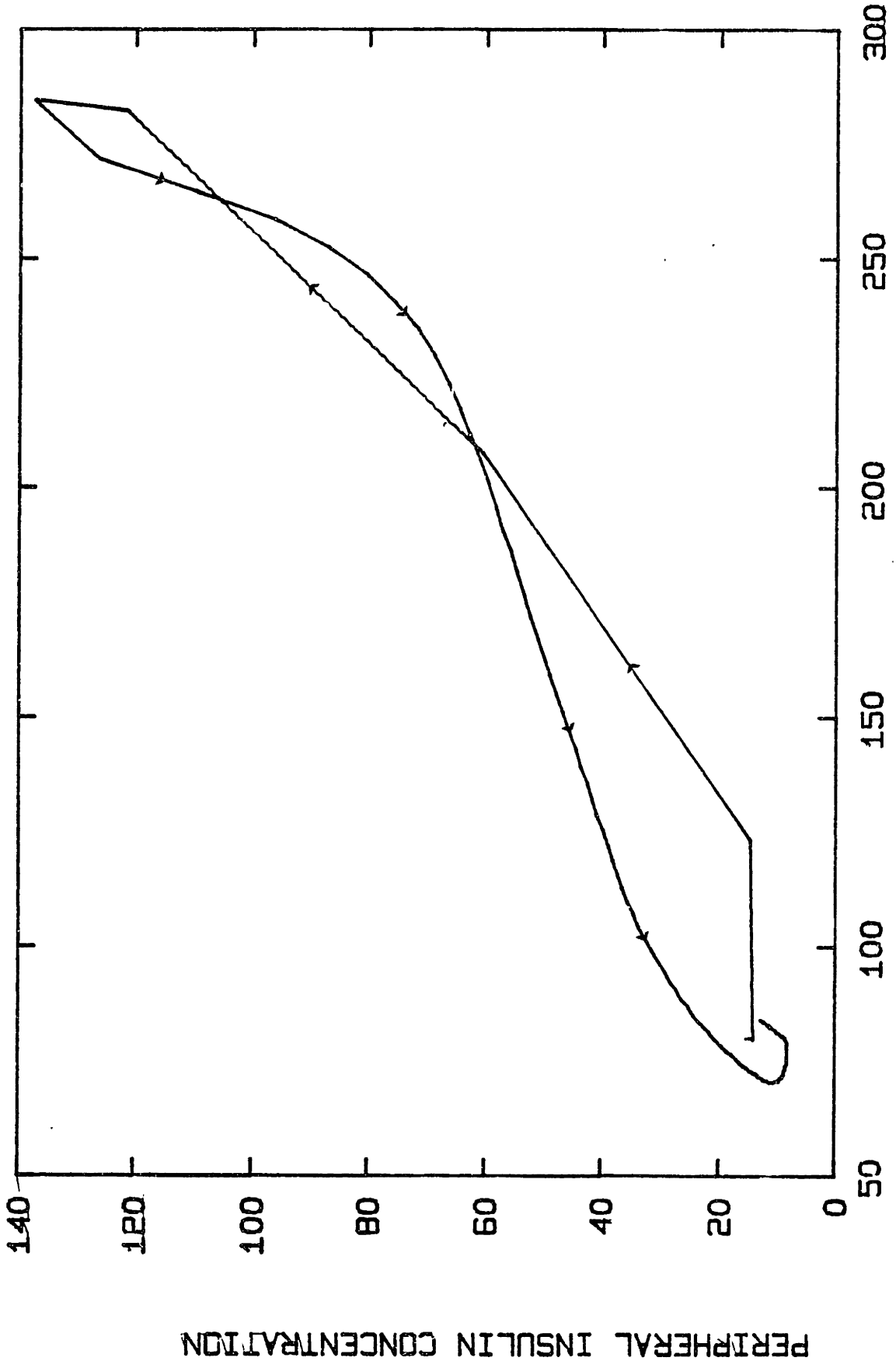

Figure 80

Phase plot of simulated peripheral insulin versus peripheral glucose concentrations following a 35 gram IVGTT.

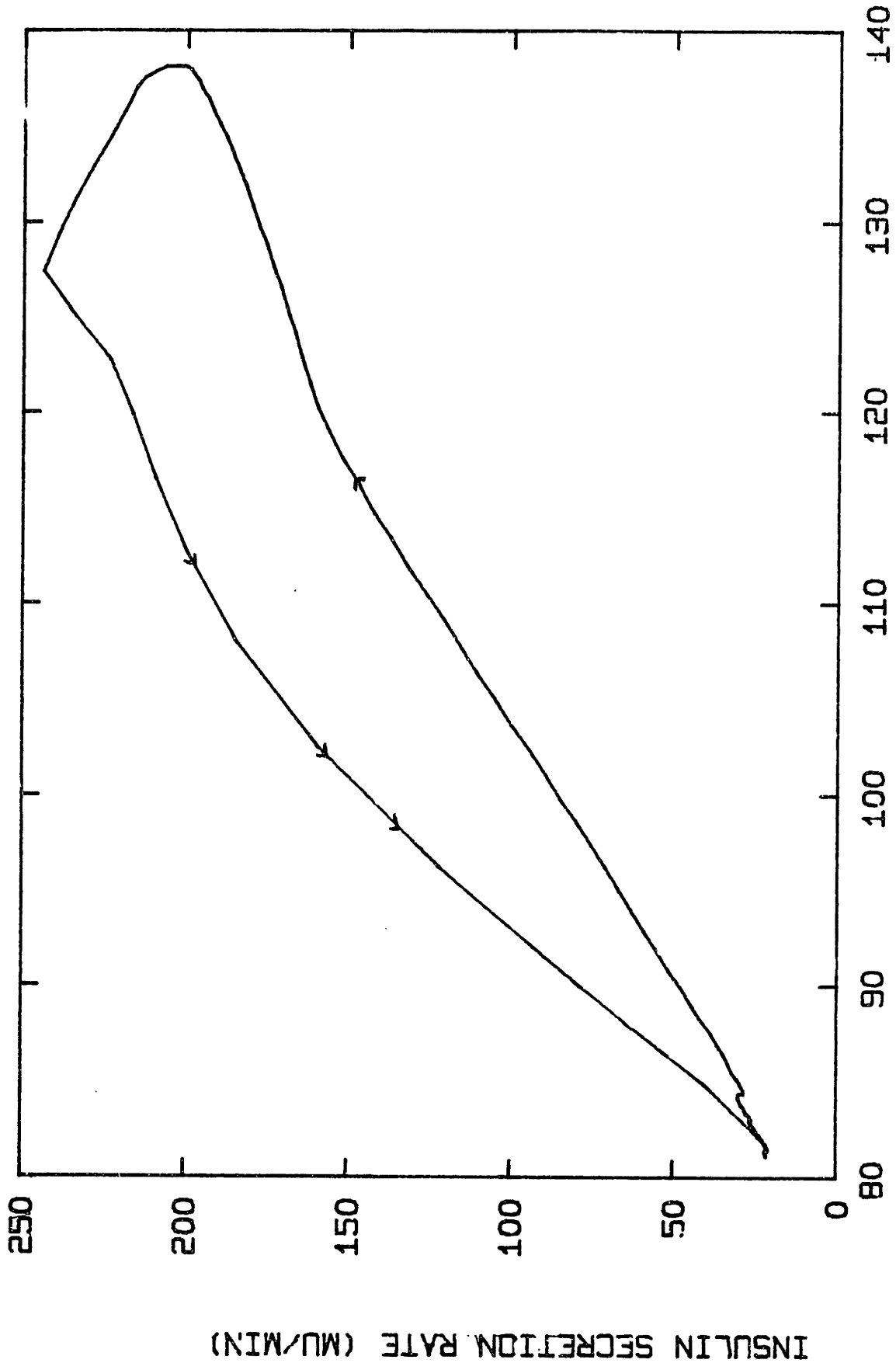

Figure 81

Phase plot of simulated insulin secretion rate versus arterial glucose concentrations following a 100 gram oral glucose tolerance test.

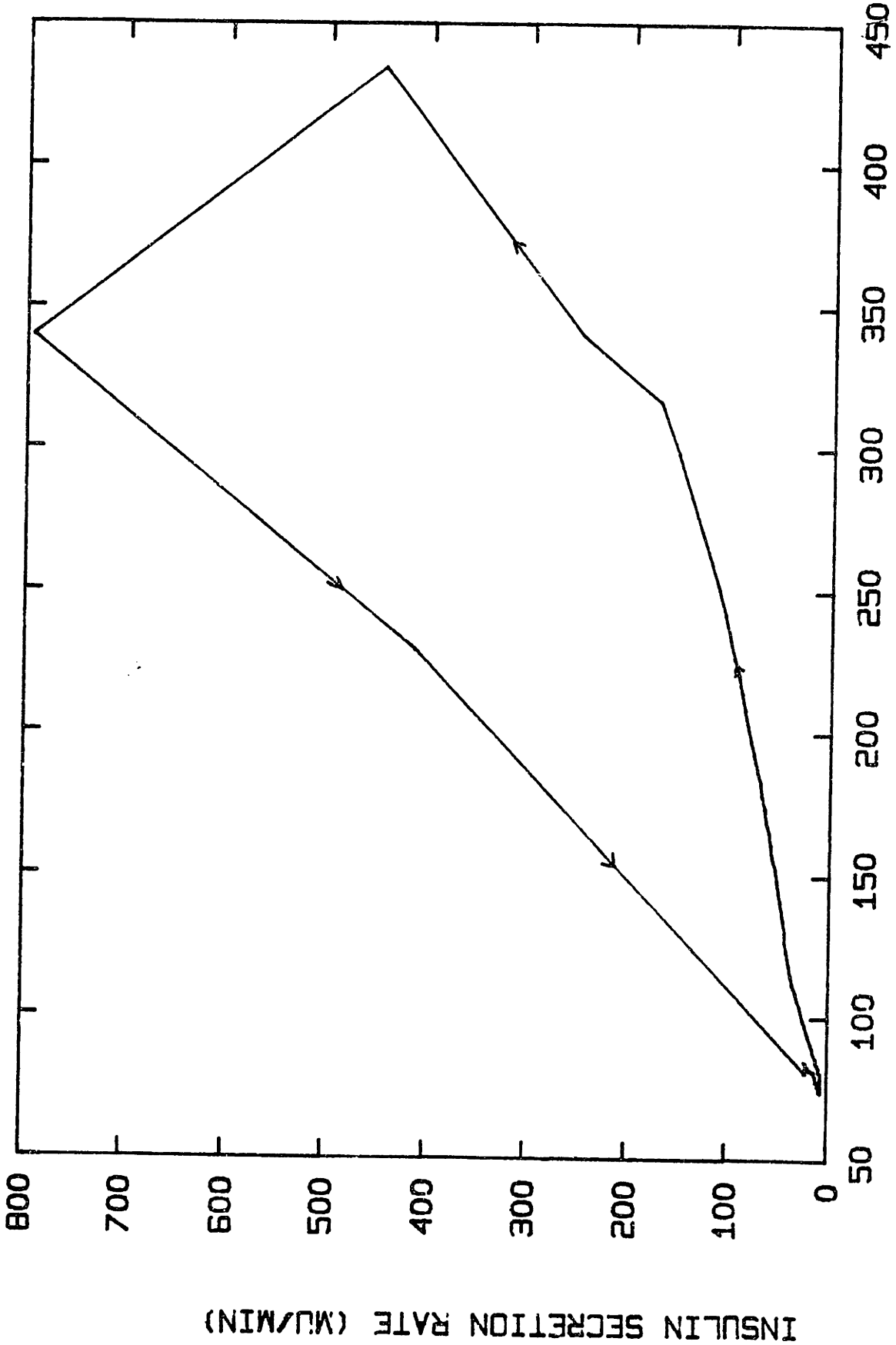

Figure 82

Phase plot of simulated insulin secretion rate versus arterial glucose concentration following a 35 gram IVGTT.

The only other dose for which data is available, is a 50 gram oral glucose tolerance test. This dose is the standard one used in Europe. Figures 83 and 84 show the experimental and simulated peripheral glucose and insulin concentrations after a 50 gram OGTT. The data from Buchanan and McKiddie (1967) represent the mean glucose and insulin concentration in 34 normal subjects. (The standard deviation for insulin measurements is presented because of the large deviations in the data).

The model developed here is a powerful tool to use in understanding the characteristics of the glucoregulatory system. In the following sections current therapies for insulin delivery for insulin-dependent (i.e. juvenile onset) diabetes will be simulated to observe the degree of control achieved by each method. Then, various aspects of the glucoregulatory system will be investigated to understand the critical variables for achieving glucose control. These results will be applied to suggest a temporal pattern of insulin secretion that closely approximates the normal response of the pancreas to glucose stimuli. Finally, this temporal pattern will be contrasted with current concepts of therapy.

A. Intramuscular Insulin Injection

The current therapy for insulin-dependent diabetics consists of intramuscular (I.M.) injections of insulin to lower blood glucose. Although there are many types of insulin preparations, the most common regimen is a single I.M. injection of intermediate acting insulin in the morning. There are two types of intermediate acting insulins - Neutral Protamine Hagedorn (NPH) and Lente. Both preparations consist of insulin mixed with various substances (e.g. zinc, protamine sulfate,

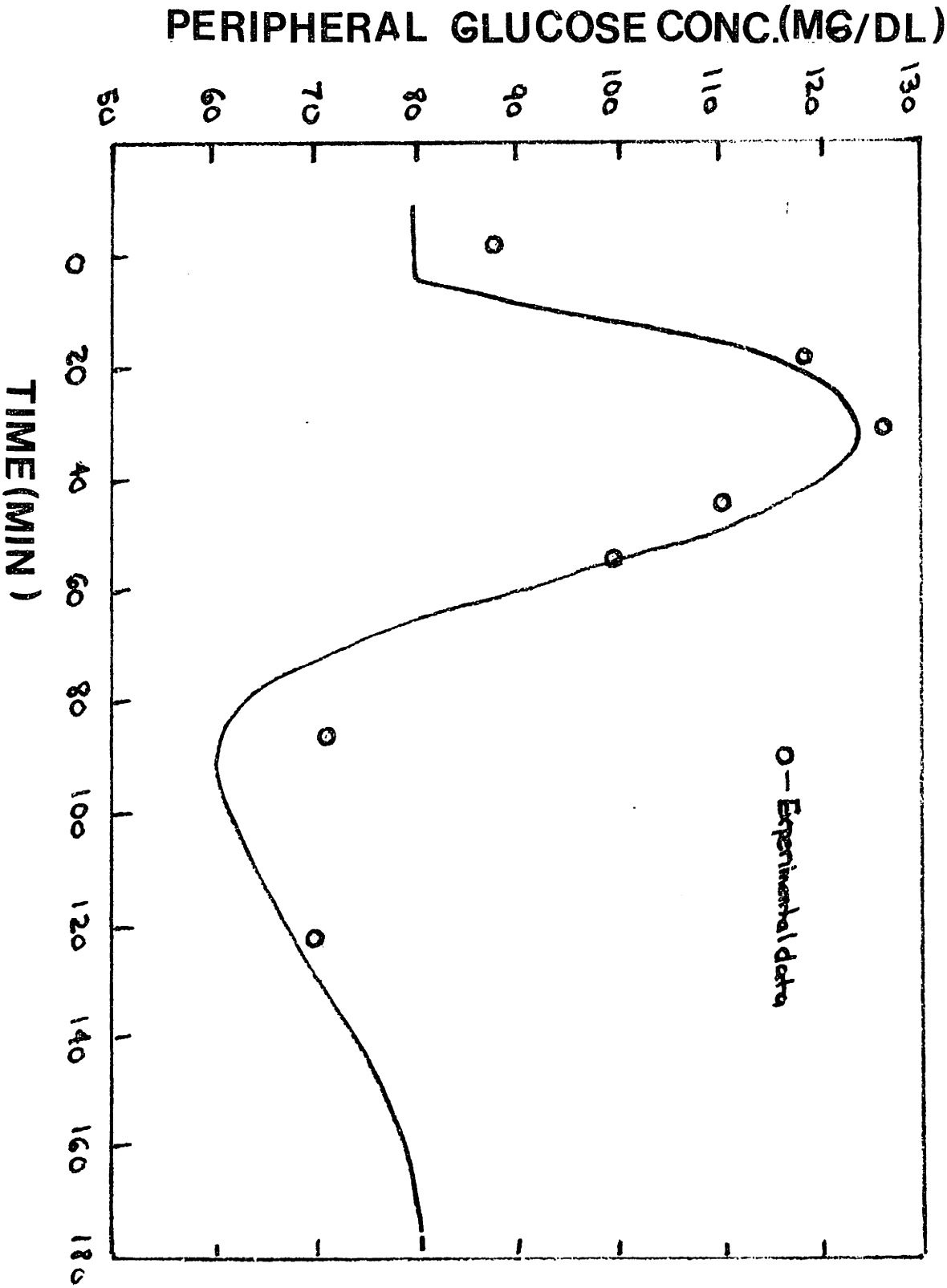

Figure 83

Experimental data and simulation of a 50 gram oral glucose tolerance test.

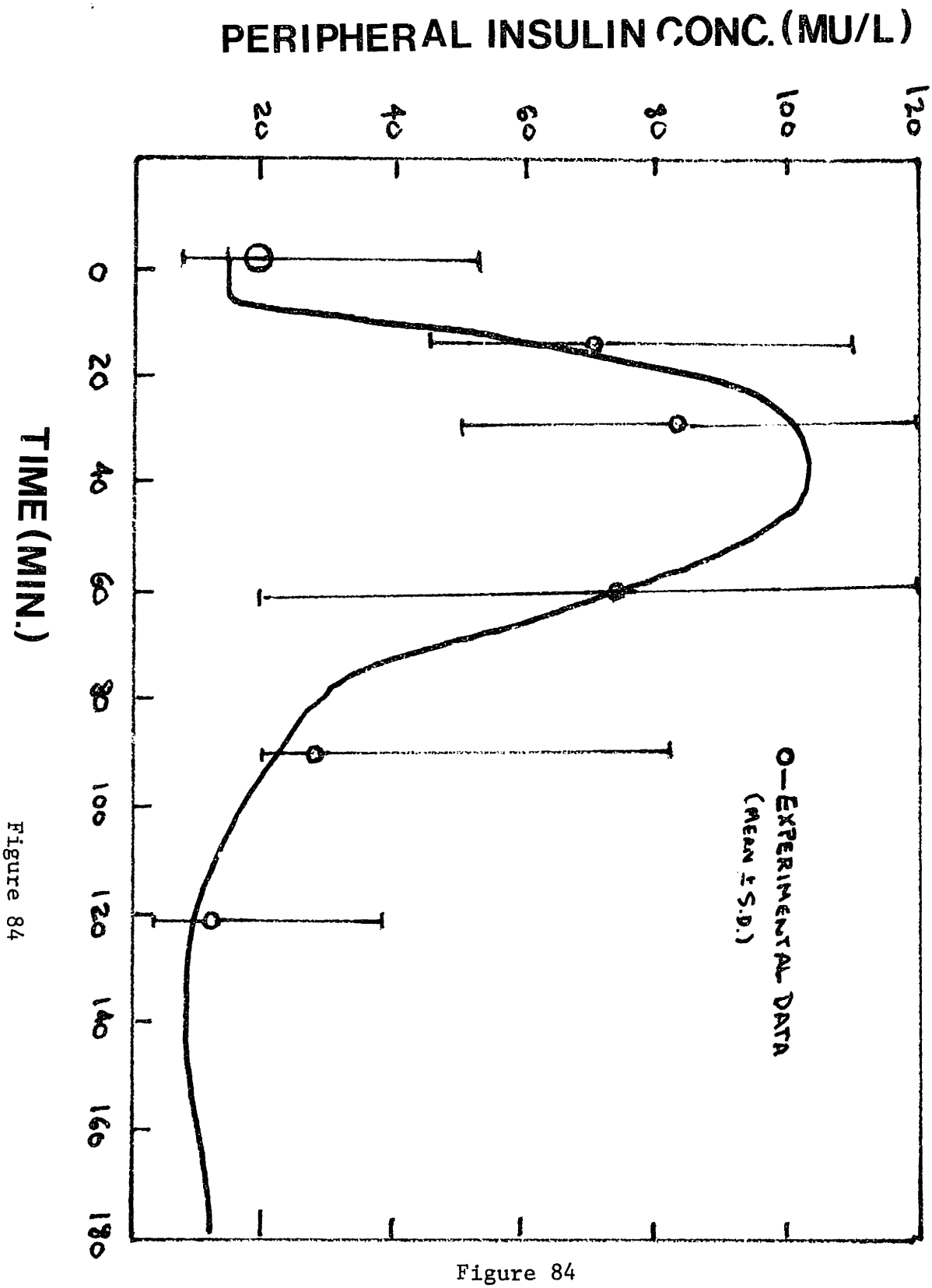

Figure 84

Figure 84

Experimental data and simulation of a 50 gram oral glucose tolerance test.

globin) to retard its rate of absorption. Binder (1969) has published data on the rate of absorption of NPH insulin following an intramuscular injection of 40 units. (Forty units is the average daily insulin requirement for a juvenile-onset diabetic). Figures 85-90 show the results of a simulation in which (1) the insulin secretion rate was set to zero, (2) 40 U of insulin were injected into the peripheral tissue compartment and (3) the rate of absorption of insulin as a function of time was specified. The model was then presented with two 100 gram oral glucose tolerance tests at 5 hour intervals. This was intended to mimic a meal at 8 A.M. (breakfast) and 1 P.M. (lunch). [Figure 86 shows the peripheral insulin concentrations which result from this absorption pattern.] From figure 85, it can be seen that this method of insulin administration poorly regulates peripheral glucose concentrations which rise as high as 300 mg/dl and drop as low as 50 mg/dl.

B. Intravenous Insulin Infusion at a Constant Rate

During a fast of less than 24 hours, insulin levels drop to about 10-20 MU/L. In other words, there is always a measurable level of insulin in the circulation. This low level presumably is the signal for glycogenolysis and lipolysis to meet the fuel requirements of the body. If the insulin concentration falls below this level (as in diabetics), excessive mobilization of free fatty acids and amino acids occur leading to hyperglycemia and glycosuria. Therefore, it has been suggested that unstable diabetics be given a constant infusion of insulin to elevate plain insulin concentrations to 20 MU/L. Two simulations were run in which (1) endogenous insulin secretion was set to zero, and

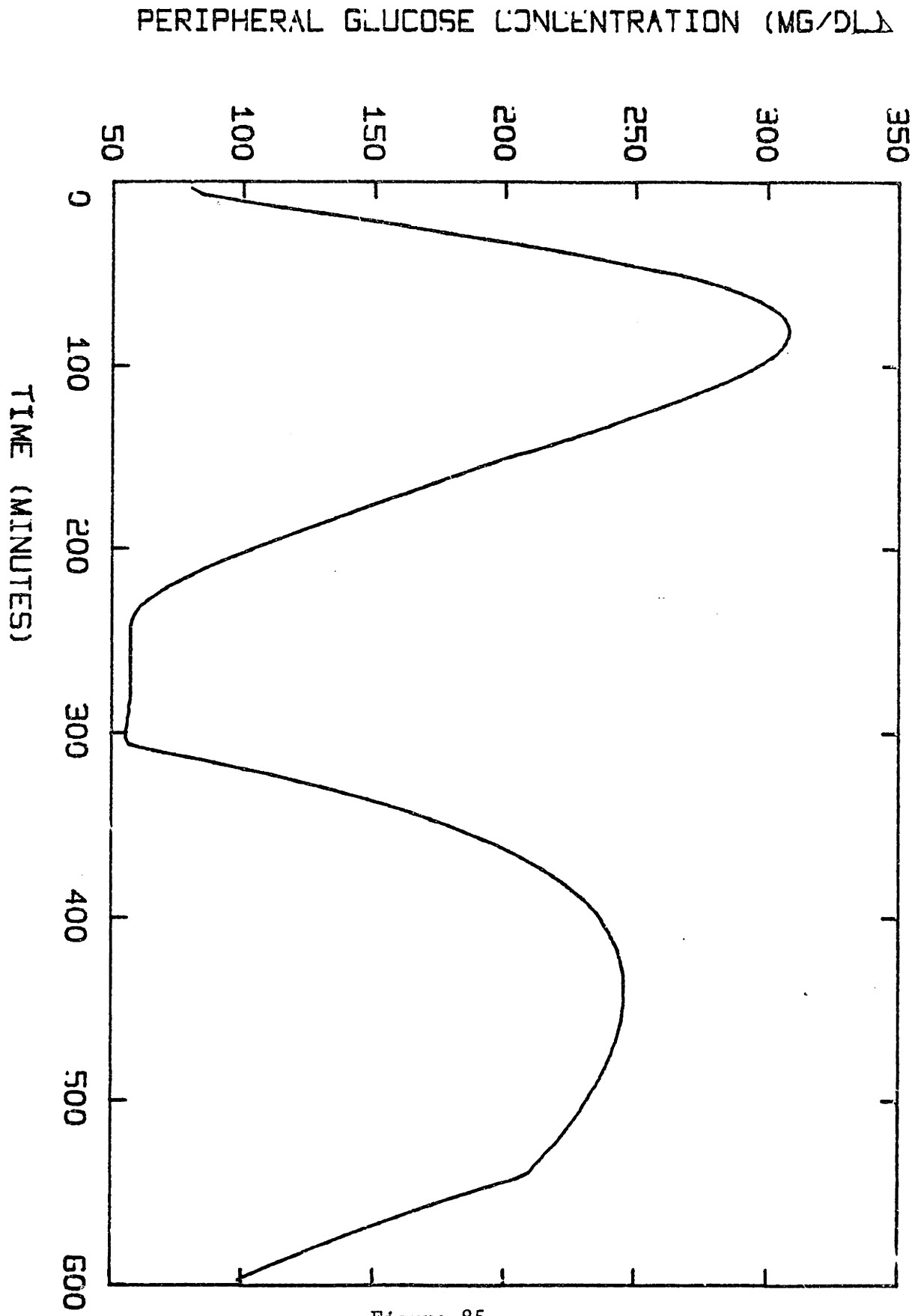

Figure 85

Intramuscular insulin injection of 40 units of intermediate-acting insulin. Simulation of response to two 100 gram OGTT at 5 hour

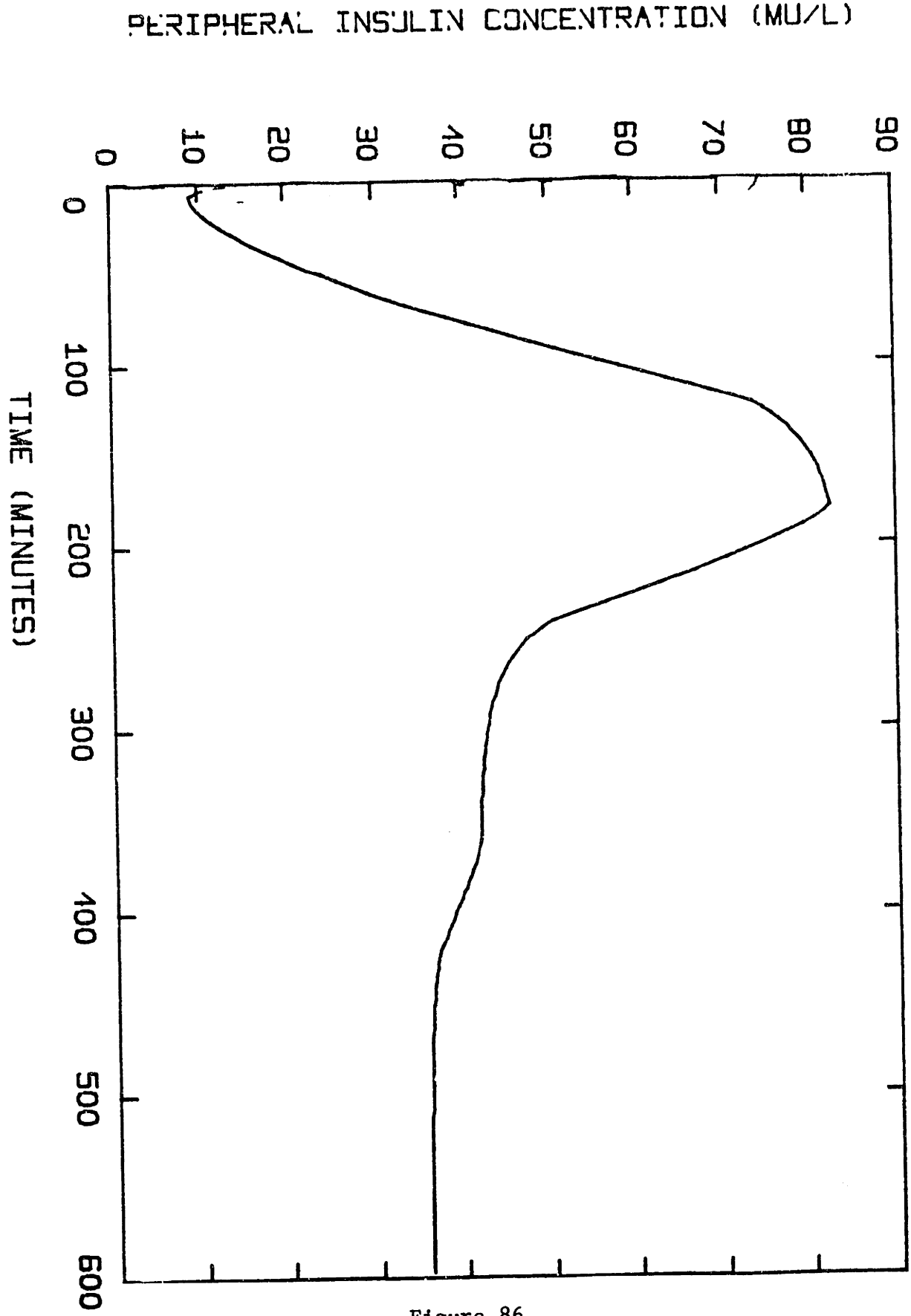

Figure 86

Intramuscular insulin injection of 40 units of intermediate-acting insulin. Simulation of response to two 100 gram OGTT at 5 hour intervals, under these conditions.

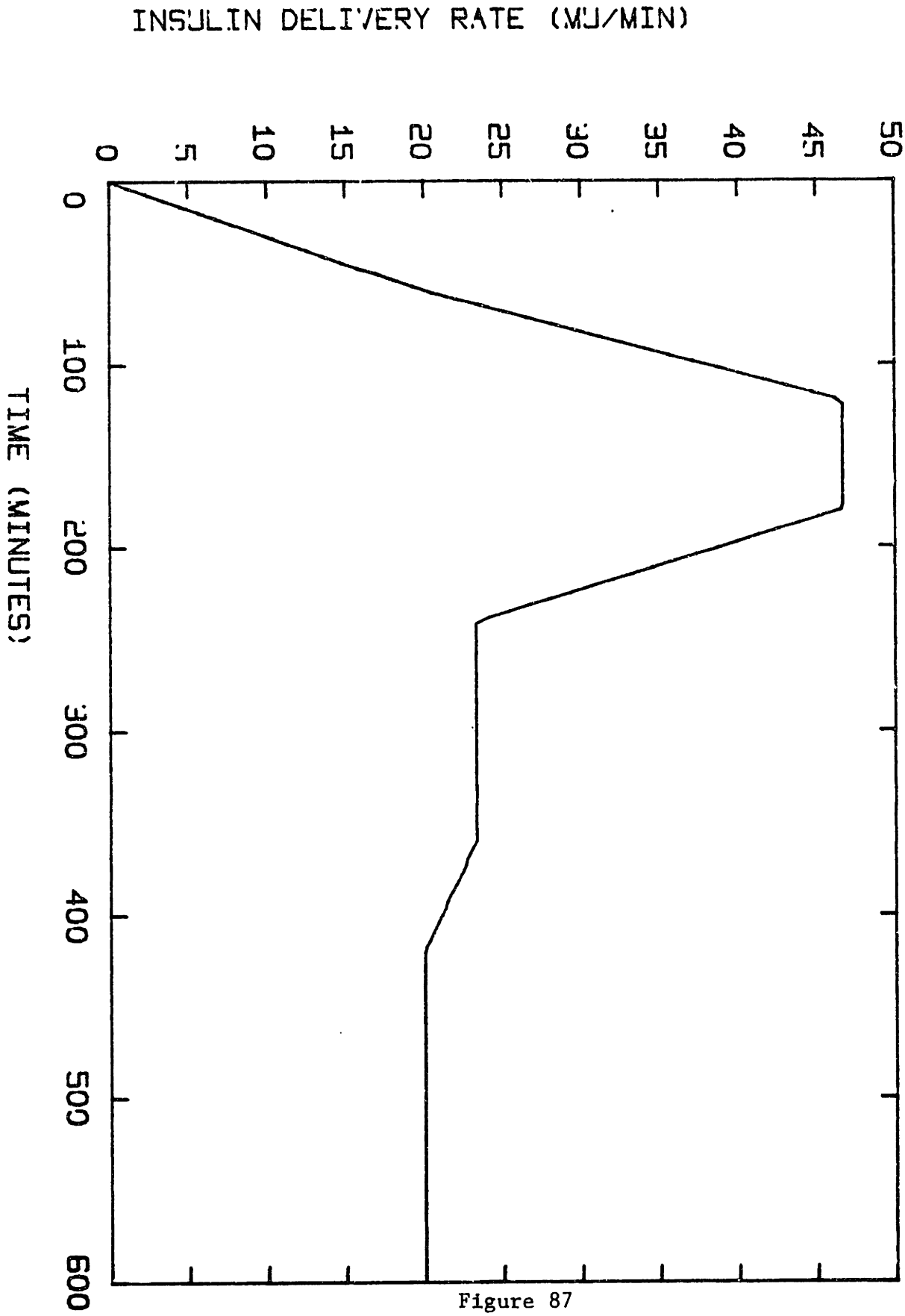

Figure 87

Intramuscular insulin injection of 40 unitsof intermediate-acting insulin. Simulation of response to two 100 gram OGTT at 5 hour intervals, under these conditions.

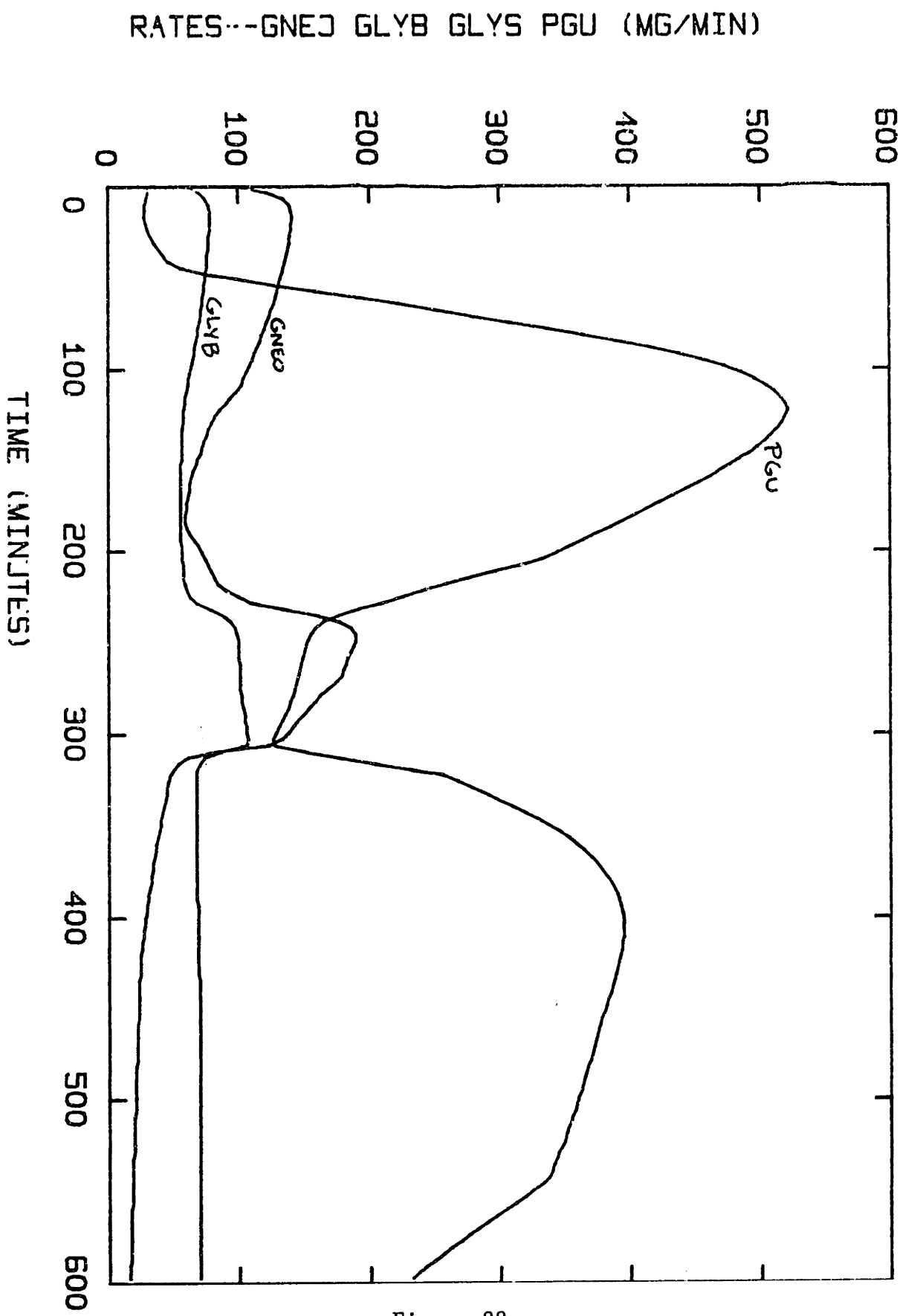

Figure 88

Intramuscular insulin injection of 40 units of intermediate-acting insulin. Simulation of response to two 100 gramm OGTT

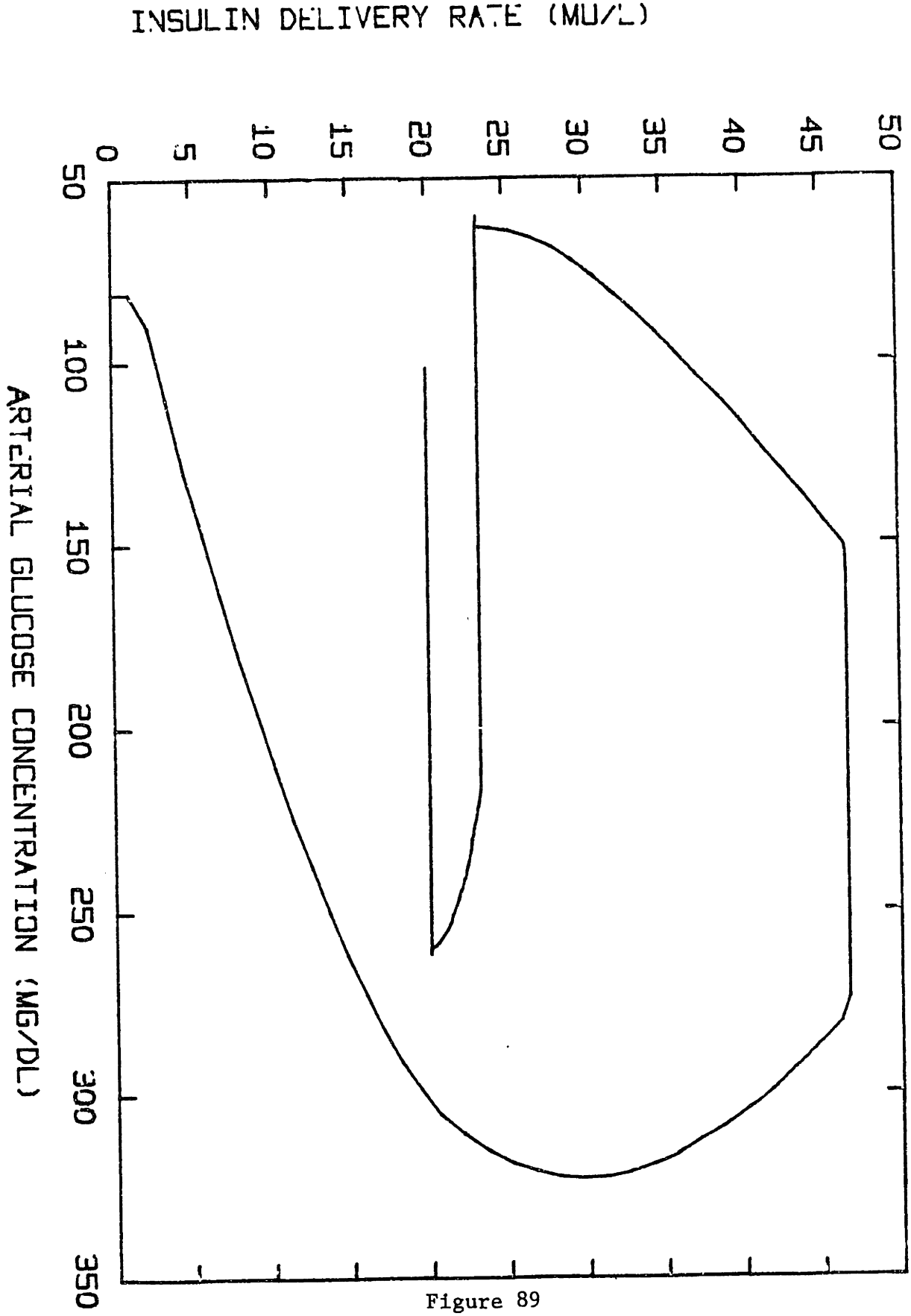

Figure 89

Intramuscular insulin injection of 40 units of intermediate-acting insulin. Simulation of response to two 100 gram OGTT at 5 hour intervals, under these conditions.

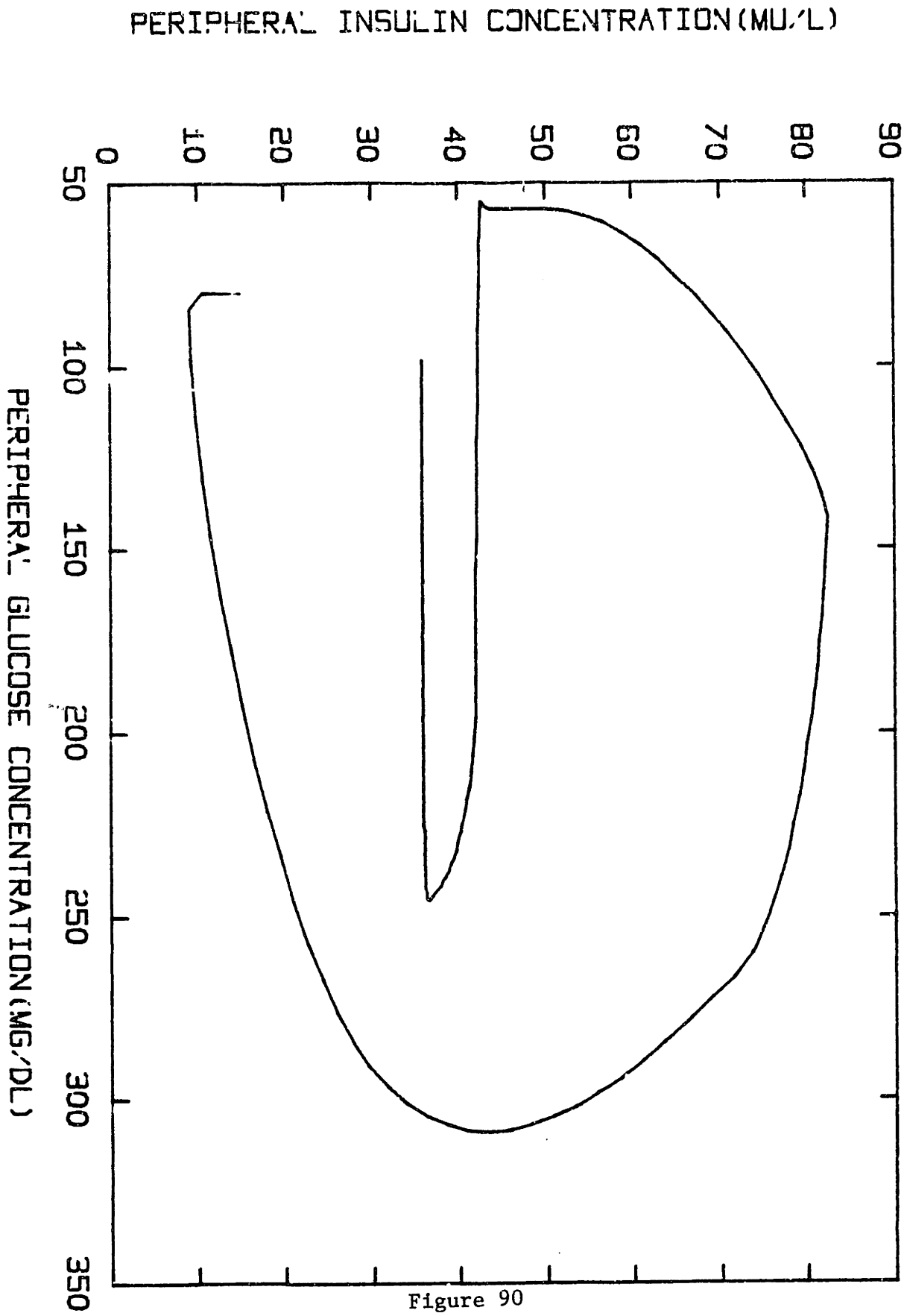

Figure 90

Intramuscular insulin injection of 40 units of intermediate-acting insulin. Simulation of response to two 100 gram OGTT at 5 hour intervals, under these conditions.

(2) constant infusions of insulin were given intravenously to elevate plasma insulin concentrations to 20 MU/L and 40 MU/L, respectively. Then the model was presented with a 100 gram oral glucose tolerance test. Figure 91-92 and 93-94 show peripheral glucose and insulin concentrations for each dose. Although glucose levels do return to the baseline, the peripheral glucose levels reach unacceptably high levels, and remain elevated for longer than normal periods. Therefore, one can conclude that constant infusions are sufficient for preventing excess glucose production during fasting, but inadequate in preventing severe hyperglycemia following an oral glucose load.

C. Pulsed Insulin Delivery

As discussed in Section II., Genuth and Martin (1977) have developed an insulin delivery system that provides pulses of insulin after each meal and a constant infusion thereafter. The pulse elevates insulin concentrations five-to-tenfold above baseline at its peak which occurs at 45 minutes. The pulse was designed to mimic the pancreatic secretion of insulin after a meal, thereby maintaining hyperglycemia within normal bounds. A simulation was run in which insulin secretion was set to zero and insulin secretion into the peripheral blood $D(t)$, was calcualted by

$$D(t) = (a_4 e^{-t/a_2} - a_5 e^{-t/a_3}) + KI_o$$

The constants chosen[3] were for a 70 Kg man and an insulin degredation time of 15 minutes (the parameters which correspond to the model).

---

[3] P. Martin, personal communication, 1977.

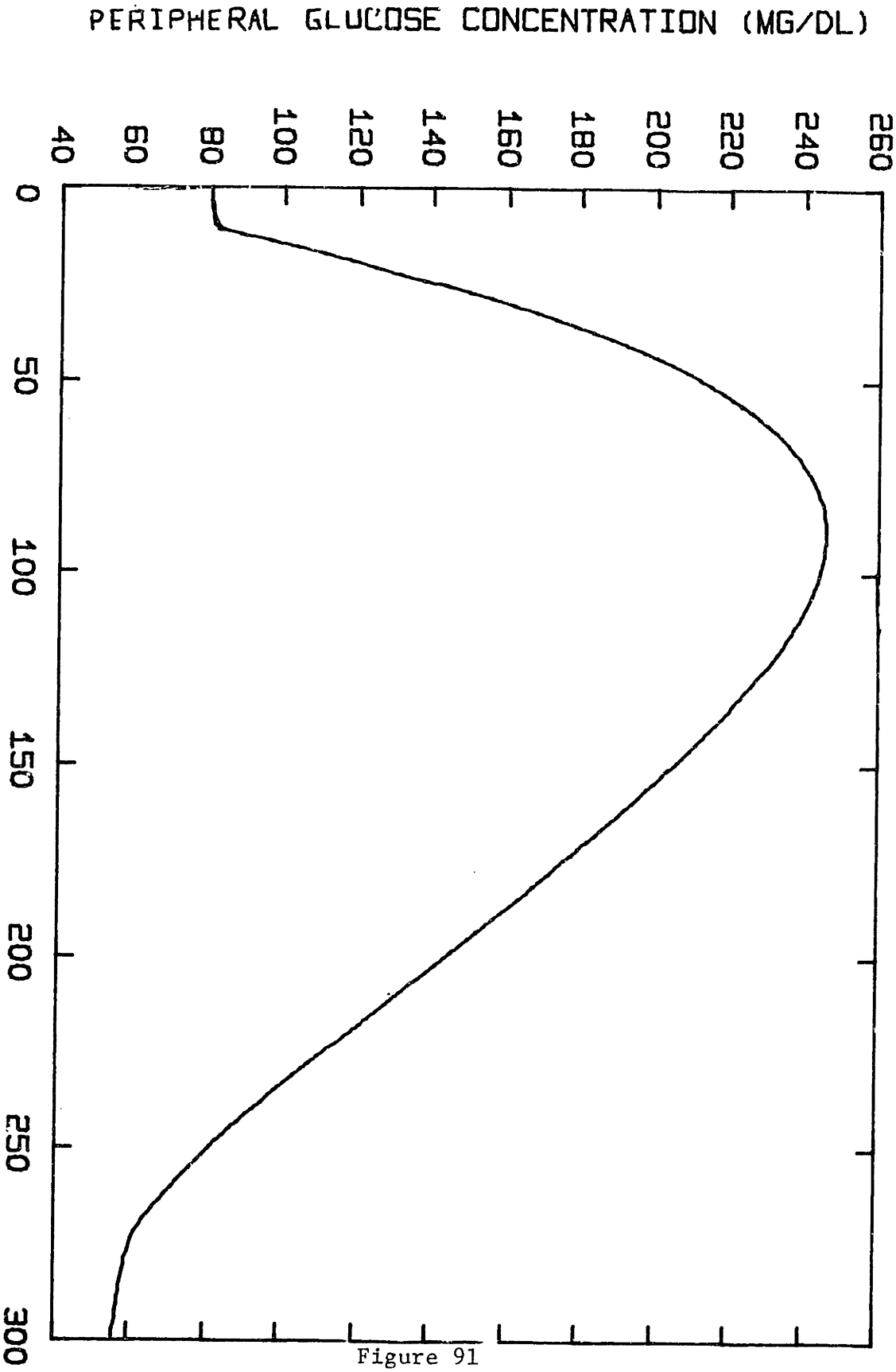

Figure 91

Intravenous insulin infusion of 10 mu/min. Simulation of response to a 100 gram OGTT, under these conditions.

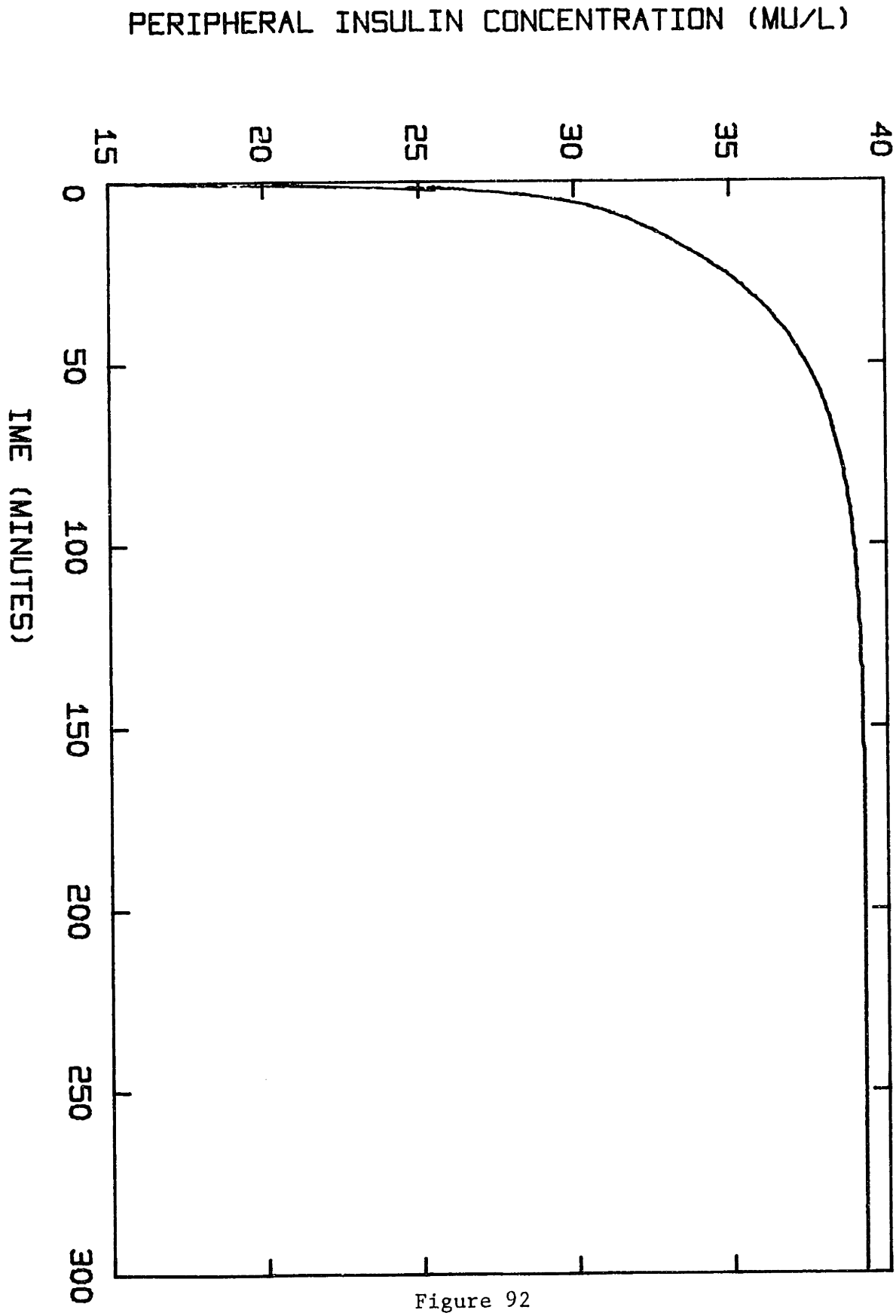

Figure 92

Intravenous insulin infusion of 10 mu/min. Simulation of response to a 100 gram OGTT, under these conditions.

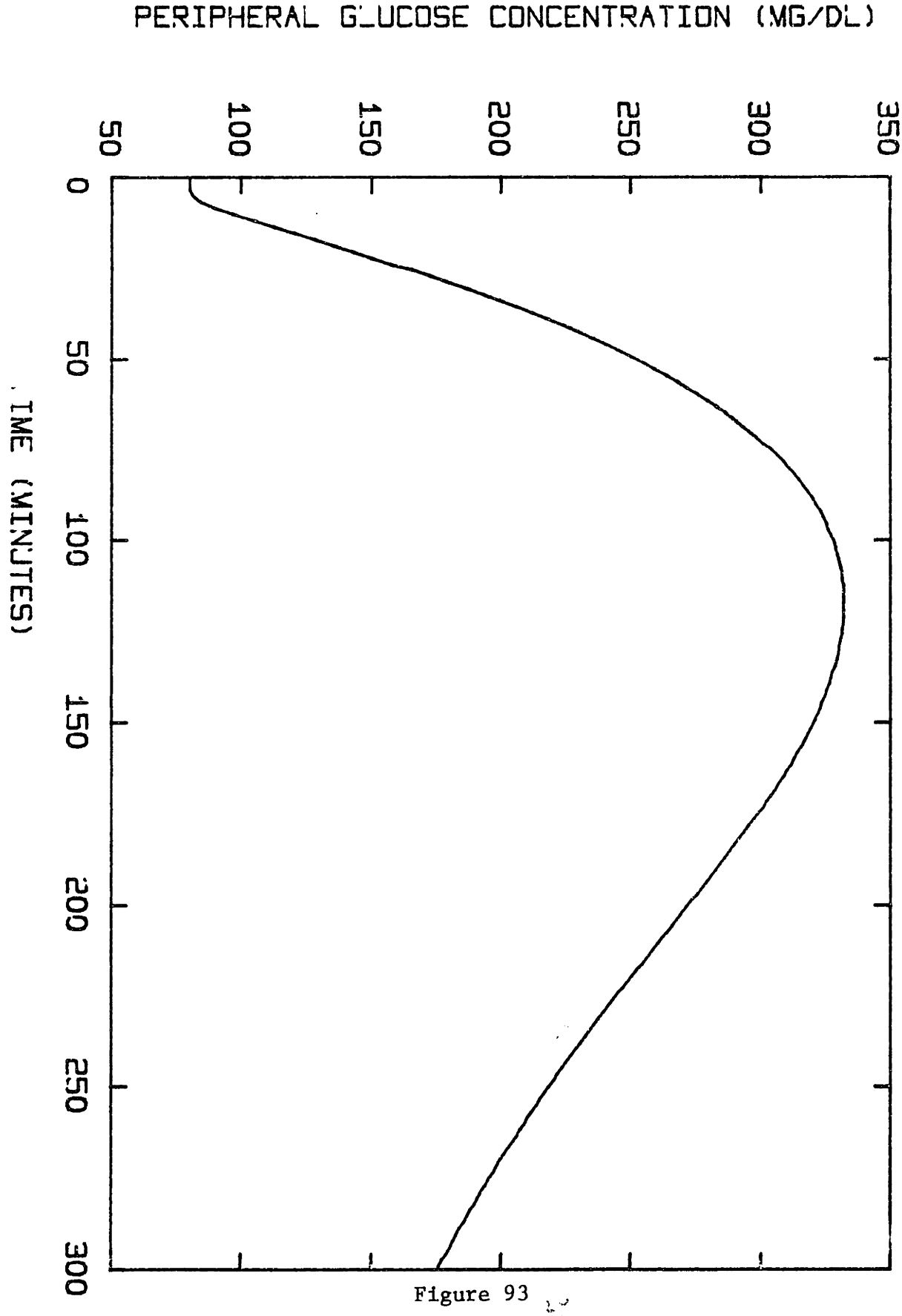

Figure 93

Intravenous insulin infusion of 10 mu/min. Simulation or response to a 100 gram OGTT, under these conditions.

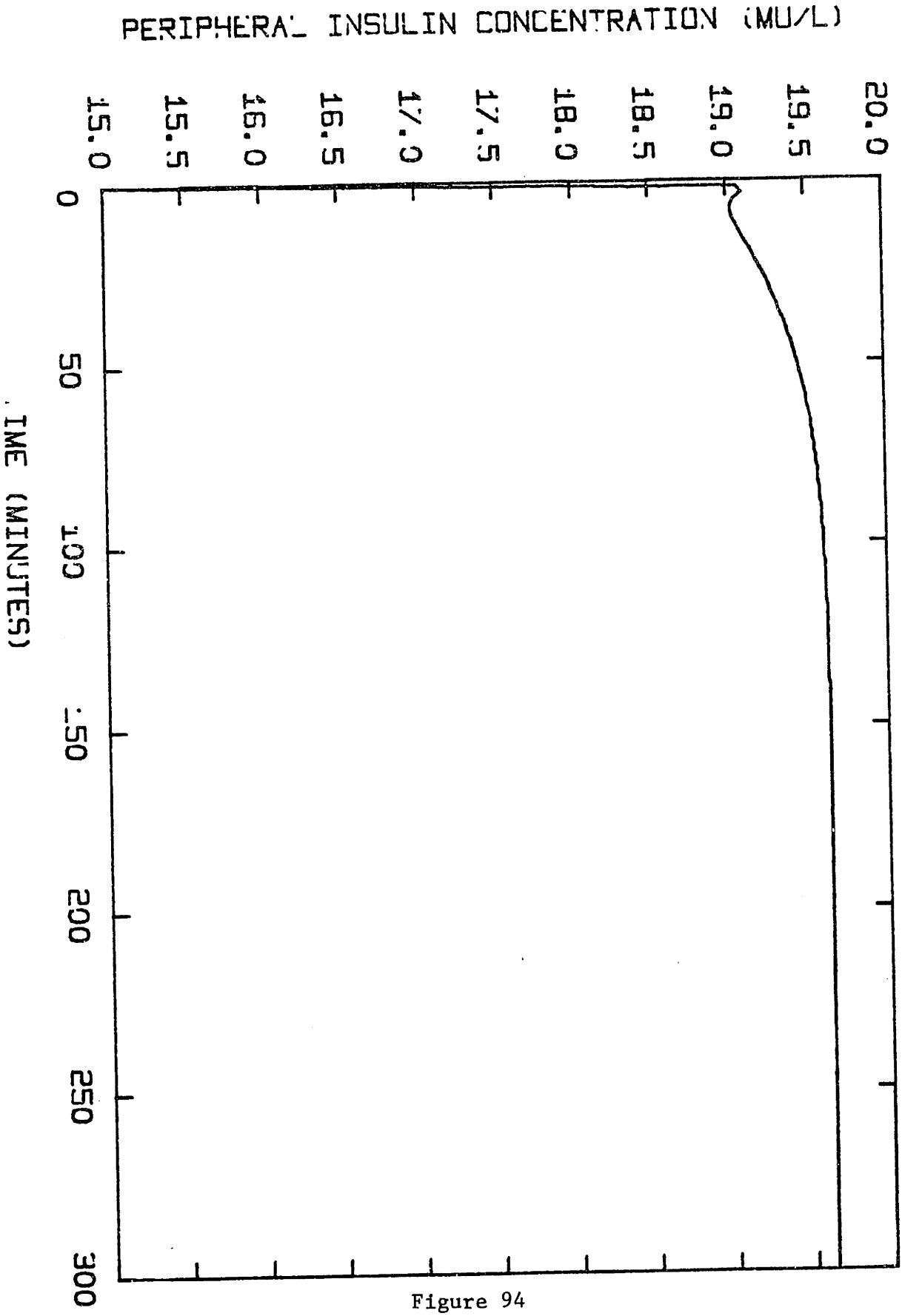

Figure 94

Intravenous insulin infusion of 20 mu/min. Simulation of response to a 100 gram OGTT, under these conditions.

Constants a_4,a_5,a_3 and a_2 were chosen for breakfast and lunch. Figures 95 to 97 show the results when model was presented with a 100 gram oral glucose load at five hour intervals, corresponding to "breakfast" and "lunch". The peripheral glucose concentrations following the first oral input were fairly well controlled (peak 140 mg %, versus a normal peak of 120 mg %). However, the second oral glucose load was not well controlled by the pulsed insulin infusion. This points out the serious drawback of this approach. Without feedback of glucose concentrations, the parameters specified for each pulse are only first approximations. The potential to overdose or underdose the patient always exists. Furthermore, with variable meal sites, and different lengths of time for completing a meal, this fixed pulse becomes a less accurate approximation of the actual beta cell response.

D. Insulin Delivery Based on Feedback Control

As described in section IV, C., Albisser et al (1974) and Clemens et al (1977) have both developed empirical algorithms for continuous intravenous insulin infusions at rates regulated by feedback from a blood glucose monitor. The algorithms have been implemented with a system consisting of two infusion pumps (one for insulin delivery and one for glucose delivery to compensate for overshoot), a glucose sensor and a minicomputer. Equations (34)-(47) describe the algorithm. The values for the parameters were obtained from a paper by Marliss et al (1977) for a 70 kg man: R_I Max = 500, S_I = .02, B_I = 150, K_1 = 100, K_2 = 10. It is important to point out that these parameters are empirically chosen. Figures 98 to 103 show the results when (1) endogenous insulin secretion is set to zero, (2) the algorithm is used to calculate insulin secretion, and (3) two 100 gram oral glucose inputs are presented at 5 hour intervals.

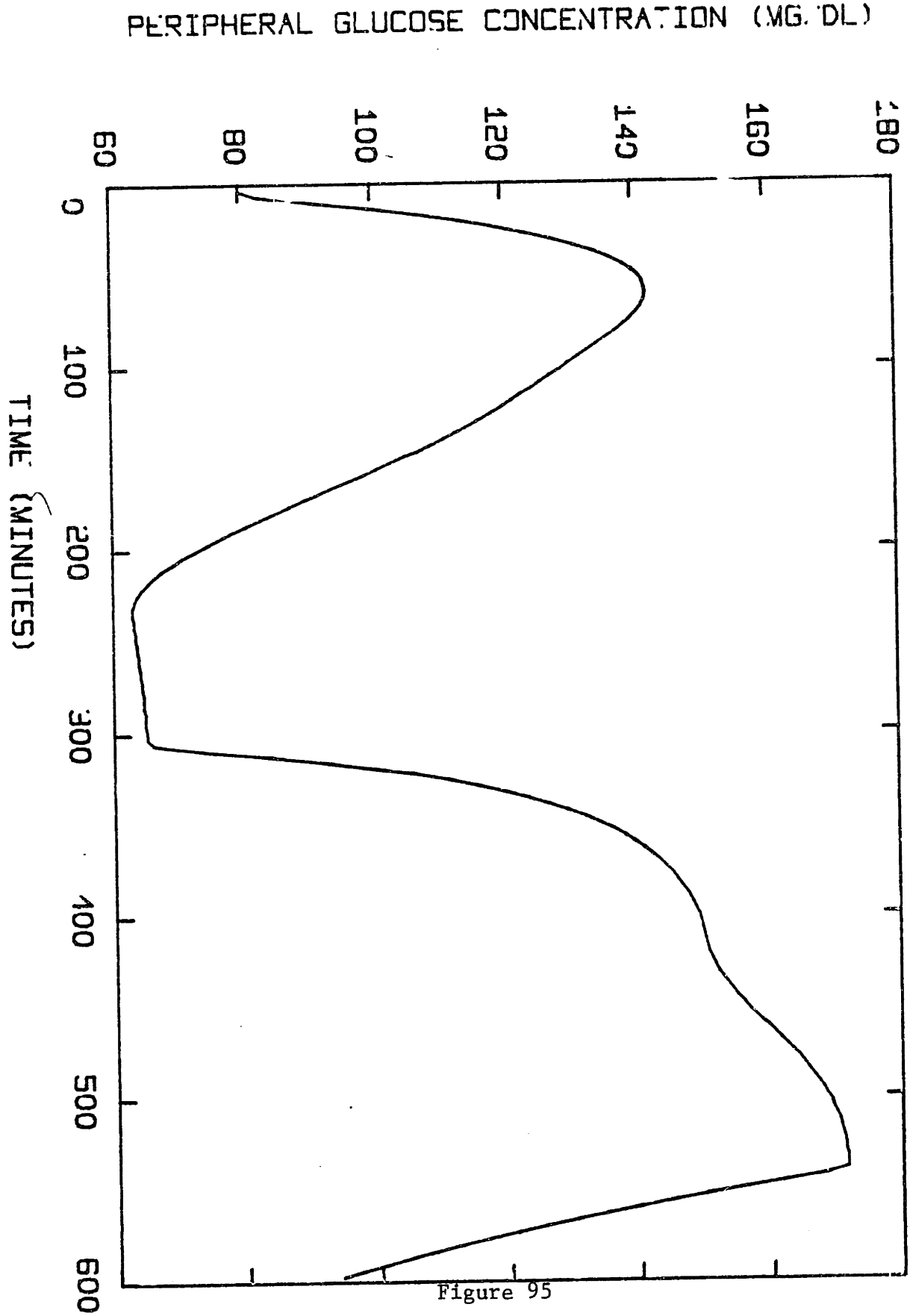

Figure 95

Pulsed intravenus insulin infusion after each meal. Simulation of response to two 100 gram OGTT at 5 hour intervals.

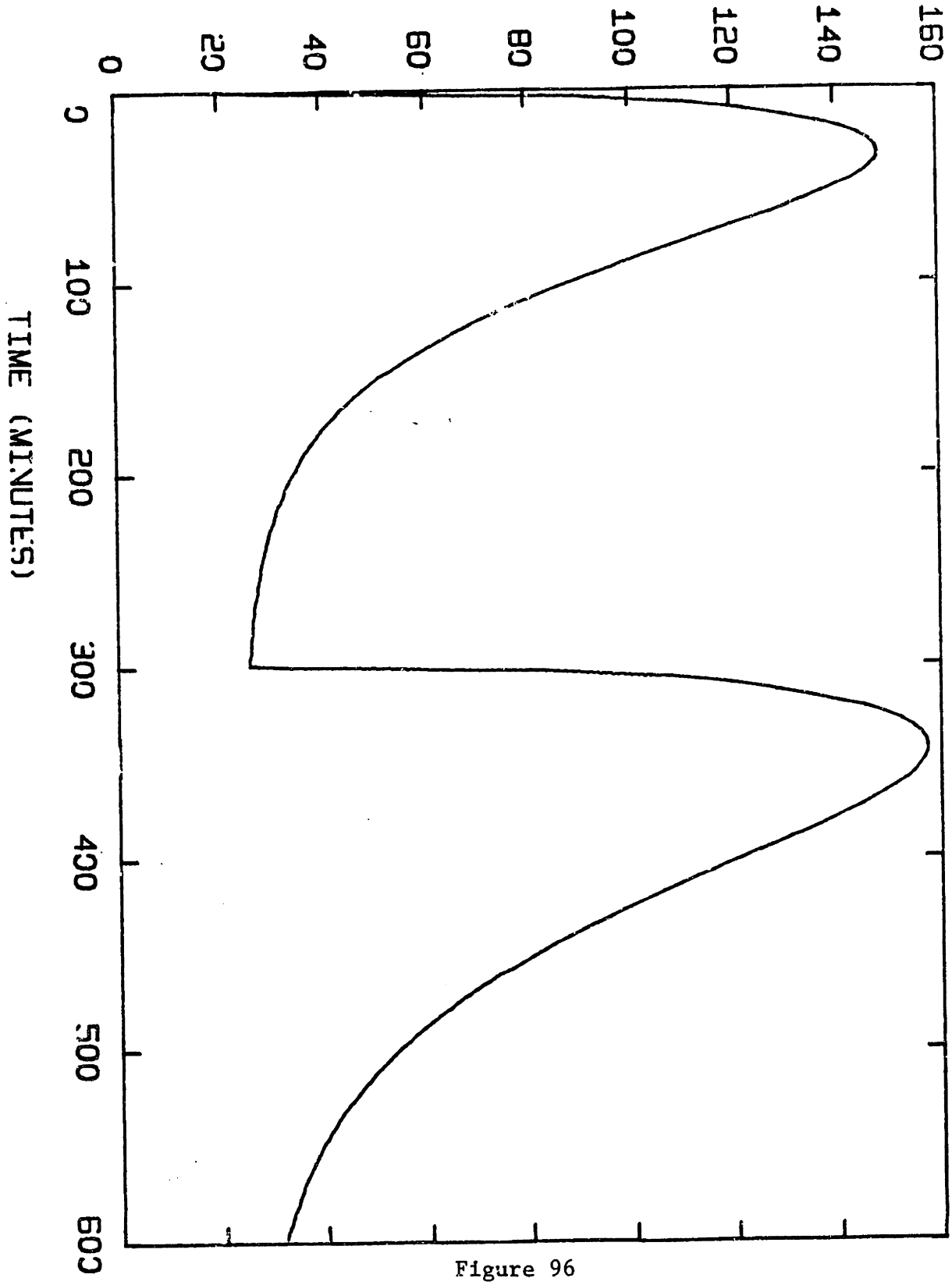

Figure 96

Pulsed intravenus insulin infusion after each meal. Simulation of response to two 100 gram OGTT at 5 hour intervals.

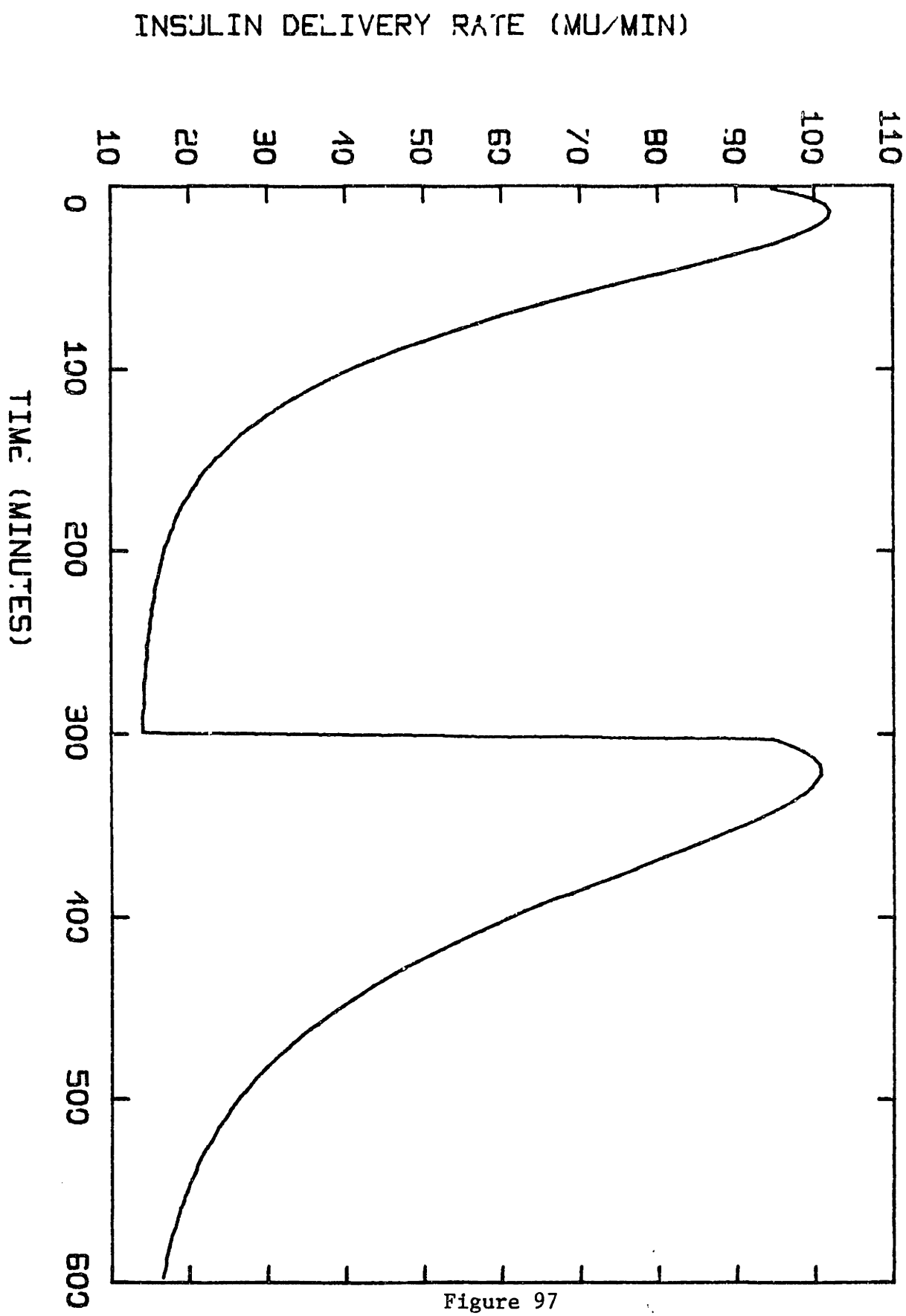

Figure 97

Pulsed intravenus insulin infusion after each meal. Simulation of response to two 100 gram OGTT at 5 hour intervals.

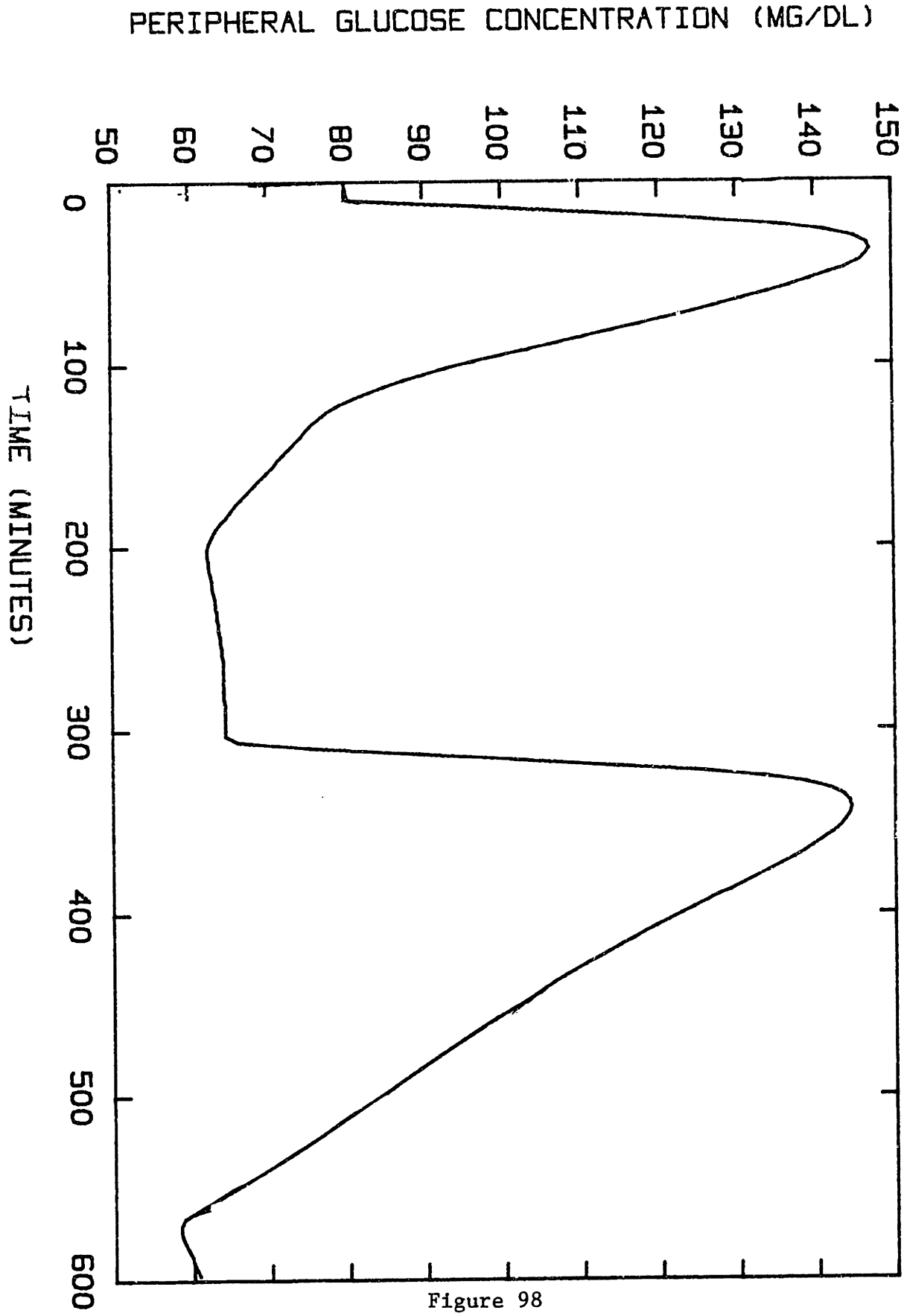

Figure 98

Continuous intravenus insulin infusion regulated by continous feedback from a glucose sensor. Simulation of response to two 100 gram OGTT at 5 hours intervals.

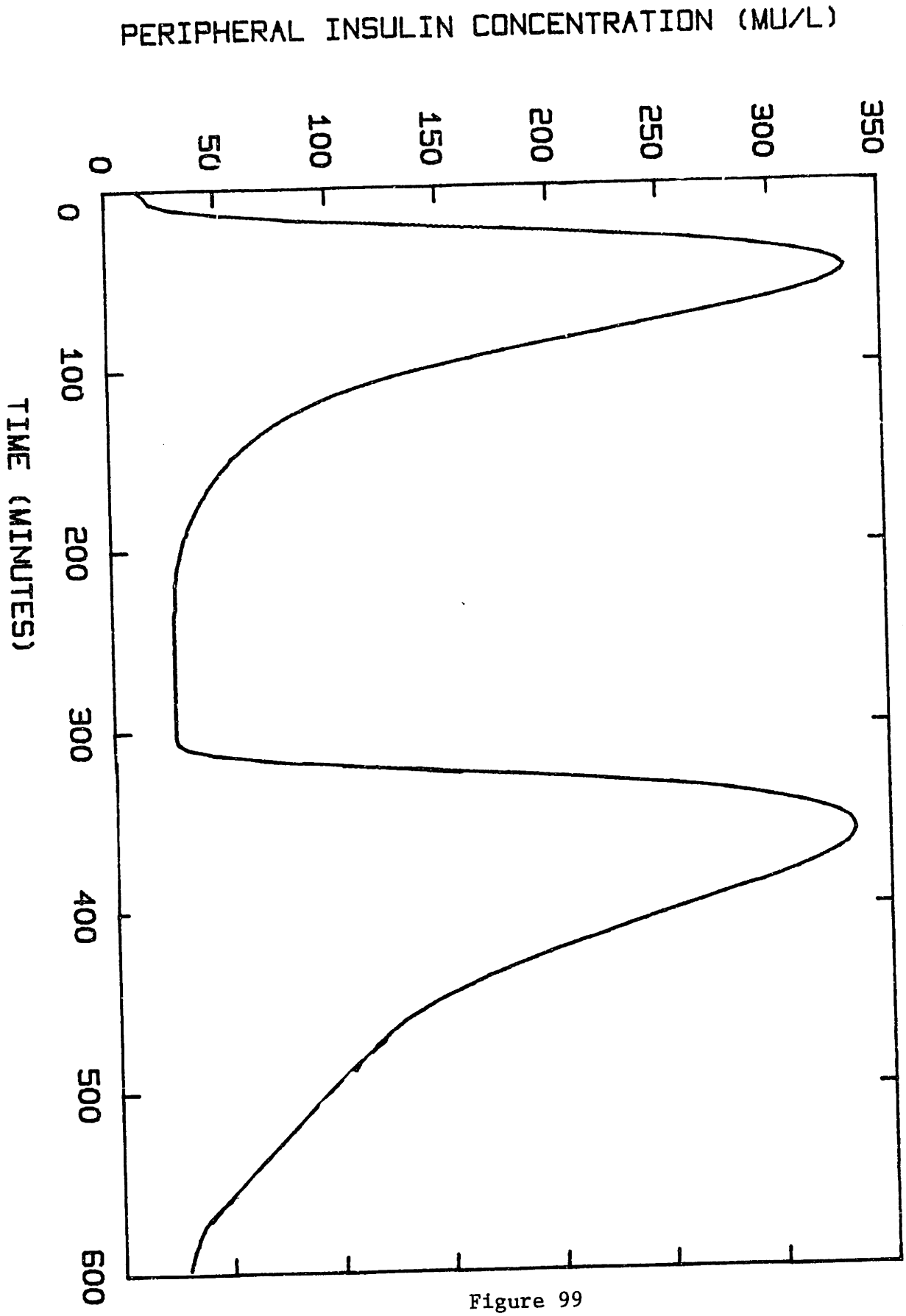

Figure 99

Continuous intravenus insulin infusion regulated by continous feedback from a glucose sensor. Simulation of response to two 100 gram OGTT at 5 hour intervals.

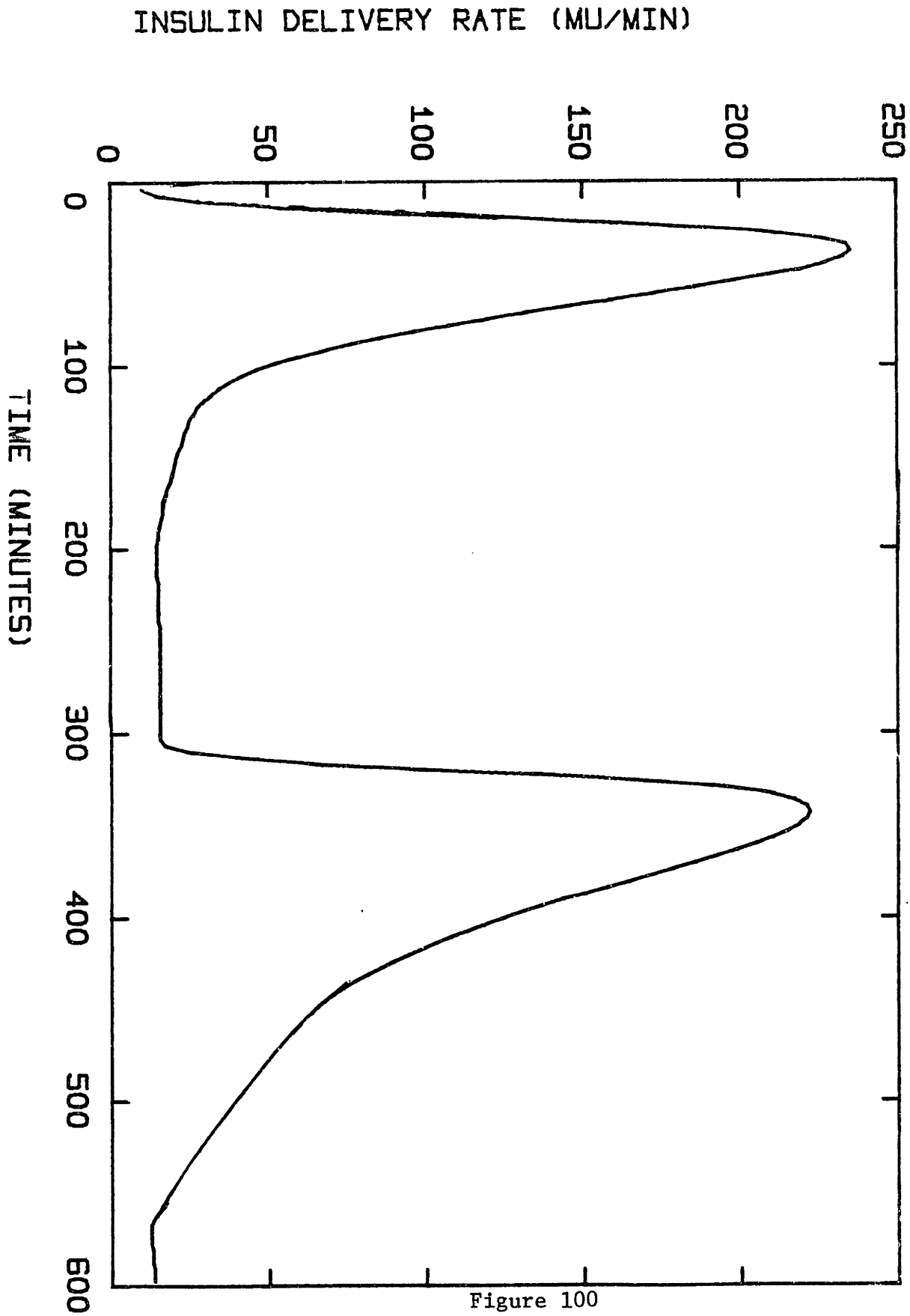

Figure 100

Continuous intravenus insulin infusion regulated by continous feedback from a glucose sensor. Simulation of response to two 100 gram OGTT at 5 hour intervals.

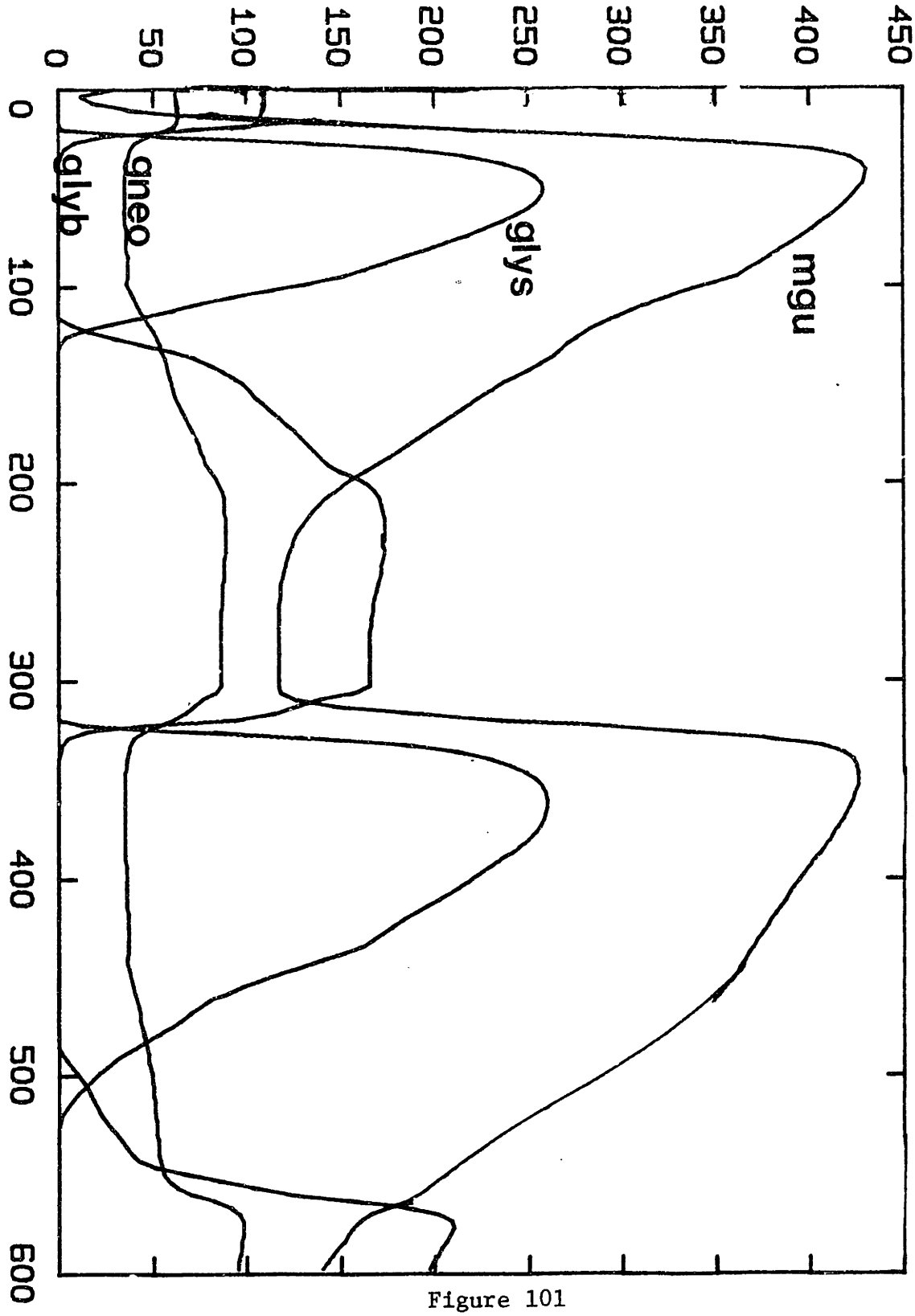

Figure 101

Continuous intravenus insulin infusion regulated by continuous feedback from a glucose sensor. Simulation of response to two 100 gram OGTT at 5 hour intervals.

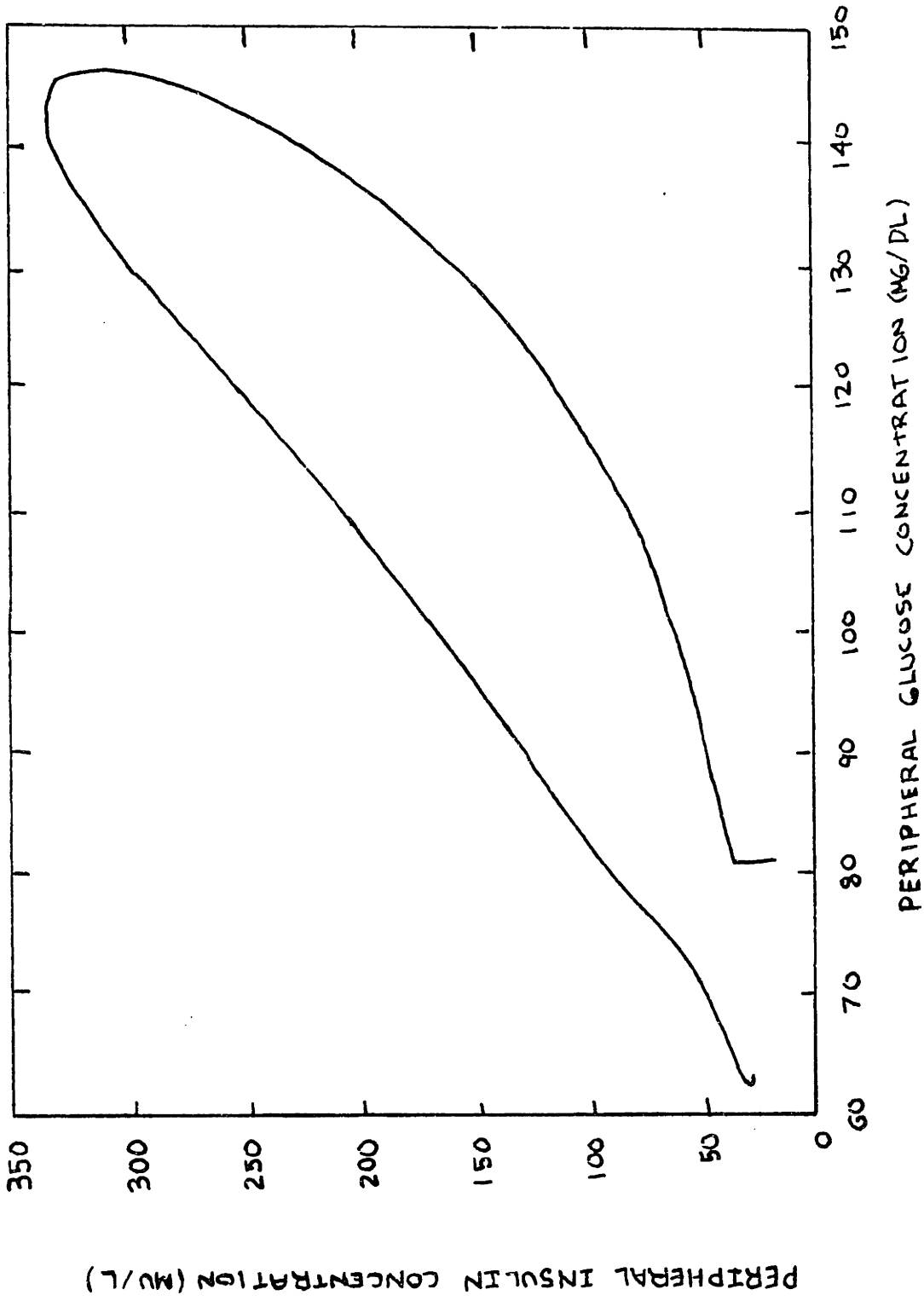

Figure 102

Continuous intravenous insulin infusion
regulated by continuous feedback from a glucose sensor.
Simulation of response to two 100 gram OGTT at 5 hour intervals.

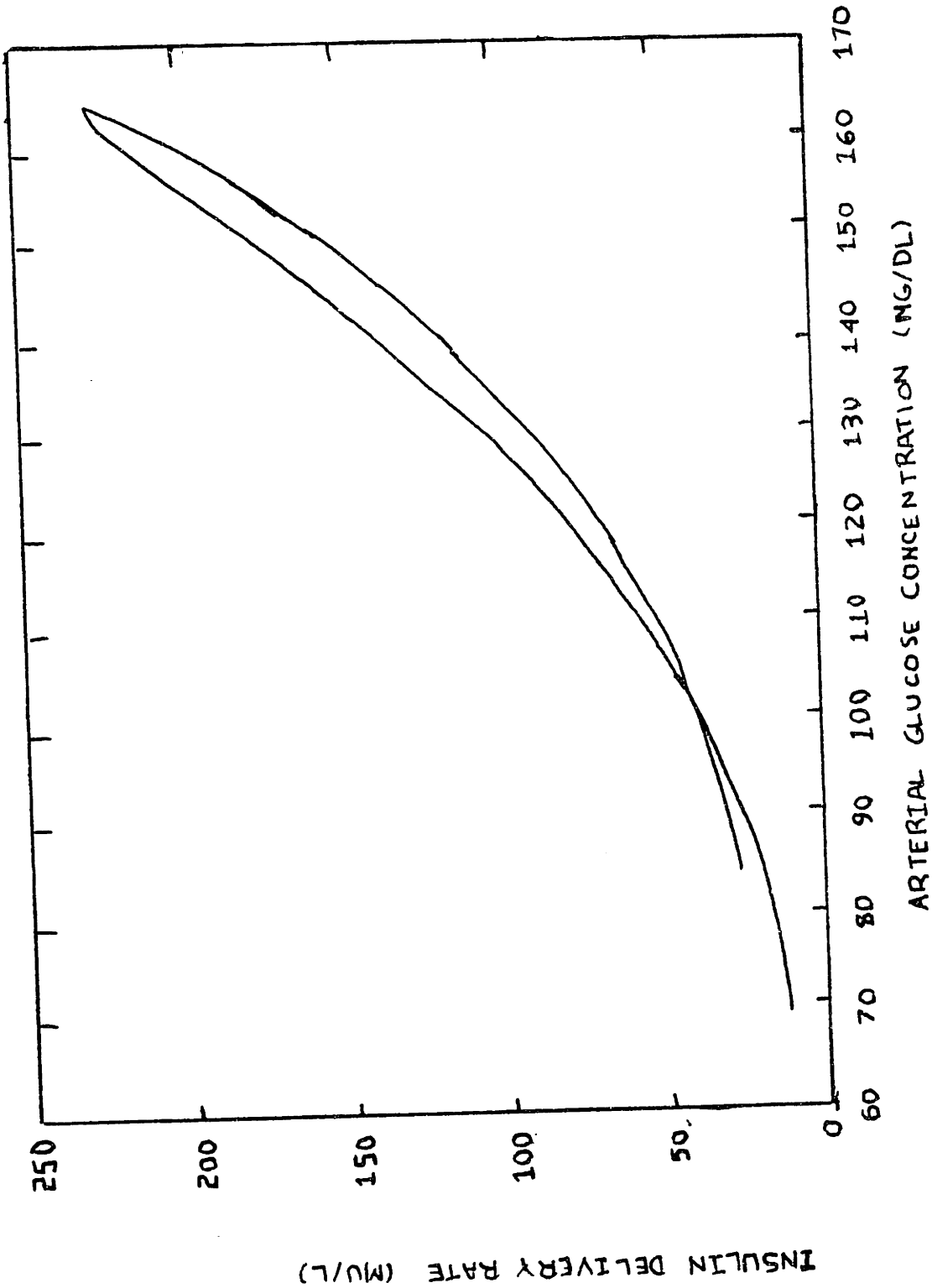

Figure 103

Continuous intravenous insulin infusion
regulated by continuous feedback from a glucose sensor.
Simulation of response to two 100 gram OGTT at 5 hour intervals.

Again, insulin secretion is based on continuous feedback of peripheral glucose concentrations-although there is a 1.5 minute measurement delay. This delay is handled by extrapolating the current data at time t, to predict a glucose concentration at t + 1.5 (see equation 45-47). The peripheral glucose concentrations are kept within a normal range. However, the peripheral insulin concentrations to achieve this control are significantly greater than normal. This is due to the fact that insulin is delivered intravenously rather than the normal intraportal route. This will be discussed in greater detail in a subsequent section.

Clemens et al (1977) have developed an algorithm which, according to published data on its function, should be equivalent to Albisser's model. Equations (48) to (49) describe the algorithm. The values for the parameters were obtained from Miles Laboratories[4]: $R_I = 15$, $B_I = 80$, $S_I = 85$, $K_R = 180$ and $K_1 = 120$. A simulation of the algorithm with these values was attempted, but resulted in a sharp spike of insulin secretion at 25 minutes. This clearly is inadequate for any reasonable glucose control. Since the constants are for the most part empirically determined, it is difficult to estimate the source of the error. As described in Section I., Benedek (1973) has shown that the normal glucoregulatory system can be characterized by a proportional-plus-derivative-plus integral controller. This observation can be translated into an insulin delivery algorithm:

$$\frac{dc_I}{dt} = K_D \frac{dc_G}{dt} + K_p(C_G - C_S)$$

---

[4]Personal communication to Dr. T. Aoki, 1977.

C_I is the insulin concentration. C_G is the concentration of glucose at time t, C_S is the setpoint (e.g. 80 mg/dl) against which the program measures the increase or decrease in glucose concentration. The coefficients for derivative, K_D, and proportional control, K_p, can be calculated by using data from Grodsky (1972). The slope of a plot of insulin secretion rate as a function of glucose concentration will give K_p. Likewise, K_D is the slope of insulin secretion rate versus rate of change of glucose concentration. The constants are $K_p = .05417$ and $K_D = .8333$. The integral element is necessary to prevent steady-state error, but is not important over the short term. Therefore, we will not consider it here. Figures 104-109 show the results when (1) endogenous insulin secretion is set to zero, (2) the above algorithm is used to calculate insulin secretion on the basis of peripheral glucose feedback, and (3) the model input is two 100 gram OGTT at 5 hour intervals. The insulin delivery is into the peripheral blood (I.V. administration). Compare the normal glucose concentrations (figure 104.1) to the glucose concentrations based on this algorithm. It appears the algorithm accurately simulates the dynamics necessary to effect glucose control. The constants could be easily tailored to each individual, to eliminate the mild hyperglycemia following the OGTT (140 mg/dl) and hypoglycemia (60 mg/dl) afterwards. Recall that K_p, K_D were analytically chosen from experiments using an isolated perfused pancreas preparation - yet they are remarkably close to what is needed. Indeed Shichiri et al[5] have demonstrated excellent control in pancreatectomized dogs. They found that with a K_D/K_p ratio

---

[5]Shichiri et al, personal communication to Dr. J.S. Soeldner, 1977.

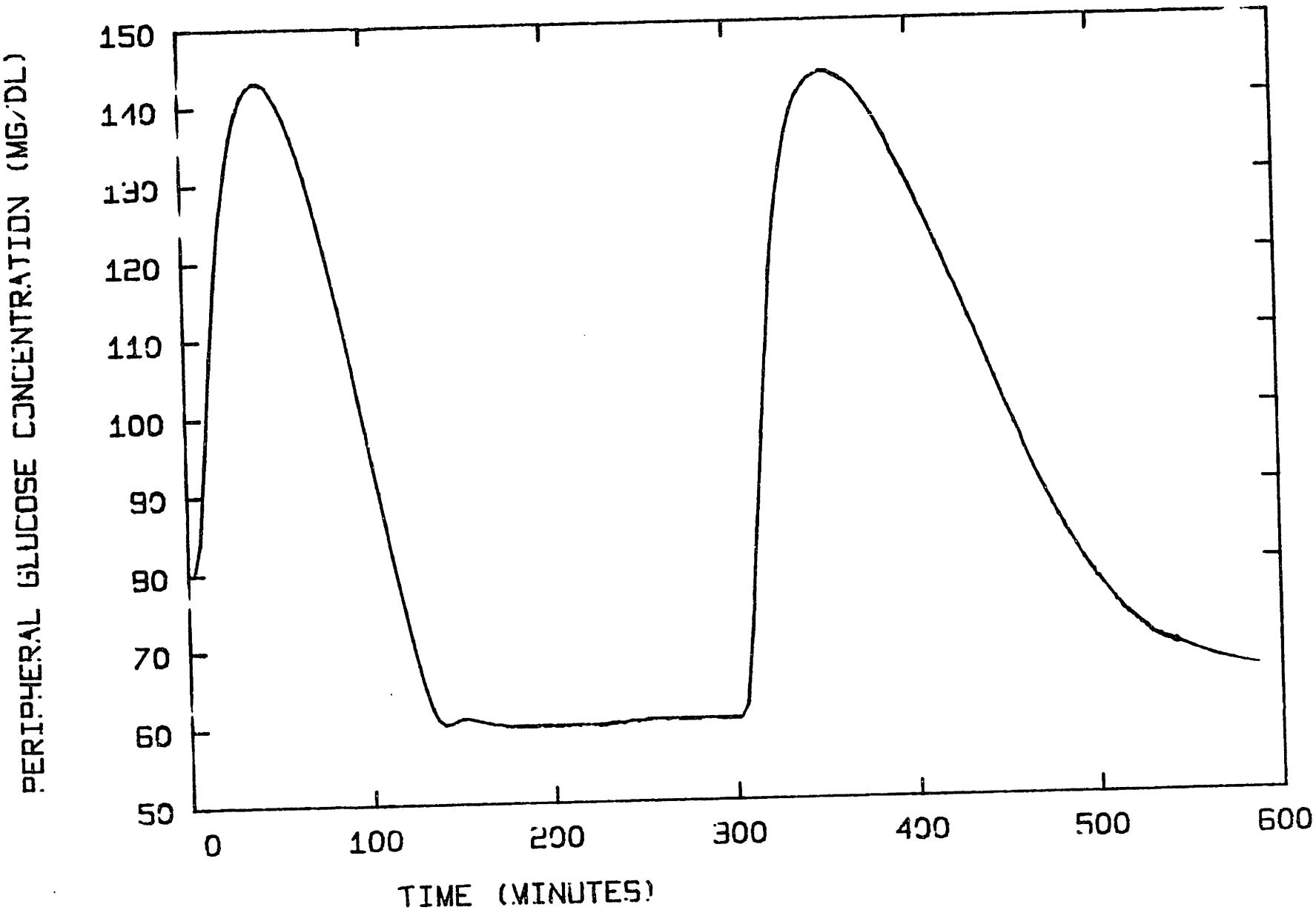

Figure 104

Continuous intravenous infusion based on a proportional-plus-derivative controller and feedback from a glucose sensor. Simulation of response to two oral glucose tolerance tests at five-hour intervals.

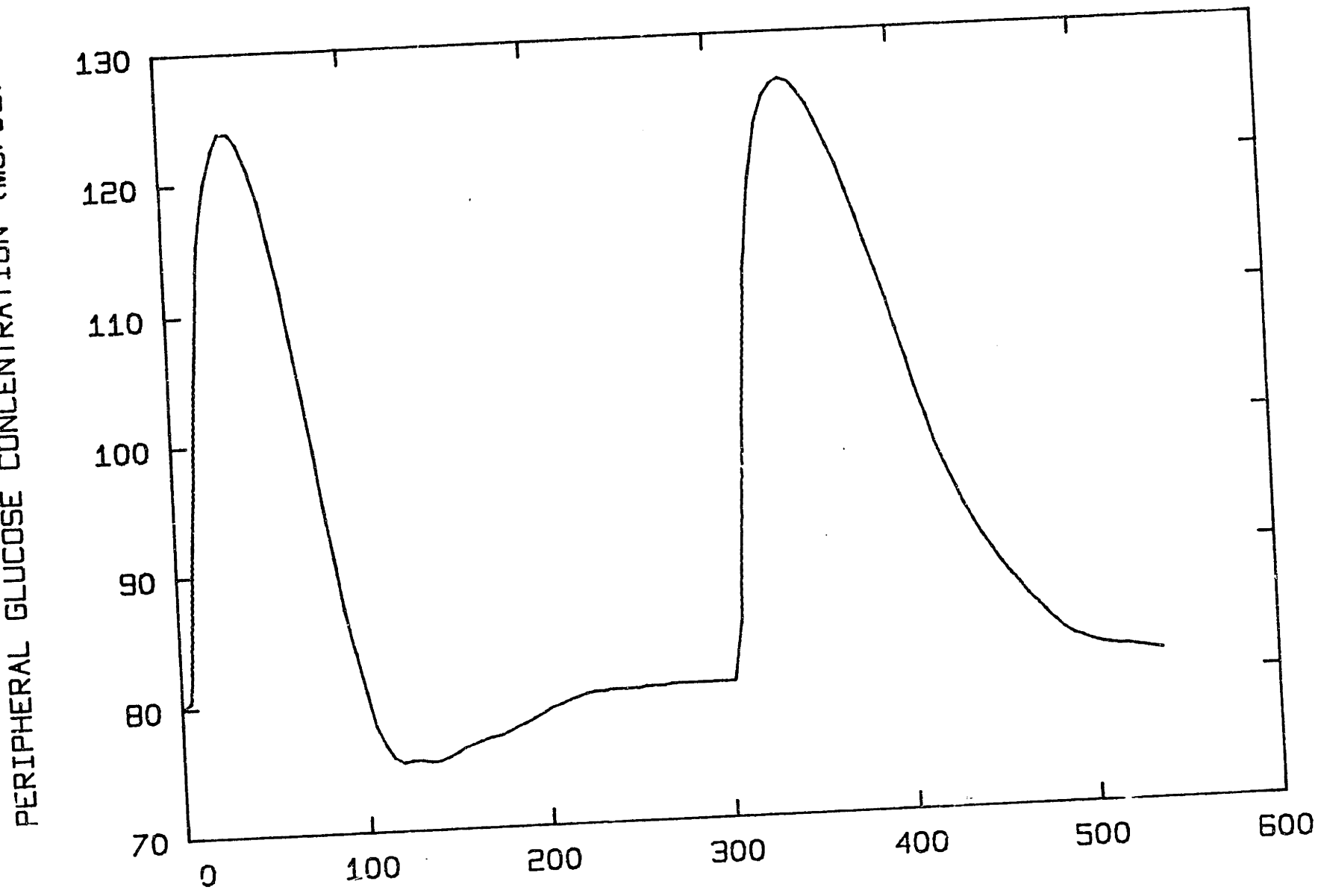
PERIPHERAL GLUCOSE CONCENTRATION (MG/DL)
130
120
110
100
90
80
70
0
100
200
300
400
500
600
TIME (MIN)

Figure 104.1

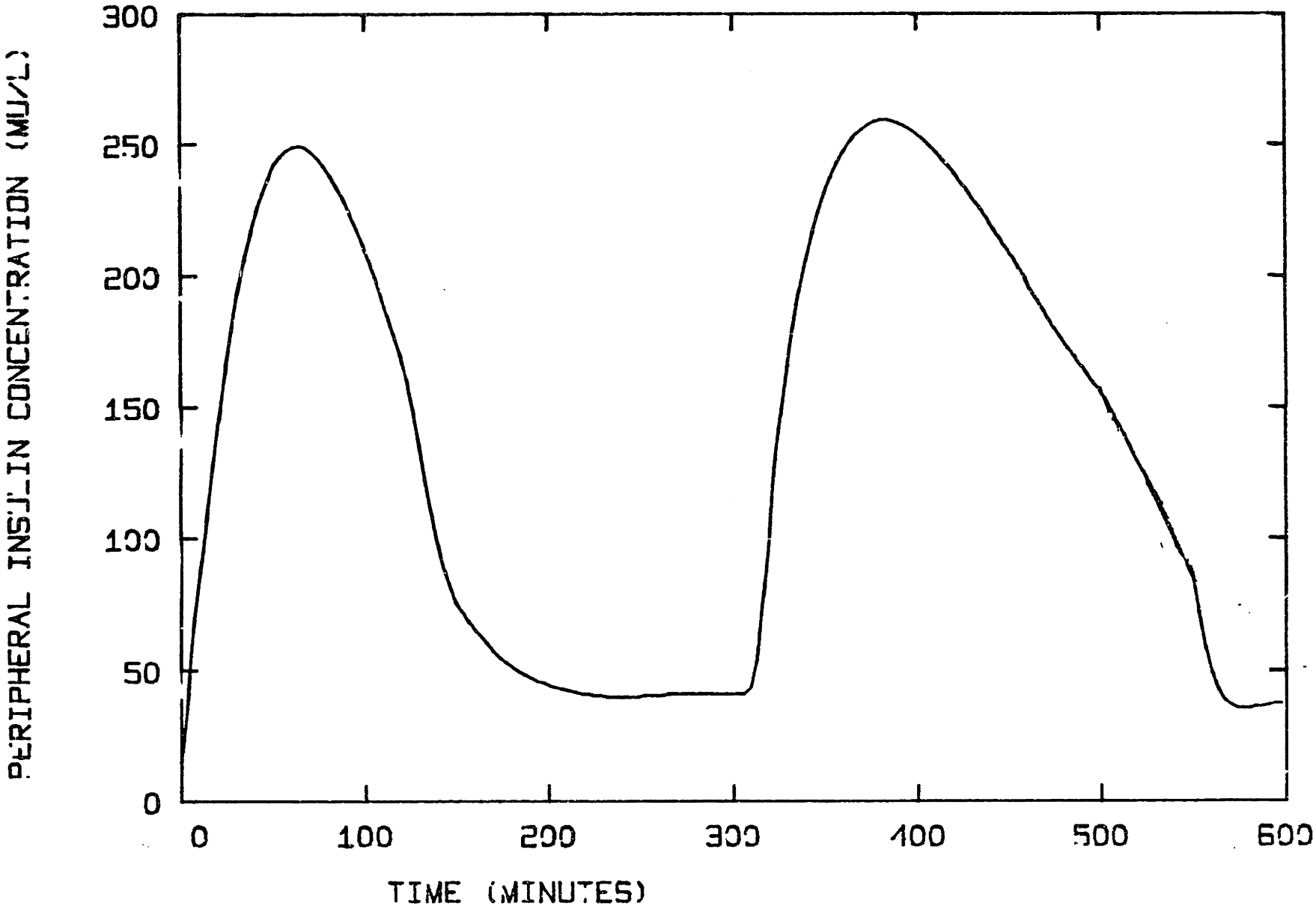

Figure 105

Continuous intravenous infusion based on a
proportional-plus-derivative controller and feedback from a glucose sensor.
Simulation of response to two oral glucose tolerance tests at five-hour intervals.

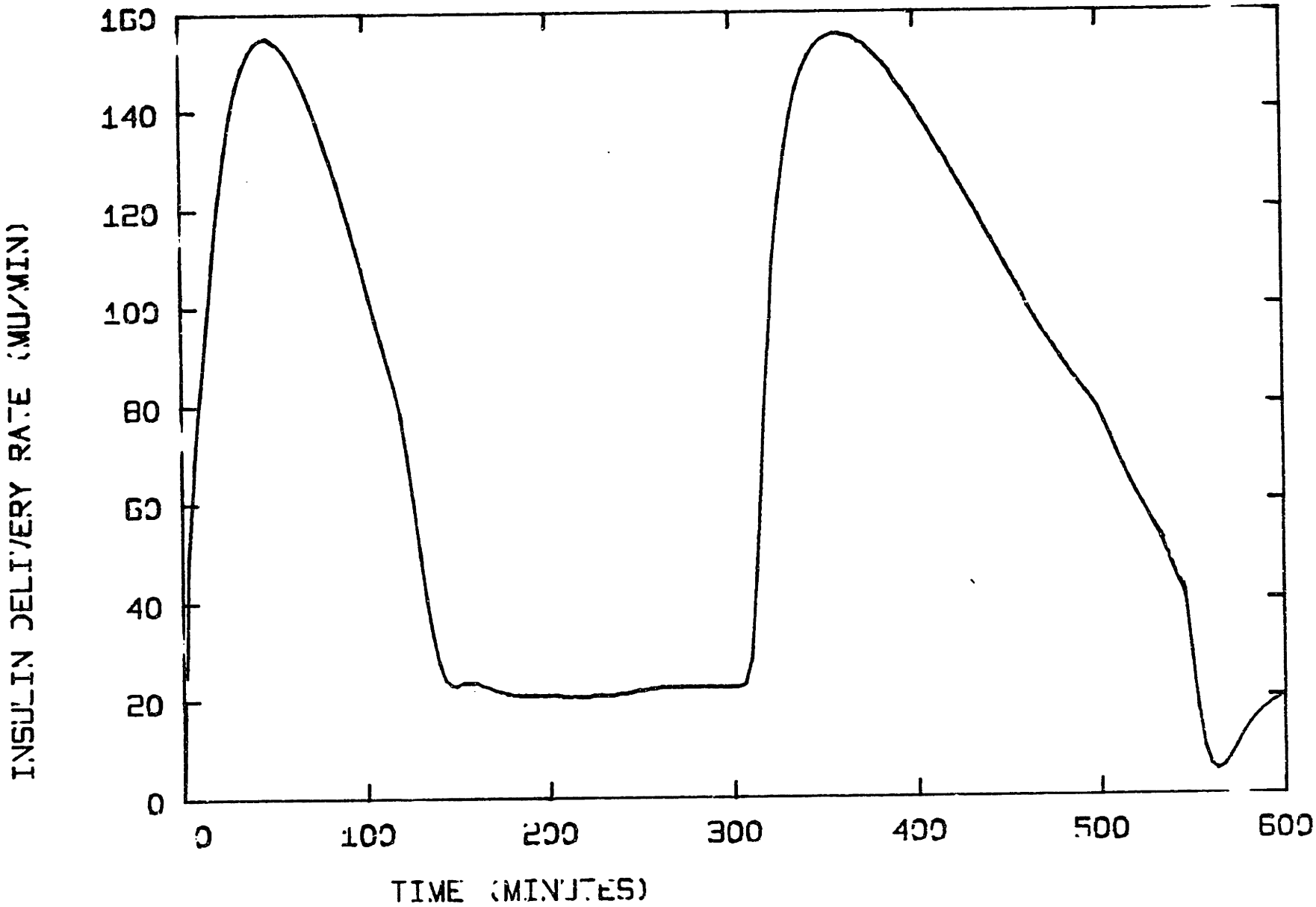

Figure 106

Continuous intravenous infusion based on a proportional-plus-derivative controller and feedback from a glucose sensor.

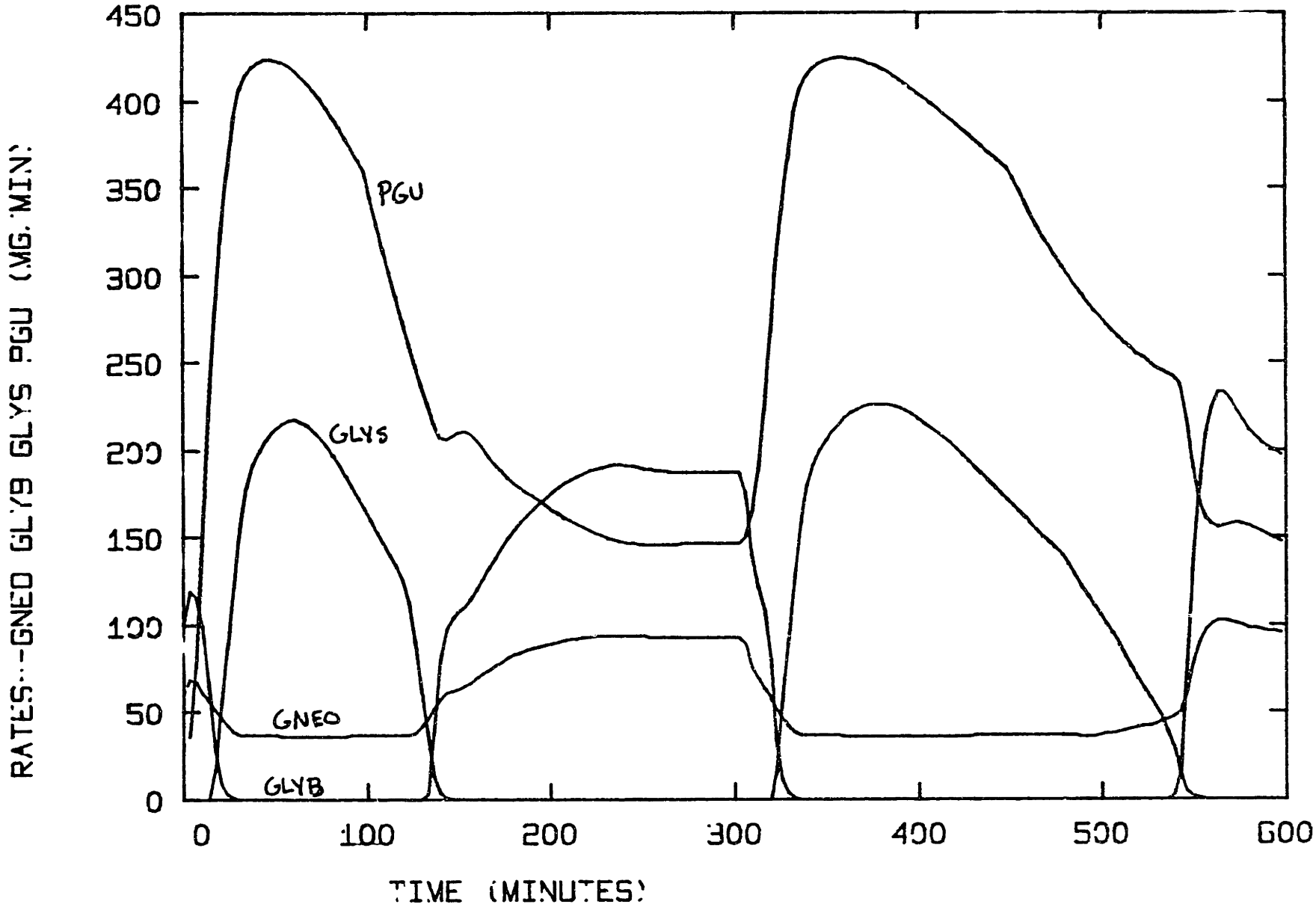

Figure 107

Continuous intravenous infusion based on a
proportional-plus-derivative controller and feedback from a glucose sensor.

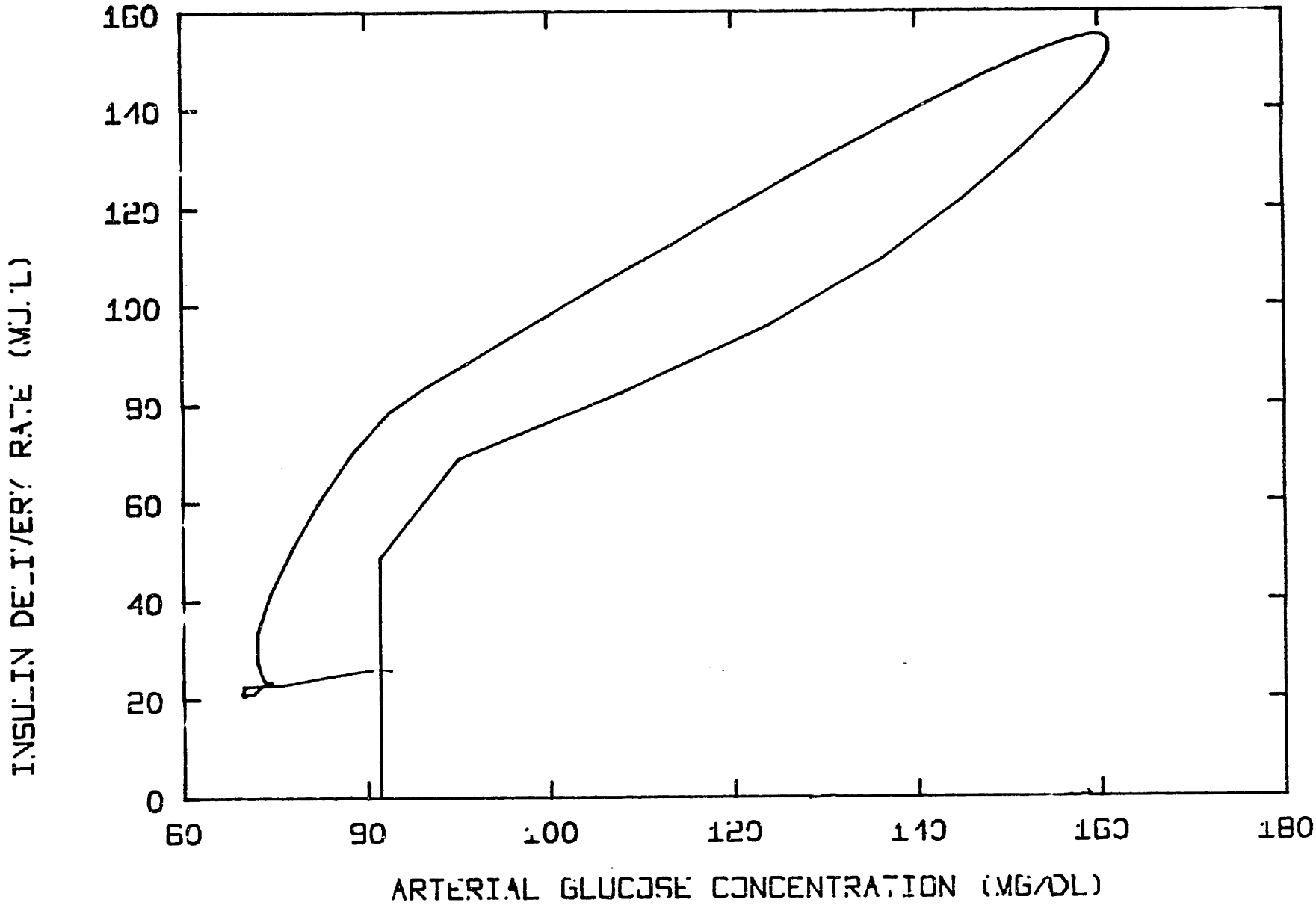

Figure 108

Continuous intravenous infusion based on a
proportional-plus-derivative controller and feedback from a glucose sensor.
Simulation of response to two oral glucose tolerance tests at five-hour intervals.

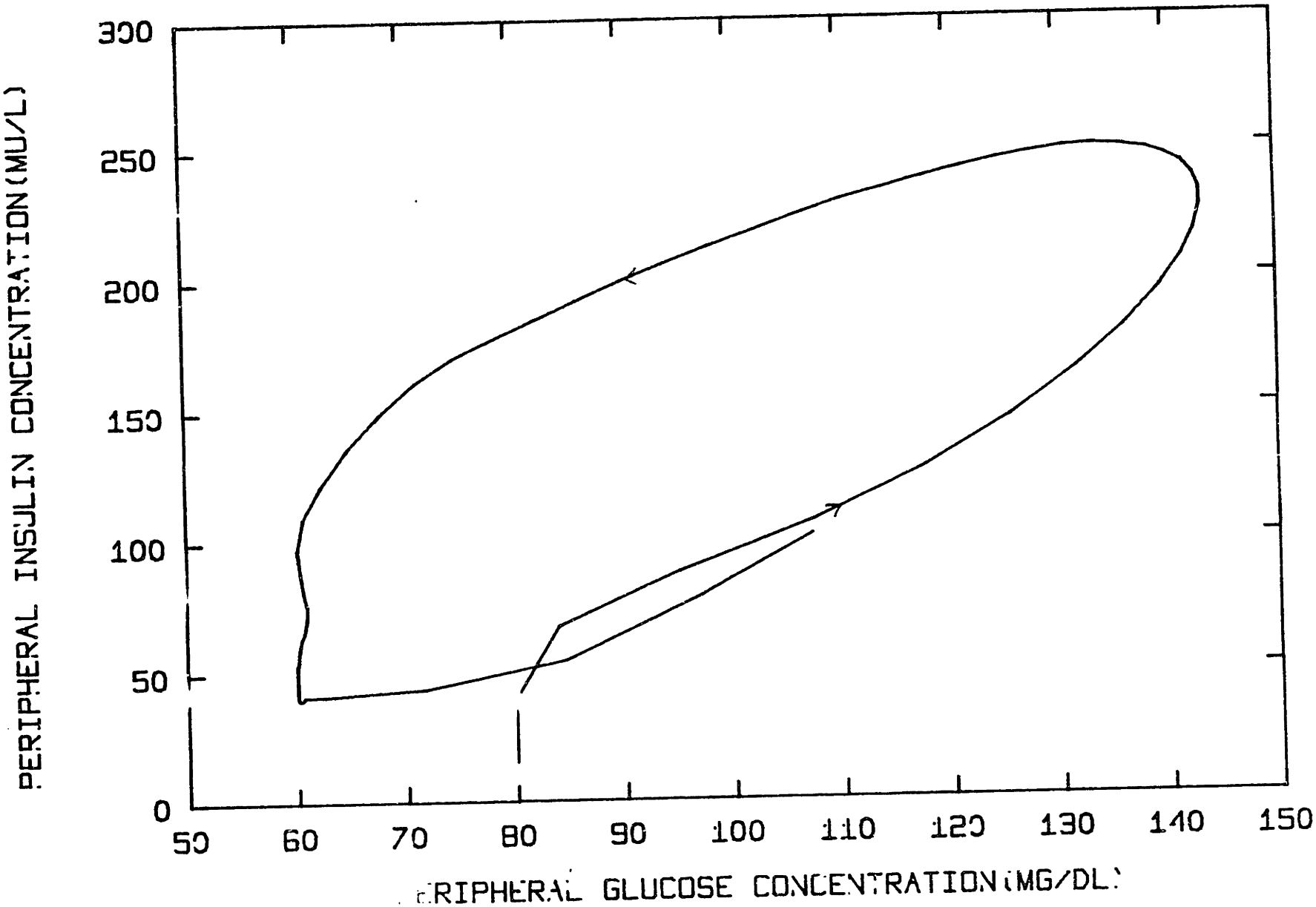

Figure 109

Continuous intravenous infusion based on a proportional-plus-derivative controller and feedback from a glucose sensor. Simulation of response to two oral glucose tolerance tests at five-hour intervals.

of 10, the glucose assimilation curve was within the physiological range of responses seen in normal dogs (our choice for this simulation was a K_D/K_p ratio of 15.4). It is interesting to note that this algorithm required less insulin secretion (150 MU/min.) than Albisser's more empirical method (240 MU/min.); a point also verified by Shichiri et al experimentally.

This use of this algorithm presupposes that continuous glucose measurements are fed back, and there is no delay in measurement. In actuality, the shortest time (transport) delay reported has been 1.5 minutes (Albisser et al, 1974). In addition, the only implantable sensor being developed for glucose measurements operates in a discontinuous mode.[6] Therefore, it is of interest to determine (1) the maximum time delay for which glucose concentration can be extrapolated and (2) the minimum number of points necessary to reconstruct the continuous change of glucose concentrations. A predictor algorithm for extrapolating blood glucose concentration developed by Albisser et al has been discussed. By simulating increasing time delays in measurement, it appears this algorithm can project data accurately for a 15 minute time delay. Beyond that, it fails. (However, a more sophisticated algorithm may be possible to extend this time, if necessary). The number of points necessary to construct a continuous function for the change of glucose concentration with time obviously depends on the delay. With a 1.5 minute delay, 6 samples per hour are adequate for maintaining glucose control. A three minute delay requires a minimum of

---

[6] J.S. Soeldner, personal communication.

12 samples per hour. A five minute time delay requires 15 samples per hour. Beyond a 5 minute delay, the algorithm is inadequate. Again, with a more sophisticated algorithm (if necessary) a greater time delay may be accomodated. The important point to note is that with a suitable data fitting procedure to extrapolate and reconstruct data, these practical difficulties can be overcome.

E. Insulin Delivery from a Hollow-fiber Artificial Pancreas

In section 2, a method for culturing beta cells on hollow fibers was discussed as a means for normalizing blood glucose levels. Blood flow is directed through the hollow fibers, and glucose diffuses to the beta cells. In response to this stimulus, the beta cells secrete insulin which diffuses back across the fibers into the blood. To date, not enough experiments have been done to characterize the transport delays for insulin and glucose, however, an estimate of a transport delay of 1-2 minutes for glucose and less than 5 minutes for insulin has been suggested.[7] Therefore, a simulation was done in which the transport delays were both taken to be 2 minutes. While this is an obvious simplification of the dynamics, some qualitative conclusions can be made. Figures 111-115 show the response of the model to a 100 gram oral glucose load. In figure 111, it can be seen that oscillations in peripheral glucose concentrations occur. Although the oscillations have a small amplitude (5 mg/dl) the underlying rates (see figure 113) of gluconeogenesis and glycogen breakdown (which represent the liver's attempt to stabilize glucose concentrations between 70-80 mg/dl) also

---

[7] W. Chick, personal communication.

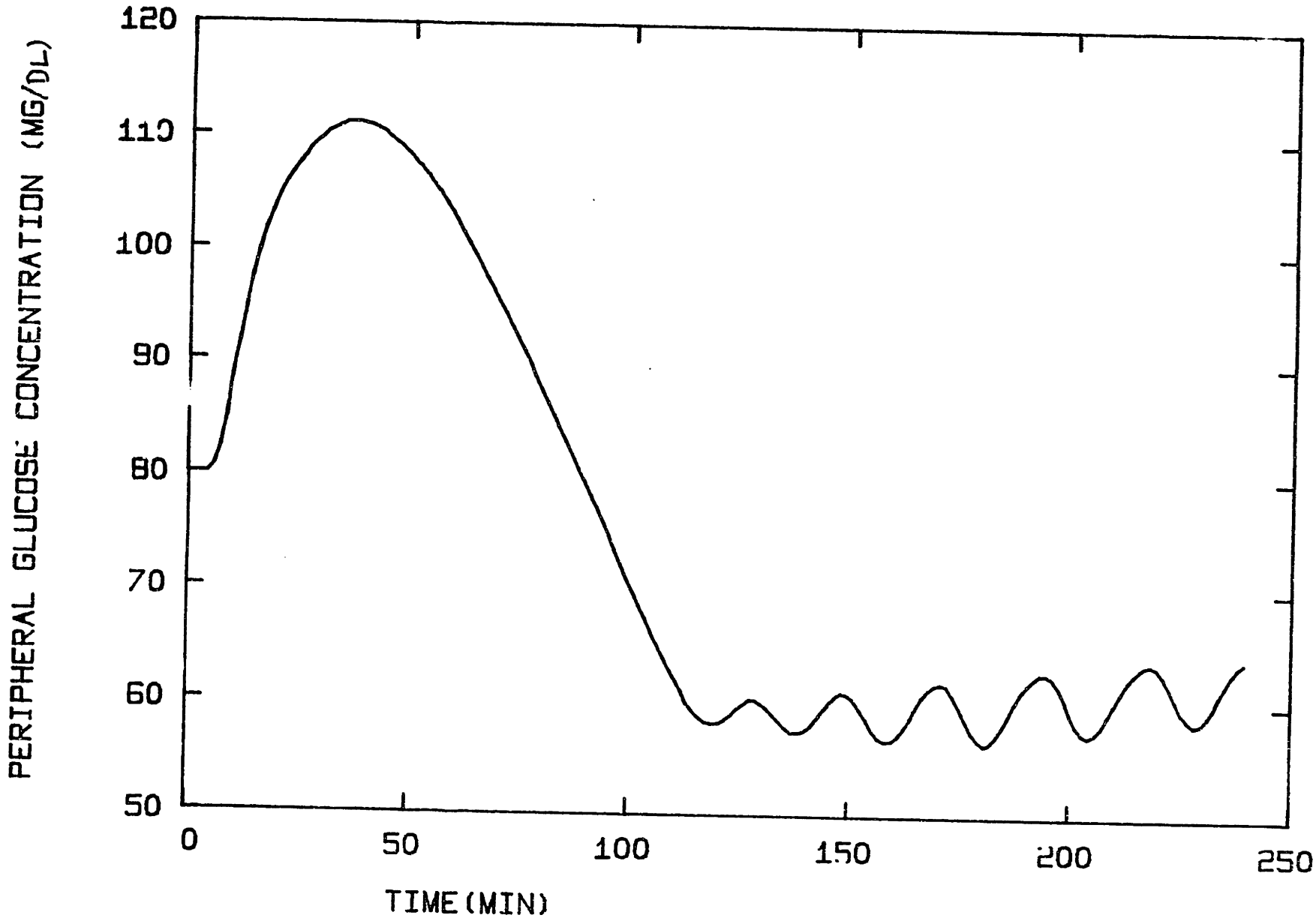

Figure 111

Insulin delivery with diffusional delay in glucose measurement and insulin secretion.
Simulation of response to a 100 gram oral glucose tolerance test.

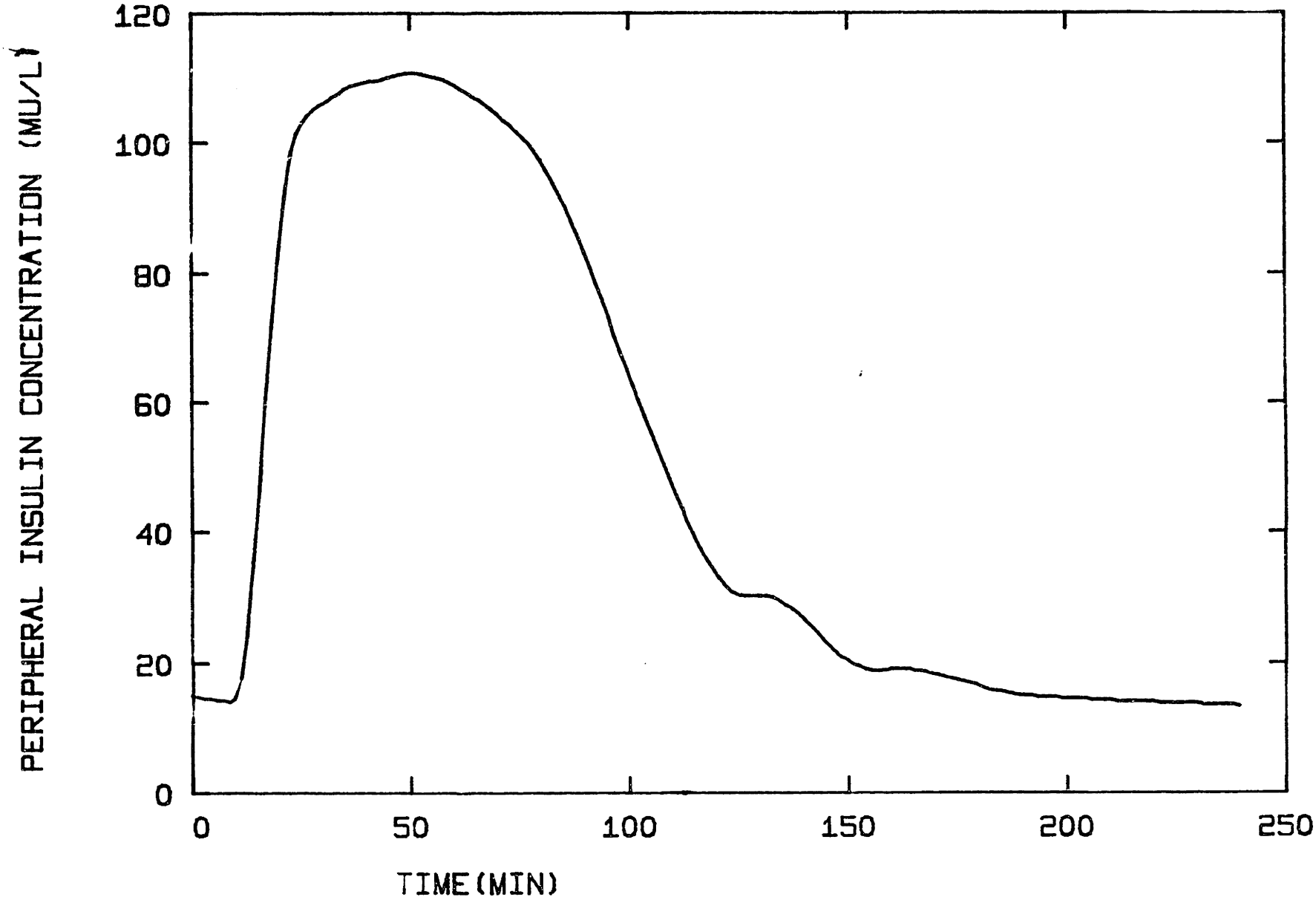

Figure 112

Insulin delivery with diffusional delay in glucose measurement and insulin secretion. Simulation of response to a 100 gram oral glucose tolerance test.

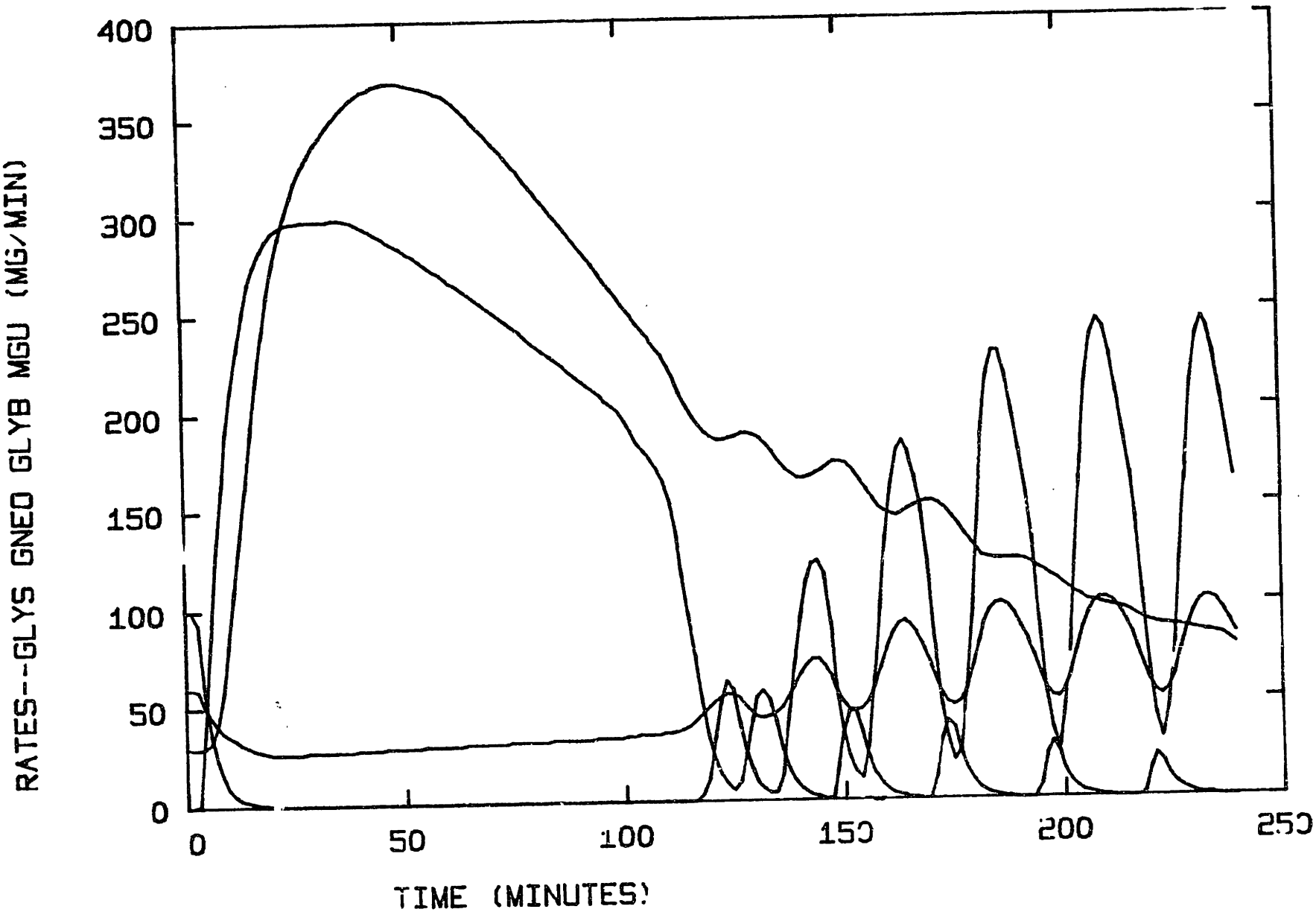

Figure 113

Insulin delivery with diffusional delay in glucose measurement and insulin secretion. Simulation of response to a 100 gram oral glucose tolerance test.

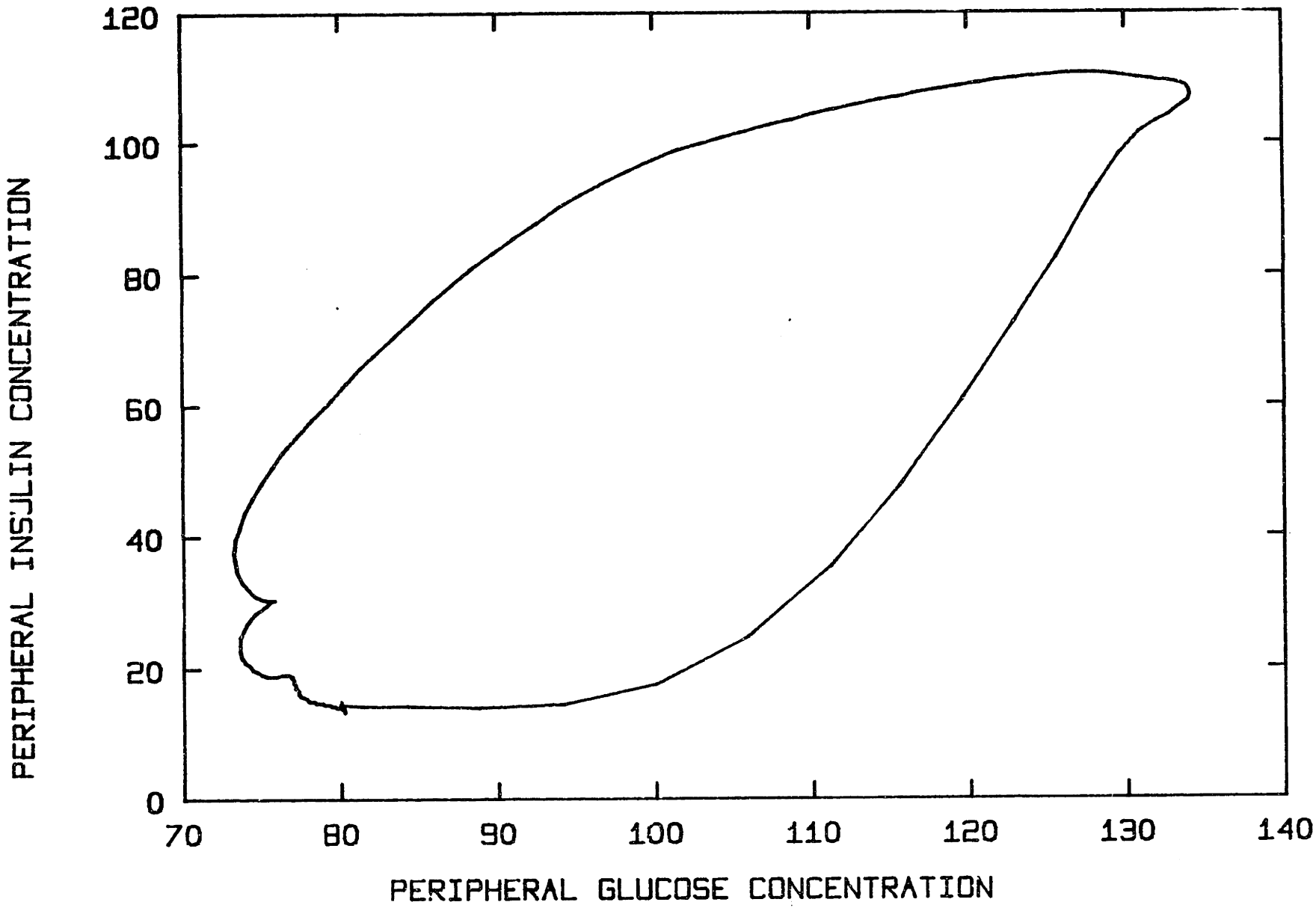

Figure 114

Insulin delivery with diffusional delay in glucose measurement and insulin secretion.
Simulation of response to a 100 gram oral glucose tolerance test.

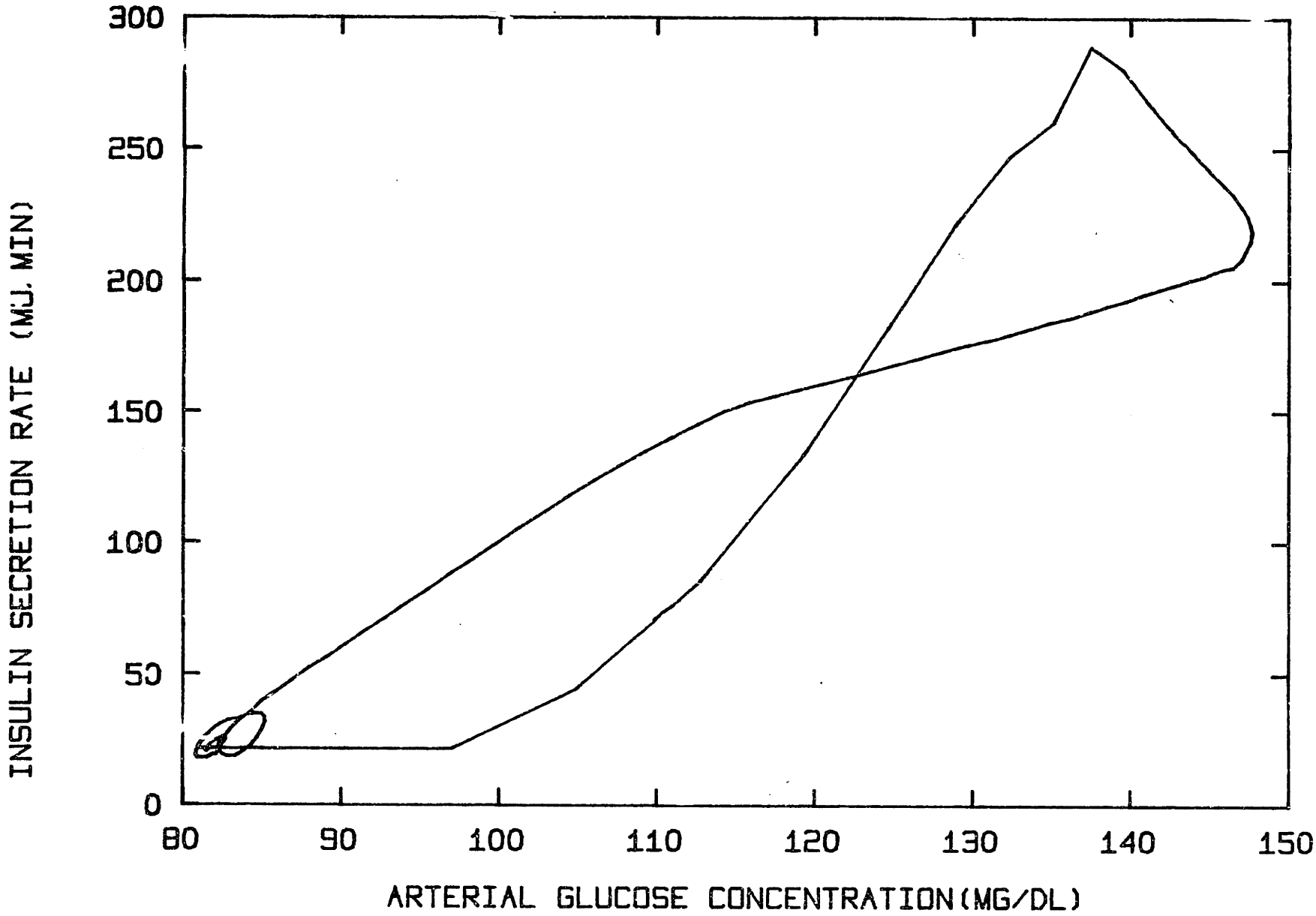

Figure 115

Insulin delivery with diffusional delay in glucose measurement and insulin secretion.
Simulation of response to a 100 gram oral glucose tolerance test.

oscillate in response. These oscillations are not surprising, due to the nature of the oral absorption rate. Because of the two diffusional delays, the pancreas and liver cannot accurately track the rising peripheral glucose concentrations following an OGTT. Again, the magnitude of these effects can only be determined if further experimentation is done to characterize (and minimize) the delays.

F. Peripheral versus Pancreatic "sensing of glucose".

Under normal physiologic conditions, glucose concentrations are "sensed" by the pancreas in the arterial blood perfusing the organ. The following simulation is presented to consider the effect of "sensing" glucose at a site different than arterial blood. Figures 116-121 show the effect when insulin secretion is based on peripheral rather than pancreatic glucose concentrations. That is, the model is adapted so the peripheral glucose levels are "sensed" and used to calculate the rate of insulin secretion. The input is a 100 gram oral glucose tolerance test comparing the insulin and glucose concentrations (figure 85 and 86) to those seen after an OGTT in normals, very little difference can be discerned. This is verified by comparing the phase plots for the two situations (figures 120-121 and 79-80). The insulin secretion rate at a given glucose concentration is identical.

G. Peripheral versus Portal Delivery of Insulin.

Under normal physiologic conditions, insulin is secreted into the portal circulation. The following simulations are presented to consider the effect of insulin secretion at a site other than the portal circulation. Figures 122-127 show the effect when insulin is secreted into the peripheral circulation following a 100 gm OGTT. As discussed

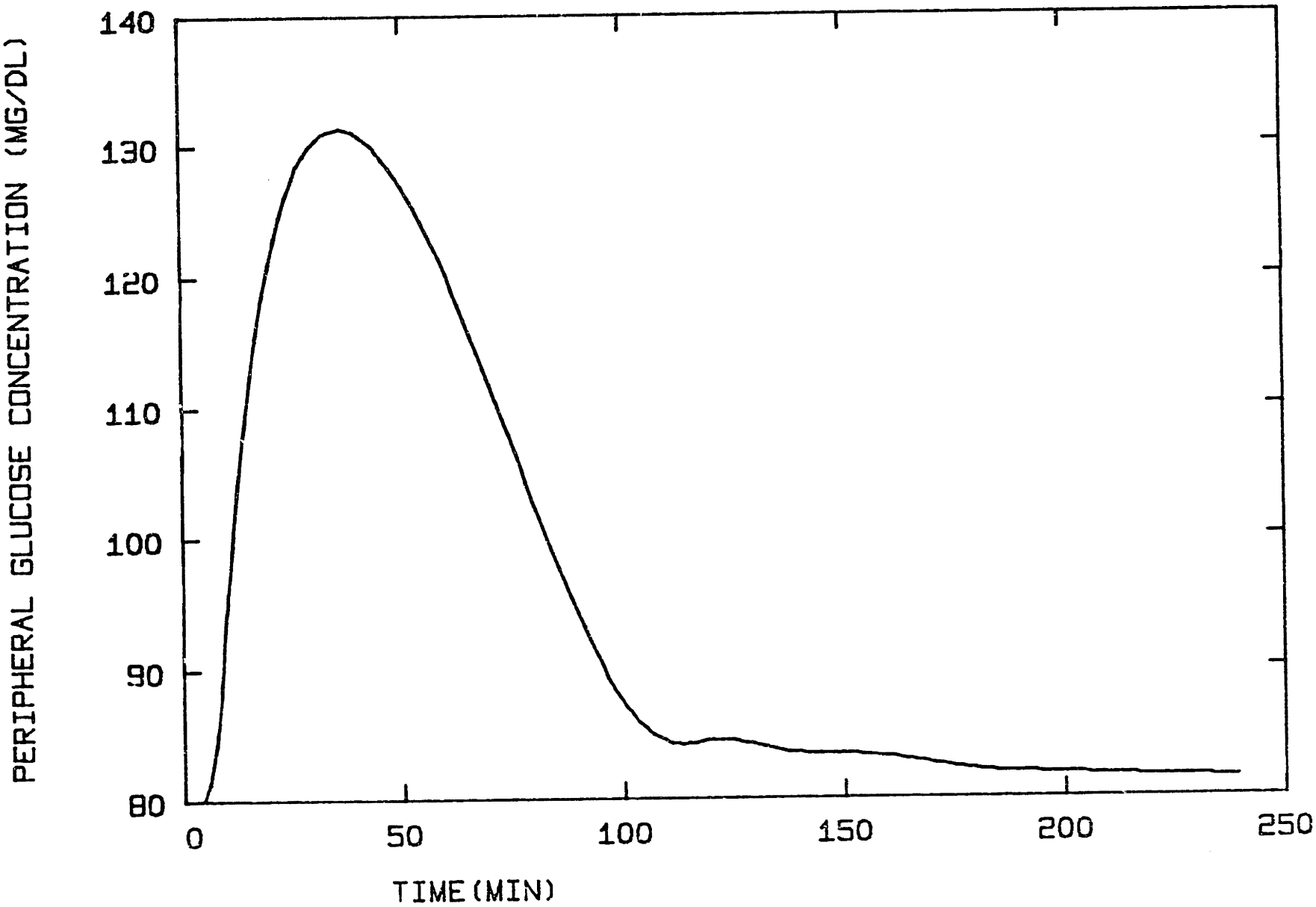

Figure 116

Pancreatic insulin secretion based on measurement of peripheral (i.v.) glucose concentration.
Simulation of response to a 100 gram oral glucose tolerance test.

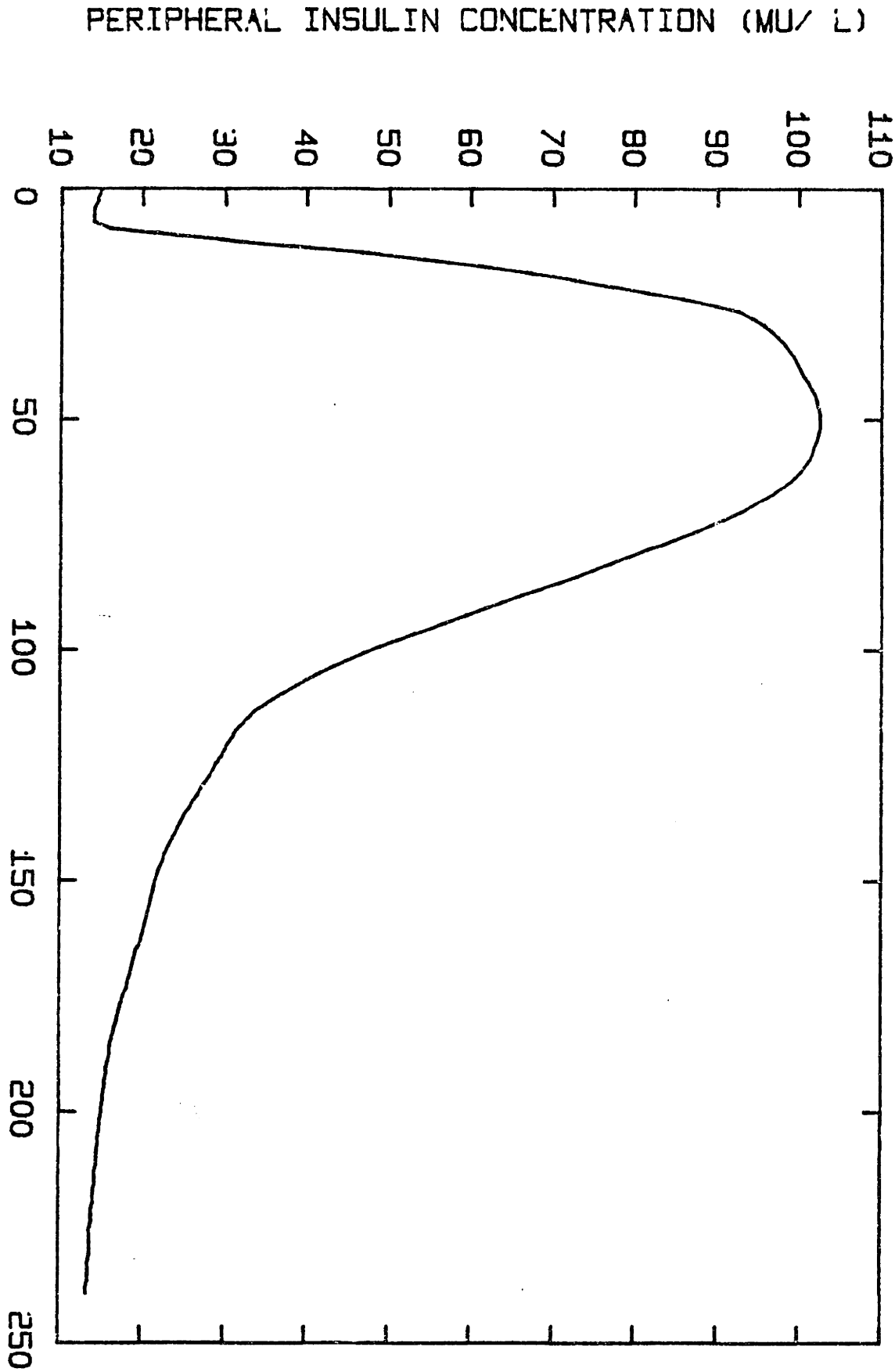

Figure 117

Pancreatic insulin secretion based on measurement of peripheral (i.v.) glucose concentration. Simulation of response to a 100 gram oral glucose tolerance test.

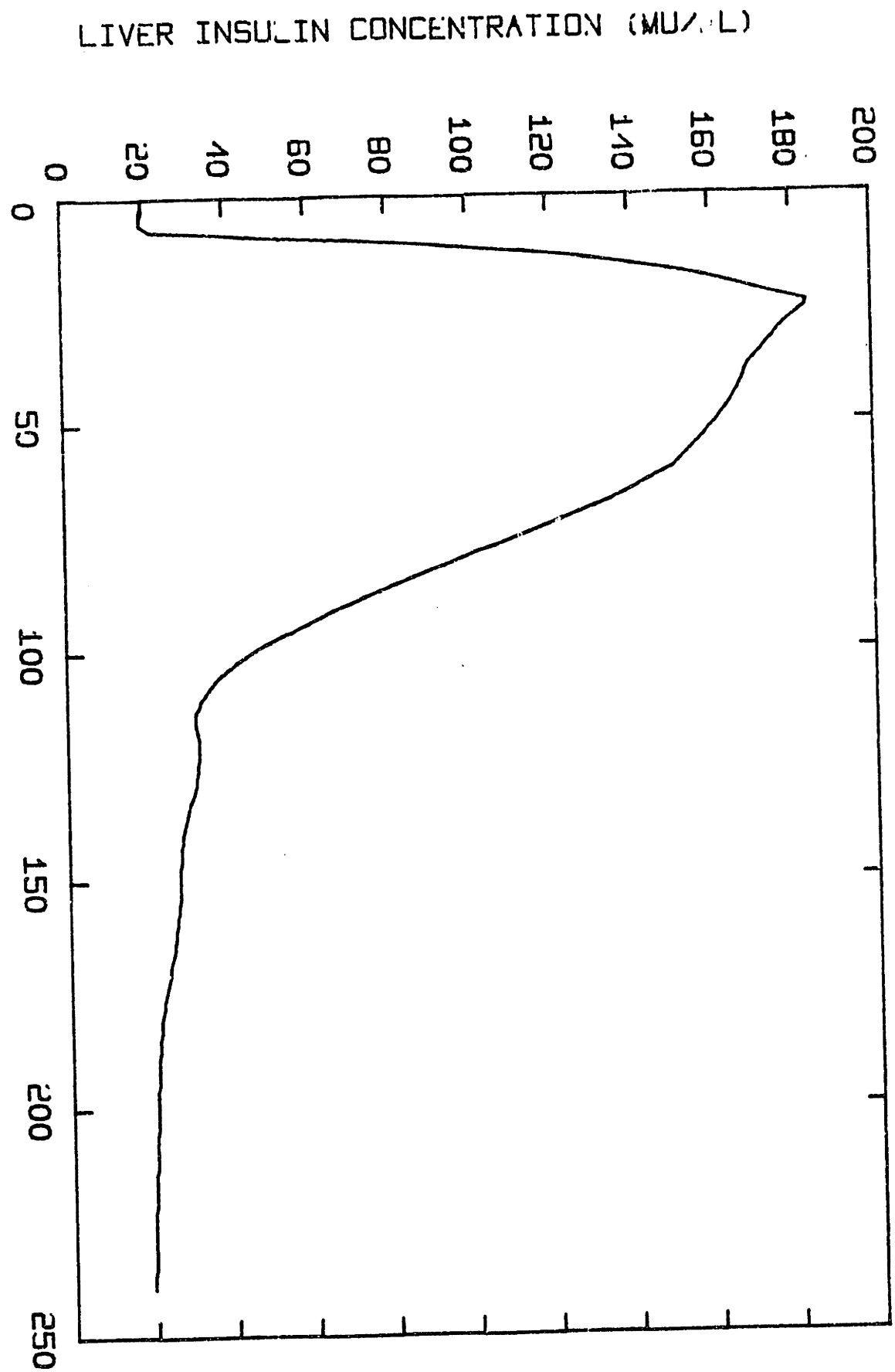

Figure 118

Pancreatic insulin secretion based on measurement of peripheral (i.v.) glucose concentration. Simulation of response to a 100 gram oral glucose tolerance test.

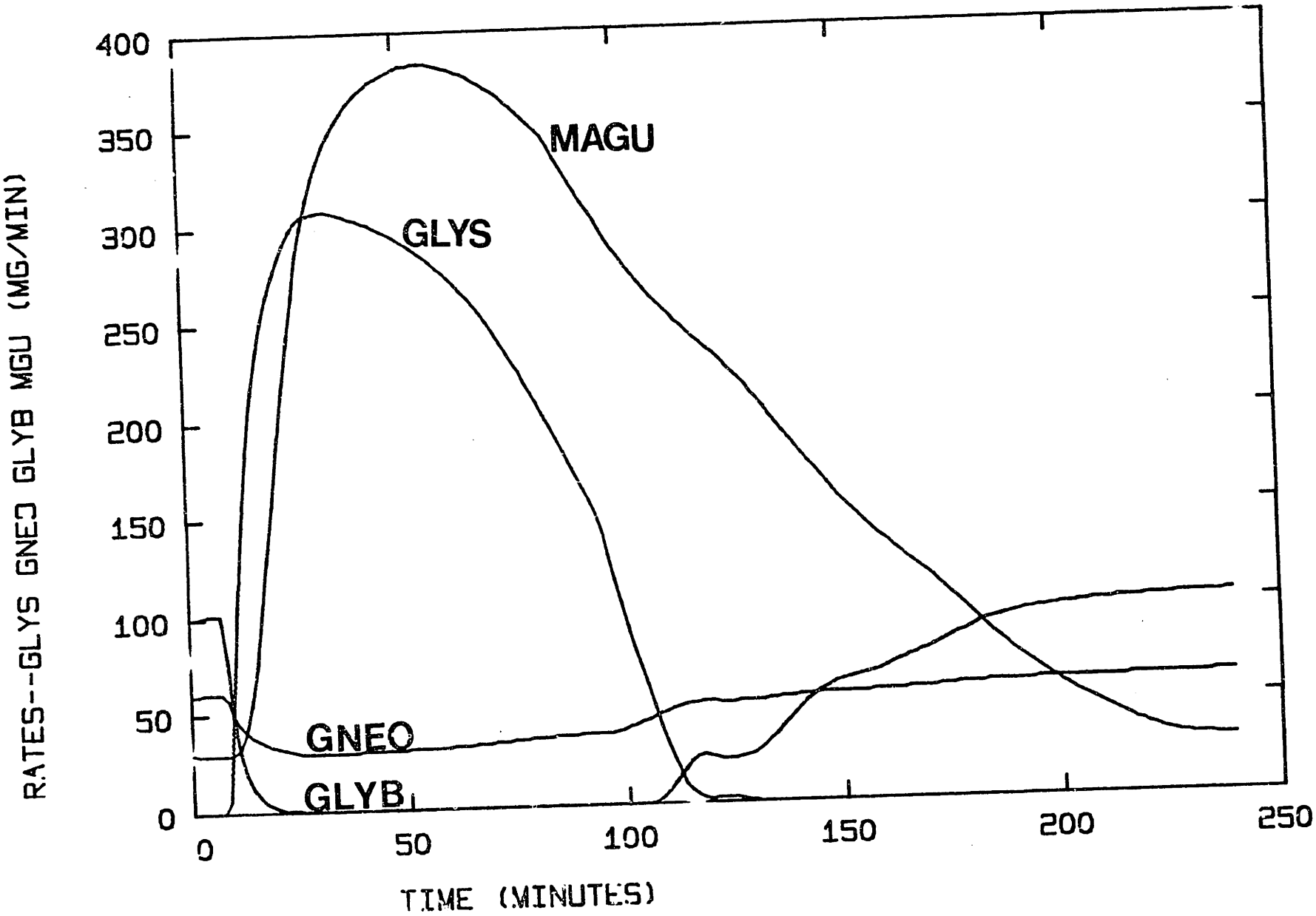

Figure 119

Pancreatic insulin secretion based on measurement of peripheral (i.v.) glucose concentration. Simulation of response to a 100 gram oral glucose tolerance test.

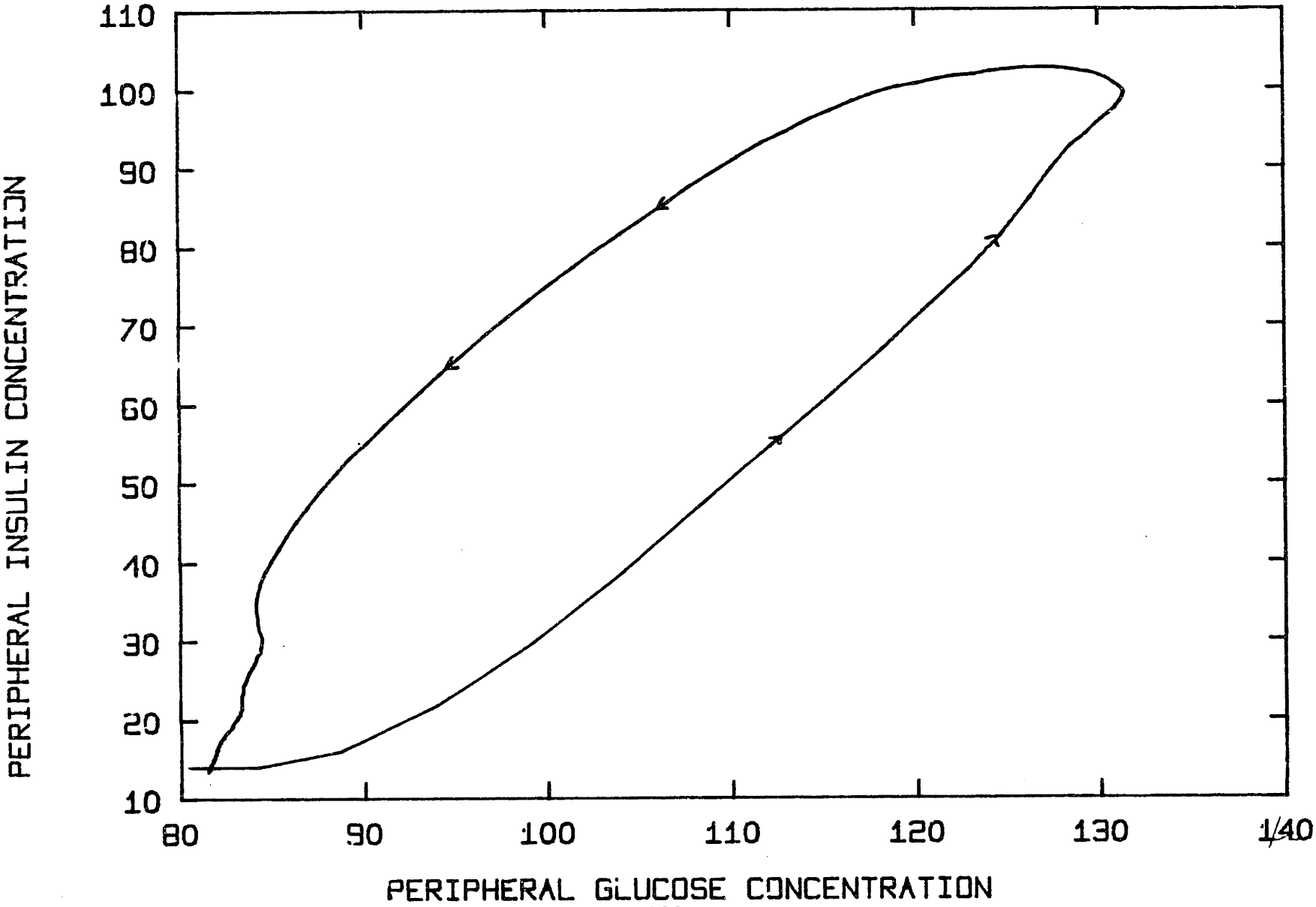

Figure 120

Pancreatic insulin secretion based on measurement of peripheral (i.v.) glucose concentration. Simulation of response to a 100 gram oral glucose tolerance test.

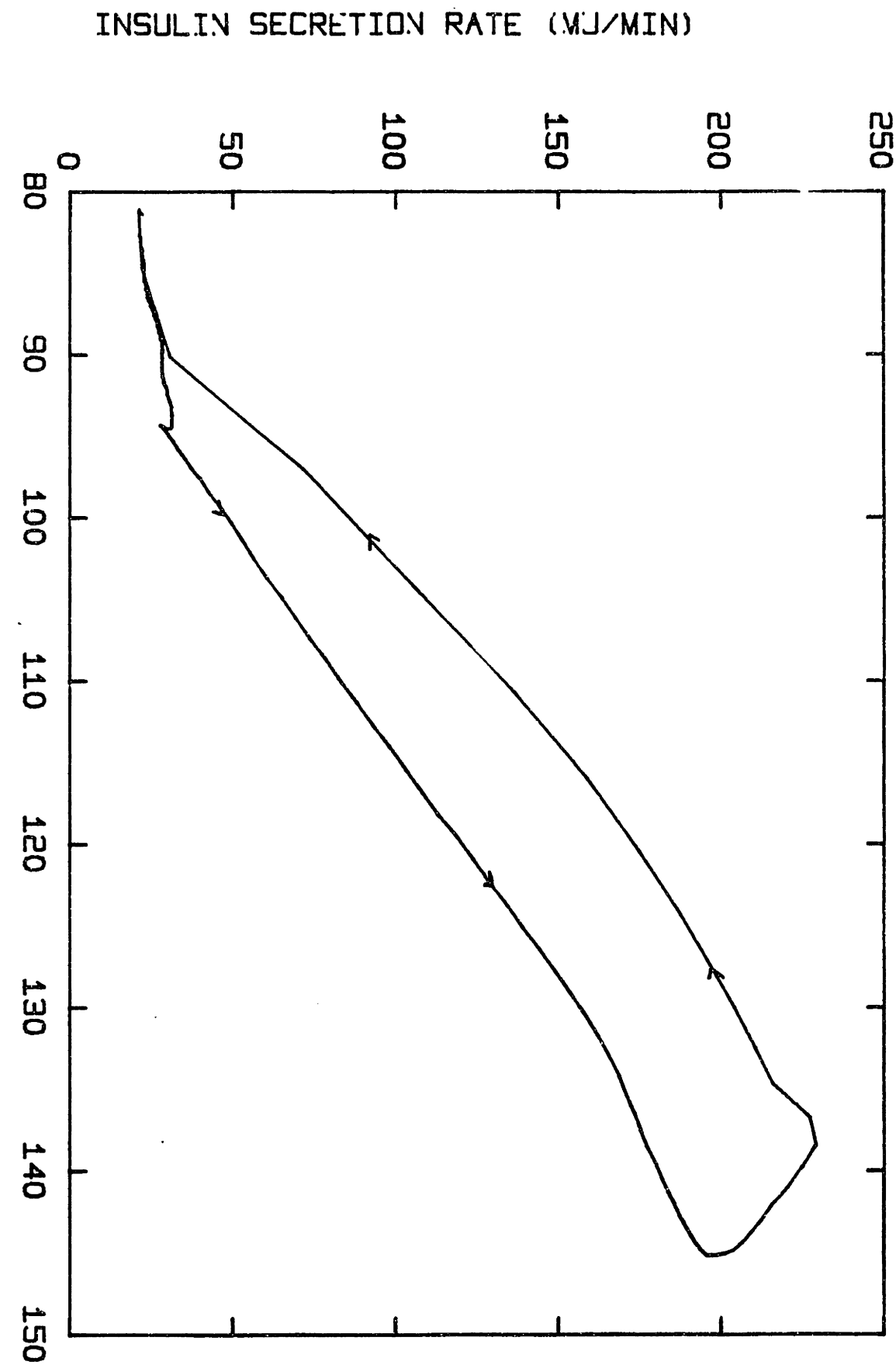

Figure 121

Pancreatic insulin secretion based on measurement of peripheral (i.v.) glucose concentration. Simulation of response to a 100 gram oral glucose tolerance test.

earlier, experiments by Botz et al (1976) have shown that equally good control of peripheral blood glucose levels can be achieved by portal or peripheral insulin delivery. Comparing figure 64 to figure 91 it can be seen that peripheral blood glucose levels are comparable for both sites of insulin delivery. However, it is important to note that by delivering insulin via the peripheral route, peripheral insulin concentrations are elevated 3 times normal (compare figure 123 to figure 65) while liver (portal) insulin concentrations are only ½ their normal values (compare figure 93 to figure 67). The normal portal-peripheral gradient is therefore reversed and peripheral insulin concentrations are actually higher than those in the liver. As a result, the rate of peripheral glucose uptake is significantly increased above normal, while the rate of glycogen synthesis is decreased. To compensate for the increased glucose uptake by muscle's adipose tissue and maintain peripheral glucose concentrations within 70-80 mg/dl, the rates of gluconeogenesis and glycogenolysis are increased to 240 mg/min. So although glucose control as measured by peripheral glucose concentrations is adequate, the underlying rates necessary to maintain this homeostasis have been severely altered. If insulin is delivered peripherally for long periods of time, it is possible that adipose tissue (fat) stores would greatly increase at the expense of liver glycogen. This may not occur due to the fact that the body may readjust to a new set point for insulin. A new set point could be achieved by (1) a reduction in the density of insulin receptors on adipose and muscle cells, with an increase in density on liver cells or (2) a change in the coupling between binding of insulin and biochemical action (i.e. glucose uptake).

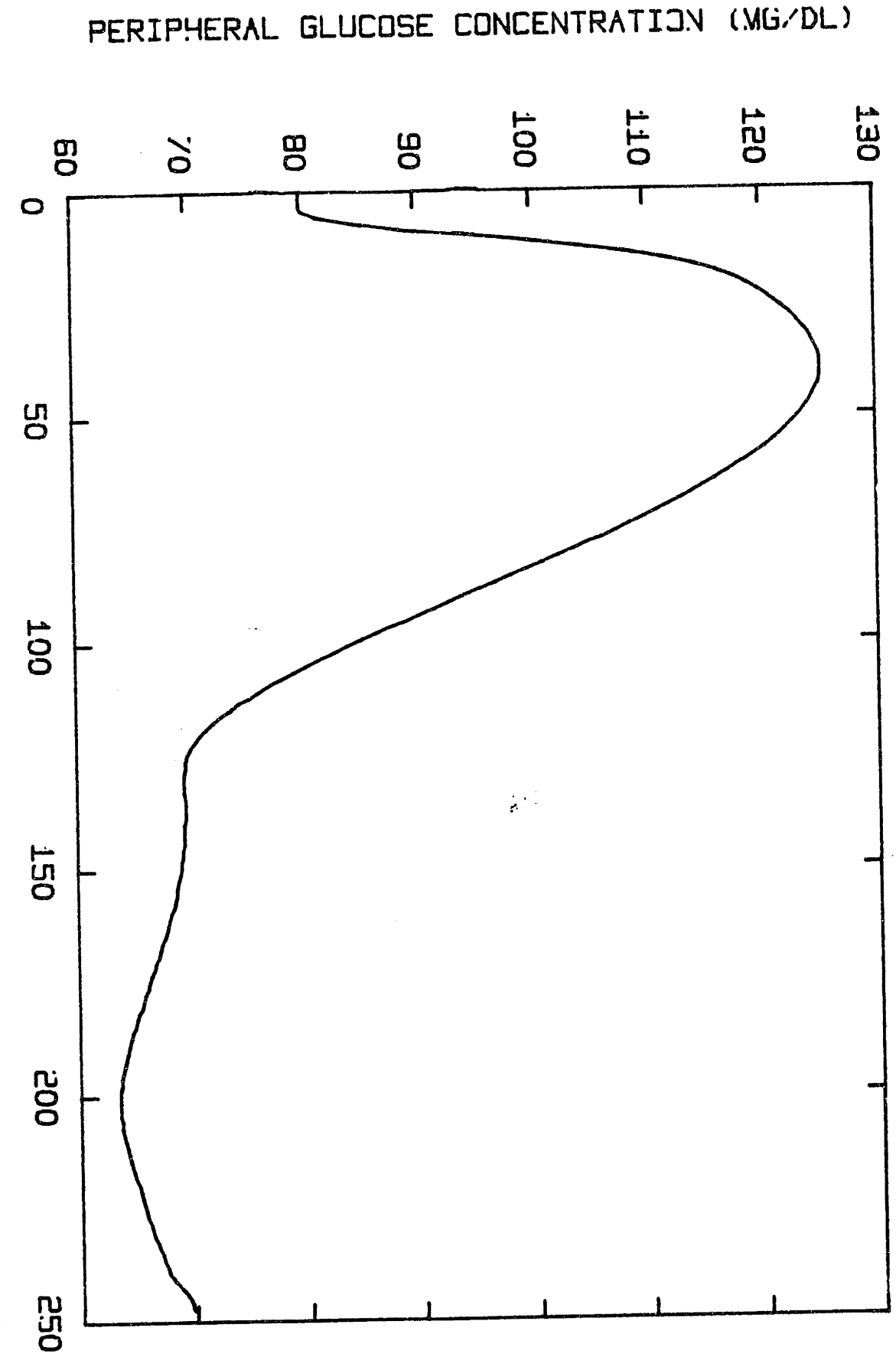

Figure 122

Pancreatic insulin secretion via the peripheral rather than portal circulation. Simulation of response to a 100 gram oral glucose tolerance test.

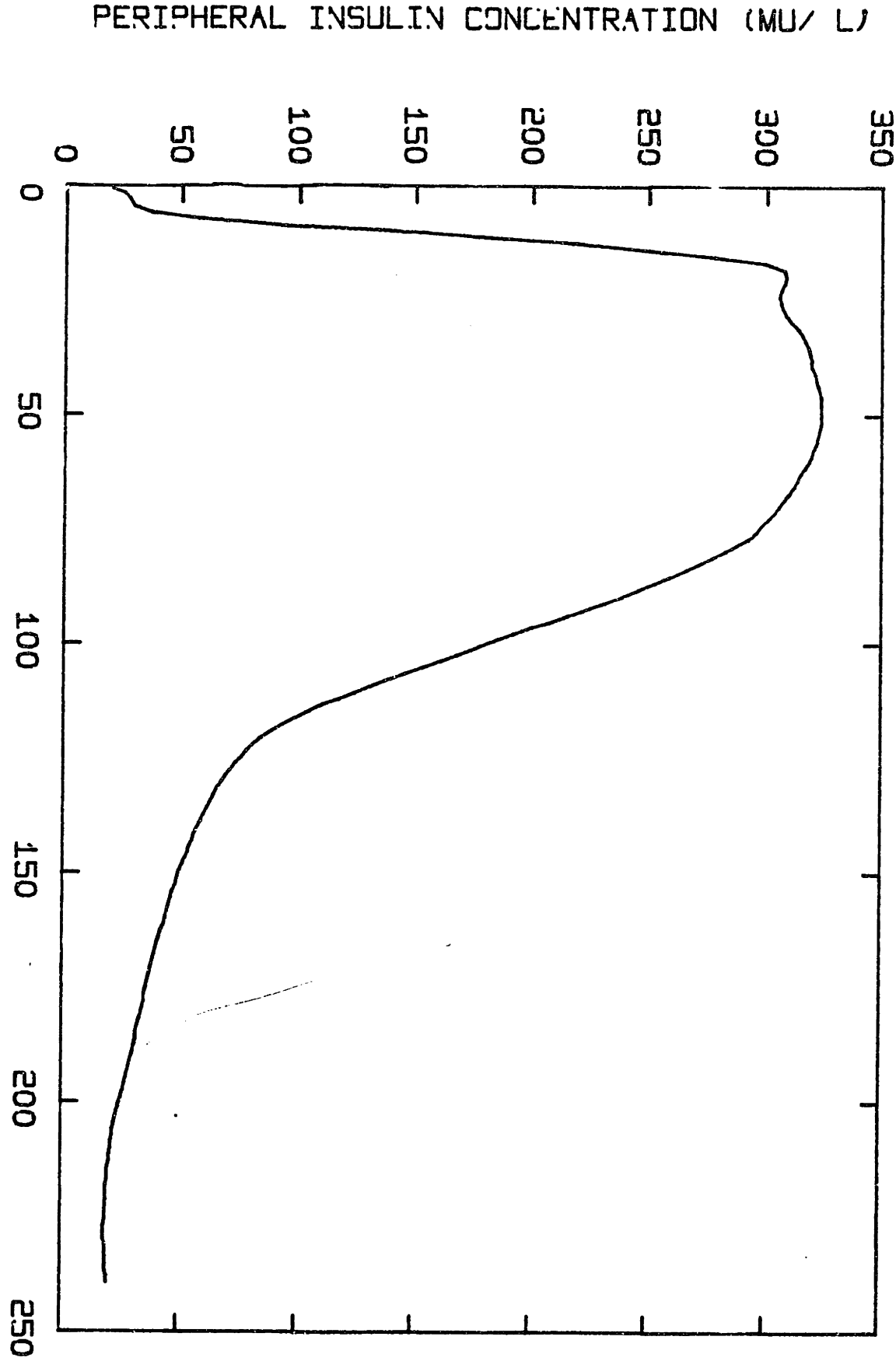

Figure 123

Pancreatic insulin secretion via the peripheral rather than portal circulation. Simulation of response to a 100 gram oral glucose tolerance test.

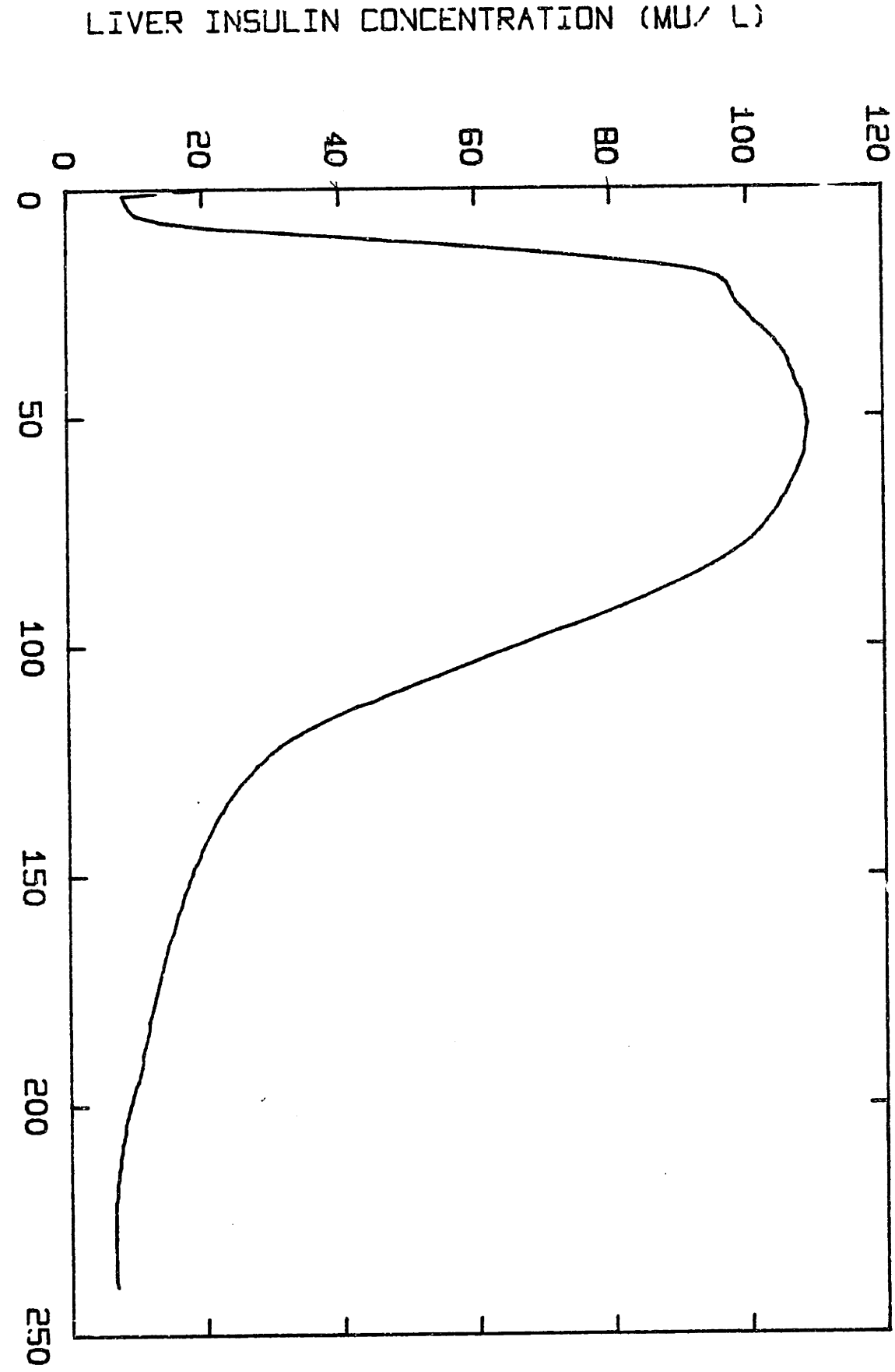

Figure 124

Pancreatic insulin secretion via the peripheral rather than portal circulation. Simulation of response to a 100 gram oral glucose tolerance test.

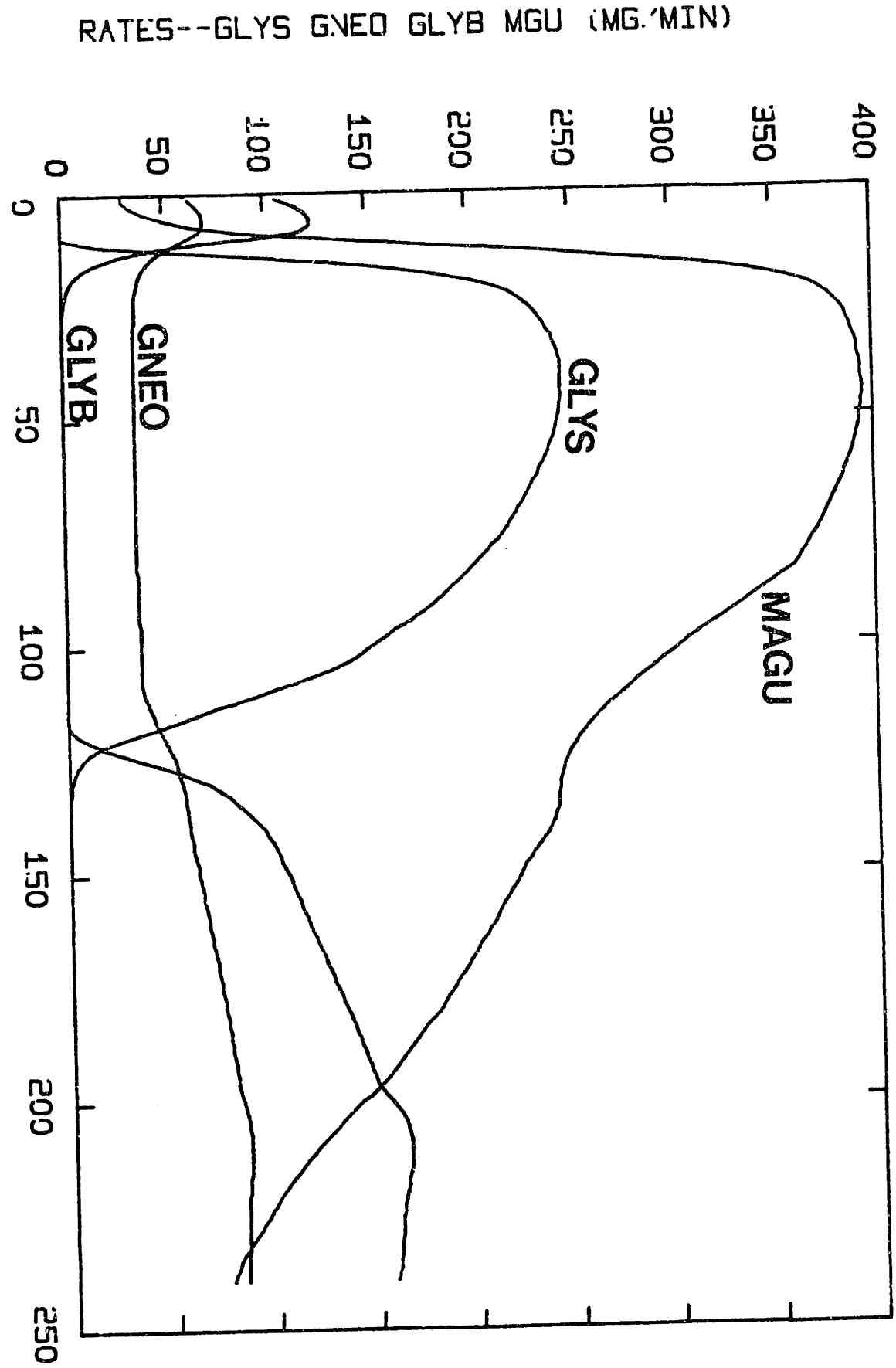

Figure 125

Pancreatic insulin secretion via the peripheral rather than portal circulation. Simulation of response to a 100 gram oral glucose tolerance test.

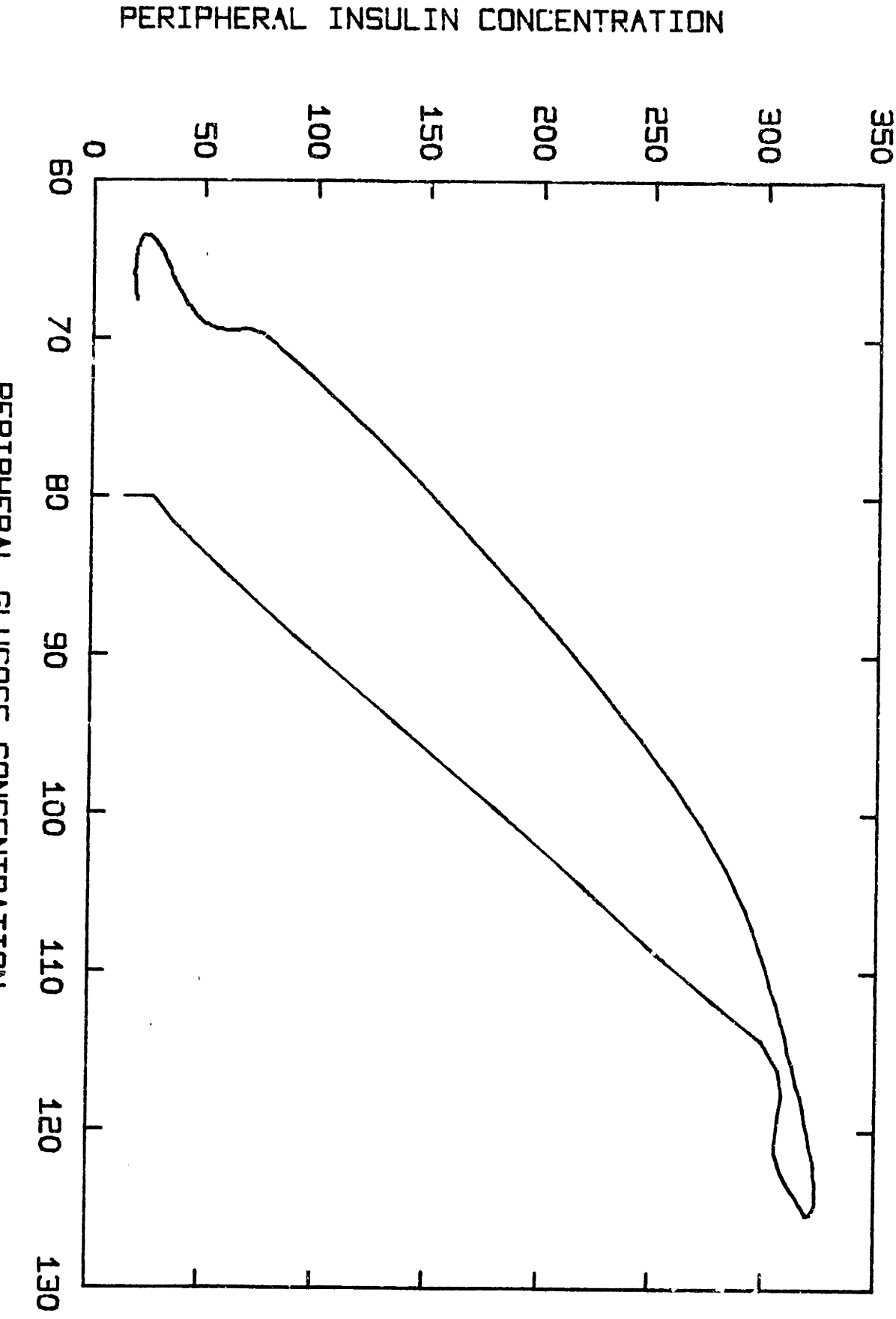

Figure 126

Pancreatic insulin secretion via the peripheral rather than portal circulation. Simulation of response to a 100 gram oral glucose tolerance test.

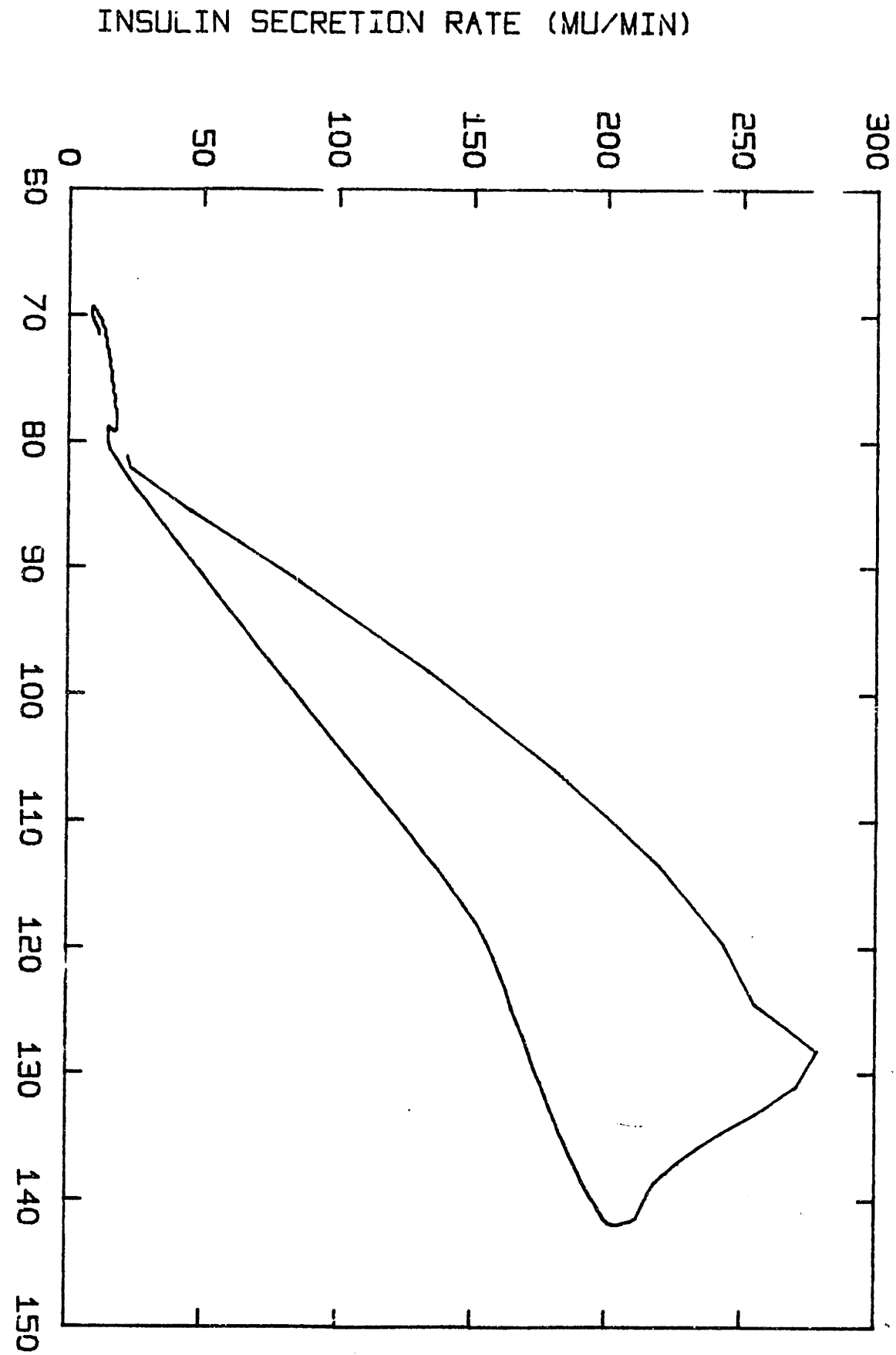

Figure 127

Pancreatic insulin secretion via the peripheral rather than portal circulation. Simulation of response to a 100 gram oral glucose tolerance test.

This mode of delivery must be reconsidered as a viable alternative, if total normalization is desired.

In conclusion, the site of glucose sensing does not appear to be an important variable for glucose control, although the site of insulin delivery appears to be important. To further demonstrate this point, two other simulations were run. Figures 128-132 show the results of peripheral glucose "sensing" and peripheral (I.V.) insulin delivery. Figures 133-138 show the results of peripheral tissue "sensing" and peripheral (I.V.) insulin delivery. Comparing these different areas of the body (pancreatic blood, peripheral blood, and peripheral tissue) as the site for measurement of glucose concentration result in small differences in overall glucose control (see figures 122, 128, 133).

H. Delay in Glucose Measurement

A delay in insulin secretion by the pancreas leads to a delayed glucose tolerance curve which is characteristic of maturity-onset diabetics. It is interesting to consider the effect a delay in the glucose signal to the pancreas would have on glucose tolerance. That is the glucose stimulus reaching the pancreas at time, t would reflect blood glucose concentrations at an earlier time, $t - dt$, where dt is the delay time. Figures 139-143 show the results when dt is equal to 5 minutes and the model input is a 100 gram glucose load. Compare the phase plots of peripheral insulin concentration as a function of peripheral glucose concentration for the normal (figure 79) and "delay" model (figure 142). From this comparison, it can be noted that a rise in insulin concentration does not occur until 110 mg/dl for the "delayed"

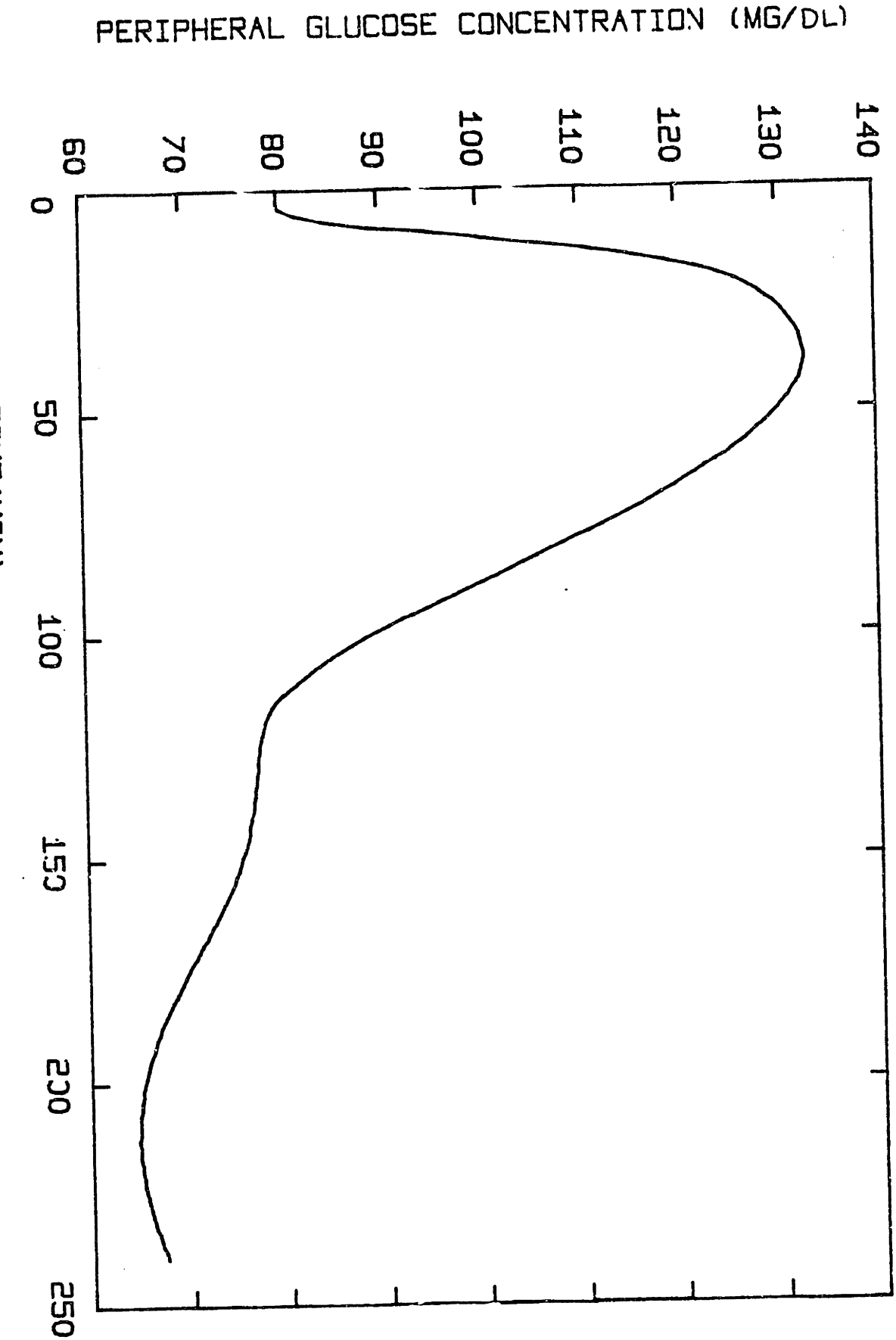

Figure 128

Pancreatic insulin secretion via the peripheral circulation based on measurement of peripheral (i.v.) glucose concentrations. Simulation of response to a 100 gram oral glucose tolerance test.

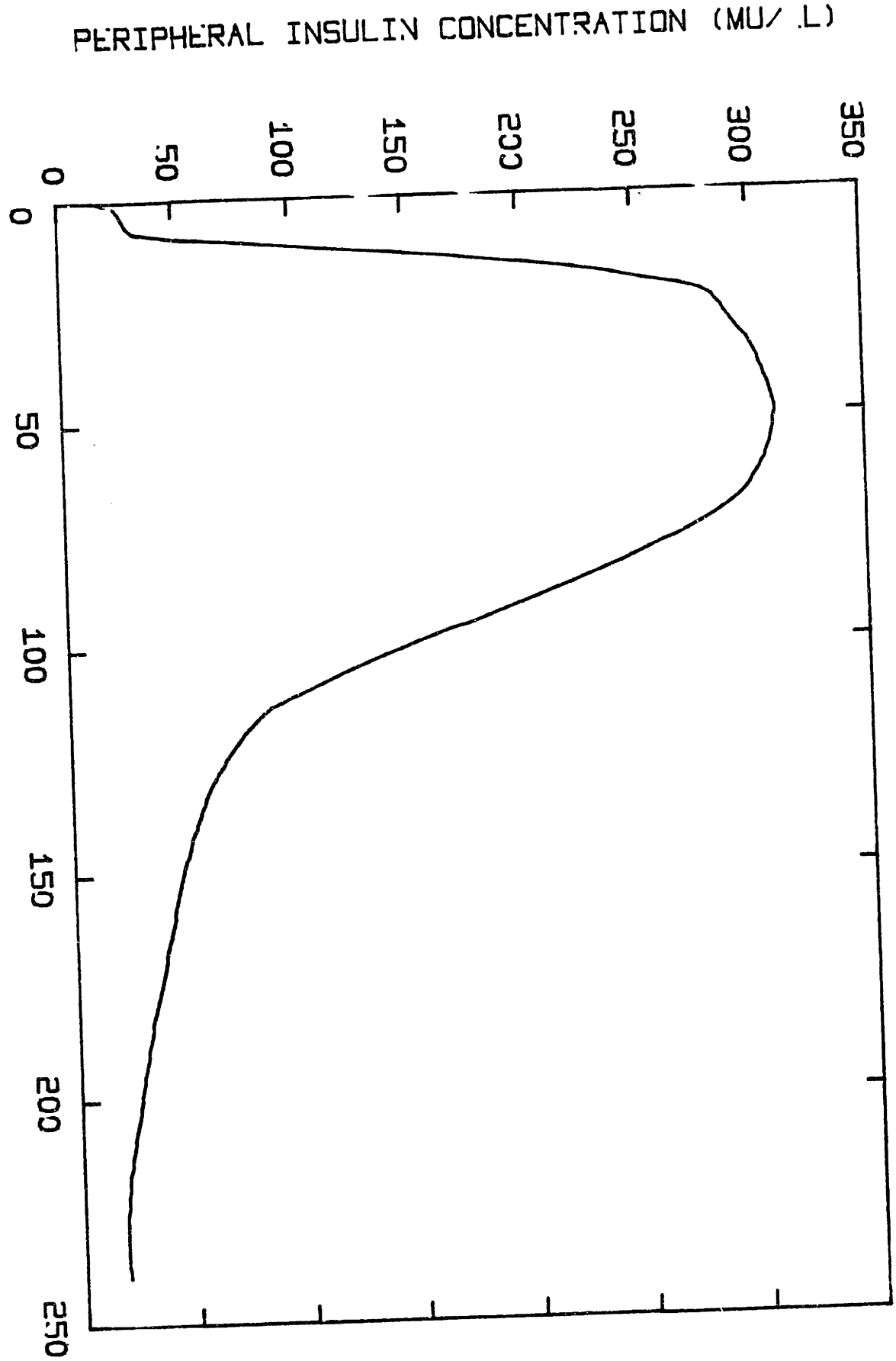

Figure 129

Pancreatic insulin secretion via the peripheral circulation based on measurement of peripheral (i.v.) glucose concentrations.

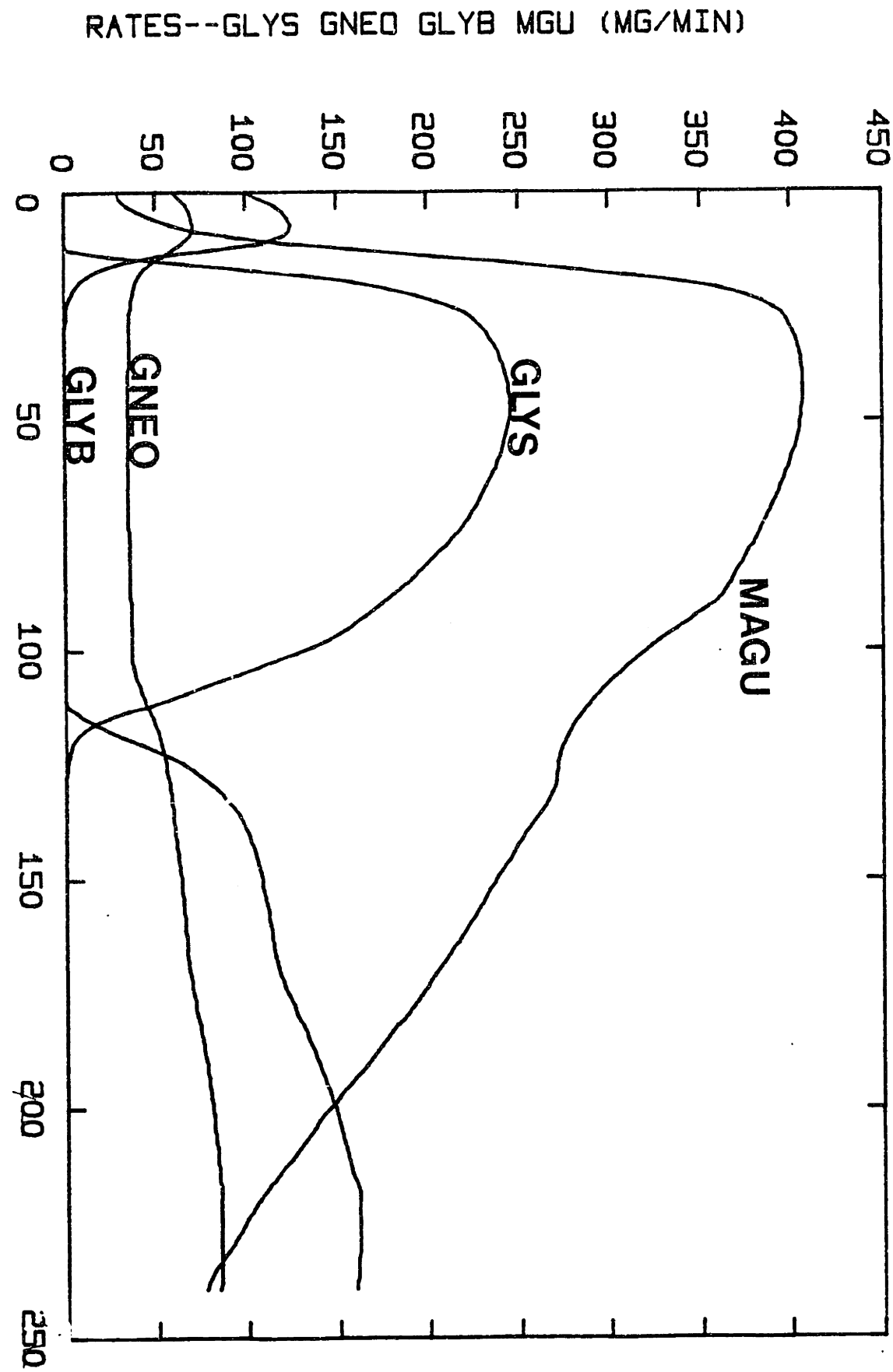

Figure 130

Pancreatic insulin secretion via the peripheral circulation based on measurement of peripheral (i.v.) glucose concentrations. Simulation of response to a 100 gram oral glucose tolerance test.

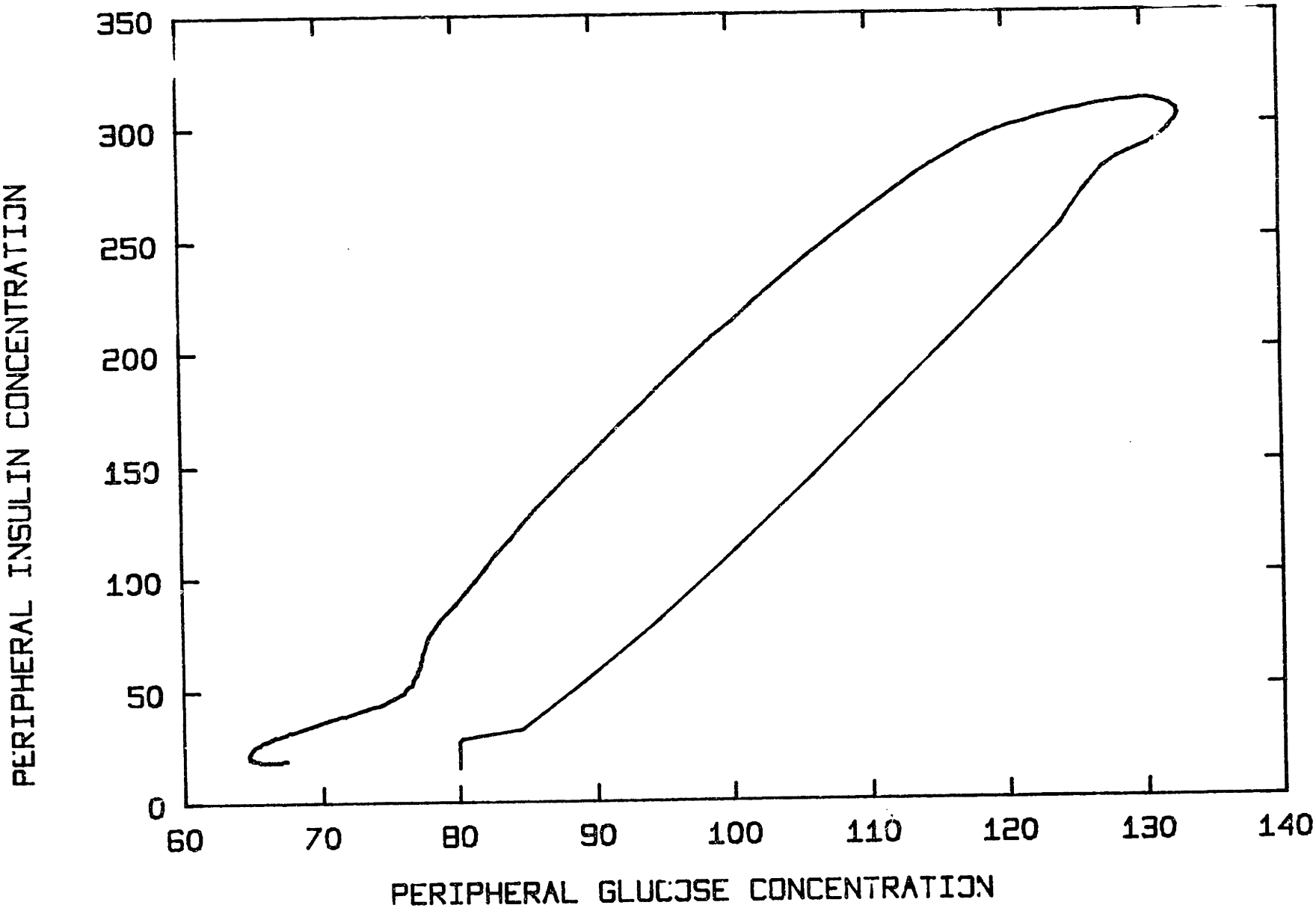

Figure 131

Pancreatic insulin secretion via the peripheral circulation based on measurement of peripheral (i.v.) glucose concentrations. Simulation of response to a 100 gram oral glucose tolerance test.

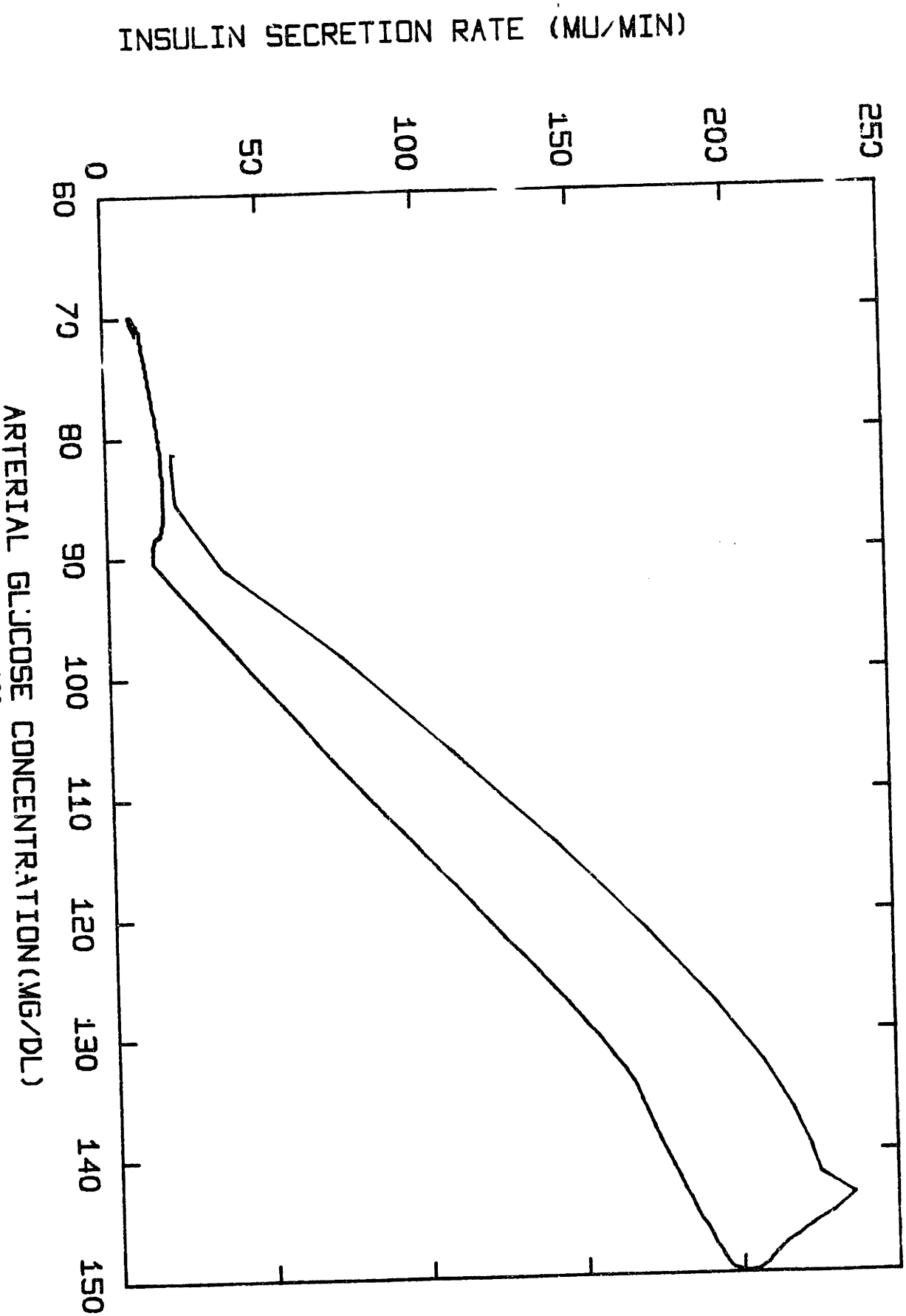

Figure 132

Pancreatic insulin secretion via the peripheral circulation based on measurement of peripheral (i.v.) glucose concentrations. Simulation of response to a 100 gram oral glucose tolerance test.

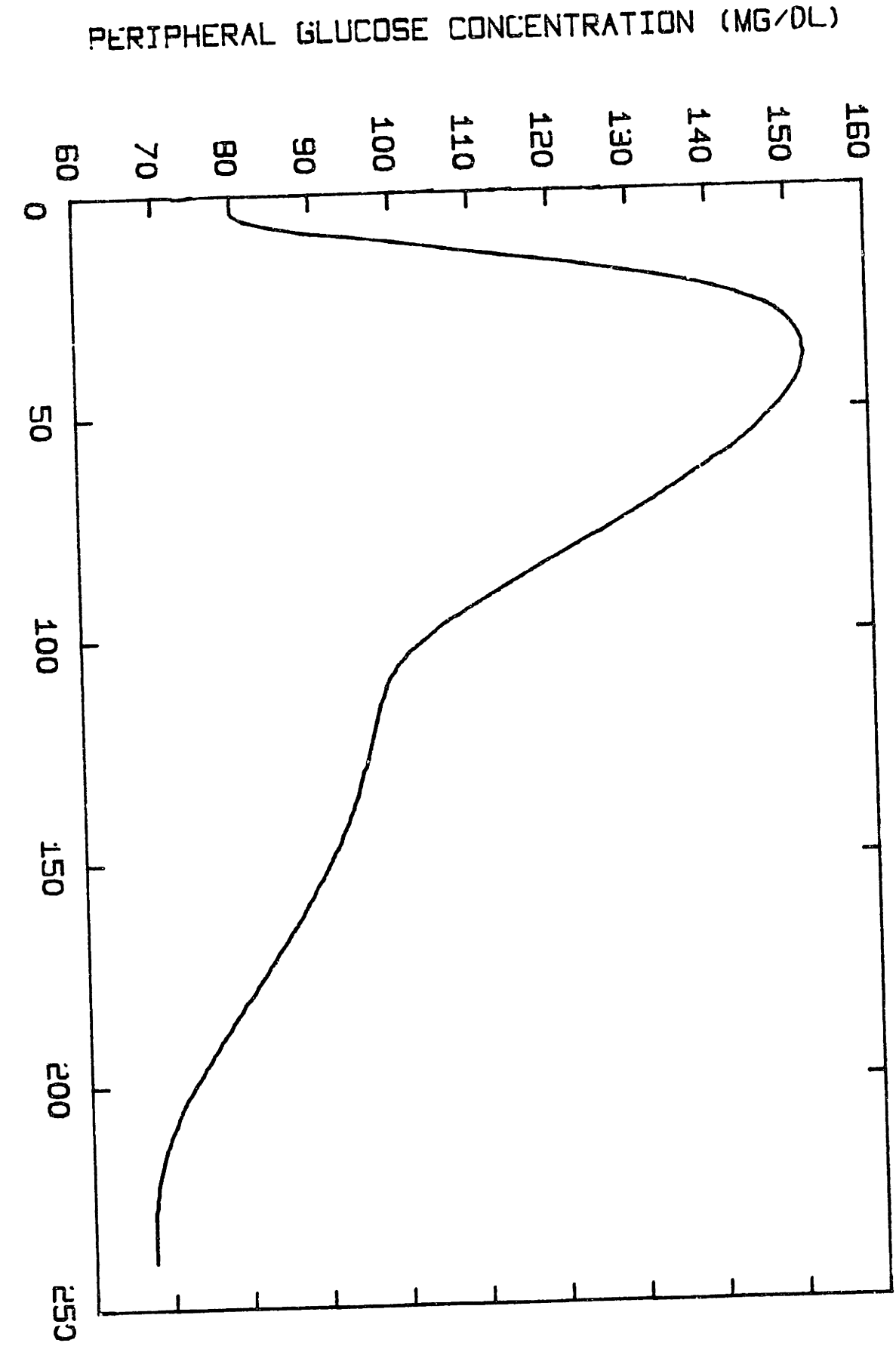

Figure 133

Pancreatic insulin secretion via the peripheral circulation based on measurement of peripheral tissue glucose concentrations. Simulation of response to a 100 gram oral glucose tolerance test.

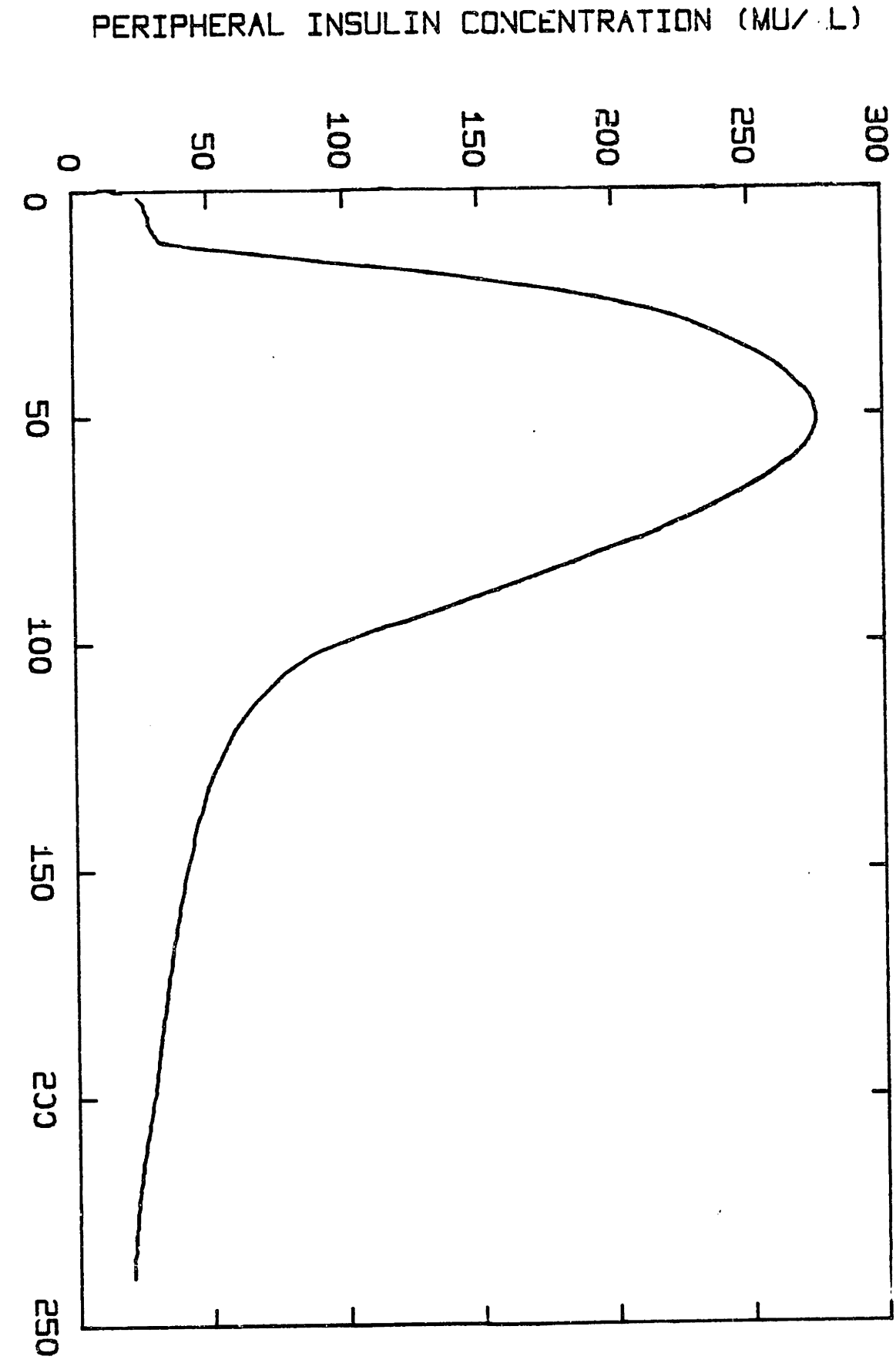

Figure 134

Pancreatic insulin secretion via the peripheral circulation based on measurement of peripheral tissue glucose concentrations. Simulation of response to a 100 gram oral glucose tolerance test.

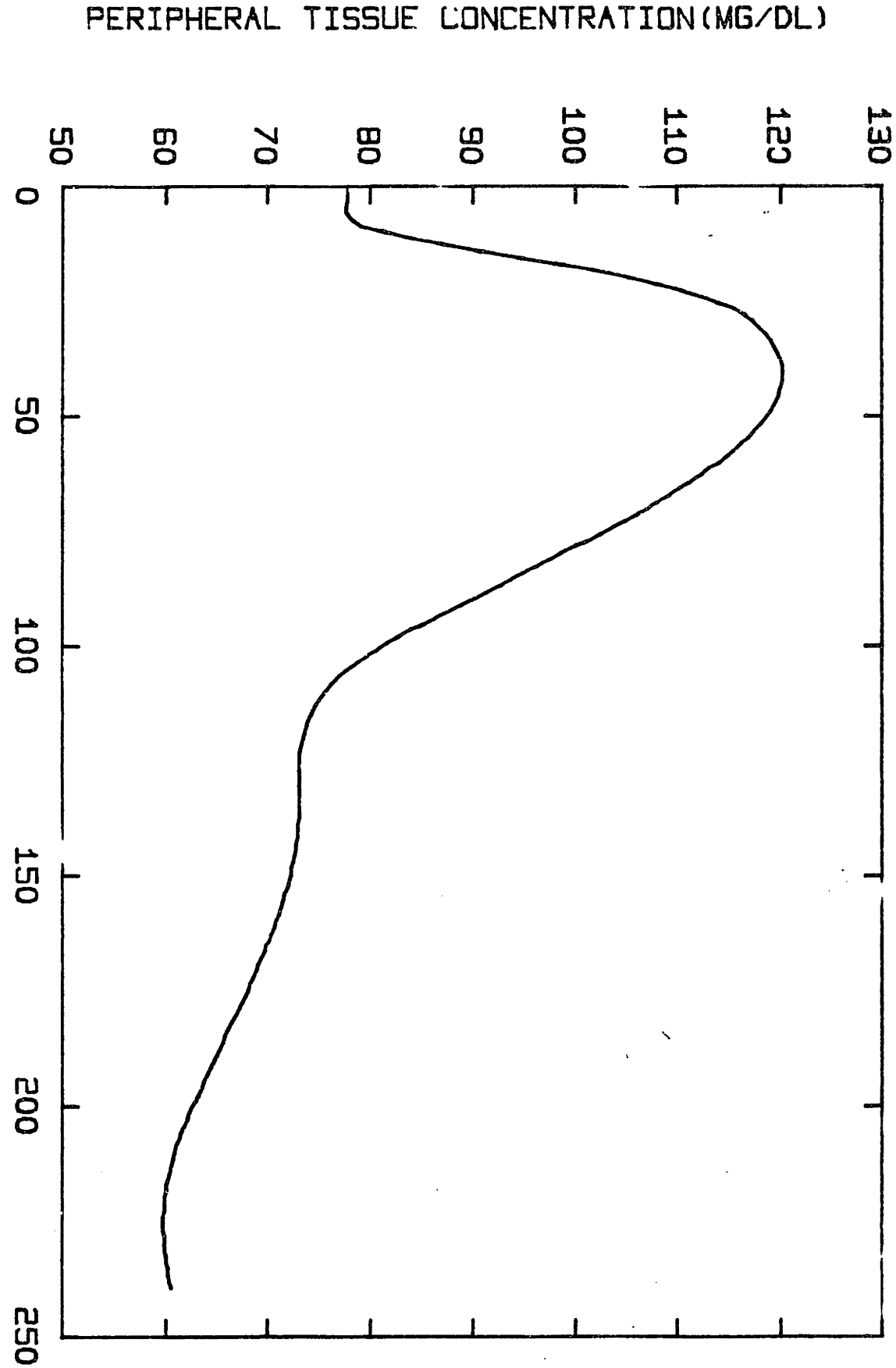

Figure 135

Pancreatic insulin secretion via the peripheral circulation based on measurement of peripheral tissue glucose concentrations. Simulation of response to a 100 gram oral glucose tolerance test.

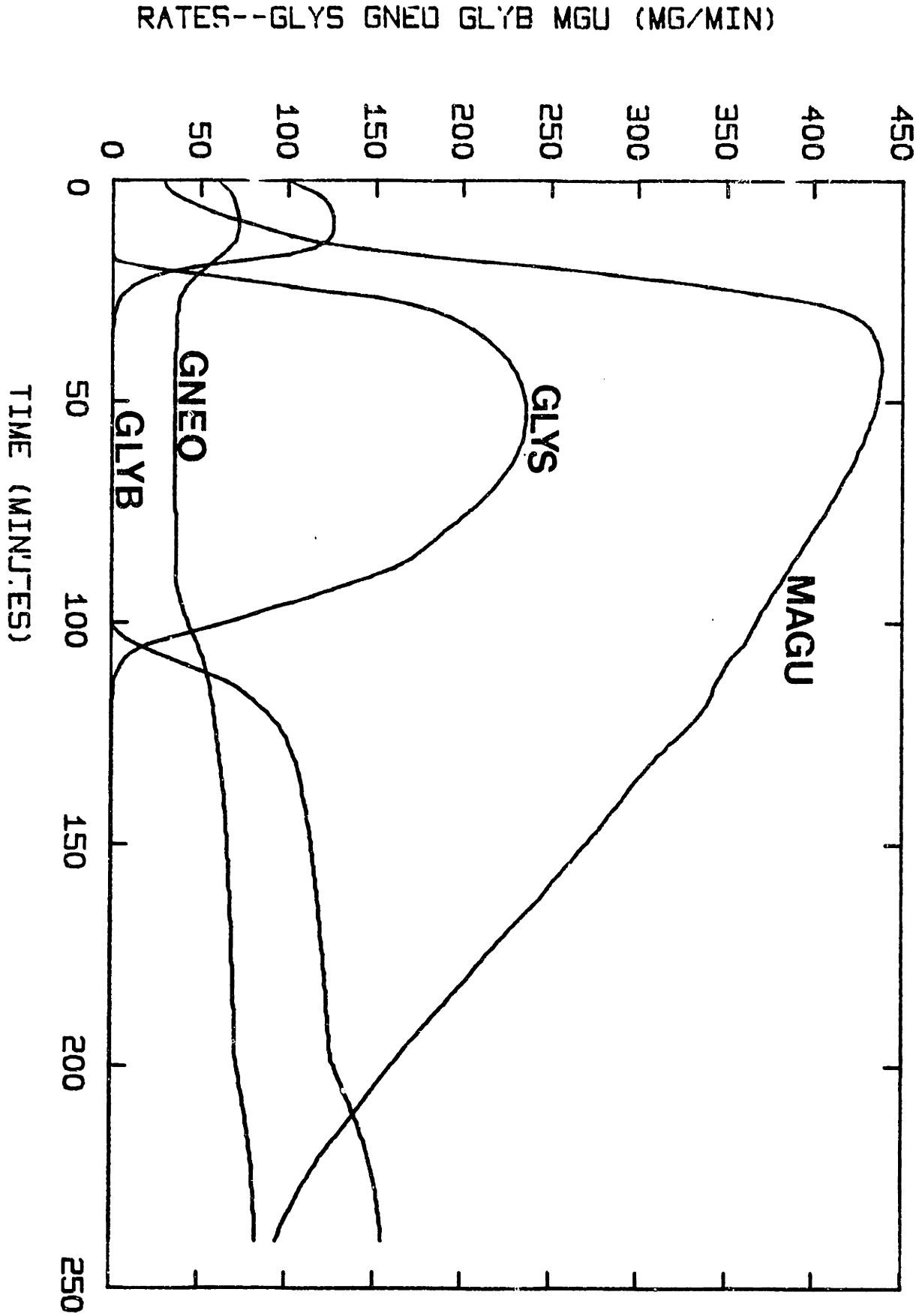

Figure 136

Pancreatic insulin secretion via the peripheral circulation based on measurement of peripheral tissue glucose concentrations. Simulation of response to a 100 gram oral glucose tolerance test.

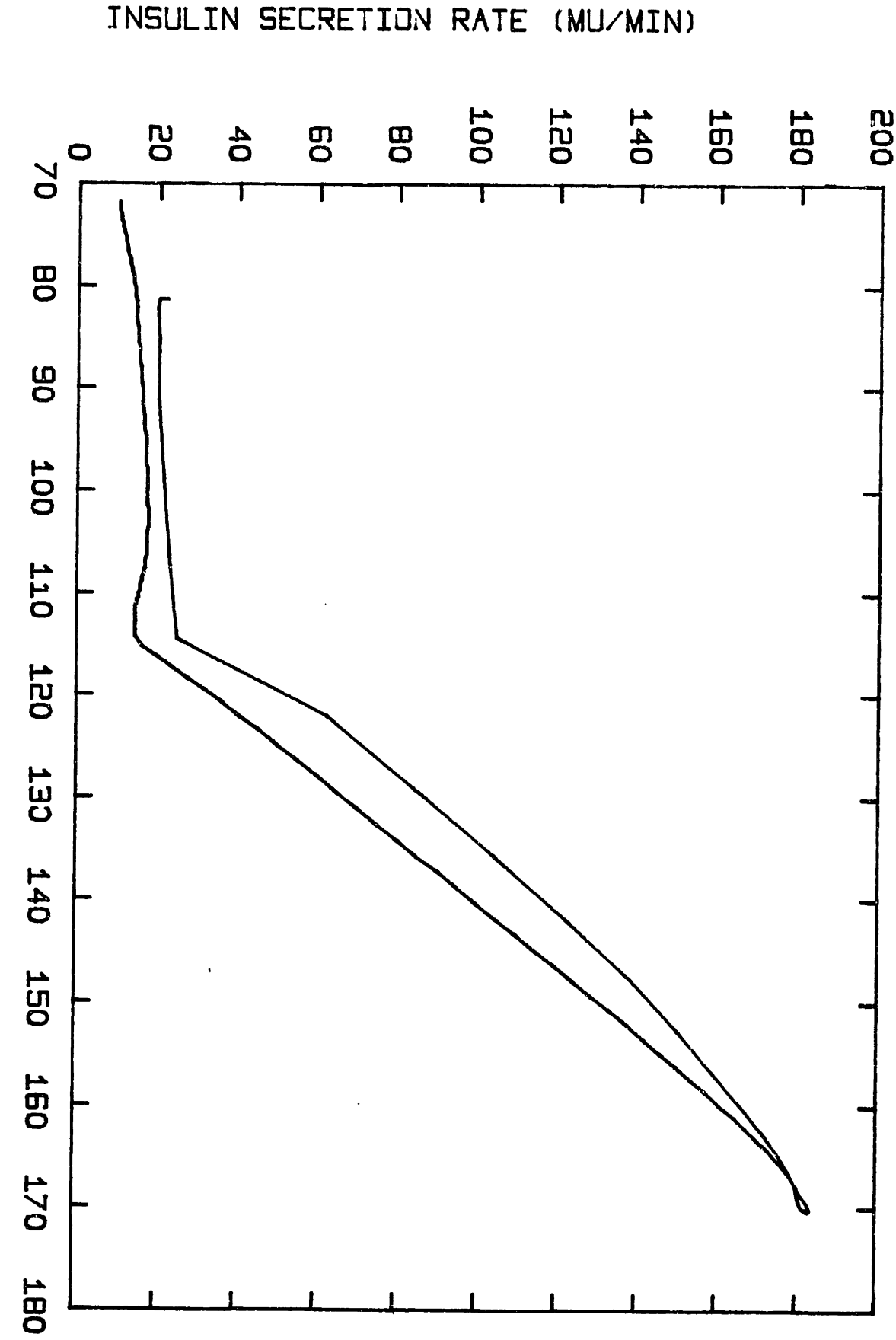

Figure 137

Pancreatic insulin secretion via the peripheral circulation based on measurement of peripheral tissue glucose concentrations. Simulation of response to a 100 gram oral glucose tolerance test.

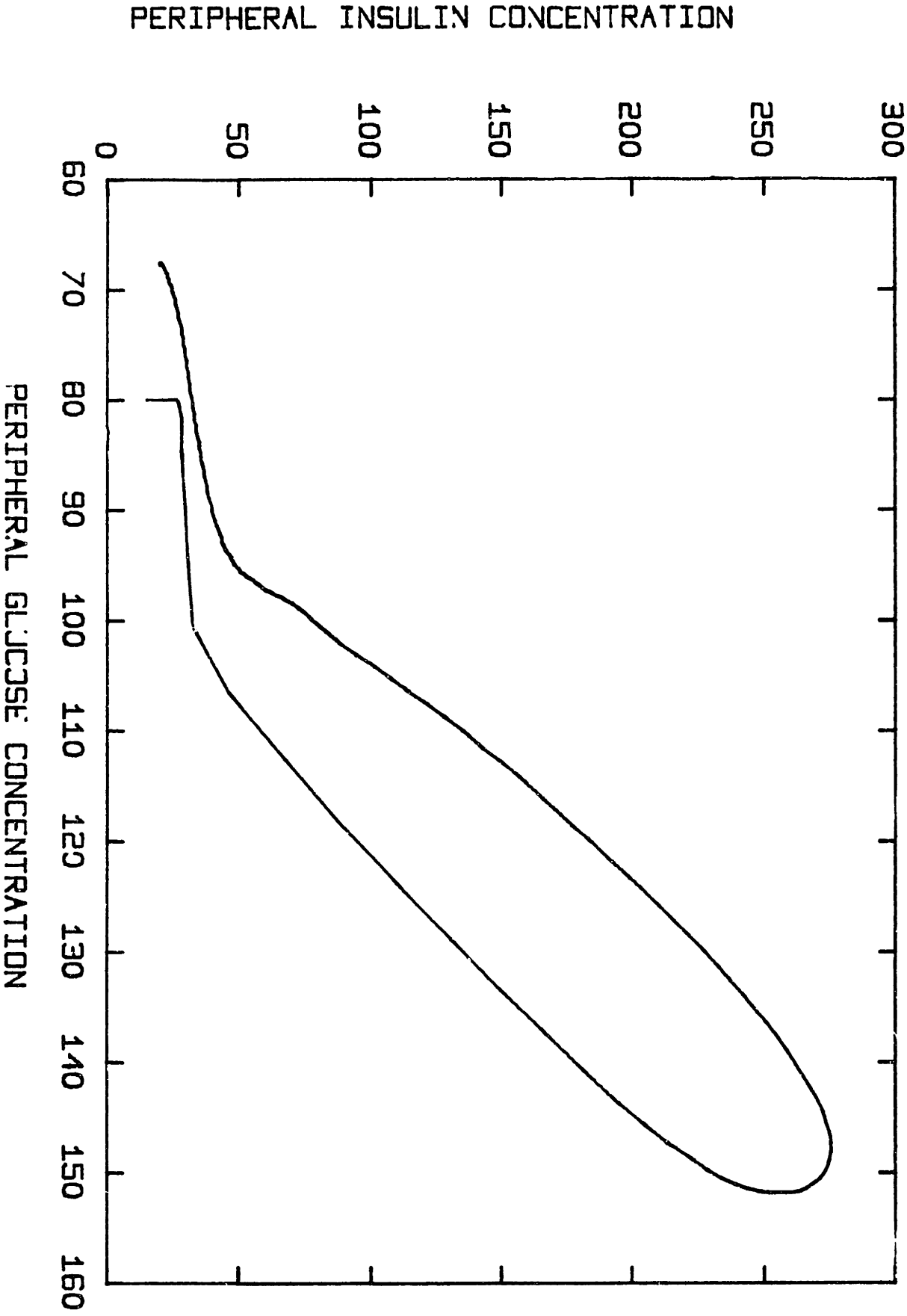

Figure 138

Pancreatic insulin secretion via the peripheral circulation based on measurement of peripheral tissue glucose concentrations. Simulation of response to a 100 gram oral glucose tolerance test.

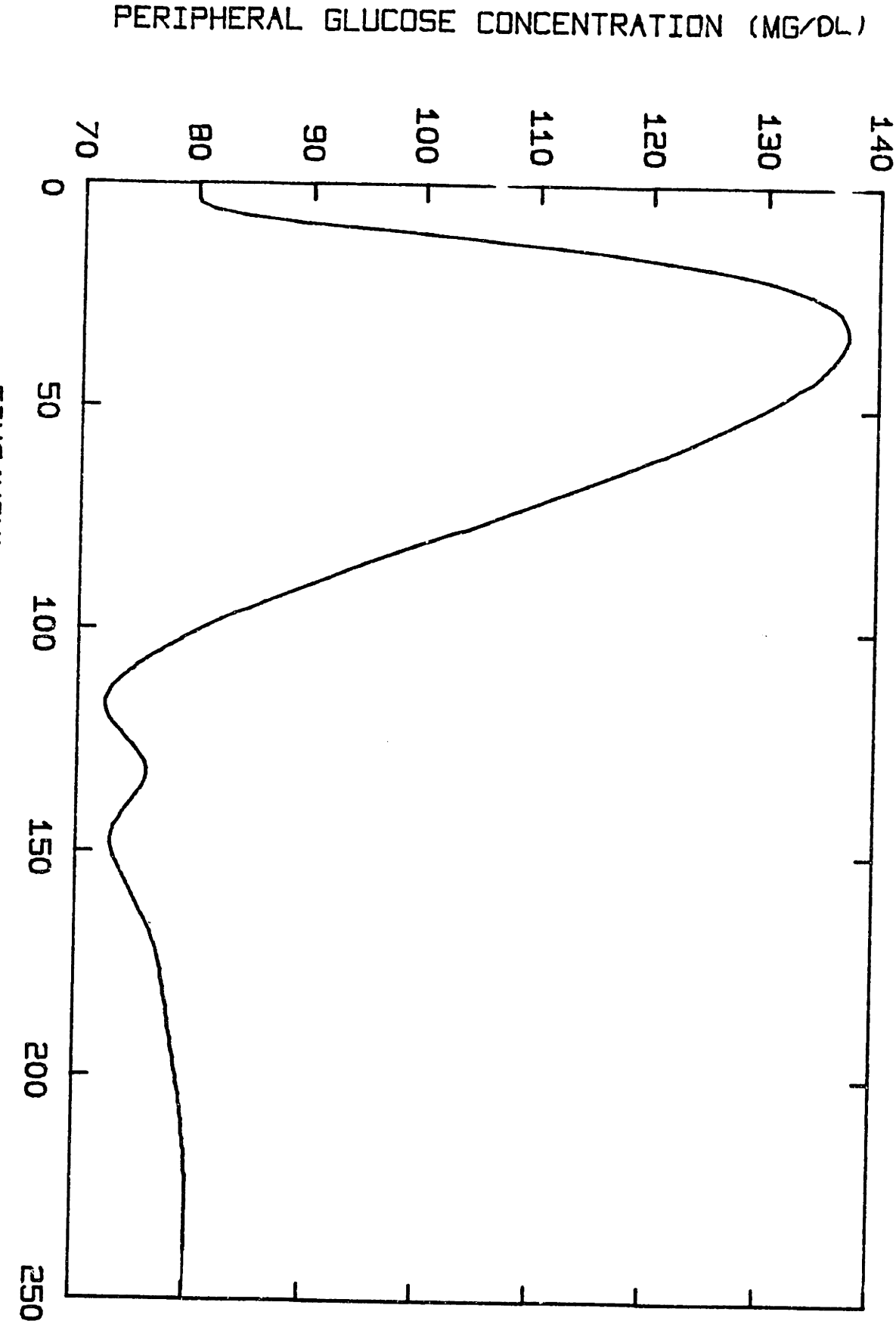

Figure 139

Five-minute delay in the glucose signal to the pancreas.
Simulation of response to a 100 gram oral glucose tolerance test.

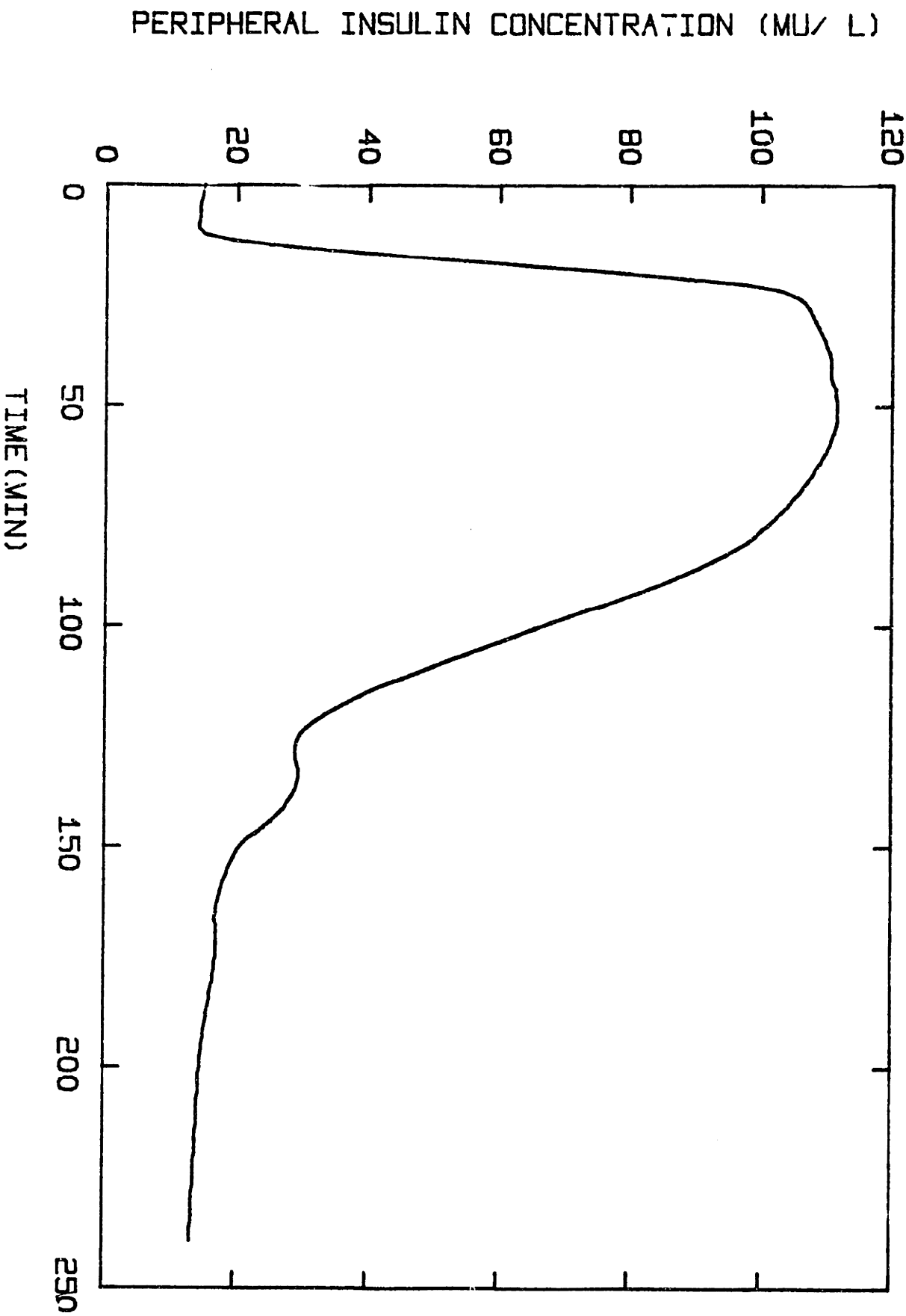

Figure 140

Five-minute delay in the glucose signal to the pancreas.
Simulation of response to a 100 gram oral glucose tolerance test.

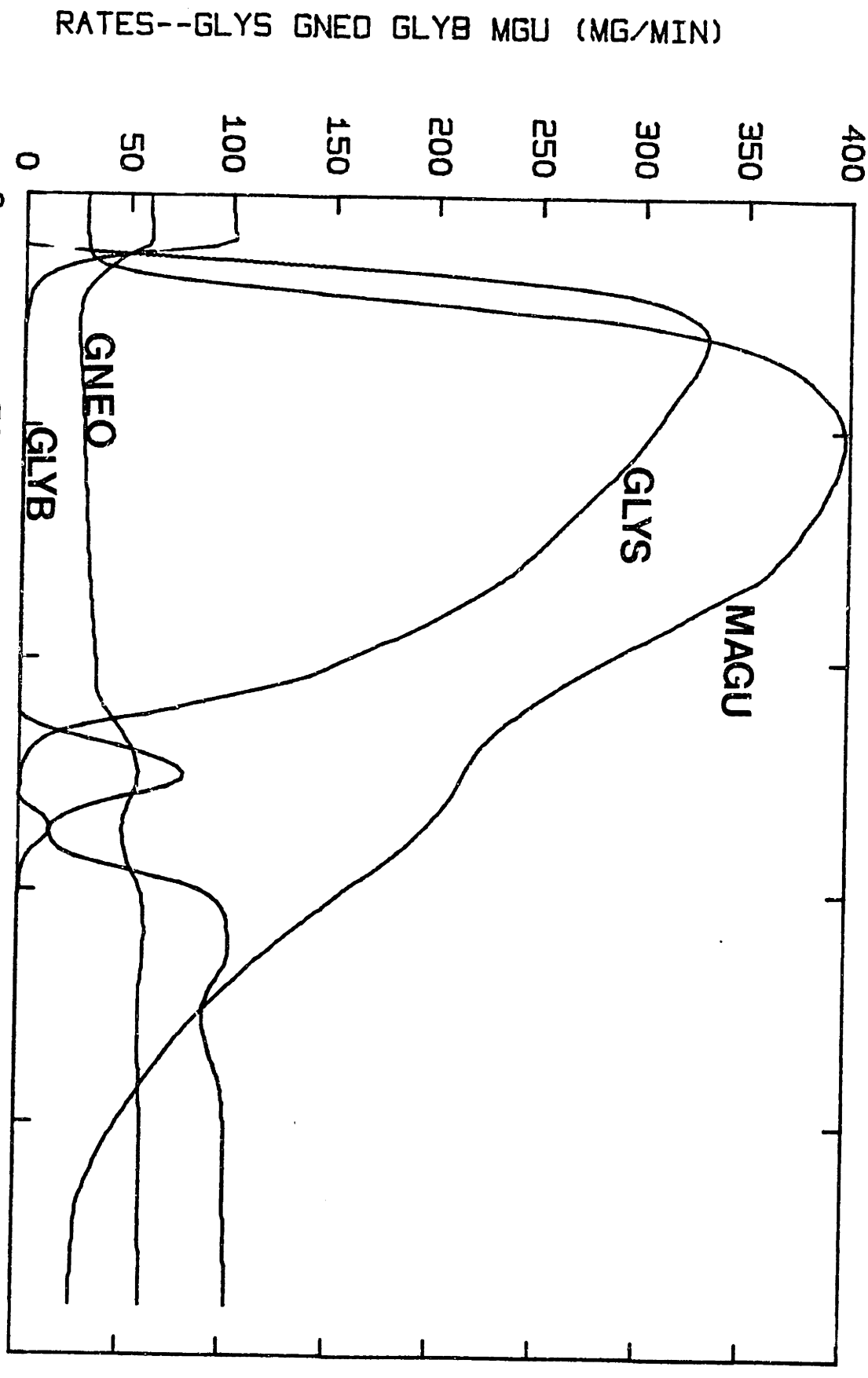

Figure 141

Five-minute delay in the glucose signal to the pancreas.
Simulation of response to a 100 gram oral glucose tolerance test.

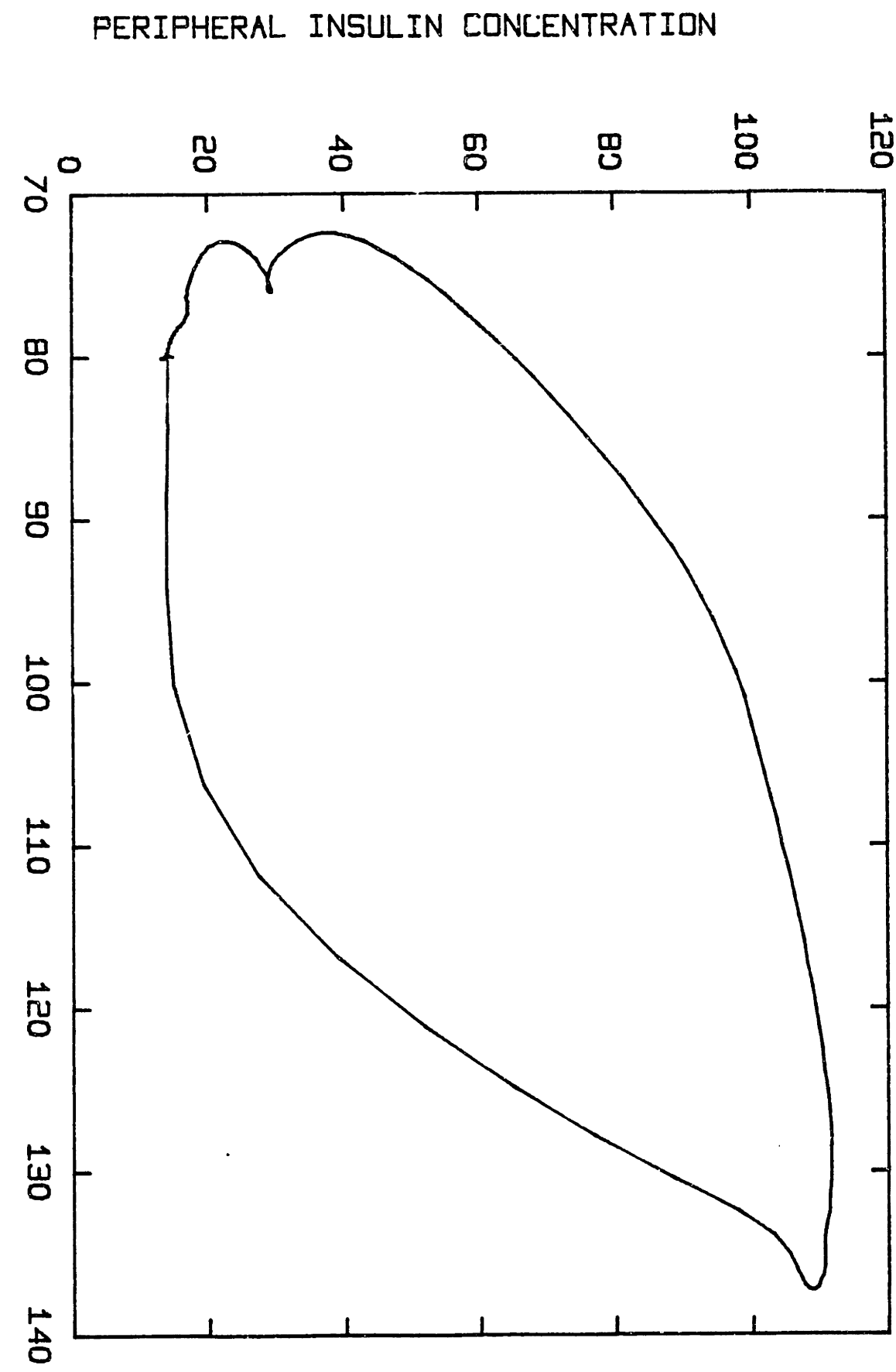

Figure 142

Five-minute delay in the glucose signal to the pancreas.
Simulation of response to a 100 gram oral glucose tolerance test.

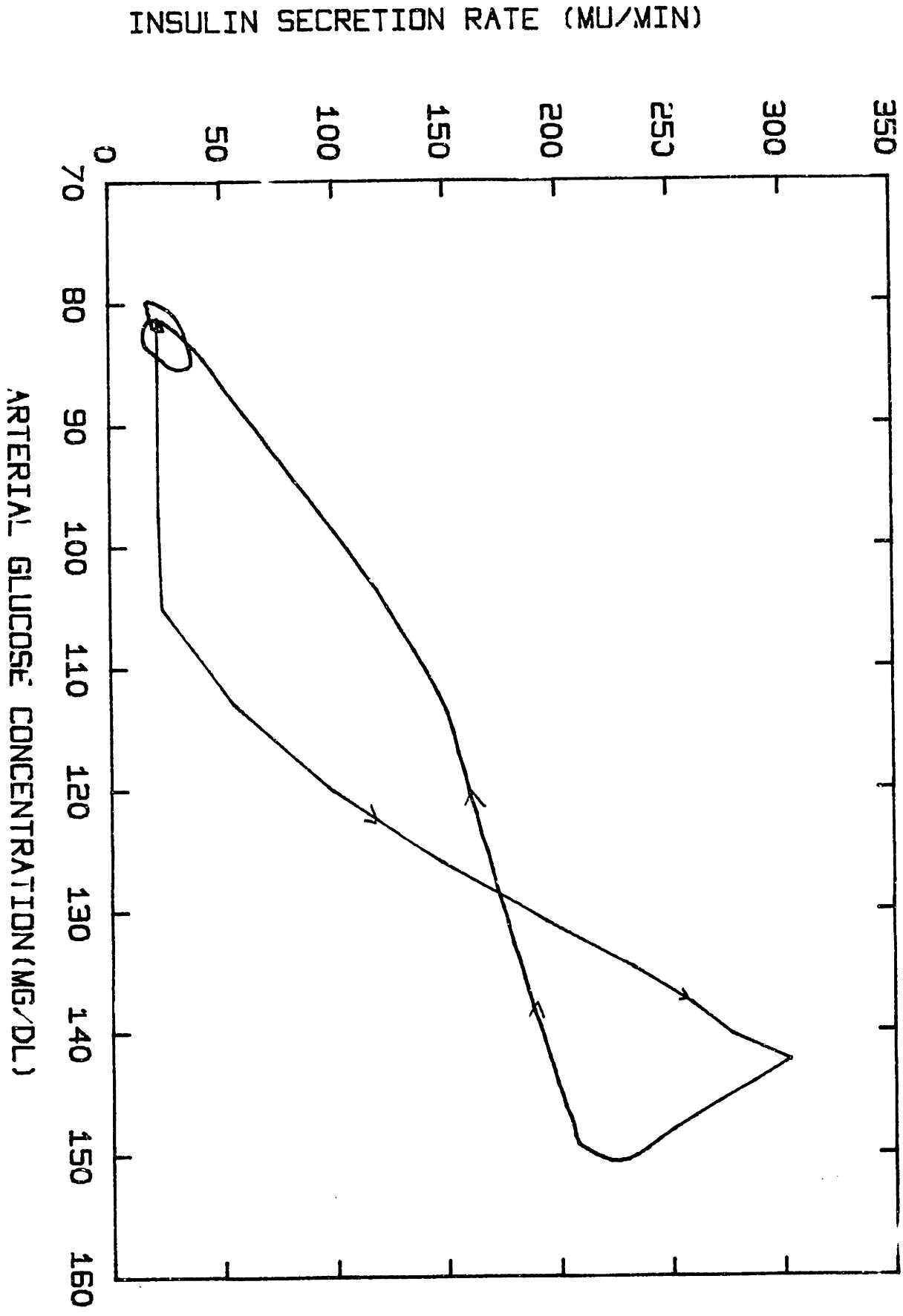

Figure 143

Five-minute delay in the glucose signal to the pancreas.
Simulation of response to a 100 gram oral glucose tolerance test.

model while in the normal model insulin concentrations rise when blood glucose goes above the fasting level of 80 mg/dl. Compare the phase plots for insulin secretion as a function of glucose concentration for the normal (figure 80) and "delayed" model (figure 143). Again note that insulin secretion is delayed till blood glucose reaches 110 mg/dl, and thereafter rises very sharply. As a result peripheral glucose concentrations rise to a peak of 140 mg/dl as opposed to the normal peak of 120 mg/dl. Interestingly enough, the time of the peak is unaffected. Figures 144-148 show the results when dt is equal to 10 minutes. Basically, the effects previously discussed are just accentuated. Insulin secretion (above fasting) is delayed until blood glucose concentrations reach 120 mg/dl and the peak peripheral glucose concentration reaches 160 mg/dl. So whereas a delay in insulin secretion results in a <u>delayed</u> peak glucose concentration, a delay in glucose signal results in an <u>increased</u> peak glucose concentration (with no delay in the time of the peak). Indeed these delays have been shown to affect the degree of control achieved with the various control algorithm discussed.

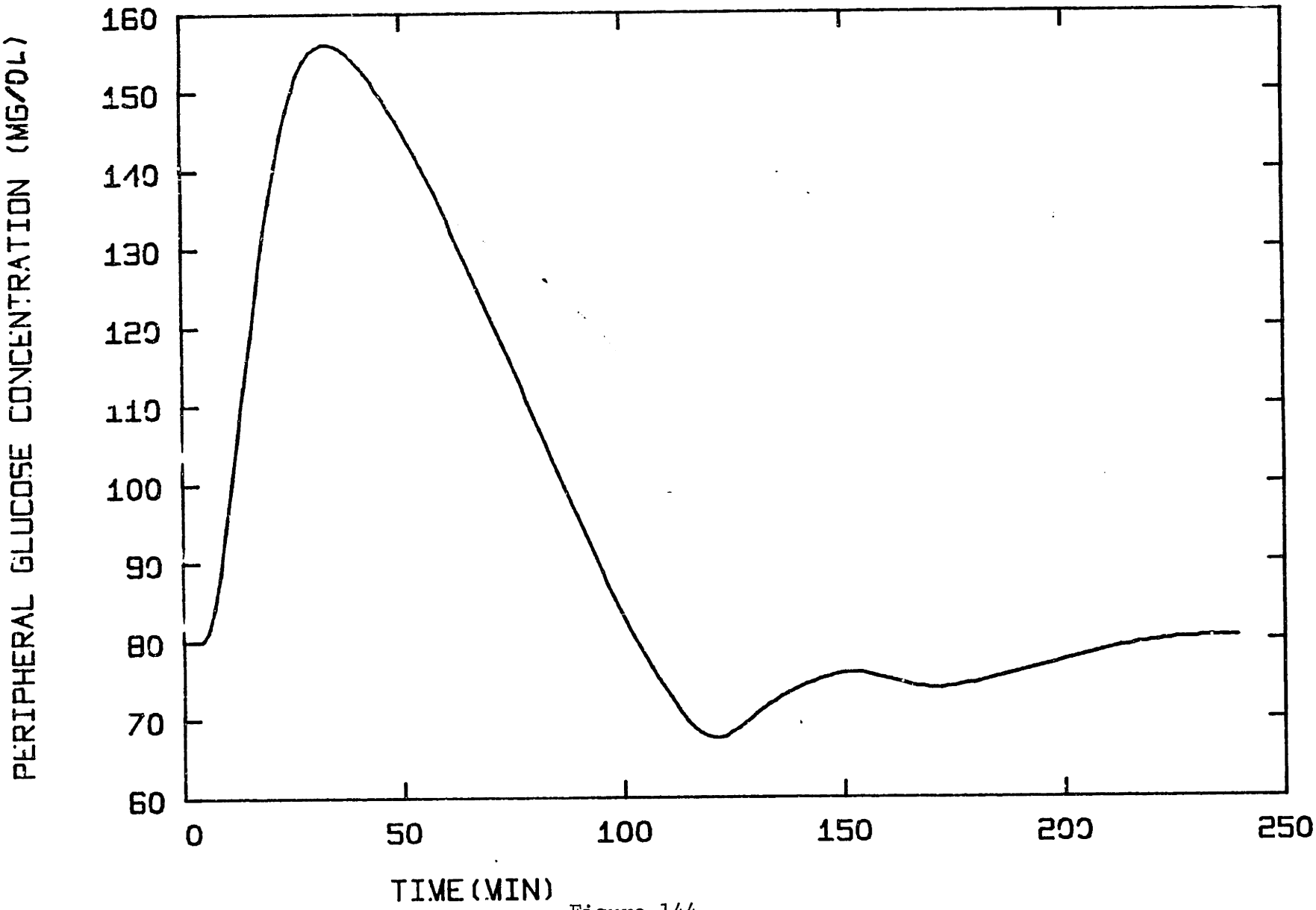

Figure 144

Ten-minute delay in the glucose signal to the pancreas.
Simulation of response to a 100 gram oral glucose tolerance test.

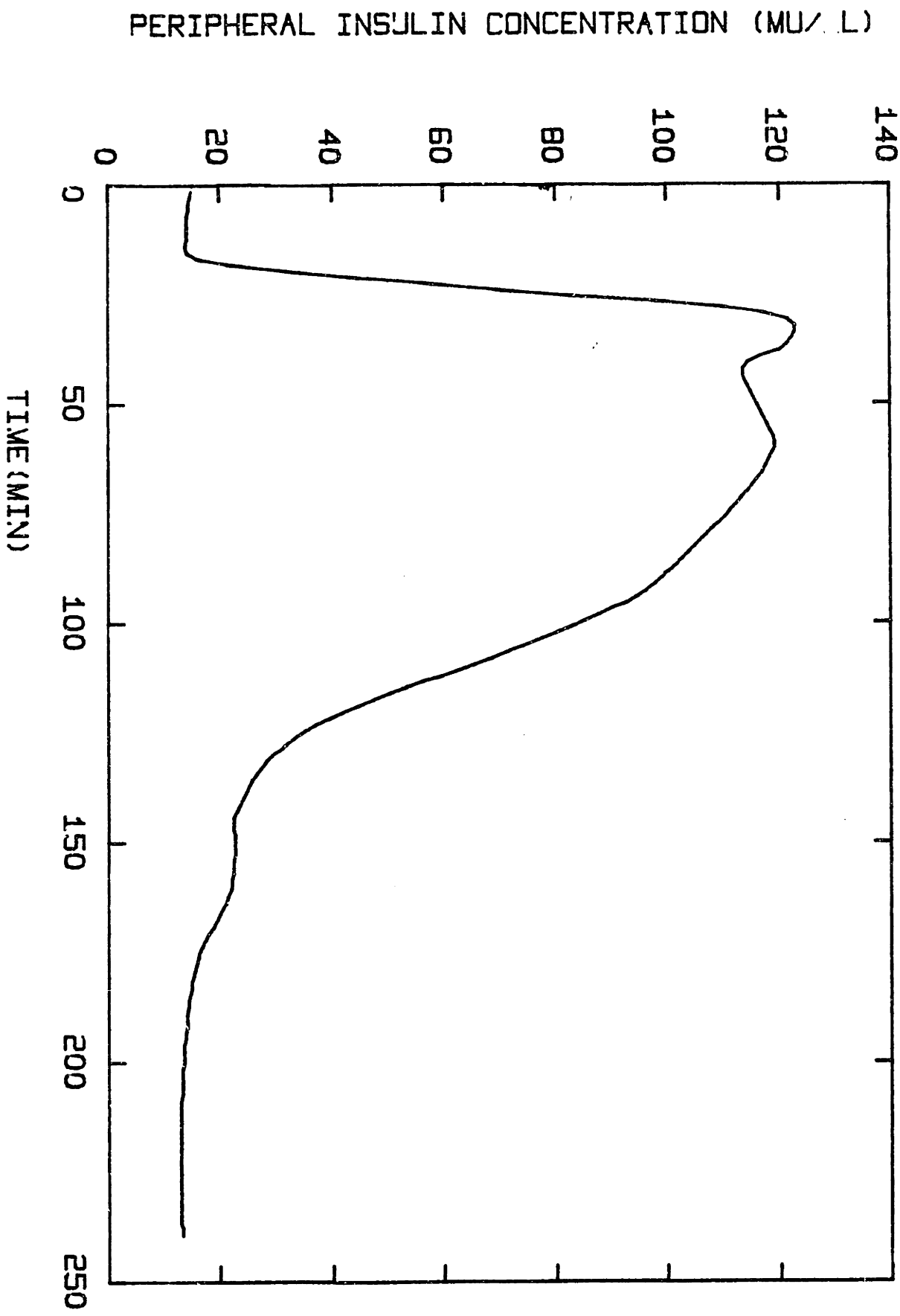

Figure 145

Ten-minute delay in the glucose signal to the pancreas.
Simulation of response to a 100 gram oral glucose tolerance test.

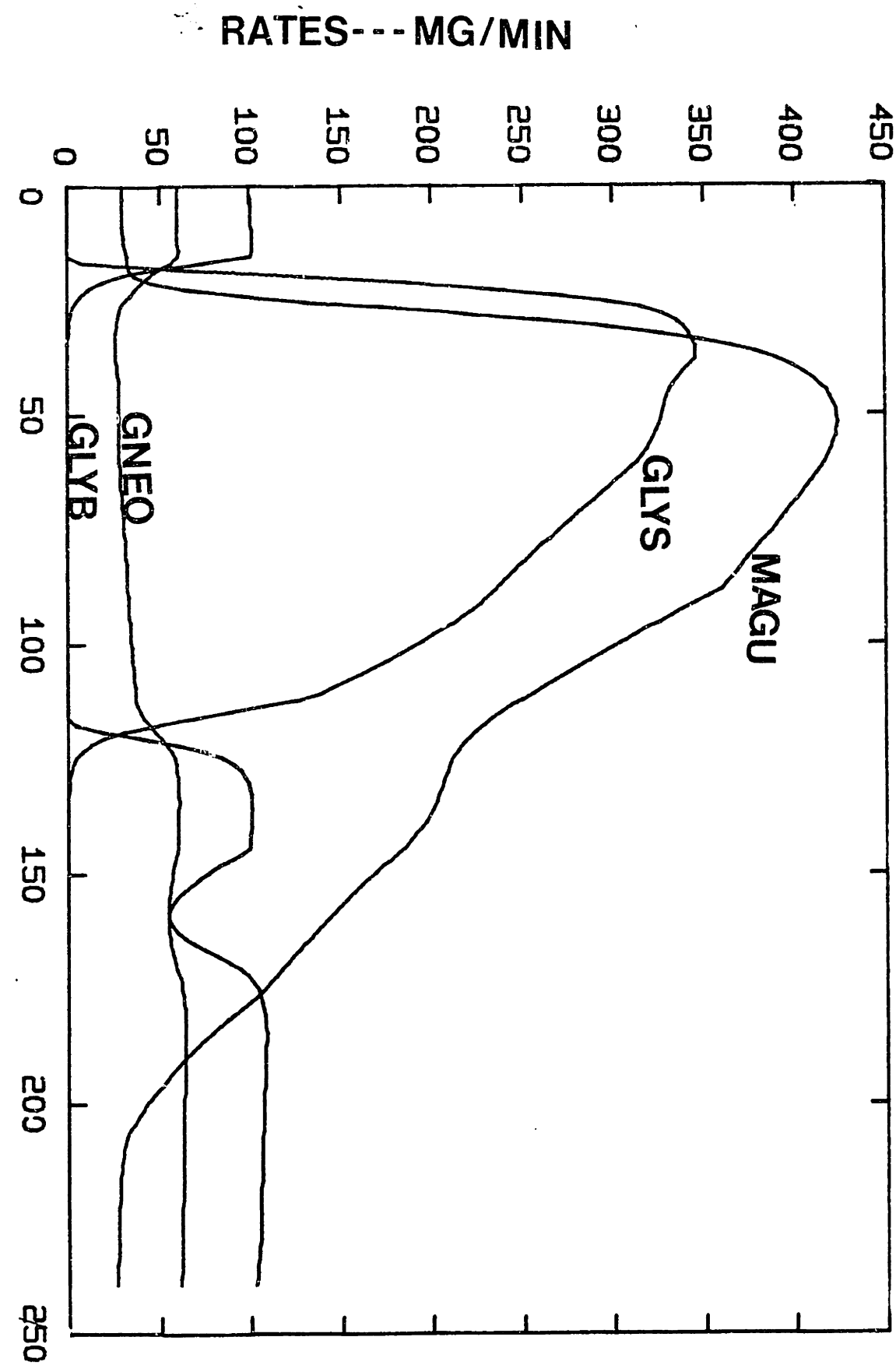

Figure 146

Ten-minute delay in the glucose signal to the pancreas.
Simulation of response to a 100 gram oral glucose tolerance test.

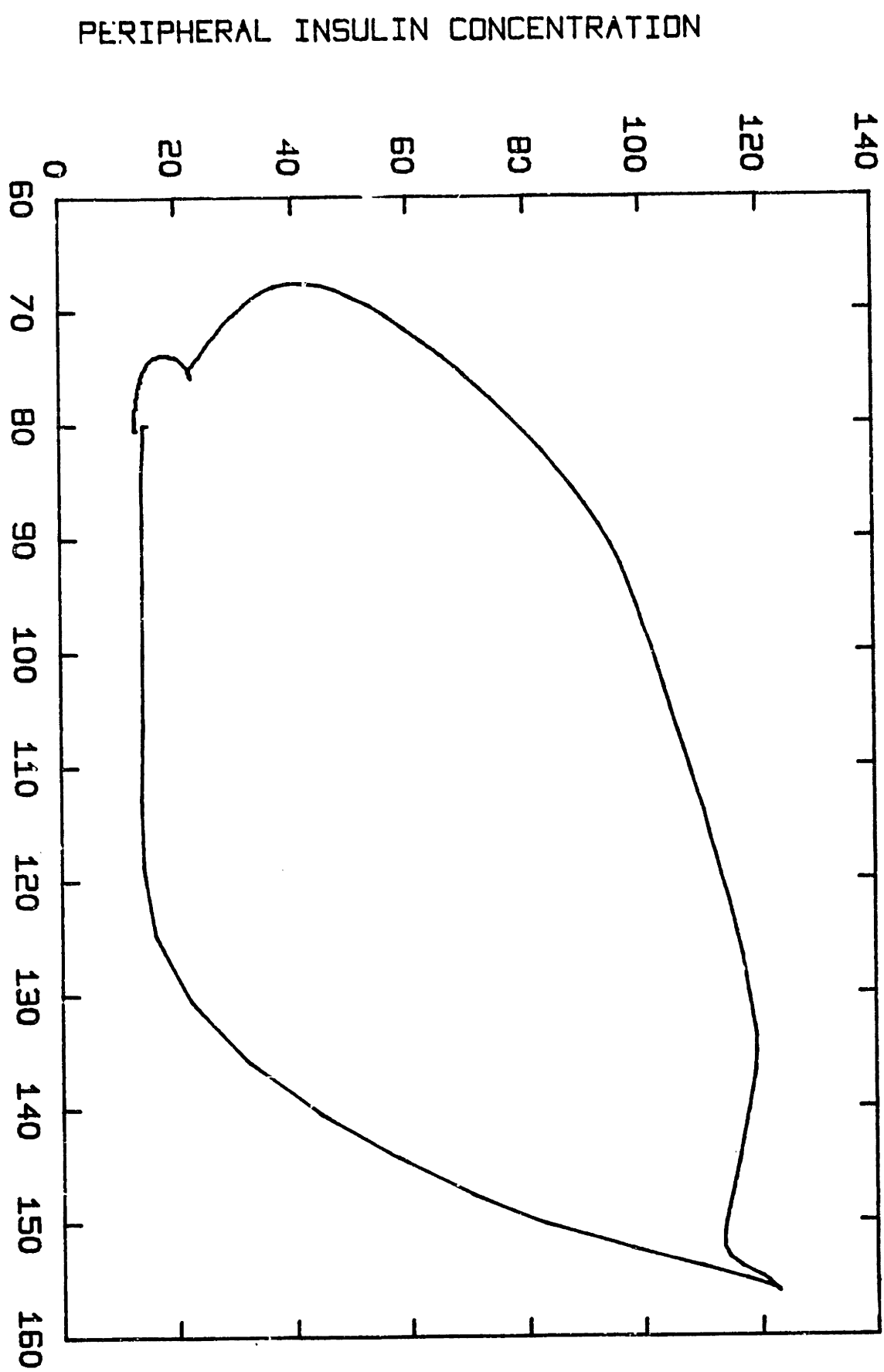

Figure 147

Ten-minute delay in the glucose signal to the pancreas.
Simulation of response to a 100 gram oral glucose tolerance test.

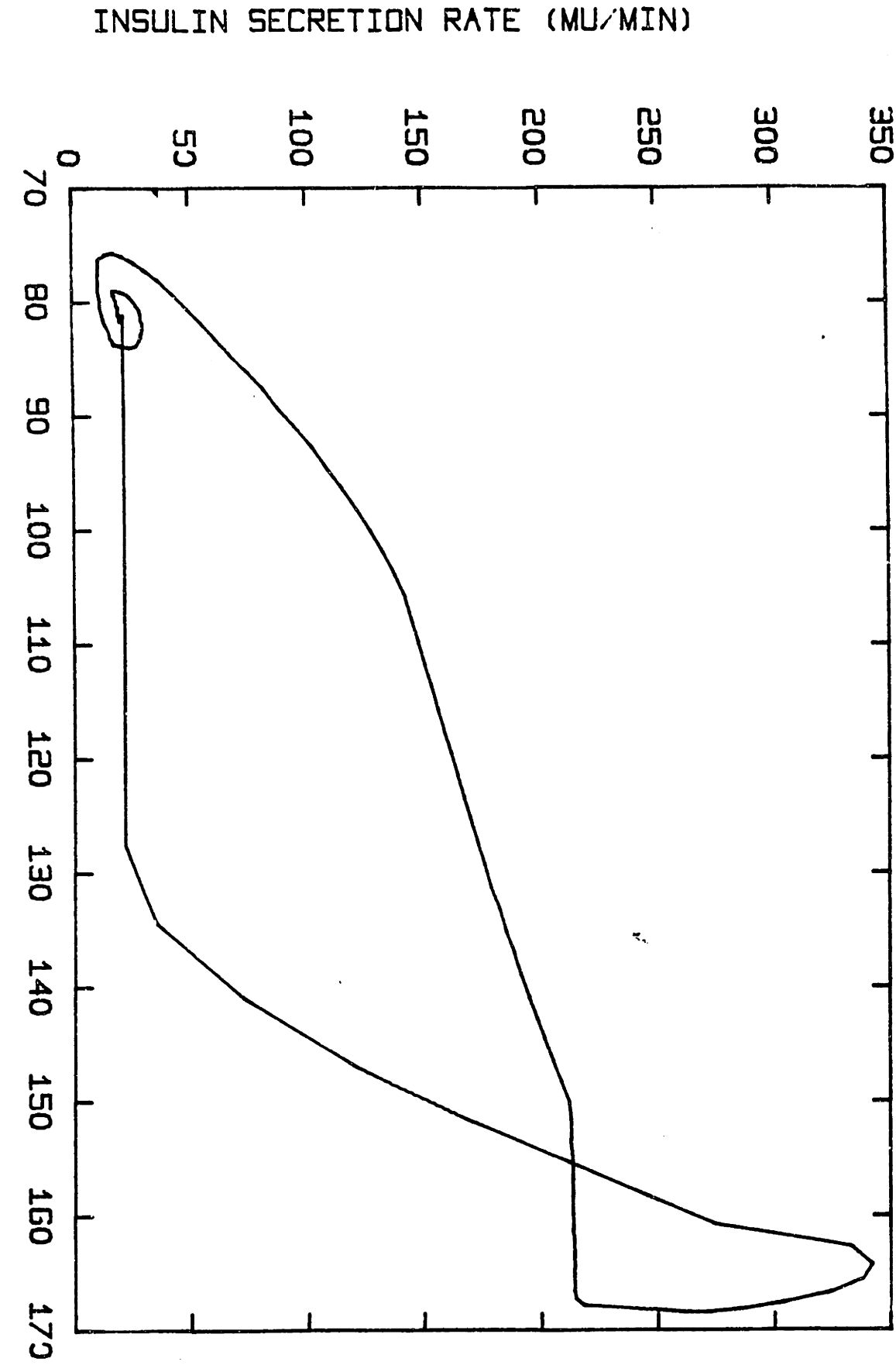

Figure 148

Ten-minute delay in the glucose signal to the pancreas.
Simulation of response to a 100 gram oral glucose tolerance test.

VI. CONCLUSION

The development of a model for glucose homeostasis based on physiological principles over a 24 hour period has been described. The model is the first, to the author's knowledge, to include gastrointestinal absorption of glucose, and the effect of gastrointestinal hormones on insulin secretion. This extension allowed the simulation of an oral as well as intravenous glucose load. In addition the model has been used to (1) test the proposed regimens for the normalization of blood glucose metabolism, (2) evaluate the characteristics of the glucoregulatory system, and (3) synthesize an effective control algorithm.

Several areas of work for future work are indicated: (1) an extension of the model to incorporate the absorption and distribution of amino acids and free fatty acids and their effect on insulin secretion and overall glucose homeostasis; (2) an extension of the model to incorporate the effects of the central nervous system and exercise an overall glucose metabolism. (3) of greatest importance would be the development of a much more general approach to study the important characteristics of the glucoregulatory system and subsequently design an "optimal control" algorithm. The conclusions drawn here have been based solely on simulating various conditions using the model. A more general methodology[8] would involve a) specifying a desired temporal and spatial distribution pattern of glucose, b) defining a performance index that will give a quantitative measure of this objective, and

---

[8] R. Hillman, M. Nathanson. 10.90 Project, M.I.T. Dept. of Chemical Engineering, Spring, 1977. C. Georgakis, Advisor, "Towards an Optimal Drug Delivery Regimen for Methotrexate Chemotherapy".

c) utilizing optimal control theorty to calculate the temporal and spatial pattern of administration of insulin that would minimize the performance index in (b). The distribution pattern then, is treated as the known function of time and the insulin secretion rate as the unknown function. The optimal strategy can then be (1) compared to the pancreatic response and (2) lead to a clinically applicable treatment plan for diabetics. Why might the "optimal" solution be different than the actual pancreatic response? Perelson et al[9] have pointed out that there is no a priori reason why any biological system should operate in an "optimal manner". Typically an organism is forced to cope with a number of competing influences so that an improvement in one direction invites a sacrifice in another direction. Thus optimality should be interpreted in a broader context as a "best compromise" solution.

---

[9] A. Perelson, M. Mirmirani, and G. Oster, "Optimal Strategies in Immunology", Journal of Mathematical Biology, 3, 325 (1967).

REFERENCES

Alberti, K. G. M. M., Christensen, N. J., Christensen, S. E., Prange-Hanson, Aa. P., Iverson, J., Lundboek, K., Seyer-Hansen, K., and Orskov, H., Inhibition of insulin by somatostatin, Lancet, 2, 1299 (1973)

Albisser, A. M., Leibel, B. S., Ewart, T. G., Davidovac, Z., Botz, C. K., Zingg, W., Schipper, H., and Gander, R., Clinical control of diabetes by the artificial pancreas, Diabetes, 23, no. 5, 397 (1974).

Albisser, A. M., Leibel, B. S., Ewart, T. G., Davidovac, Z., Botz, D. K., Zingg, W., An artificial endocrine pancreas, Diabetes, 23, no. 5, 389 (1974).

Atkins, G. L., Investigations of some theoretical models relating the concentrations of glucose and insulin in plasma, Journal of Theoretical Biology, 32, 471 (1971).

Atkinson, R. M., Parsons, B. J., and Smyth, D. H., The intestinal absorption of glucose, Journal of Physiology, 135, 581 (1957).

Avruch, J., Carte, J. R., and Martin, D. B., The effect of insulin on the metabolism of adipose tissue, Handbook of Physiology Endocrinology, Sec. 7. Vol. 1, R. O. Greep, E. B. Astwood (eds.), Physiol. Soc., Washington, D. C., 473, 1972.

Balasse, E. O., and Ooms, H. A., Role of plasma free fatty acids in the control of insulin secretion in man, Diabetologica, 9, 145 (1973).

Benedek, G., Unpublished notes, Topics in Quantitative Physiology, Harvard-M.I.T. Health Science and Technology Program, (1973).

Benedek, G., and Villars, F., In Physics with Illustrative Examples from Medicine and Biology, Volume 1, Mechanics, Addison-Wesley Publishing Co., Massachusetts, 1974.

Bergman, R. N., and Urquhart, J., The pilot gland approach to the study of insulin secretory dynamics, Recent Progr. Hormone Res., 27, 583 (1971).

Bessman, S. P., and Schultz, R. D., Sugar electrode for the "artificial pancreas", Horm. Metab. Res., 4, 415, (1972).

Bischoff, K. B., and Brown, R. G., Drug distribution in mammals, Chem. Eng. Prog. Symp. Ser., 62, No. 66, 33, (1966).

Bischoff, K. B., Dedrick, R. L., Zaharko, D. S., and Longstreth, J. A., Methotrexate pharmacokinetics, J. Pharm. Sci., 60, No. 8, 1128, (1971).

Bischoff, K. B., Some fundamental considerations of the applications of pharmacokinetics to cancer chemotherapy, Cancer Chemotherapy Rep., 59, 777-793, (1975).

Blackard, W. G., and Nelson, N. C., Portal and peripheral vein immunoreactive insulin concentrations before and after glucose infusion, Diabetes, 19, 302, (1970).

Bloodworth, J. M. B., Jr., Experimental diabetic glomerulosclerosis, II, the dog, Arch. Path., 79, 113-125, (1965).

Bolie, V., Coefficients of normal blood glucose regulation, J. Appl. Physiol., 16, 783, (1961).

Botz, C. K., An improved control algorithm for an artificial beta-cell, IEEE Transactions on Biomedical Engineering, 23, No. 3, 252, (1976).

Botz, C. K., Leibel, B. S., Zingg, W., Gander, R. E., and Albisser, A. M., Comparison of peripheral and portal routes of insulin infusion by computer-controlled insulin infusion system, Diabetes, 25, No. 8, 691, (1976).

Brown, J. C., Dryburgh, J. R., Ross, S. A., and Dupré, J., Identification and actions of gastric inhibiting polypeptide, Recent Prog. Hormone Res., 31, 487, (1975).

Bunn, H. F., Haney, D. N., Gabbay, K. H., et. al., Further identification of the nature and linkage of the carbohydrate in hemoglobin A_{Ic}, Biochem. Biophys. Res. Commun., 67, 103-109, (1975).

Cahill, G. F., Jr., Ashmore J., Earles, A. S., and Zutto, S., Glucose penetration into liver, Am. J. Physiology, 192, 491, (1958).

Cahill, G. F., Jr., Herrera, M. G., Morgan, A. P., Soeldner, J. S., Steinke, J., Levy, P. L., Reichard, G. A., and Kipnis, D. M., Hormone-fuel interrelationships during fasting, J. Clin. Invest., 45, 1851, (1966).

Cahill, G. F., Jr., and Owen, D. E., Some observations on carbohydrate metabolism in man, In Carbohydrate Metabolism and Its Disorders, Dickens, F., Randle, P. J., and Whelan, W. J. (eds), Academic Press, London, 143, 1968.

Cahill, G. F., and Soeldner, J. S., Glucose homeostasis: a brief review, In Hormonal Control Systems, Supplement I, E. B. Steer and A. H. Kadish (eds), American Elsevier Press, 88, 1969.

Cahill, G. F., Physiology of insulin in man, Diabetes, 20, No. 12, 785, (1971).

Cahill, G. F., Hyperglycemia, Ann. of N. Y. Acad. Sci., 230, 161, (1974).

Cahill, G. F., Jr., Etzwiler, D. D., and Freinkel, N., Blood glucose control in diabetes, Diabetes, 25, 237-8, (1976 a).

Cahill, G. F., Jr., Etzwiler, D. D., and Freinkel, N., Control and diabetes (editorial), N. Eng. J. Med., 294, 1004-5, (1976 b).

Cahill, G. F., Insulin and glucagun, Peptide Hormones, J. A. Parsons (ed.), Macmillan Press, London, 85, 1976 C.

Cerasi, E., and Luft, R., The plasma insulin response to glucose infusion in healthy subjects and in diabetes mellitus, Acta Endocr., 55, 278, (1967).

Cerasi, E., Fick, G., and Rudermo, M., A mathematical model for the glucose induced insulin release in man, Europ. J. Clin. Invest., 4, 267, (1974).

Charette, W. P., Kadish, A. H., Sridhar, R., Modeling and control aspects of glucose homeostasis, In Hormonal Control Systems - Supplement I, Stear, E. B., Kadish, A. H. (eds), Mathematical Bioscience, American Elsevier, New York, 115, 1969.

Chick, W. L., Like, A. A., Lavris, V., Galleti, P. M., Richardson, P. D., Panol, G., Mix, T. W., and Colton, C. K., A hybrid artificial pancreas, Trans. Amer. Soc. Art. Int. Organs, 21, 8, (1975).

Christensen, N. J., and Orskov, H., The relationship between endogeous glucose, serum insulin concentrations and glucose uptake in the forearm muscle of nondiabetics, J. Clin. Invest., 47, 1262, (1968).

Clemens, A. H., Chang, P. H., and Myers, R. W., The development of a Biostater, a glucose controlled insulin infusion system, In Blood Glucose Monitoring, Hormones and Metabolic Research, 7, (Supplement), 23, 1977.

Costrini, N. V., Ganeshappa, K. P., Wu, W., Whalen, G. E., and Soergel, K.H., Effect of insulin, glucose, and controlled diabetes mellitus on human jejunal function, Am. J. Physiol., 233 (3), E181-E187, 1977.

Creutzfeldt, W., and Perings, E., Is the frequency of vascular complications in human secondary diabetes related to nutritional factors?, In Nutrition and Diabetes Mellitus, Proc. of the 6th Capril. Conf., Acta Diab. Lat., 9

Csaky, T. Z., Intestinal Absorption and Malabsorption, New York, Raven Press.

Curry, D. L., Bennet, L. L., and Grodsky, G. M., Dynamics of insulin secretion by the perfused rat pancreas, Endocrinology, 83, 572, (1968).

Dean, P. M., and Matthews, E. L., Electrical activity in pancreatic islet cells: effect of ions, J. Physiol. (London), 210, 265, (1970).

Engerman, R. L., and Bloodworth, J. M. B., Experimental retinopathy in dogs, Arch. Opthal., 73, 204-210, (1965).

Erwald, R., Hed, R., Nygren, A., Röjdmark, S., Wiechel, K. L., Comparison of the effect of intraportal and intravenous infusion of insulin on blood glucose and free fatty acids in peripheral venous blood of man, Acta Med-Scand., 195, 351, (1974).

Exton, J. H., Gluconeogenesis, Metabolism, 21, 945, (1972).

Fajans, S. S., and Floyd, J. C., Jr., Stimulation of islet cell secretion by nutrients and by gastrointestinal hormones released during ingestion. In Handbook of Physiol. Endocrinology, Sec. 7, Vol. 1, Greep, R. O., Astwood, E. B. (eds), Am. Physiol. Soc., Washington, D. C., 473, 1972.

Felig, P., and Wahren, J., Influence of endogenous insulin secretion of splanchnic glucose and amino acid metabolism in man, J. Clin. Invest., 50, 1702, (1971).

Felig, P., Insulin: rates and rates of delivery, New Eng. J. Med., 291, No. 19, 1031, (1974 a).

Felig, P., Wahren, J., and Hendler, R., Primary role of the liver in the disposal and metabolic response to oral glucose, Clin. Res., 22, 476A, (1974 b).

Felig, P., and Wahren, J., The liver as a site of insulin and glucagon action in normal, diabetic, and obese humans, Isr. J. Med. Sci., 11, 528, (1975 a).

Felig, P., Wahren, J., and Hendter, R., Influence of oral glucose ingestion on spinchnic glucose and gluconeogenic substrate metabolism in man, Diabetes, 24, 468, (1975 b).

Felig, P., Wahren, J., Sherwin, R., and Hendler, R., Insulin, glucagon, and somatostatin in normal physiology and diabetes mellitus, Diabetes, 25, No. 12, 1092, (1976 a).

Felig, P., Wahren, J., and Hendler, R., Influence of physiologic hyperglucagonemia on basal and insulin-inhibited splanchnic glucose output in normal man, J. Clin. Invest., 58, 761, (1976 b).

Forbath, N., and Hetenyi, G., Glucose dynamics in normal subjects and diabetics before and after a glucose load, Diabetes, 15, 778, (1966).

Fordtran, J. S., Clodi, P. H., Konrad, H. S., and Ingelfinger, F. S., Sugar absorption tests with special reference to 3-O-Methyl-d-Glucose and d-Xylose, Annals of Int. Medicine, 57, 983, (1962).

Foster, R. O., Soeldner, J. S., Tan, M. H., and Guyton, J. R., Short term glucose homeostasis in man: a system dynamics model, ASME Journal of Dynamic Systems Measurements and Control, 308, (1973).

Gabby, K. H., and O'Sullivan, J. B., The sorbitol pathyway, enzyme localization and content in normal and diabetic nerve and cord, Diabetes, 17, 239-243, (1968).

Gatewood, L. C., Ackerman, E. A., Roseveor, J. W., and Molner, G. D., Computers and Biomedical Research, 2, 15, (1968).

Genuth, S. M., Metabolic clearance of insulin in man, Diabetes, 21, 1003, (1972).

Genuth, S., and Martin, P., Control of hyperglycemia in adult diabetics by pulsed insulin delivery, Diabetes, 26, No. 6, 571, (1977).

Gerich, J. E., Lorenzi, M., Schneider, V., Karan, J. H., Rivier, J., Guillemin, R., and Forsham, Ph. H., Effects of somatostatin on plasma glucose and glucagon levels in human diabetes mellitus, N. Eng. J. Med., 291, 544, (1974).

Grodsky, G. M., Bennett, L. L., Smith, D., Nemechck, K., The effect of tolbutamide and glucose on the timed release of insulin from the isolated perfused pancreas. In Tolbutamide After Ten Years, W. J. H. Butterfield and W. Westering (eds.), Excerpta Media, Amsterday, 11, 1967.

Grodsky, G. M., Cumy, D., Landahl, H., Bennett, L. L., Further studies on the dynamic aspects of insulin release in vitro with evidence of a two compartmental storage system, Acta. Diabet. Lat., 6, Suppl. 1, 554, (1969).

Grodsky, G. M., A threshold distribution hypothesis for packet storage of insulin and its mathematical modeling, J. of Clin. Invest., 51, 2047, (1972).

Guyton, A. C., Textbook of Medical Physiology, 2nd edition, W. B. Saunders Co., Philadelphia, 1961.

Guyton, J. R., Foster, R. O. Soeldner, J. S., Tan, M. H., Kahn, C. B., Koncz, L., and Gleason, R. E., A model of glucose-insulin homeostasis in man incorporating the heterogenous fast pool theory of pancreatic insulin release, Diabetes (accepted for publication).

Hetenyl, G., Jr., Pagurek, B., Fluker, G., Anthony, J., Popeseu, I., and Norwich, K.H., Computer controlled glucoregulation in the diabetic dog, Annals of Biomedical Engineering, 5, 61, (1977).

Holdsworth, C. D., and Dawson, A. M., The absorption of monosaccharides in man, Clin. Sci., 27, 317, (1964).

Ikkos, D., and Luft, R., On the volume of distribution of glucose in man, Acta. Endocrinol., 25, 235, (1957).

Insel, P. A., Liljenquist, J. E., Tobin, J. D., Sherwin, R. S., Watkins, P., Andres, R. and Berman, M., Insulin control of glucose metabolism in man, J. of Clin. Invest., 55, 1057, (1975).

Kadish, A. H., and Little, R. L., Automation control of blood glucose homeostasis, 7th Int. Cong. Clin. Chem., Methods in Clinical Chem. Vol. 1, Karger, Basel, 231, (1970)

Karam, J. H., Grodsky, G. M., Ching, K. N., Schmid, F., Burrill, K. and Forsham, P., "Staircase" glucose stimulation of insulin secretion in obesity, Diabetes, 23, 763, (1974).

Kerner, W., Thum, Ch., jun Gy, Tamas, Beischer, W., Clemens, A. H., and Pfeifter, E. F., Attempts at perfect normalization of blood glucose tolerance test of severe diabetics by artificial beta cell, Horm. Metab. Res., 8 256, (1976).

Kety, S. S., The general metabolism of the brain in vivo, In Metabolism of the Nervous System, Richter, D. (ed.), Pergammon Press, New York, 225, (1957).

Kline, N. S., Shimano, E., Stearns, H., McWilliams, C., Kohn, M., and Blair, J. H., Technique for automatic in vivo regulation of blood sugar, Medical Research Eng., 14, (1968).

Lacy, P. G., Howell, S. L., Yang, D. A., and Fink, C. J., New hypothesis of insulin secretion, Nature (London), 219, 1177, (1968).

Lagerlöf, H. O., Johansson, C., and Ekelund, K., Human gastric and intestinal response to meals by a multiple indicator dilution method, Mount Sinai Journal of Medicine, 43, 1-98, (1976).

Licko, V., Threshold secretary mechanism: a model of a derivative element in biological control, Bull. of Math. Bio., 35, 51, (1973).

Madison, L. L., Role of insulin in hepatic handling of glucose, Arch. Intern. Med., 123, 284, (1969).

Mallinson, C. N., Bloom, S. R., Warin, A. P., Salmon, P. R., and Cos, B., A glucagonoma syndrome, Lancet, 2, 1, (1974).

Malmendier, C. L., Deleroix, C., and Berman, M., Interrelations in oxidative metabolism of free-fatty acids, glucose and glycerol in normal and hyperlipemic patients, J. Clin. Invest., 54, 461, (1974).

Marliss, E. B., Murray, F. T., Stokes, E. F., Zinman, B., Nakhouda, A. F., Dernoga, A., Leibel, B. S., and Albisser, M., Normalization of glycemia in diabetes with insulin and glucagon delivery by the artificial pancreas, Diabetes, 26, No. 7, 663, (1977).

Matas, A. J., Sutherland, D. E. R., and Najarian, J. S., Current status of islet and pancreas transplantation in diabetes, Diabetes, 25, No. 9, 785, (1976).

McIntyre, N., Holdsworth, C. D., and Turner, Intestinal factors in the control of insulin secretion, J. Clin. Endocrin. Metab., 25, 1317, (1965).

Mirouze, J., Selam, J. L., Pharm, T. C., and Caradore, D., Evaluation of exogenus insulin homeostasis by the artificial pancreas in insulin-dependent diabetics, Diabetologica, 13, 273-278, 1977.

Morgan, H. E., Henderson, M. J., Regen, D. M., and Park, C. R., Regulation of glucose uptake in muscle, I, the effects of insulin and anoxia on glucose transport and phosphorylation in the isolated perfused heart of normal rats, Journal of Biol. Chem., 236, 253, (1961).

Mortimore, G. E., Influence of insulin on the hepatic uptake and release of glucose and amino acids, In Handbook of Physiology, Section 7, Endocrinology, Vol. 1, Baltimore, Waverly Press, 495, 1972.

Najarian, J. S., Sutherland, D. E. R., and Steftes, M. W., Isolation of human islets of langerhans for transplantation, Transpl. Proc., 7, Suppl. 1, 611, (1975).

Neely, J. R. and Morgan, H. F., Relationship between carbohydrate and lipid metabolism and the energy balance of the heart, Am. Rev. Physiol., 36, 413, (1974).

Nilsson, L. H., Furst, P., and Hultman, E., Carbohydrate metabolism of the liver in normal man under varying dietary conditions, Scand. J. Clin. Lab. Invest., 32, 331, (1973).

Norwich, K. H., Fluker, G., Anthony, J., Popeseu, I., Pagurek, B., and Hetenyi, G., Jr., The development of a glucose clamp, Metabolism, 24, 1221, (1975).

O'Connell, R., Morgan, A. P., Aoki, T. T., Ball, M. R., and Moore, F. O., Nitrogen conservation in starvation: graded responses to intravenous glucose studies in normal human volunteer subjects, J. Clin. Invest., 50, 1536, (1974).

O'Connor, M. D., Landahl, H. D., and Grodsky, G. M., Role of rate of change of glucose concentration as a signal for insulin release, Endocrinology, 101, 85, (1977).

Owen, O. E. and Reichard, G. A., Fuels consumed by man: the interplay between carbohydrates and fatty acids, Progr. Biochem. Pharm., 6, 177, (1971).

Perley, M., and Kipnis, D. M., Plasma insulin responses to glucose and tolbutamide of normal weight and obese diabetic and non-diabetic subjects, Diabetes, 15, 867, (1966).

Pfeiffer, E. F., Thum, Ch., Clemens, A. H., The artificial beta cell - a continuous control of blood sugar by external regulation of insulin infusion, Horm. Metab. Res., 487, 339, (1974).

Porte, D., Jr., Stimulation of insulin release by beta-adrenergic receptor, Diabetes, 15, 543, (1966 a).

Porte, D., Graber, A. L., Kuzuya, T., and Williams, R. H., The effect of epinephrine and immunoreactive insulin levels in man, J. Clin. Invest., 45, 228, (1966 b).

Porte, D., and Pupo, A. A., Insulin response to glucose: evidence for a two pool system in man, J. of Clin. Invest., 48, 2309, (1969).

Prankerd, T. A. J., The Red Cell, Blackwell, Oxford, 59, 1961.

Rasio, E., Whichelau, M. J., Butterfield, W. J. A., and Hicks, B. H., Insulin fixation and glucose uptake by forearm tissue in reponse to infusions of physiological amounts of insulin in nondiabetic subjects, Diabetologia, 8, 244, (1972).

Reichard, G. A., Jr., Jacobs, A. G., Kimbel, P., Hochella, N. J., and Weinhouse, S., Blood glucose replacement rates in normal and diabetic humans. J. Appl. Physiol., 16, 789, 1961.

Renold, A. E., the Beta cell and its response: summarizing remarks and some contributions from Geneva, Diabetes, 21, 619, (1972).

Reynell, P. C., and Spray, G. H., The absorption of glucose by the intact rat, J. Physiol., 134, 531, (1956).

Robinson, J. R., Principles of renal physiology, in Renal Disease, Black, D. A. K. (ed.), Blackwell Press, Oxford, 76, 1967.

Seltzer, H. S., Allen, E. W., Herron, A. L., and Brenna, M. T., Insulin secretion in response to glycemic stimulus, relation of delayed initial release to carbohydrate intolerance in mild diabetes mellitus, J. Clin. Invest., 46 323, (1967).

Service, F. J., Molnar, G. D., Rosevear, J. W., Ackerman, J. W., Gatewood, L. C., and Taylor, W. F., Mean amplitude of glycemic excursions, a measure of diabetic instability, Diabetes, 19, 644, (1970).

Shames, D. M., Berman, M., and Segal, S., Effects of thyroid disease on glucose oxidative metabolism in man. A compartmental model analysis, J. Clin. Invest., 50, 627, (1971).

Sherwin, R. S., Kramer, K. J., Tobin, J. D., Insel, P. A., Liljenquist, J. E., Berman, M., and Andres, R., A model of the kinetics of insulin in man, J. of Clin. Invest., 53, 1481, (1974).

Sherwin, R. S., Fischer, M., Hendler, R., and Felig, P., Hyperglucagonemia and blood glucose regulation in normal, obese and diabetic subjects, N. Eng. J. Med., 244, 455, (1976).

Shoemake, W. C., Yanof, A. M., Turk, L. N., and Wilson, T. H., Glucose and fructose absorption in the unanesthetized dog, Gastroenterology, 44 (5), 654, (1963).

Slamer, G. Hautecouverture, M. Assan, R., and Tchobrovtsky, G., One to five days of continuous intravenous insulin infusion on seven diabetic patients, Diabetes, 23, 732, (1974).

Soeldner, J. S., and Slone, D., Critical variables in the radio immunoassay of serum insulin using the double antibody technique, Diabetes, 14, 771, (1965).

Soeldner, J. S., The intravenous glucose tolerance test, In Diabetes Mellitus: Diagnosis and Treatment, Volume 3, S. S. Fajans and K. E. Sussman (eds.), American Diabetes Association, New York, 1971.

Soeldner, J. S., Chang, K. W., Aisenberg, S., and Hiebert, J. M., Progress towards an implantable glucose sensor and an artificial beta cell. Temporal Aspects of Therapeutics, J. Urquhert and F. E. Yates (eds.), Plenum Press, New York-London, 181, 1973.

Sokal, J. E., and Gerasi, K. E., Human liver glycogen levels, J. Lab. Clin. Med., 53, 878, (1959).

Spencer, J. L., Long, C. L., and Kinney, T. M., A model for glucose metabolism in man, Ind. Chem. Eng. Fund., 10, No. 1, 2, (1971).

Spiro, R. G., Biochemistry of the renal glomerular basement membrane and its alteration in diabetes mellitus, N. Eng. J. Med., 288, 1337-1342, (1973).

Unger, R. H., The pancreas as a regulator of metabolism, In MTP International Review of Science, Vol. 5, Endocrine Physiology, S. McCann (ed.), University press, Baltimore, 179, 1975.

Unger, R. H., and Orci, L., Physiology and pathophysiology of glucagon, Physiological Reviews, SG, No. 4, 798, (1976).

University Diabetes Program, A study of the effects of hypoglycemic agents on vascular complications in patients with adult-onset diabetes, Diabetes, 19 (Supplement 2), 747-830, (1970).

Wade, O. L., and Bishop, J. M., Cardiac Output and Regional Blood Flow, F. A. Davis Co., Philadelphia, 86, 1962.

Wagner, J. G., Fundamentals of Clinical Pharmacokinetics, Drug Intelligence Publications, Illinois, (1975).

Wahren, J., Felig, P., and Cerasi, E., Splanchnic and peripheral glucose and amino acid metabolism in diabetes mellitus, J. Clin. Invest., 51, 1870, (1976).

Wiesman, G., Absorption from the Intestine , London, Academic Press, 1964.

Wick, A. N., and Drury, D. R., Influence of glucose concentration on the action of insulin, Am. J. Physiol., 174, 445, (1953).

Wilson, T. H., Intestinal Absorption, Philadelphia, W. B. Saunders, 1962.

Yates, F. E., Benson, H., Buckles, R., Urquahart, J., and Zaffaroni, A., Engineering development of therapeutic systems: a new class of dosage forms for the controlled delivery of drugs, In Advances in Biomedical Engineering, J. Dickson (ed.), New York, Academic Press, 5, 1975.

Zierler, K. L., and Rabinowitz, D., Roles of insulin and growth hormone on peripheral glucose metabolism based on studies of forearm metabolism in man, Medicine, 42, 385, (1963).

Appendix A

Listing of the computer program for the model

PRINT ON THE FOLLOWING PAGES IS PARTIALLY ILLEGIBLE


```
C FLOW-LIMITED MODEL FOR THE DISTRIBUTION AND METABOLISM OF
C GLUCOSE AND INSULIN IN A 70 KILOGRAM MAN
C DYSYS (DYNAMIC SYSTEM SIMULATION) IS A MAINLINE COMPUTER PROGRAM WHICH
C SOLVES A SYSTEM OF FIRST ORDER LINEAR OR NONLINEAR DIFFERENTIAL
C EQUATIONS BY A FOURTH ORDER RUNGE-KUTTA INTEGRATION.  DYSYS CALLS THE
C FORTRAN SUBROUTINE EQSIM (EQUATION SIMULATION) TO CALCULATE THE
C ELEMENTS OF THE F (F=DY/DT) VECTOR GIVEN THE APPROPRIATE Y VECTOR
C AND THE CURRENT VALUE OF TIME
      SUBROUTINE EQSIM
      COMMON T,DT,Y(97),F(97),STIME,FTIME,NEWDT,TFWRT,
     *       N,IPR,ICD,ICN,TNEXT,PNEXT,TBACK
      COMMON /XZ/ X(16,16),Z(16,16)
C   CONSTANT  DEFINITION
C   QII       FLOWRATE OUT OF COMPARTMENT I (ML/MIN)
C   QIJ       FLOWRATE FROM COMPARTMENT J TO I (ML/MIN)
C   RBCU      RATE OF RED BLOOD CELL UPTAKE OF GLUCOSE (MG/MIN)
C   CNSU      RATE OF CENTRAL NERVOUS SYSTEM UPTAKE OF GLUCOSE (MG/MIN)
C   HUG       RATE OF HEART UPTAKE OF GLUCOSE (MG/MIN)
C   ***       FASTING REFERS TO 12-16 HR. ABSENCE OF CARBOHYDRATE INTAKE
C   GNEOF     FASTING RATE OF GLUCONEOGENESIS (MG/MIN)
C   GLYBNF    FASTING RATE OF GLYCOGEN BREAKDOWN (MG/MIN)
C   GLYSN     FASTING RATE OF GLYCOGEN SYNTHESIS
C   MAGUF     FASTING RATE OF MUSCLE & ADIPOSE UPTAKE OF GLUCOSE(MG/MIN)
C   GKNF      FASTING LIVER GLUCOSE CONCENTRATION (MG/DL)
C   GPSNF     FASTING PERIPHERAL TISSUE GLUCOSE CONCENTRATION (MG/DL)
C   IPSNF     FASTING PERIPHERAL TISSUE INSULIN CONCENTRATION (MU/LITER)
C   ILSNF     FASTING LIVER TISSUE CONCENTRATION OF INSULIN ((MU/L)
C   GDC       GLUCOSE DIFFUSION COEFFICIENT FOR BETA CELL (MG/MG%/MIN)
C   GMET      FASTING GLUCOSE METABOLITE CONCENTRATION (MG/DL)
C   ISPF      FASTING RATE OF INSULIN TRANSFER (MU/MIN)
C   PISNF     FASTING RATE OF PROINSULIN SYNTHESIS (MU/MIN)
C   IRRF      FASTING RATE OF INSULIN RELEASE FROM BETA-CELL (MU/MIN)
C   MRNASN    FASTING RATE OF MRNA SYNTHESIS (MOLECULES/MIN)
C   FMMPM     FRACTION OF GLUCOSE METABOLITE METABOLIZED  (FRAC/MIN)
C   FMMPM     FRACTION OF GLUCOSE METABOLITE METABOLIZED  (FRAC/MIN)
C   FGTMPM    FRACTION OF GLUCOSE METABOLIZED  (FRAC/MIN)
```

```
C     FMTGM      FRACTION OF METABOLITE TO GLUCOSE (FRACTION/MIN)
C     GNEMTM     TRANSPORT DELAY IN ACTION OF GLUCONEOGENSIS (MIN)
C     MAGMTM     TRANSPORT DELAY IN ACTION OF MUSCLE & ADIPOSE UPTAKE(MIN
C     GLYBMTM    TRANSPORT DELAY IN ACTION OF GLYCOGEN BREAKDOWN (MIN)
C     GLYSMTM    TRANSPORT DELAY IN ACTION OF GLYCOGEN SYNTHESIS (MIN)
C     DEGRTM     DELAYED EFFECT OF GLUCOSE ON INSULIN REL--TIME CONST(MIN
C     PITIME     PROINSULIN TIME CONSTANT (MIN)
C     MRTIME     MRNA TIME CONSTANT (MIN)
C     IGTIME     INSULIN-IN-GOLGI COMPLEX TIME CONSTANT (MIN)
C     RHSDTM     RELEASING-HOLDING SITES DEGREDATION TIME (MIN)
C     DISTM      RELEASING-HOLDING SITES DISTRIBUTION TIME  (MIN)
C     IRTM       INSULIN RELEASE TIME CONSTANT (MIN)
      REAL ILSN,IPSN
      REAL MAGUF,MAGMTM,ILSNF,IPSNF
      REAL MRNASN,MRTIME,IGTIME,IRTM,IRRF,ISPF,IFTSF
      DIMENSION EOGISF(16),EOGRHS(16),XBUFF1(200),XBUFF2(200)
      DATA EOGRHS/0.,0.,1.,1.,1.667,1.429,1.370,1.190,1.124,1.087,1.0
     *1.020,1.,0.,0.,0./
      DATA EOGISF/0.,1.0,1.0,7.273,5.714,3.636,2.667,2.,1.6,1.333,1.1
     *1.,1.,0.,0.,0./
      DATA IC/1/
      DATA GLNF,ILSNF,IPSNF,GPSNF/1846.44,4.70609,84.24,5450./
      DATA GNEOF,GNEMTM,MAGUF,MAGMTM,GLYBTM/60.,3.,30.,3.,3./
      DATA GDC,GMET,FMTGM,FGTMPM,FMMPM,MRNASN,MRTIME,PISNF,
     *PITIME,IGTIME,RHSDTM,DISTM,IRTM,IRRF,ISPF,DEGRTM,IFTSF/
     *.01,.465000,.5,2.,1.,.05,20.,21.88,20.,20.,45.,.2,.4,
     *21.88,200000.,45.,44.405/
      DATA RBCU,CNSU,HUG,GLYBNF,GLYSTM,GLYSN/3.67,100.,20.,100.,3.0,
     *100./
      DATA Q11,Q12,Q13,Q15,Q16,Q18,Q1B/-4.2273,1.0,3.625,1.933,
     *.7250,1.02078,-.3667/
      DATA Q21,Q22/1.591,-1.0/
      DATA Q31,Q33,Q34,Q3B/.3296,-8.625,5.0,-0.333/
      DATA Q43,Q44/5.,-5./
      DATA Q51,Q55,Q5B,Q562/.5273,-1.9333,-.0667,-1./
```

```
      DATA Q61,Q66,Q6B,Q637,Q660,Q661/0.6591,-0.7250,-0.1333,1.,-1.,1./
      DATA Q81,Q87,Q8B,Q88/1.12045,.2,-.4,-1.6104/
      DATA Q78,Q77,Q745/.5833,-0.2,-1.0/
      DATA Q1515,Q1516,Q1517,Q1519,Q1521/-2.4380,0.1,2.9,1.8125,1.0278/
      DATA Q1615,Q1616/.25694,-0.1/
      DATA Q1715,Q1717,Q1718/.48334,-7.0667,5./
      DATA Q1817,Q1818/4.1667,-7./
      DATA Q1915,Q1919,Q1920,Q1932/.604168,-5.972,5.,2.5/
      DATA Q2019,Q2020/4.1667,-8.75/
      DATA Q2115,Q2121,Q2122/1.02708,-1.27014,.05/
      DATA Q2221,Q2222/.2430556,-.0625/
      IF(NEWDT.EQ.-1) GO TO 2
      GO TO 3
    2 READ(8,50)((X(I,J),J=1,16),I=1,16)
   50 FORMAT(16F8.2)
      READ(8,50)((Z(I,J),J=1,16),I=1,16)
      WRITE(5,52)
   52 FORMAT('  X-Y FUNCTION VALUES')
      DO 4 I=1,16
      WRITE(5,51) I,(X(I,J),J=1,16)
   51 FORMAT('0',I3,16F7.2)
      WRITE(5,54) (Z(I,J),J=1,16)
   54 FORMAT('    ',16F7.2)
    4 CONTINUE
    3 CONTINUE
C GLUCOSE DISTRIBUTION EQUATIONS
C  INDEX  COMPARTMENT
C    1     HEART,LUNG,AND CENTRAL VASCULAR BLOOD(MG)
C    2     HEART,LUNG,AND CENTRAL VASCULAR TISSUE
C    3     HEAD BLOOD
C    4     HEAD TISSUE
C    5     KIDNEY BLOOD
C    6     LIVER BLOOD
C    7     PERIPHERAL TISSUE
C    8     PERIPHERAL BLOOD
```

```
C MEDIATORS ACT AS TRANSPROT DELAY (DELAY TIME SPECIFIED BY ---MTM)
C AND AS COMMON SITE OF ACTION OF INSULIN AND GLUCOSE
C   9      MEDIATOR OF LIVER GLYCOGEN BREAKDOWN (NORMALIZED)
C   10     MEDIATOR OF LIVER GLUCOSE METABOLISM (MEDLGM)
C   11     MEDIATOR OF LIVER GLYCOGEN SYNTHESIS (NORMALIZED)
C   12     MEDIATOR OF GLUCONEOGENESIS (NORM)
C   13     LIVER GLYCOGEN (MG)
C  INDEX   FUNCTION
C   14     MEDIATOR OF MUSCLE AND ADIPOSE TISSUE GLUCOSE UPTAKE (NORM)
C   60     RATE OF GLYCOGEN SYNTHESIS (MG/MIN)
C   61     RATE OF GLUCONEOGENESIS (MG/MIN)
C   62     RATE OF KIDNEYEXCRETION OF GLUCOSE (MG/MIN)
    37     RATE OF GLYCOGEN BREAKDOWN (MG/MIN)
C   38     EFFECT OF GLYCOGEN ON GLYCOGEN BREAKDOWN
C   39     EFFECT OF MEDLGM ON GLYCOGEN BREAKDOWN
C   40     EFFECT OF INSULIN ON MEDLGM
C   41     EFFECT OF ARTERIAL GLUCOSE ON MEDLGM
C   42     EFFECT OF LIVER GLUCOSE CONC. ON RATE OF GLYCOGEN SYNTHESIS
C   43     EFFECT OF MEDLGM ON RATE OF GLYCOGEN SYNTHESIS
C   44     EFFECT OF MEDLGM ON GLUCONEOGENESIS
C   45     MUSCLE AND ADIPOSE TISSUE GLUCOSE UPTAKE (MG/MIN)
C   46     EFFECT OF GLUCOSE ON PERIPHERAL GLUCOSE UPTAKE
C   47     EFFECT OF INSULIN ON PERIPHERAL GLUCOSE UPTAKE
C   48     EFFECT OF ARTERIAL GLUCOSE ON PERIPHERAL GLUCOSE UPTAKE
      Y(59)=0.
      F(1)=Q11*Y(1)+Q12*Y(2)+Q13*Y(3)+Q15*Y(5)+Q16*Y(6)+Q18*Y(8)+
     *Q1B*RBCU+Y(59)
      F(2)=Q21*Y(1)+Q22*Y(2)-HUG
      F(3)=Q31*Y(1)+Q33*Y(3)+Q34*Y(4)+Q3B*RBCU
      F(4)=Q43*Y(3)+Q44*Y(4)-CNSU
      F(5)=Q51*Y(1)+Q55*Y(5)+Q562*Y(62)+Q5B*RBCU
      GKC=Y(5)/6.0
      Y(62)=R(GKC,Y(62),1,6)
      F(6)=Q61*Y(1)+Q66*Y(6)+Q6B*RBCU+Q637*Y(37)+Q660*Y(60)+Q661*Y(61)
     *+Y(77)
```

```
      F(13)=.001*(Y(60)-Y(37))
      Y(37)=Y(38)*Y(9)*GLYBNF
      Y(38)=R(Y(13),Y(38),2,6)
      F(9)=(Y(10)*Y(39)-Y(9))/GLYBTM
      Y(39)=R(Y(10),Y(39),3,6)
      Y(10)=Y(40)*Y(41)
      ILSN=Y(20)/ILSNF
      Y(40)=R(ILSN,Y(40),4,11)
      GLC=Y(1)/22.
      Y(41)=R(GLC,Y(41),5,7)
      Y(60)=GLYSN*Y(11)
      F(11)=(Y(42)*Y(43)-Y(11))/GLYBTM
      GLN=Y(6)/GLNF
      Y(42)=R(GLN,Y(42),6,6)
      Y(43)=R(Y(10),Y(43),7,9)
      Y(61)=Y(12)*GNEOF
      F(12)=(Y(44)*Y(10)-Y(12))/GNEMTM
      Y(44)=R(Y(10),Y(44),8,8)
      F(8)=Q81*Y(1)+Q88*Y(8)+Q8B*RBCU+Q87*Y(7)
      F(7)=Q78*Y(8)+Q77*Y(7)+Q745*Y(45)
      Y(45)=MAGUF*Y(46)*Y(14)
      F(14)=(Y(47)*Y(48)-Y(14))/MAGMTM
      IPSN=Y(22)/IPSNF
      Y(47)=R(IPSN,Y(47),10,15)
      GPSN=Y(7)/GPSNF
      Y(46)=R(GPSN,Y(46),9,6)
      GHC=Y(1)/22.
      Y(48)=R(GHC,Y(48),11,4)
C   77    RATE OF GLUCOSE ABSORPTION (MG/MIN)
C   36    TOTAL GLUCOSE ABSORPTION (MG)
C   RA    MAXIMUM RATE OF ABSORPTION (MG/MIN)
C   TO    ONSET OF ABSORPTION (MINUTES)
C   TEND  END OF ABSORPTION (MIN)
C   EOGISF    EFFECT OF ORAL GLUCOSE ON INSULIN TRANSFER
C   EOGRHS    EFFECT OF ORAL GLUCOSE ON DISTR OF RELEASING-HOLDING SITES
```

```
      RA=800.
      TEND=240.
      T0=30.
      IF(T.LT.3.0) GO TO 64
      IF(T.GE.3.0.AND.T.LE.10.) GO TO 63
      IF(T.GT.10..AND.T.LE.30.) GO TO 61
      IF(T.GT.TEND) GO TO 160
      Y(77)=RA*(1.-SIN(((T-T0)/(TEND-T0))*PI(1.)/2.))
      GO TO 62
   64 Y(77)=0.
      GO TO 62
   61 Y(77)=RA
      GO TO 62
   63 Y(77)=RA*SIN(((T-3.0)/(10.-3.))*PI(1.)/2.)
   62 CONTINUE
      GO TO 300
  160 T0=330.
      TEND=540.
      IF(T.LT.303.) GO TO 164
      IF(T.GE.303.0.AND.T.LE.310.) GO TO 163
      IF(T.GT.310..AND.T.LE.330.) GO TO 161
      IF(T.GT.TEND) GO TO 164
      Y(77)=RA*(1.-SIN(((T-T0)/(TEND-T0))*PI(1.)/2.))
      GO TO 162
  164 Y(77)=0.
      GO TO 162
  161 Y(77)=RA
      GO TO 162
  163 Y(77)=RA*SIN(((T-303.)/(310.-303.)*PI(1.)/2.))
  162 CONTINUE
  300 CONTINUE
      IF(NEWDT.EQ.-1) GO TO 68
      GO TO 76
   68 DO 69 I=1,16
      Z(14,I)=Z(14,I)*EOGISF(I)
```

```
      Z(16,I)=Z(16,I)*EOGRHS(I)
   69 CONTINUE
      WRITE(5,77)
   77 FORMAT('0')
      WRITE(5,54) (Z(14,I),I=1,16)
      WRITE(5,54) (Z(16,I),I=1,16)
   76 CONTINUE
C INSULIN DISTRIBUTION EQUATIONS
C  INDEX  COMPARTMENT
C   15     HEART,LUNG,CENTRAL VASCULAR AND HEAD PLASMA
C   16     HEART,LUNG,CENTRAL VASCULAR AND HEAD TISSUE
C   17     KIDNEY PLASMA
C   18     KIDNEY TISSUE
C   19     LIVER PLASMA
C   20     LIVER TISSUE
C   21     PERIPHERAL PLASMA
C   22     PERIPHERAL TISSUE
      F(15)=Q1516*Y(16)+Q1517*Y(17)+Q1519*Y(19)+Q1521*Y(21)+Q1515*Y(1
      F(16)=Q1615*Y(15)+Q1616*Y(16)
      F(17)=Q1715*Y(15)+Q1717*Y(17)+Q1718*Y(18)
      F(18)=Q1817*Y(17)+Q1818*Y(18)
      F(19)=Q1915*Y(15)+Q1919*Y(19)+Q1920*Y(20)
     *+Q1932*Y(32)
      F(20)=Q2019*Y(19)+Q2020*Y(20)
      F(21)=Q2115*Y(15)+Q2121*Y(21)+Q2122*Y(22)
      F(22)=Q2221*Y(21)+Q2222*Y(22)
C INSULIN SYNTHESIS AND SECRECTION     BETA CELL
C  INDEX  COMPARTMENT
C   23     GLUCOSE IN BETA CELL (MG)
C   24     GLUCOSE METABOLITE (MG)
C   25     MESSENGER RNA (MOLECULES)
C   26     PROINSULIN(MILLIUNITS)
C   27     INSULIN IN GOLGI COMPLEX(MILLIUNITS)
C   28     INSULIN IN SLOW POOL (MILLIUNITS)
C   29     HOLDING SITES EMPTY(MILLIUNITS)
```

```
C   30    HOLDING SITES INSULIN-OCCUPIED(MILLIUNITS)
C   31    RELEASING SITES EMPTY (MILLIUNITS)
C   32    RELEASING SITES INSULIN-OCCUPIED(MILLIUNITS)
C   33    DELAYED EFFECT OF GLUCOSE ON INSULIN RELEASE
C   49    EFFECT OF GLUCOSE ON MRNA
C   50    EFFECT OF GLUCOSE ON INSULIN RELEASE
C   51    EFFECT OF GLUCOSE ON INSULIN SLOW TO FAST PO
C   52    EFFECT OF ARTERIAL GLUCOSE ON INSULIN TRANSFER SLOW TO FAST
C   53    ERROR FOR RELEASING SITES(MILLIUNITS)
C   54    RATE OF INSULIN TRANSFER SLOW TO FAST POOL  (MU/MIN)
C   55    SITES EMPTY TO INSULIN OCCUPIED (MU/MIN)
C   56    RELEASING TO HOLDING SITES (MU/MIN)
C   57    HOLDING TO RELEASING SITES (MU/MIN)
      F(23)=GDC*GHC-Y(23)*(GDC*100.+FGTMPM)+FMTGM
      F(24)=Y(23)*FGTMPM-Y(24)*(FMTGM+FMMPM)
      F(25)=MRNASN*Y(49)-Y(25)/MRTIME
      GMETC=80.*Y(24)/GMET
      Y(49)=R(GMETC,Y(49),12,11)
      F(26)=Y(25)*PISNF-Y(26)/PITIME
      F(27)=Y(26)/PITIME-Y(27)/IGTIME
      F(28)=Y(27)/IGTIME-(Y(29)+Y(31))*Y(55)+(Y(30)+Y(32))/RHSDTM
      Y(55)=(1./(Y(29)+Y(31)))*Y(54)
      Y(54)=(Y(28)*Y(51)*Y(33)*IRRF/ISPF+IFTSF)*Y(52)
      Y(51)=R(GMETC,Y(51),14,13)
      Y(52)=R(GHC,Y(52),15,3)
      Y(50)=R(GMETC,Y(50),13,7)
      F(33)=(Y(50)-Y(33))/DEGRTM
      F(30)=Y(29)*Y(55)+Y(32)*Y(56)-Y(30)*(Y(57)+1./RHSDTM)
      F(29)=Y(50)*(Y(29)+Y(30))/RHSDTM+Y(31)*Y(56)-Y(29)*(Y(57)+Y(55)-
     *1./RHSDTM)
      F(32)=Y(31)*Y(55)+Y(30)*Y(57)-Y(32)*(Y(56)+1./RHSDTM+1./IRTM)
      F(31)=Y(32)/IRTM+Y(50)*(Y(31)+Y(32))/RHSDTM
     *-Y(31)*(Y(55)+1./RHSDTM+Y(56))+Y(29)*Y(57)
      Y(56)=(1./(Y(31)+Y(32)))*ALIMIT(Y(53),0.,1.E50,IST1,NEWDT)/DIST
      Y(57)=-(1./(Y(29)+Y(30)))*ALIMIT(Y(53),-1.E50,0.,IST2,NEWDT)/DI
```

```
      Y(53)=(Y(31)+Y(32))-(Y(31)+Y(32)+Y(29)+Y(30))*Y(58)
      Y(58)=R(GMETC,Y(58),16,13)
C GLUCOSE CONCENTRATION
C   63    HEART,LUNG, AND CENTRAL VASCULAR BLOOD (MG/DL)
C   64    PERIPHERAL BLOOD
C   65    PERIPHERAL TISSUE
C   66    KIDNEY BLOOD
C   67    LIVER  LOOD
C   73    GLYCOG N SYNTHESIS PLUS CONSTANT GLUCOSE UPTAKE
   74    MUSCLE AND ADIPOSE TISSUE GLUCOSE UPTAKE PLUS CSTUG &GLYS
C   75    URINARY SPILLAGE AND ALL OTHER UPTAKE (MG/MIN)
C INSULIN CONCENTRATION
C   34    INSULIN AREA (MU-MIN/LITER)
C   35    TOTAL PANCREATIC INSULIN RELEASE (MILLIUNITS)
C   68    HEART,LUNG,HEAD, AND CENTRAL VASCULAR PLASMA (MU/ML)
C   69    PERIPHERAL PLASMA
C   70    KIDNEY PLASMA
C   71    LIVER PLASMA
C   72    INSULIN RELEASE RATE FROM BETA CELL
C   76    TOTAL INSULIN LOSS IN BODY
      PCF=15.
      F(34)=Y(21)/1.44-PCF
      F(35)=Y(32)/IRTM
      Y(63)=Y(1)/22.
      Y(64)=Y(8)/24.
      Y(65)=Y(7)/70.
      Y(66)=Y(5)/6.0
      Y(67)=Y(6)/20.
      Y(68)=Y(15)/1.44
      Y(69)=Y(21)/1.44
      Y(70)=Y(17)/.24
      Y(71)=Y(19)/.48
      RBCUP=10.
      CSTUG=CNSU+HUG+RBCUP+MAGUF
      Y(72)=Y(32)/IRTM
```

```
      Y(73)=Y(60)+CSTUG
      Y(74)=Y(73)+Y(45)-MAGUF
      Y(75)=Y(62)+Y(74)
      Y(76)=Y(15)+Y(16)+Y(17)+Y(18)+Y(19)+Y(20)+Y(21)+Y(22)
      RETURN
      END
      FUNCTION R(C,A,TN,L)
C LINEAR INTERPOLATION SUBROUTINE
C    C      CONCENTRATION
C    A      RATE
C    TN     TABLE NUMBER
C    L      NUMBER OF ENTRIES
      INTEGER TN
      COMMON /XZ/ X(16,16),Z(16,16)
      IF(C.LT.X(TN,1)) GO TO 30
      IF(C.GE.X(TN,L)) GO TO 20
      IF(X(TN,1).EQ.0.) GO TO 10
      CA=C-X(TN,1)
      I=CA/(X(TN,2)-X(TN,1))+1.
      GO TO 15
   10 I=C/X(TN,2)+1.
   15 J=I+1
      R=((X(TN,J)-C)*Z(TN,I)+(C-X(TN,I))*Z(TN,J))/(X(TN,J)-X(TN,I))
      RETURN
   20 R=Z(TN,L)
      RETURN
   30 R=Z(TN,1)
      RETURN
      END
// DUP
FILE DAFILE 1
// XEQ DYSYS97 4
*EL BINARY
*EL DYSYS,DYSYSLIB
*LC 800
```

```
*BC 600
FTIME=120.,DT=.1,N=22
Y(1)=1790.345,Y(2)=2828.76,Y(3)=135.0804,Y(4)=115.08,Y(5)=487.931,
Y(6)=1846.44,Y(7)=5450.,Y(8)=1920.,Y(9)=1.0,Y(10)=1.0,
Y(11)=0.0,Y(12)=1.0,Y(13)=50.,Y(14)=1.,Y(15)=22.6226,
Y(16)=58.1300,Y(17)=2.6731,Y(18)=1.591,Y(19)=9.8757,Y(20)=4.70609
Y(21)=21.6,Y(22)=84.,Y(23)=.34876,Y(24)=.46501,Y(25)=1.0,
Y(26)=437.5964,Y(27)=437.5964,Y(28)=200000.,Y(29)=216.9341
Y(30)=1989.4737,Y(31)=107.3608,Y(32)=8.7519,Y(33)=1.0
Y(34)=0.,Y(35)=0.0,Y(36)=0.,Y(37)=100.,Y(38)=1.,Y(39)=1.,Y(40)=1.,
Y(41)=1.,Y(42)=1.,Y(43)=0.,Y(44)=1.,Y(45)=30.,Y(46)=1.,Y(47)=1.,
Y(48)=1.,Y(49)=1.,Y(50)=1.,Y(51)=1.,Y(52)=1.,Y(53)=-0.0133,Y(54)=66.3,
Y(55)=.20431,Y(56)=0.,Y(57)=0.,Y(58)=.05,Y(59)=0.,
Y(60)=0.,Y(61)=60.
IPRNT=23,24,25,26,27,64,69, PRNTC(3)=10.
 &
0.,180.,360.,540.,720.,900.,0.,0.,0.,0.,0.,0.,0.,0.,0.,0.,0.
0.,10.,20.,30.,40.,50.,0.,0.,0.,0.,0.,0.,0.,0.,0.,0.
.5,.6,.7,.8,.9,1.,0.,0.,0.,0.,0.,0.,0.,0.,0.,0.
0.,1.,2.,3.,4.,5.,6.,7.,8.,9.,10.,0.,0.,0.,0.,0.
20.,30.,40.,50.,60.,70.,80.,0.,0.,0.,0.,0.,0.,0.,0.,0.
0.,1.,2.,3.,4.,5.,0.,0.,0.,0.,0.,0.,0.,0.,0.,0.
0.,.1,.2,.3,.4,.5,.6,.7,.8,0.,0.,0.,0.,0.,0.,0.
0.,.5,1.,1.5,2.,2.5,3.,3.5,0.,0.,0.,0.,0.,0.,0.,0.
0.,1.,2.,3.,4.,5.,0.,0.,0.,0.,0.,0.,0.,0.,0.,0.
0.,.5,1.,1.5,2.,2.5,3.,3.5,4.,4.5,5.,5.5,6.,6.5,7.,0.
50.,60.,70.,80.,0.,0.,0.,0.,0.,0.,0.,0.,0.,0.,0.,0.
0.,40.,80.,120.,160.,200.,240.,280.,320.,360.,400.,0.,0.,0.,0.,0.
0.,80.,160.,240.,320.,400.,480.,0.,0.,0.,0.,0.,0.,0.,0.,0.
0.,40.,80.,120.,160.,200.,240.,280.,320.,360.,400.,440.,480.TO.,0.,0.
61.0345,71.2069,81.3793,0.,0.,0.,0.,0.,0.,0.,0.,0.,0.,0.,0.,0.
0.,40.,80.,120.,160.,200.,240.,280.,320.,360.,400.,440.,480.,0.,0.,0.
0.,0.,230.,460.,690.,920.,0.,0.,0.,0.,0.,0.,0.,0.,0.,0.
0.,.2,.8,1.,1.,1.,0.,0.,0.,0.,0.,0.,0.,0.,0.,0.
0.,0.,0.,.3,.8,1.,0.,0.,0.TOC,0.,0.,0.,0.,0.,0.
```

```
1.5,1.,.64,.45,.39,.35,.32,.29,.26,.23,.20,0.,0.,0.,0.,0.
4.5,4.3,3.9,3.4,2.4,1.2,1.,0.,0.,0.,0.,0.,0.,0.,0.,0.
0.,1.,1.5,1.75,2.,2.,0.,0.,0.,0.,0.,0.,0.,0.,0.,0.
2.25,2.25,2.25,1.9,1.4,1.,.6,.3,0.,0.,0.,0.,0.,0.,0.,0.
2.8,1.2,1.,.9,.8,.7,.6,.5,0.,0.,0.,0.,0.,0.,0.,0.
0.,1.,1.4,1.75,2.,2.,0.,0.,0.,0.,0.,0.,0.,0.,0.,0.
0.,.5,1.,4.,6.,7.7,8.8,9.5,10.,10.4,10.8,11.1,11.5,11.8,12.,0.
.2,.8,1.,1.,0.,0.,0.,0.,0.,0.,0.,0.,0.,0.,0.,0.
0.,.2,1.,2.,3.,4.,4.8,5.4,5.7,5.9,6.,0.,0.,0.,0.,0.
1.,1.,1.,1.3,1.6,1.8,2.,0.,0.,0.,0.,0.,0.,0.,0.,0.
0.,.5,1.,1.1,1.4,2.2,3.,4.,5.,6.,7.,8.,9.,0.,0.,0.
0.,.9,1.,0.,0.,0.,0.,0.,0.,0.,0.,0.,0.,0.,0.,0.
0.,0.,.05,.43,.6,.7,.78,.84,.89,.92,.95,.98,1.,0.,0.,0.
```